INVESTIGATING THE INTERACTIONS OF BISMUTH AND OTHER METALS WITH BIOLOGICALLY RELEVANT MOLECULES

by

Heather A. Phillips

Submitted in partial fulfillment of the requirements
for the degree of Doctor of Philosophy

at

Dalhousie University
Halifax, Nova Scotia
August 2007

Your file Votre référence
ISBN: 978-0-494-31492-0
Our file Notre référence
ISBN: 978-0-494-31492-0

DALHOUSIE UNIVERSITY

To comply with the Canadian Privacy Act the National Library of Canada has requested that the following pages be removed from this copy of the thesis:

Preliminary Pages
- Examiners Signature Page (pii)
- Dalhousie Library Copyright Agreement (piii)

Appendices
- Copyright Releases (if applicable)

For Sean, John, Elaine, and Pete

Table of Contents

List of Tables

List of Figures

Abstract

For more than two centuries, the medicinal potential of bismuth compounds has been exploited to yield positive health effects in humans. Pepto-Bismol®, De-Nol®, and Pylorid® are modern remedies for gastrointestinal ailments, containing bismuth subsalicylate, colloidal bismuth subcitrate, and ranitidine bismuth citrate, respectively. Given the strength of bismuth-sulfur bonds compared to bonds between bismuth and other heteroatoms, it is likely that sulfur is involved in biological transformations of bismuth compounds. However, the biological chemistry of bismuth is still not understood at a molecular level. Among other characterization techniques, electrospray ionization mass spectrometry (ESI-MS) has recently been established as a data-rich tool for examining reaction mixtures containing metals and biological molecules. To build on previous studies and to further investigate the utility of ESI-MS as a method for examining bioinorganic chemical systems, this thesis primarily describes endeavours to examine new, biologically significant combinations of bismuth and biological molecules. For comparison, the chemistry of relatively toxic metals - mercury, thallium, and lead, which reside in the same row as bismuth in the periodic table - has also been examined. From these experiments, numerous new complex ions have been observed containing bismuth or other metals and various biologically relevant ligands, including amino acids and monosaccharides. In particular, the first bismuth-citrate complexes to be observed by mass spectrometry are described. This research not only contributes to a growing library of known metal-biomolecule complexes, but also confirms that mass spectrometry is a valid and preferred technique for the examination of bioinorganic complexes. Because bismuth compounds are effective in many different medicinal applications, and particularly with respect to gastrointestinal disorders, the fundamental work presented herein may be helpful to other medicinal chemists who are interested in the biological chemistry of bismuth, and particularly to those involved in the future production of new bismuth-based pharmaceuticals.

List of Abbreviations and Symbols Used

A	adenine	CP	cross-polarization
Å	angstrom(s)	Cys	L-cysteine
AA	amino acid	Cys-Gly	cysteinyl-glycine
Ac	acetyl	δ	chemical shift
ADH	alcohol dehydrogenase	Δ	change
Ala	L-alanine	D	dextrorotatory
APCI	atmospheric pressure chemical ionization	Da	dalton(s)
Arg	L-arginine	deg or °	angle degree(s)
Asn	L-asparagine	DMF	N,N-dimethylformamide
Asp	L-aspartic acid	DMSA	2,3-dimercaptosuccinic acid
BDH	chemical supplier	DNA	deoxyribonucleic acid
biomolecule	biologically relevant molecule	DP	dipeptide
bipy	2,2′-bipyridine	E	OCOR, OH, NR_2
BSS	bismuth subsalicylate	e.g.	for example
©	copyright	EI	electron ionization
C	cytosine	ESI	electrospray ionization
°C	degree(s) Celsius	ESI-MS	electrospray ionization mass spectrometry
ca.	circa = of approximately	Et	ethyl
CBS	colloidal bismuth subcitrate	ETG	ethylthioglycolate
CCD	charge-coupled device	EtOH	ethanol
CI	chemical ionization	eV	electron volt(s)
CID	collision-induced dissociation	*F*	structure factor
cit	tetradeprotonated citric acid	Fru	D-fructose
Cit	citric acid	g	gram(s)
cm	centimetre(s)	G	guanine

Gal	D-galactose	*I*	intensity
GERD	gastroesophageal reflux disease	ICP-MS	inductively coupled plasma mass spectrometry
GI	gastrointestinal	i.e.	that is
Glc	D-glucose	Ile	L-isoleucine
GlcN	D-glucosamine	*in vitro*	outside a living entity
GlcNAc	N-acetyl-D-glucosamine	*in vivo*	in a living entity
Gln	L-glutamine	IR	infrared
Glu	L-glutamic acid	*J*	coupling constant
Gly	glycine	K	kelvin(s)
Gly-Gln	glycyl-glutamine	kg	kilogram(s)
Gly-Glu	glycyl-glutamic acid	kHz	kilohertz
Gly-Gly	glycyl-glycine	kJ	kilojoule(s)
Gly-His	glycyl-histidine	KMTS	potassium methylthiosalicylate
Gly-Leu	glycyl-leucine	kV	kilovolt(s)
Gly-Phe	glycyl-phenylalanine	λ	wavelength
Gly-Ser	glycyl-serine	L	levorotatory
GS	deprotonated glutathione	L	ligand
GSH	glutathione	Leu	L-leucine
h	hour(s)	Lys	L-lysine
H	proton	μ	indicates a bridging atom or other chemical moiety
Hcy	DL-homocysteine	μL	microlitre(s)
His	L-histidine	μm	micrometre(s)
HPLC	high-performance liquid chromatography	μs	microsecond(s)
H. pylori	*Helicobacter pylori*	m	mass of an ion in atomic mass units or metre
Hz	hertz	M	molarity (moles/litre)
I	spin quantum number	*M*	metal

MALDI	matrix-assisted laser desorption/ionization	nm	nanometre(s)
Man	D-mannose	NMR	nuclear magnetic resonance
MAS	magic angle spinning	ORTEP	Oak Ridge Thermal Ellipsoid Plot
Me	methyl	p	type of orbital
MEA	2-mercaptoethylamine	P	primitive
Met	L-methionine	PEEK	polyetheretherketone
Met-Gly	methionyl-glycine	Ph	phenyl
MHz	megahertz	Phe	L-phenylalanine
min	minute(s)	phen	1,10-phenanthroline
mL	millilitre(s)	ppm	parts per million
mm	millimetre(s)	Pro	L-proline
mM	millimolar	PTFE	polytetrafluoroethylene (teflon)
mmol	millimole(s)	Q	quadrupole moment
mol	mole(s)	®	registered
Mon	monosaccharide	ρ	density
MPA	3-mercaptopropionic acid	R	alkyl or H substituent
MS	mass spectrometry	*R*	residual factor
MS/MS	mass spectrometry/ mass spectrometry	RBC	ranitidine bismuth citrate
MTG	methylthioglycolate	Rib	D-ribose
MTS	methylthiosalicylate	RNA	ribonucleic acid
mW	milliwatt(s)	RT	run time
m/z	mass-to-charge ratio(s)	σ	error or type of bond
NB	nucleobase	Σ	sum
Nd:YAG	neodymium-doped yttrium aluminum garnet	s	type of orbital
NL	normalized spectral intensity	SA	salicylic acid

SARS	severe acute respiratory syndrome	Tyr	L-tyrosine
SB	subtracted background	υ	frequency difference
Ser	L-serine	u	atomic mass unit(s)
T	thymine or tesla	U	uracil
TGSS	1-thio-β-D-glucose sodium salt	UV	ultraviolet
TGTA	1-thio-β-D-glucose tetraacetate	V	volume
Thr	L-threonine	Val	L-valine
TLA	thiolactic acid (2-mercaptopropionic acid)	X	Cys, MPA, or MEA
TlDLCys	DL-cysteinatothallium(I)	X-ray	electromagnetic radiation (λ ca. 10^{-12} to 10^{-9} m)
TlLCys	L-cysteinatothallium(I)	XRD	X-ray diffraction
TM	trademark	z	number of charges
TMA	thiomalic acid (mercaptosuccinic acid)	Z	OH or H
Trp	L-tryptophan	Z	formula units per unit cell
TSA	thiosalicylic acid		

Acknowledgements

The author is grateful for financial support from the Natural Sciences and Engineering Research Council of Canada, the Killam Program of the Canada Council for the Arts, the Canada Research Chairs program, the Canada Foundation for Innovation, and the Nova Scotia Research and Innovation Trust Fund. The author recognizes Dalhousie University, including the Department of Chemistry, the Faculty of Graduate Studies, the Chemistry Graduate Student Society, and the Dalhousie Student Union for providing funds in the form of a stipend and for related conference traveling. Faculty and staff in the Department of Chemistry have consistently helped the author, personally and intellectually. The author thanks committee members, Dr. A. A. Doucette, Dr. N. P. Schepp, and Dr. M. Stradiotto; X. Feng and Dr. A. Thompson of the Maritime Mass Spectrometry Laboratories; Dr. B. Berno, Dr. M. D. Lumsden, and Dr. U. Werner-Zwanziger for NMR collaborations; departmental representative, Dr. P. D. Wentzell; administrative personnel, G. Andrews, S. Dorey, G. Power, C. Stanton, and D. Wentzell; machinists M. Boutilier and M. R. Conrad; B. Moore and J. Sutton of Chemistry Stores; computer technicians, B. Millier and G. Ranieri; glassblower, J. Mueller. The author also acknowledges the contributions of Dr. R. McDonald and Dr. M. J. Ferguson of the Department of Chemistry X-ray Crystallography Laboratory at the University of Alberta, external examiner, Dr. J. S. McIndoe, of the Department of Chemistry at the University of Victoria, and Dr. D. E. Mahony of the Dalhousie Department of Microbiology and Immunology. Of course, research and study cannot be accomplished without discussion and support from immediate colleagues. The author has truly appreciated interactions with current members of the Burford Research Team: Y. S. Carpenter, E. D. Conrad, R. J. Davidson, R. Ovans, and especially C. D. L. Saunders; past group members, P. N. Duchesne, Dr. C. A. Dyker, P. Edem, Dr. M. D. Eelman, K. A. Groom, Dr. J. C. Landry, W. G. LeBlanc, J. K. Lee, M. W. Little, R. Neu, S. Neupane, S. D. Riegel, K. Sharp, Dr. H. A. Spinney, and Dr. J. J. Weigand; members of the Doucette Research Team: D. Mataija, G. A. Simms, J. C. Tran, and M. Wall; members of the Stradiotto Research Team: Dr. J. Cipot, M. A. Rankin, D. Wechsler, and Dr. B. M. Wile; other Canadian colleagues: Dr. A. Carnini, G. D. MacInnis, and S. T. McCann. The author is especially indebted to Dr. N. Burford for unrelenting encouragement, humour, and guidance.

Chapter 1 Introduction

Compounds of the element bismuth have been used to treat a variety of human ailments for over two hundred years.[1;2] Since 1919, bismuth subsalicylate (BSS, now in Pepto-Bismol®, Procter & Gamble), has been used widely to prevent and remedy gastrointestinal (GI) afflictions. In 1976, colloidal bismuth subcitrate (CBS, in De-Nol®, Gist-Brocades) was introduced,[1] and became one of the most commonly researched bismuth drugs due to the successful use of this substance against peptic ulcers.[3] More recently, ranitidine bismuth citrate (RBC, in Pylorid®, GlaxoSmithKline) has been investigated and administered to patients as a dual therapy for gastric acid suppression and treatment of gastric mucosa.[4;5] Given the considerable history of benefits for which bismuth compounds are known – coupled with continual advancements in chemical characterization – it is curious that the structures of BSS, CBS and RBC have not been unambiguously identified and that the chemistry associated with the bioactivity of bismuth is not understood.

Along with other bismuth compounds, BSS, CBS, and RBC show antimicrobial activity toward the bacterium, *Helicobacter pylori* (*H. pylori*),[6-8] which after many years of controversy regarding the origin of gastrointestinal disorders, has been established as a cause of peptic ulcers.[9] First reported in 1983,[10] the Nobel Prize in Medicine was awarded in 2005 for this finding.[11]Although the biochemical pathways of bismuth have not been comprehensively charted, it is possible that bismuth interacts with biological molecules in the human GI system or the *H. pylori* organism. Alternatively, a combination of human and bacterial biological components may be involved. Bismuth has a particular affinity for coordination by sulfur;[12] hence, while bismuth-based pharmaceuticals are typically bismuth-oxygen complexes, the biological target(s) of these compounds are most likely sulfur-containing molecules such as the amino acid, cysteine. For this reason, the interactions of bismuth with biological molecules[13-19] or other organic compounds[20-29] containing one or more thiol functionalities are under investigation.

The synthesis and characterization of bismuth compounds can be challenging, mainly due to the analytical hurdle of low solubility; however, accepted techniques including nuclear

magnetic resonance (NMR)[13;30] and X-ray diffraction (XRD)[31;32] have been employed to learn more about the biological chemistry and structures of bismuth compounds. Relatively recent success has been achieved by using electrospray ionization mass spectrometry (ESI-MS) to examine reaction mixtures containing bismuth or other metals with small biological molecules, including amino acids and peptides.[16-18;27;33] Given these results, the ESI-MS technique is a promising tool for further identification of other interesting and important interactions involving metals and biologically relevant ligands. Consequently, the work presented in this thesis focuses on how ESI-MS can be used to successfully examine reaction mixtures containing bismuth or comparatively toxic metals (mercury, thallium, and lead) in the presence of monosaccharides, constituents of nucleic acids, citric acid, and various thiol-carboxylic acids with structural similarities to the amino acid, cysteine.

In general, this document is intended as a contribution to the young but growing field of bioinorganic chemistry. The results described may well have an impact on the future development of new metal chelation therapies or new bismuth-based drugs for GI and other ailments. In order to set the stage for a discussion of results that have been obtained (Chapters 2 to 6), the following Sections of Chapter 1 provide more information on medicinal inorganic chemistry, the relationship between bismuth and *H. pylori*, prominent bismuth pharmaceuticals, toxic metals, biologically relevant molecules, known bismuth-thiolate chemistry, and the characterization of bismuth compounds using a variety of methods.

1.1 Medicinal Inorganic Chemistry

Since the late 1800s, a number of important discoveries have been made in the often independent research areas of inorganic chemistry and medicinal chemistry. Such breakthroughs include the study and characterization of some of the first known transition metal compounds (Werner complexes, Nobel Prize in Chemistry, 1913),[34;35] as well as the isolation of insulin, achieved at the University of Toronto (Nobel Prize in Medicine, 1923).[36] In contrast, the inception of medicinal inorganic chemistry as a subject of formal study is typically associated with the more recent 1965 report that *Escherichia coli* cells

no longer divide when exposed to low concentrations (1 to 10 ppm) of various transition metal complexes, including ammonium salts of $[PtCl_6]^{2-}$ and $[RhCl_6]^{3-}$.[37;38]

Prior to 1970 it was determined that *cis*-$Pt(NH_3)_2Cl_2$ was active against sarcoma and leukemia tumours in mice, a finding which notably led researchers to comment that, "at present, inorganic chemistry is largely unexplored for this [antitumor] property."[39] Since being sanctioned by the American Food and Drug Administration in 1978, the same platinum compound is now recognized as the prototypical inorganic pharmaceutical known as cisplatin, which – despite side effects – has been used successfully for the treatment of a range of cancers in humans.[40] Moreover, the words quoted above have rung true, leading to many new scientific initiatives to better understand the chemistry of bioinorganic compounds.[3;41-51]

In general, there are two main pursuits for chemists interested in the biology of inorganic elements. One area of research involves understanding and mimicking bioinorganic reactions, often for applications in non-biological syntheses. One example of this is the study of biomineralization processes.[52;53] Depending on the characteristics of a particular organic framework, inorganic materials with novel properties are generated. For instance, the ability to replicate the formation of a mollusc shell or coccolithophore shield may bring about useful new applications in the realm of materials science.[53] Another relevant example is the investigation of metalloenzymes. These natural catalysts allow many biological reactions to occur, often with remarkable substrate selectivity. Understanding how these metalloenzymes function in a biological environment will enable chemists to design similar metal catalysts for use in large-scale industrial processes.[52]

A second objective for bioinorganic chemists is to understand the details of medicinal inorganic reactions in order to develop improved detection and treatment methods for medical disorders. In this case, the study of metalloenzymes provides information on the mechanisms of binding and release of metal ions to and from these catalytic biomolecules.[52] This information benefits both scientists and physicians, enabling the differentiation between normal protein function in healthy individuals and abnormal protein activity as a result of disease. A related endeavour for bioinorganic chemists, and

one for which bismuth will be the focus of this document, is the study and design of inorganic compounds that are relevant in therapeutic and diagnostic medical applications.[43] Although the pharmaceutical industry has an extensive history, much of the work that has been done to introduce new treatments for disease has involved the discovery and development of organic drug products. This is in spite of a substantial history of observations and experiments that show inorganic compounds to be capable of producing positive health effects.[45]

Of course, when the consumption of inorganic elements and metal compounds is considered, it is not surprising that concern is raised over the negative impacts that some of these compounds have on living organisms. Familiar examples of toxins include tetraethyllead, which was employed as an anti-knock gasoline additive until the poisonous nature of lead induced a shift to the use of unleaded gasoline.[54] Methylmercury consumed by ingesting fish products can also result in poisoning. Of particular concern is prenatal contact with methylmercury.[55] Chromium(VI) is a strong oxidizing agent and causes biological corrosion.[55] In contrast to these and other examples, it is equally possible that inorganic compounds can have beneficial medicinal effects. Trace amounts of many metal ions, including those of molybdenum, manganese, iron, cobalt, nickel, copper and zinc, as well as vanadium, chromium(III) and tin, are vital to the health of living organisms.[42]

Considering the previous information, it is critical to realize that the toxicity of an element depends primarily on the quantity of complex consumed.[45] For instance, in appropriate amounts, copper is an important component of certain proteins necessary for biological electron-transfer reactions.[42] Oppositely, Wilson's disease (of genetic origin) results from the buildup of copper in various tissues, meaning that copper is toxic in high quantities.[56] The bioactivity of any metal-containing compound is also dependent on the characteristics of the ligands that are coordinated to the metal; therefore, the type and arrangement of ligands are both important considerations in the design and understanding of medicinal inorganic complexes. With this in mind, the reader's attention can be returned to cisplatin (Figure 1.1a), in which the two chloride ligands are known to be

easily displaced within cancer cells, allowing binding to deoxyribonucleic acid (DNA) and ultimately resulting in cell death. Alternatively, in transplatin (Figure 1.1b) the *trans* arrangement of ligands prevents the complex from acting as an effective cancer treatment.[57] A diverse set of inorganic compounds show promise or are already employed in the treatment and detection of a range of health afflictions (see Figure 1.1, continued on the following page after the caption below).

Figure 1.1 Compounds relevant to medicinal inorganic applications. a) Cisplatin combats some cancers, while b) transplatin is not an anti-cancer complex. c) Lithium carbonate is administered to patients suffering from depression.[45] d) Barium sulfate provides imaging contrast when detecting gastrointestinal infirmity.[45] e) Bis-(maltolato)-oxovanadium(IV) is currently the standard for comparison to other vanadium complexes under investigation for use as insulin mimics in diabetes therapy.[58] f) Chloroquine is an organic compound used in the treatment of the malaria parasite which consumes human hemoglobin,[59] and g) ferrochloroquine is under study as a replacement for chloroquine, to which the malaria parasite is becoming resistant.[60] h) Gold(I) compound, Auranofin®, is employed in patients with rheumatoid arthritis.[61] i) Ceretec™ is a ^{99m}technetium radioimaging complex, used in obtaining information on stroke victims.[62] j) *p*-Boronophenylalanine is one of the most common Boron Neutron Capture Therapy agents.[63] k) Solid state structures of colloidal bismuth subcitrate, deployed to battle ulcers, typically involve this dianionic bismuth-citrate dimer.[2] l) Ranitidine is an organic H_2 antagonist that can be reacted with bismuth citrate to produce another treatment for gastrointestinal disorders.[8]

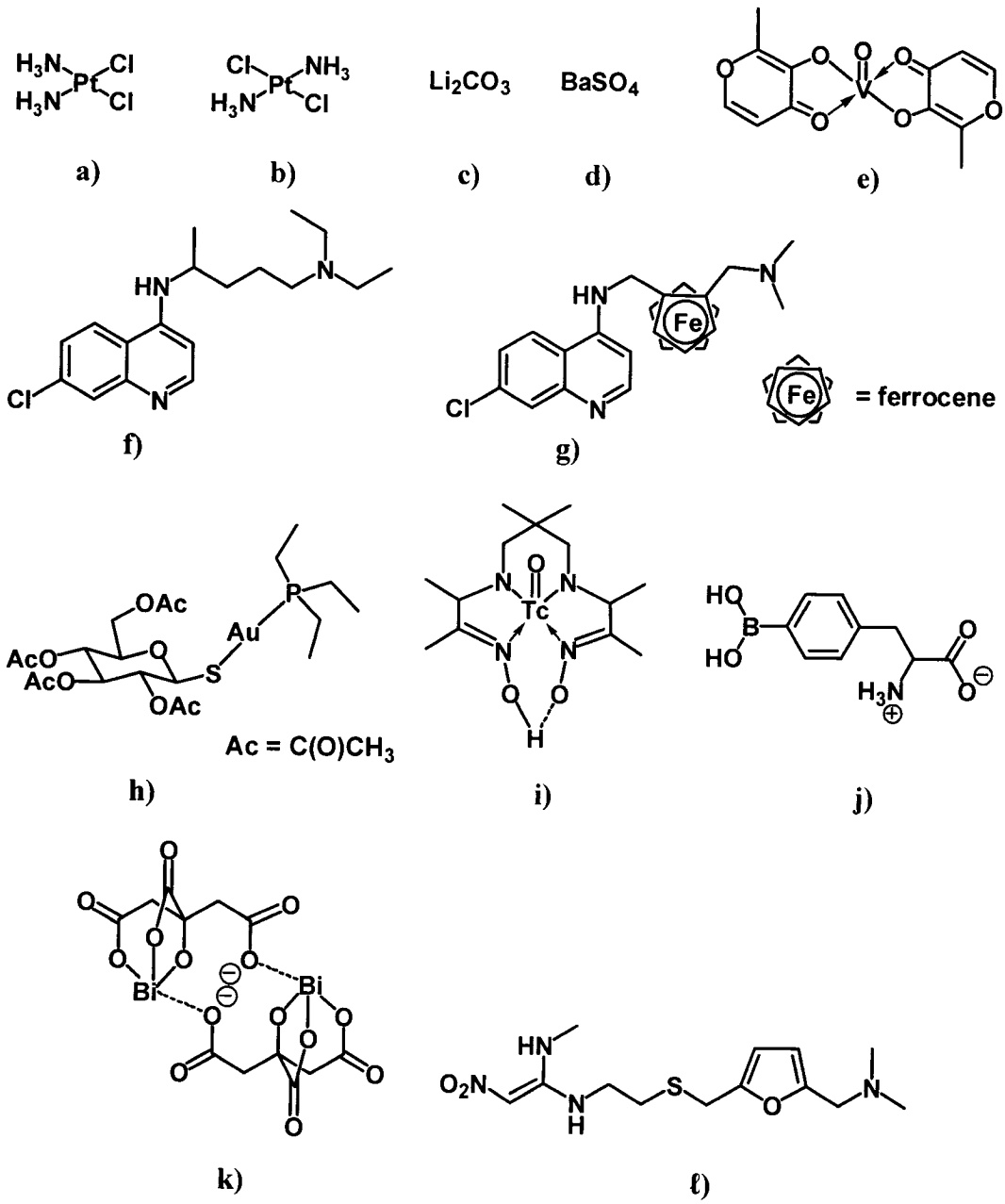

1.1.1 Biologically Relevant Molecules

It is well-established that there are four main types of macromolecules found in the cells of living systems, namely, proteins, carbohydrates, nucleic acids, and lipids. Because all of these molecules are in some way essential to a properly functioning biological system, it is reasonable that such compounds, and components of such compounds, be considered biologically relevant. Many other endogenous molecules (e.g., metabolites, and even

H_2O) are also biologically important but will not be discussed herein. For molecules endogenous to living organisms, a shorter classification term, biomolecule, may be used.

Composed of unique arrangements of different amino acid monomers, proteins are involved in many critical biological processes, ranging from the selective movement of small molecules to catalysis of biological reactions.[64] Both bacterial[65] and human proteins[66] are known to bind bismuth, and the interaction of bismuth with cysteine, a biologically important thiol, is considered to be the most likely route for the bioactivity of bismuth. A chiral carbon atom is present in all amino acids (excluding glycine); therefore, it is possible for these structures to exist in either a D- or L-stereochemical configuration. It is interesting to note that the amino acids found in biological proteins are present as L-enantiomers, and a definitive explanation for this biological preference, though explored, has not yet been established.[64;67] Figure 1.2 shows twenty common amino acids as Fisher projections of the L-enantiomers of these compounds at physiological pH (7.4). Other amino acids are known, including homocysteine, which is involved in the biosynthesis of methionine.[68] Bismuth has been shown to form gas phase complexes with seven amino acids and a number of different peptides.[13;16-18;69] Described in Chapter 5 are new results revealing that bismuth complex ions containing any of eight other amino acids can be generated in the presence of thiol-containing, cysteine.[70]

The carbohydrate class of biological molecules includes polysaccharides, which are chains of monosaccharides (sugars) linked together by glycosidic bonds.[71] Complexes of bismuth and other metals with common sugars (e.g., D-glucose, D-fructose) are described in Chapter 2. Nucleic acids are also important biological molecules, involved in the storage and replication of heritable biological information.[72] The interactions of bismuth with nucleobases are discussed in Chapter 3. Lipids play a variety of roles in biological systems; however, they are mainly concentrated in cell and other membranes to serve as part of a selective system that determines which direction across a membrane other molecules will be granted access.[73] The chemistry of lipids with bismuth and other metals is beyond the scope of this thesis.

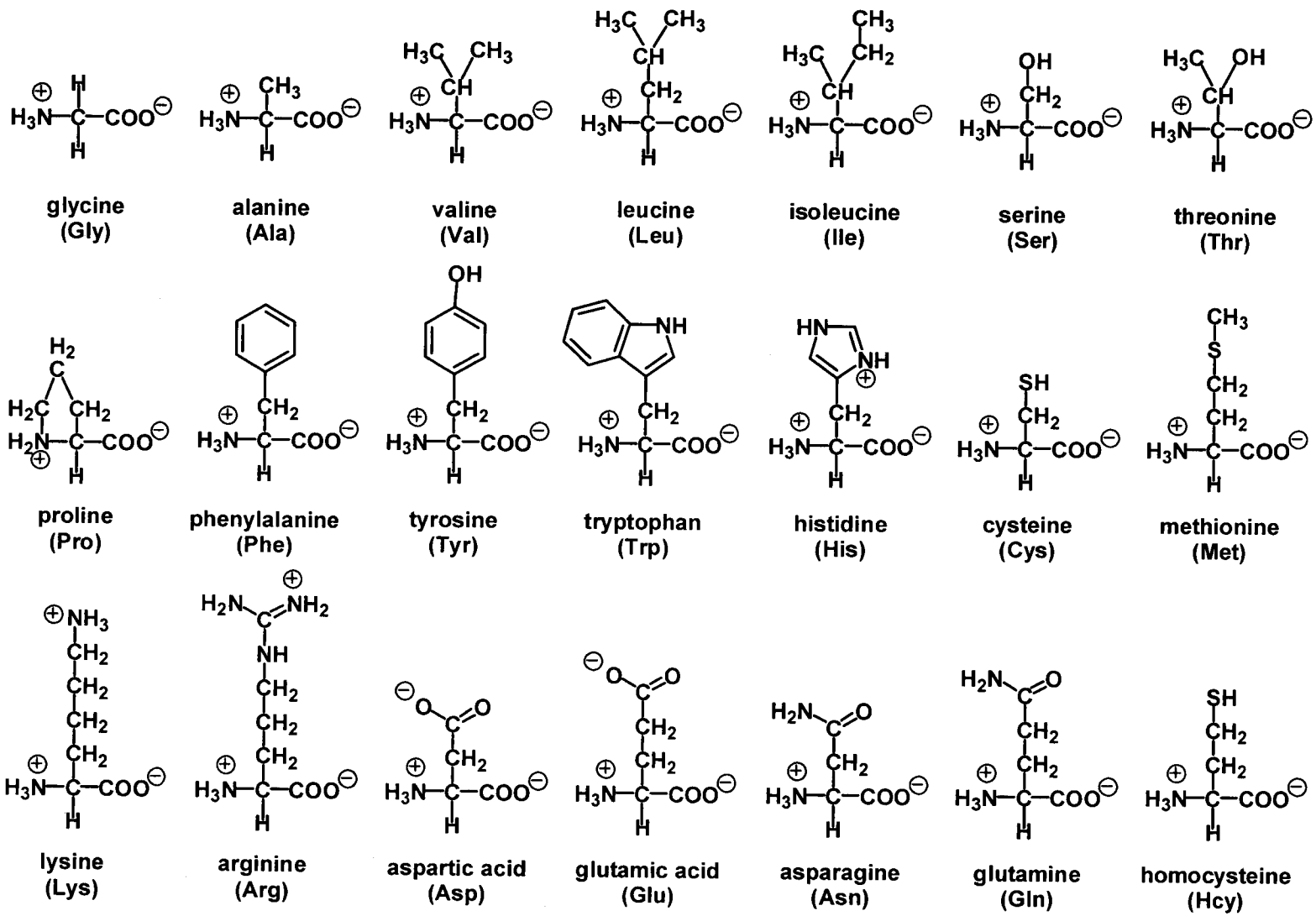

Figure 1.2 Homocysteine and twenty common amino acids present in biological proteins.

Given that biological systems are chemically sophisticated, it is important to design scientific experiments that are not overly complex, and that aim to yield unambiguous results. With this in mind, at times it may be useful to employ a small, relatively simple molecule, containing a particular functional group to represent a larger, more complex biological molecule. In such a case, the smaller molecule will not necessarily be present in any biological system (and therefore is not technically a biomolecule) but it is nevertheless expected to be helpful or interesting as a model species, and it is important that it be considered biologically relevant. A variety of non-endogenous biologically relevant molecules are shown in Figure 1.3.

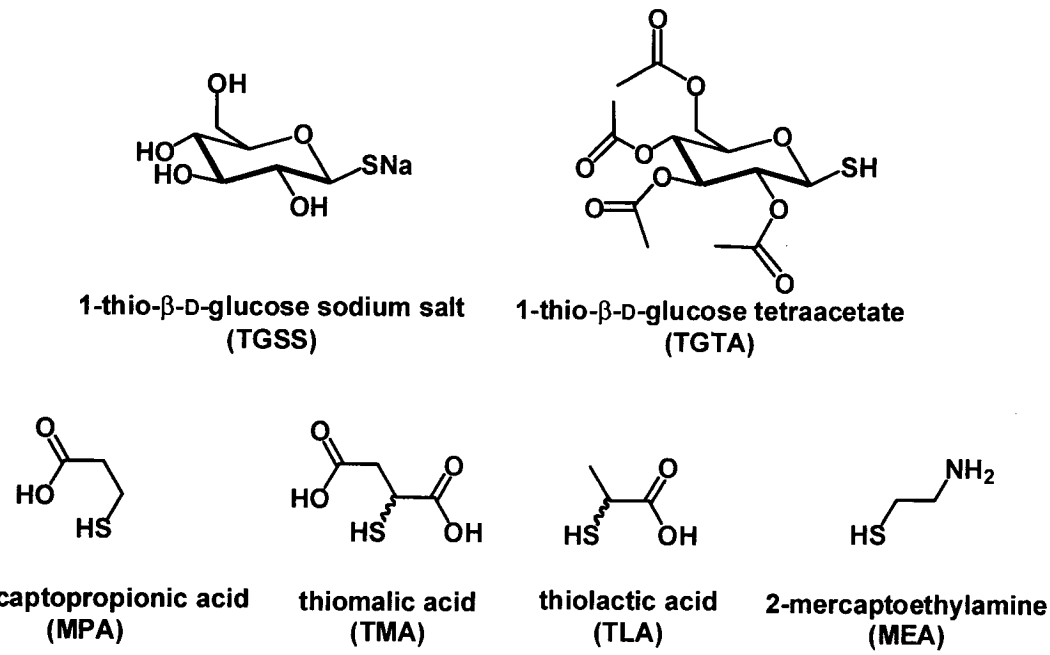

Figure 1.3 Non-endogenous biological molecules examined in this thesis.

For the purposes of this report, the term 'biologically relevant molecule' will refer not only to molecules such as amino acids that are normally present in biological systems, but also to other organic molecules with specific and biologically significant functional groups. For instance, both cysteine (Cys) and the structural analogue, 3-mercaptopropionic acid (MPA), can be considered biologically relevant (Figure 1.4). As mentioned above, Cys is a well-known amino acid found in the majority of human proteins. Although MPA is not endogenous to living systems, it can be viewed as an

amine-free model of Cys. Given the structural relationship between the two compounds, an investigation of both Cys and MPA as ligands may potentially shed more light on the fundamental chemistry of bismuth compared to examining Cys only (see Chapters 5, 6).

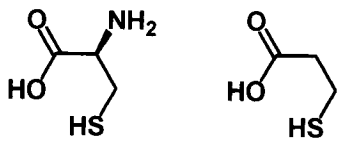

Figure 1.4 Examples of biologically relevant molecules, L-cysteine (Cys) and 3-mercaptopropionic acid (MPA).

1.2 Medicinal Bismuth Chemistry

Many medicinal inorganic compounds have had a long record of use,[38] and those of bismuth have played a role in a variety of medicinal applications over the last two and a half centuries.[2] During this time period, bismuth-containing compounds have been employed against a wide range of health afflictions, including high blood pressure, syphilis, infections and as wound dressings, persistent nasal mucous membrane inflammation, and most often GI disorders.[1;a;b]

As mentioned previously, three main bismuth preparations (BSS, CBS, and RBC) are used extensively for the relief of pain and discomfort associated with GI ailments. One of these treatments is Pepto-Bismol®, containing the active ingredient BSS and intended for use in cases of diarrhea and dyspepsia. The latter term refers to central upper abdominal irritation or pain which initiates in the upper GI region of the body.[76] A second well-known bismuth-based remedy is De-Nol®, which contains CBS and is active against peptic ulcers.[1;25] A third bismuth drug of interest is RBC, which offers a two-in-one

---

[a] ^{212}Bi has a half-life of one hour and has been employed in cancer radiotherapy.[1] Bismuth was once thought to have the highest atomic number, 83, for elements with at least one naturally occurring stable isotope; however, it is now known that ^{209}Bi has a half-life of ca. 2×10^{19} years.[74]

[b] Specifically, gastroenterology is the study of the human alimentary system, including within its boundaries the biological machinery involved in functions from ingestion and digestion, to nutrient absorption and waste elimination. The GI tract is considered to include the esophagus, stomach and intestine.[75]

antisecretory and anti-*H. pylori* treatment.[77] RBC is an amorphous solid, generated by combining bismuth citrate and ranitidine,[7] an organic compound (Figure 1.1ℓ) which is known to reduce acid production by gastric epithelium cells. It is worth noting that GI soreness and discomfort are in some cases attributed to ulcers, reflux disorders, or even gastric cancer. In other situations, designated 'non-ulcer' or 'functional' dyspepsia, it is very difficult to ascribe the symptoms of a patient to a particular syndrome.[78]

Although bismuth compounds including BSS and CBS possess considerable healing potential, the details of the chemistry by which this element exerts a biological effect have not been fully explained. In order to shed light on the route(s) by which medicinal bismuth compounds are effective against GI afflictions, it is worthwhile to further discuss *H. pylori*, which is currently considered a major cause of GI illnesses.[76;77;79;80]

1.2.1 Helicobacter pylori

H. pylori is a species of bacteria found in the majority of human stomachs[81;82] and recognized since the early 1980s as a cause of GI disorders.[10;83;84] The organism is remarkably resilient to acidic conditions in the stomach and can thrive for over ten years in this environment.[85] The treatment of *H. pylori* with either antibiotics or bismuth alone leads in both cases to low rates of successful elimination of the bacterium. Although drug resistance or undesirable side effects remain possibilities, symptoms of an *H. pylori* infection can be best treated with a combination of drugs. Two antibiotics, clarithromycin and amoxicillin[86] (or metronidazole), are commonly administered to patients along with a proton pump inhibitor (e.g., omeprazole) for at least seven days.[87;88] Due to the antisecretory effects of ranitidine bismuth citrate, this substance is in some cases substituted for the proton pump inhibitor.[88] This type of regime is known as triple therapy, and it is mostly successful in eradicating *H. pylori*. In some instances, a secondary treatment option, quadruple therapy, is applied, in which bismuth subsalicylate or subcitrate is combined with metronidazole and tetracycline antibiotics.[88] Hence, bismuth-containing drugs are an important feature of *H. pylori* treatment and the treatment of various other gastrointestinal disorders.

The negative impact of *H. pylori* on humans arises from a number of factors which affect mucous membranes in the human stomach. Due to its coiled shape and flagella (tail-like appendages), the gram-negative bacterium can essentially drill into and damage cell membranes.[1] The biological effects of *H. pylori* may also stem from the release of two enzymes, catalase and urease. Catalase inhibits the natural immune response of the human body to invading species, while urease assists in the generation of ammonia (Figure 1.5). Ammonia not only protects the bacterium from surrounding gastric acid, but it is also poisonous to human cells.[1] In general, *H. pylori* has the ability to fasten itself to the lining of the stomach, thereby preventing the bacterium from succumbing to the surrounding acid or being displaced from the stomach entirely.[89]

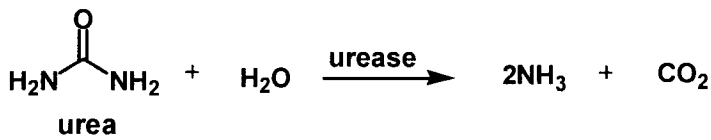

Figure 1.5 Ammonia is generated from urea in the presence of urease enzyme.

Bismuth inhibits urease and other enzymes produced by *H. pylori*, hampering normal enzyme operations of the bacterium.[1] A number of urease enzymes from different species have been characterized, all of which possess similar arrangements of amino acids and contain two nickel cations at the location of catalytic activity. 2-Mercaptoethanol ($HSCH_2CH_2OH$) interferes with urease from microorganism, *Bacillus pasteurii*, by coordinating to the Ni(II) ions in the active site of the enzyme.[90] Notably, bismuth-2-mercaptoethanol coordination complexes are more active against *H. pylori* urease than free 2-mercaptoethanol.[1;91]

Bismuth disrupts *H. pylori* alcohol dehydrogenase (ADH) by preventing the generation of acetaldehyde which otherwise damages human mucosal cells. A Zn(II) cation resides in the active site of the ADH enzyme in the presence of two cysteine residues, one histidine residue, and one molecule of water. Another Zn(II) ion plays a structural role in ADH and is coordinated by sulfur from four cysteine units. Given the affinity of bismuth for coordination by thiolate ligands, it is most likely the Zn(II) ion found in the tetrathiolate

binding region of ADH that is substituted by Bi(III).[1] Colloidal bismuth subcitrate has been suggested to counter the effects of *H. pylori* by strengthening mucous in the gastric environment and by promoting chemical mechanisms of human cell protection.[2] CBS may interfere with *H. pylori* enzymes such as phospholipase A2, important in the production of fatty acids,[92] and in which Bi(III) likely replaces endogenous Ca(II).[1] Another bacterial enzyme affected by bismuth subcitrate is F_1-adenosine triphosphate synthase. Without this enzyme, normal bacterial energy metabolism is hindered.[1] The antibacterial nature of various other bismuth compounds has also been documented.[91;93]

There is an interesting corollary to the *H. pylori* story. While antibiotics and bismuth-containing pharmaceuticals are promoted for reduction of the bacterium and for prevention and healing of GI disorders, studies indicate that *H. pylori* may actually have positive health effects that are concurrently on the decline. In developed countries, the incidence of ulcers and gastric cancer, along with *H. pylori* levels, has decreased significantly over the last century due to enhanced personal health practices and the use of antibiotics. Unfortunately serious esophageal problems, including gastroesophageal (acid) reflux disease (GERD) and cancer of this organ, are simultaneously increasing. The decreased risk of GI ailments and the increased prevalence of esophageal illnesses may be connected. Given that *H. pylori* is known to control acid levels within its surroundings (e.g., within the human stomach), it is postulated that the bacterium may actually defend humans against GERD and related diseases.[94] In an assessment of literature on both bacterial and drug-induced origins of GERD, a recent report states that exposure to either entity may aggravate but likely does not cause GERD.[95]

The complex dynamics of the relationship between *H. pylori*, GI disorders, and bismuth chemistry are far from understood; however, the interference of bismuth compounds with bacterial enzyme functions is significant. A complete elucidation of the details of this medicinal issue will certainly require a multifaceted approach, involving the time and resources of scientists with expertise in various fields of knowledge.

1.2.2 Medicinal Bismuth Complexes

Structures of bismuth-containing pharmaceuticals, BSS, CBS, and RBC, have not yet been unambiguously determined. Due to the insolubility of BSS in water and other solvents, neither solution state nor solid state data other than the experimental formula has been obtained for this compound. The experimental formula of BSS has been established as $BiC_7H_5O_4$ by elemental analysis, and a proposed structure (Figure 1.6a) includes the salicylate functionality which contributes to the name of the compound, also known as a 2-hydroxybenzoic acid bismuth(III) salt.[96] To learn more about bismuth-salicylate interactions, a number of bismuth-salicylate,[32;97;98] -alkoxybenzoate,[99;100] and -thiosalicylate[25;101] solid state structures have been prepared, including several which contain bismuth and other metals (e.g., Ti, Ni, Cu, Nb, Ta, Al).[102-106] A crystallographically characterized bismuth-salicylate compound that does not contain other metals or other non-salicylate ligands has yet to be reported.

In terms of citric acid as a ligand for bismuth, a considerable number of solid state structures are referred to as CBS.[31;107-113] Each structure is slightly different from the others; however, more than one of these structures contain the dianionic dimer, $Bi_2(C_6H_4O_7)_2^{2-}$ (Figure 1.6b), where $(C_6H_4O_7)^{4-}$ is the tetradeprotonated conjugate base of citric acid. It is likely that the extended, often polymeric, and labile interactions of bismuth with citrate in solution have thus far prevented the establishment of a single solid state arrangement of atoms for CBS. For the same reasons, the structure of CBS in solution is not understood; however, the formation of CBS appears to be pH-dependent. Increasing the pH of a mixture of insoluble bismuth citrate ($BiC_6H_5O_7$) in water allows bismuth to be solubilized as CBS.[2] The solubility of CBS is a unique property, considering that bismuth compounds are insoluble in most solvents.

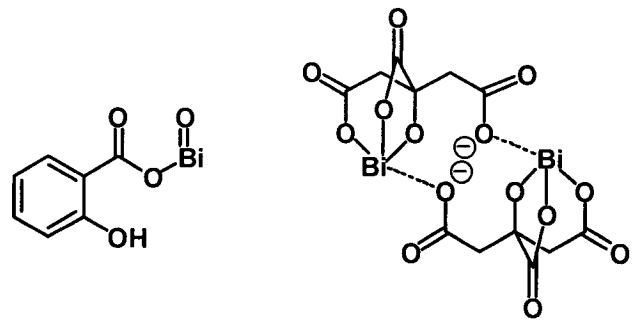

a) b)

Figure 1.6 Structural representations of medicinal bismuth compounds. a) The structure of bismuth subsalicylate is based on the experimental formula known for this compound. b) The $[Bi_2(C_6H_4O_7)_2]_2^-$ anion is common to a number of solid state structures characterized as colloidal bismuth subcitrate.

Given that the structures proposed for CBS and BSS possess multiple bismuth-oxygen bonds, the reactivity of bismuth salts with other oxygen-containing ligands has also been investigated. A number of solid state structures are known to contain bismuth coordinated by the conjugate bases of hydroxycarboxylic acids, including succinic,[28] malic,[28;114] tartaric,[114;115] lactic,[116] and oxalic acids.[117-120] Other methods of analysis including ^{13}C NMR spectroscopy were also used to identify a 1:1 complex of Bi(III) and D-gluconic acid.[121] A variety of hydroxycarboxylic acid ligands are shown in Figure 1.7. In general, refined synthetic and characterization strategies are still needed to better understand the structures of biologically relevant bismuth-oxygen complexes.

Given that CBS is known for its capacity as an antibacterial and mucous membrane fortification agent, bismuth(III) citrate has been combined with ranitidine and clinically investigated in an effort to produce a medicinal preparation providing the beneficial effects of both compounds. RBC is also soluble in water.[122] The structure of RBC has not been fully characterized; however, it is known to be polymeric as a result of bismuth-citrate bonding, hydrogen bonding, and interactions between bismuth(III) citrate and protonated dimethylamine in ranitidine.[122] Recently, RBC and other bismuth compounds have been reported to diminish the adenosine triphosphatase activity of a helicase protein associated with the severe acute respiratory syndrome (SARS) coronavirus.[123]

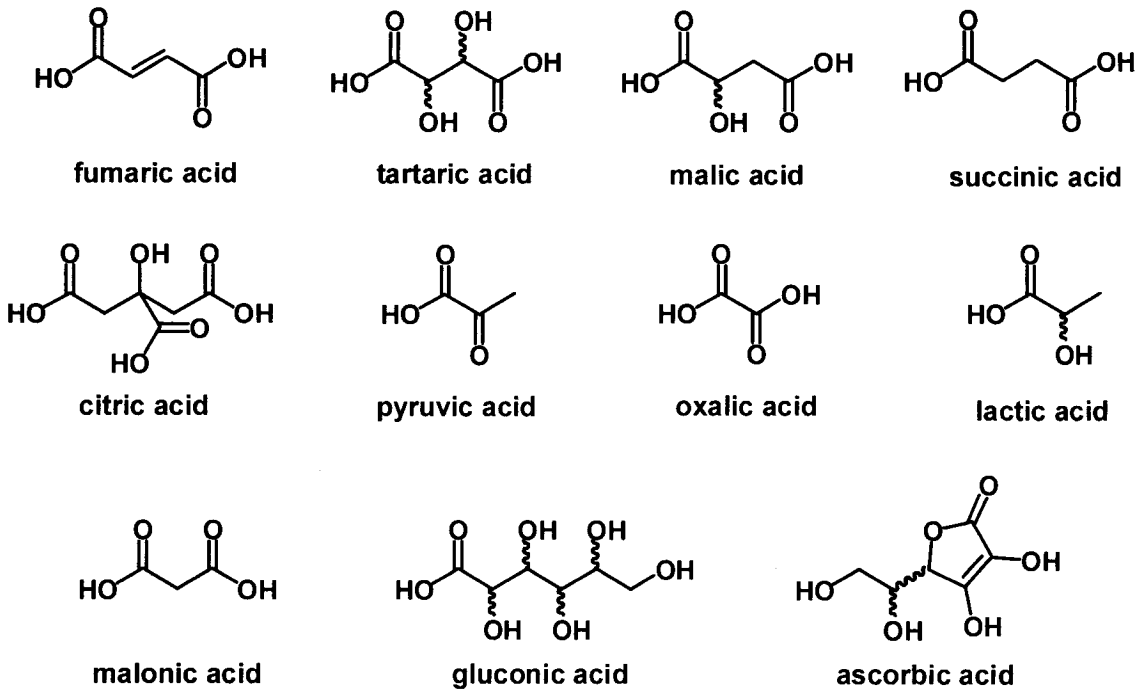

Figure 1.7 Hydroxycarboxylic acid ligands as models for BSS or CBS.

1.3 Bismuth-Thiolate Complexes

With respect to bismuth and other metals, the term thiophilicity (thiophilic = sulfur-loving) denotes the experimentally observed[12] tendency of some metals to readily form bonds with sulfur. Thiophilicity has also been defined as the nucleophilicity of a thiolate;[124] however, the former definition will be applied herein. A quantitative measure of the strength of a Bi-S bond is the bond dissociation energy, 315.5 ± 4.6 kJ/mol (298 K). One way to understand why the coordination of sulfur to bismuth is favourable is to consider these two elements in terms of the well-known Hard and Soft Acids and Bases system of classification.[125;126] Relatively small, moderately polarizable 'hard' Lewis bases (e.g., NH_3, O^{2-}, F^-) generally coordinate to 'hard' Lewis acids (e.g., H^+, BF_3, Sn^{4+}) with similar properties. Likewise, coordination is generally observed between relatively large, polarizable 'soft' Lewis bases (e.g., PR_3, I^-, RS^-) and 'soft' Lewis acids (e.g., $GaCl_3$, Hg^{2+}, Tl^+). Polarizability is a qualitative descriptor of the extent of attraction or repulsion of electrons in the presence of other atoms or molecules.[127] Thiols, thiolates and thioethers are considered to be soft bases, which bond effectively to bismuth(III), a borderline acid[126] due the large size, moderate electronegativity (1.9),[128] and relatively

high oxidation state of this metal ion. Due to the soft properties of Bi(III) and RSH, RS^-, or R_2S, bonds of a covalent nature are formed, enhanced by electrostatic attraction in the case of bismuth-thiolate bonding.

Typically the gap between the highest occupied and lowest unoccupied molecular orbitals is smaller for soft-soft interactions and larger for hard-hard interactions.[127] Up to three 3p-6p bismuth-thiolate σ bonds can be formed at one bismuth centre. Due to polarization of the Bi-S bonding electrons toward sulfur (electronegativity = 2.5),[128] the Lewis acidity of the bismuth centre is enhanced. Because bismuth can also accommodate a coordination number of up to ten,[1] subsequent coordination or chelation of ligands to $Bi(SR)_3$ is understood to occur by donation of electron density into an empty bismuth-thiolate σ^* orbital.[129]

The mode of action of bismuth pharmaceuticals most likely involves the interaction of bismuth with one or more thiolate groups in gastrointestinal peptides or proteins. These biological molecules contain numerous other functional groups; therefore, bismuth may be coordinated both by sulfur and/or other heteroatoms. Given the strength of bismuth-sulfur bonds with respect to cleavage under hydrolytic conditions and at high temperatures,[12] many initial studies of bismuth complexes have not thoroughly explored the properties of bismuth systems containing weaker, non-sulfur donor atoms. Consequently, emphasis has recently been placed on the chemistry of bismuth in the presence of heterobifunctional thiolates in addition to multi-thiolate ligands.

From a chemical perspective, discrete dithiolate complexes of bismuth can actually be more challenging to examine compared to those containing heterobifunctional thiolates. Ligands in which sulfur is the only donor atom (e.g., 1,2-ethanedithiol: $HSCH_2CH_2SH$) tend to form numerous bismuth-sulfur bonds readily, leading to multiple ligands coordinated to bismuth even if the starting bismuth:ligand stoichiometry is 1:1. In addition, the solubility of bismuth-thiolate compounds is often low, impeding solution analysis.[27] Employing a coordinating solvent can improve solubility; however, the coordination of solvent molecules to bismuth is not necessarily reversible, nor

biologically significant. As a result, the structures of bismuth-thiolate compounds in the presence of donor solvents may be inherently altered, thereby inhibiting the characterization of desired bismuth-thiolate species.

In a heterobifunctional ligand, the coordination of a non-thiolate donor atom to bismuth is assisted by the strong interaction between bismuth and sulfur which secures the ligand to the metal. Chelation of a heterobifunctional ligand to bismuth can actually prevent more bismuth-sulfur bonds from forming at the same bismuth centre; therefore, the synthesis of bismuth compounds containing heterobifunctional thiolate ligands typically allows for better control of product stoichiometry compared to reactions involving dithiolate donors only.

1.3.1 Bismuth-Thiolate Complexes with Heterobifunctional Ligands

The selective preparation and characterization of heterobifunctional bismuth-thiolate complexes with bismuth:ligand ratios of 1:1, 1:2, and 1:3 has been achieved, as illustrated in Figure 1.8.[23;27] The ability of a weaker oxygen or nitrogen donor atom to chelate to bismuth once the bismuth-sulfur anchor is established also improves solubility of the bismuth complex without requiring an additional solubilizing agent.[21] The improved solubility of bismuth compounds having desired metal:ligand stoichiometries can also be expected to better facilitate crystallization processes and solution analyses.

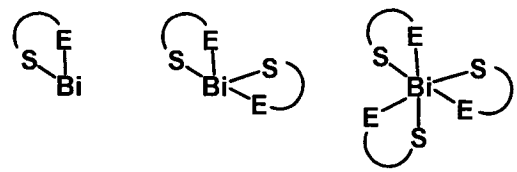

Figure 1.8 A consecutive series of ligand arrangements known for various heterobifunctional thiolates coordinated to bismuth (E = OCOR, OH, NR_2, where R = alkyl or H).

Other studies have revealed that not only dithiolate[20] but also heterobifunctional thiolate ligands[21;23;24;27] can coordinate to bismuth in a variety of ways. For instance, structural drawings of some of the first-characterized solid state bismuth-esterthiolate compounds

are shown in Figure 1.9. In all three bismuth-thioglycolate complexes, esterthiolate ligands chelate to bismuth via sulfur and oxygen.[27] The compound shown in Figure 1.9a exhibits two modes of coordination: bidentate chelation to a single bismuth atom, and tethering between two bismuth atoms. Specifically, two esterthiolate ligands coordinate through sulfur and oxygen to each bismuth centre, while two other esterthiolate ligands link the two bismuth atoms such that coordination occurs to each bismuth via only one heteroatom (S or O).[24;27] In this dimer of tri(methylthioglycolate) bismuth(III), a distorted facial thiolate geometry exists at each hexacoordinate bismuth atom. This structure can be compared to the $Bi_2(C_6H_4O_7)_2^{2-}$ dimer (Figure 1.6b), found in a number of different crystalline structures identified as CBS, in which the association between two bismuth atoms occurs through two tethering citrate tetraanions.

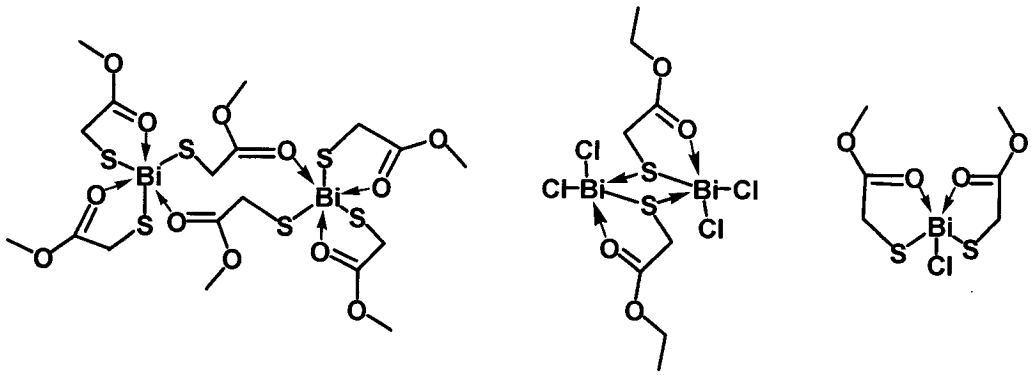

Figure 1.9 Bismuth-esterthiolate compounds. a) Dimer of tri(methylthioglycolate) bismuth(III), b) dimer of dichloro(ethylthioglycolate) bismuth(III), and c) chlorodi(methylthioglycolate) bismuth(III).

Single crystals of two other bismuth-thioglycolate compounds (Figure 1.9b, c) were obtained for XRD analysis from reactions of bismuth(III) chloride with methylthioglycolate (MTG) in molar ratios of 1:1 and 1:2. Like the 1:3 Bi:MTG structure in Figure 1.9a, the dichloro(ethylthioglycolate) bismuth(III) structure in Figure 1.9b is also a dimer in the solid state, containing μ-thiolate units that link the two bismuth atoms, each of which is pentacoordinate. The resulting geometry at bismuth can be described as a distorted square pyramid. The 1:2 Bi:MTG compound (Figure 1.9c) is polymeric due to intermolecular interactions. In the full structure of the 1:2 Bi:MTG complex, bismuth is

heptacoordinate and interacts with two sulfur atoms from ligands on neighbouring bismuth atoms, in addition to the five bismuth-element interactions shown.

Further examination of the three structures in Figure 1.9 reveals that it is the carbonyl oxygen atoms in the thioglycolate ligands that coordinate to bismuth. Due to the relatively low basicity of an ester carbonyl oxygen atom compared to donor atoms in other non-thiolate functional groups ($CO_2^- \sim NR_2 > OH > COOR$), $Bi\text{-}O_{carbonyl}$ bonds are not common; however, it is of interest to note that $Bi\text{-}O_{carbonyl}$ bonding also occurs in the bismuth citrate dimer that is common to solid state structures of CBS (Figure 1.6b).[27] The $Bi\text{-}O_{carbonyl}$ bonds in CBS range in length from 2.4 to 2.6 Å, while typical $Bi\text{-}O_{carbonyl}$ bond distances have lengths of 2.31 to 2.46 Å. In the esterthiolate structures shown in Figure 1.9, the $Bi\text{-}O_{carbonyl}$ bond lengths are between 2.56 to 2.86 Å for the chelating ligands, while the $Bi\text{-}O_{carbonyl}$ bond involved in the tethering ligand (Figure 1.9a) has a length of 3.07 Å. The relatively long $Bi\text{-}O_{carbonyl}$ bonds in the esterthiolate complexes may be a consequence of the stronger bismuth-sulfur interactions that are also present.[27]

Supporting information for the structures illustrated in Figure 1.9 was gained from infrared (IR) radiation and Raman spectroscopy, as well as mass spectrometry. A variety of ionization methods, including ESI-MS, were used to identify gas phase ions with bismuth:thioglycolate ratios including 1:1, 1:2, and 1:3.[27] Comparable to the solid state structures discussed above, interactions of bismuth with both MTG and ETG were observed upon examination of solution reaction mixtures by way of ESI-MS.

It is important to reiterate that neutral ethylthioglycolate (ETG) was not initially reacted with bismuth(III) chloride; however, transesterification has been proposed to yield ETG ions in solution. Therefore, persistence of the ETG ligand in the gas phase within the mass spectrometer is not unexpected. Figure 1.10 illustrates the mechanism proposed for the quantitative conversion of a 1:1 stoichiometric mixture of bismuth(III) chloride and MTG, in the presence of absolute ethanol, to dichloro(ethylthioglycolate) bismuth(III), methanol, and hydrochloric acid. The equilibrium constant for transesterification is approximately one; therefore, the presence of excess ethanol propels the reaction towards

the products observed. In summary, when a 1:2 ratio of bismuth(III) chloride and MTG was prepared, both MTG and ETG products were observed. In the case of a 1:3:3 ratio of bismuth(III) chloride, MTG and potassium hydroxide, bismuth instead underwent thiolation as a result of potassium chloride metathesis, and only MTG products were identified.

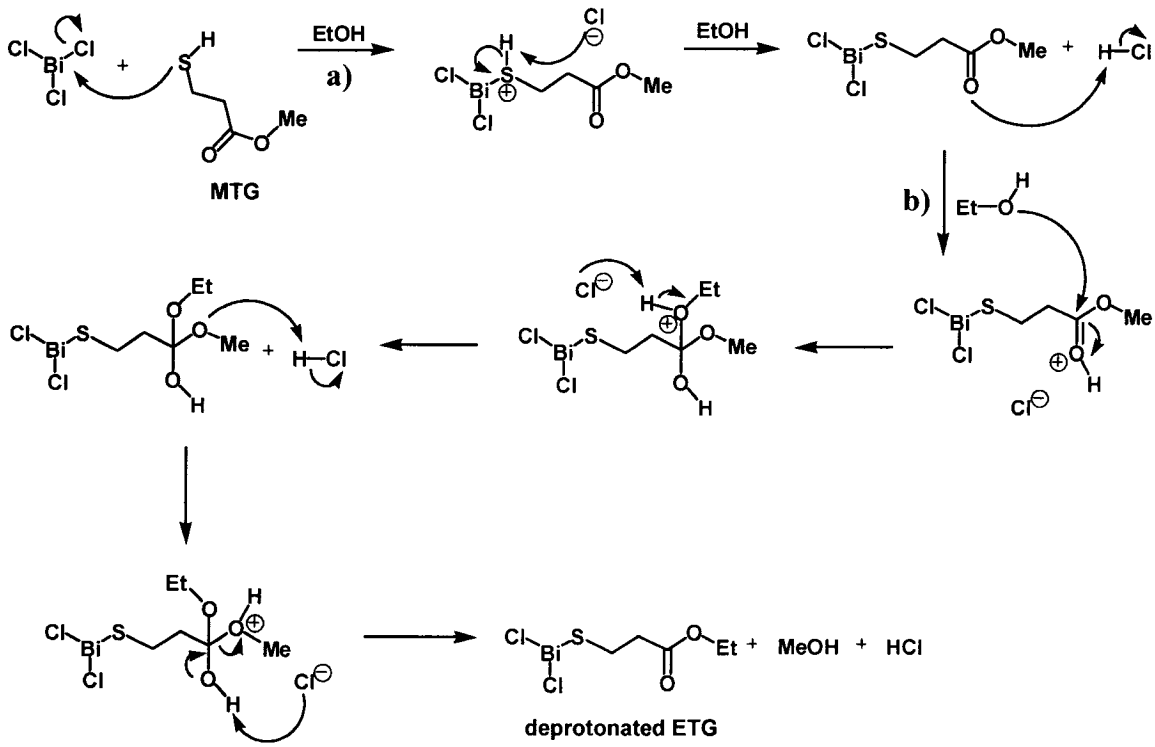

Figure 1.10 Proposed mechanism yielding dichloro(ethylthioglycolate) bismuth(III). a) A metathesis reaction produces bismuth dichloro(methylthioglycolate) and hydrochloric acid, followed by b) transesterification in the presence of hydrochloric acid and solvent ethanol.

Building on what is already known about bismuth coordination chemistry, solutions containing bismuth(III) chloride and the heterobifunctional methylthioglycolate ligand were prepared and carefully manipulated to reveal interesting structural features of bismuth-esterthiolate coordination complexes. Bismuth:thioglycolate ratios of 1:1, 1:2 and 1:3 were observed in the solid state, and a variety of coordination numbers and geometries for bismuth were recorded. Numerous gas phase bismuth-esterthiolate interactions were also identified through the use of ESI-MS. The latter results validate the

usefulness of the ESI technique in bringing to light new details that are significant to advancing the study of bismuth-thiolate chemistry.[27]

Analogous to salicylic acid (SA) – the conjugate base of which is thought to play an important role in bismuth pharmaceutical, BSS – thiosalicylic acid (TSA) is an example of a heterobifunctional thiol that has been studied as a ligand for Bi(III). Using ESI-MS, interactions have been observed between bismuth(III) chloride and each of TSA, methylthiosalicylate (MTS), and potassium methylthiosalicylate (KMTS) (Figure 1.11).[25]

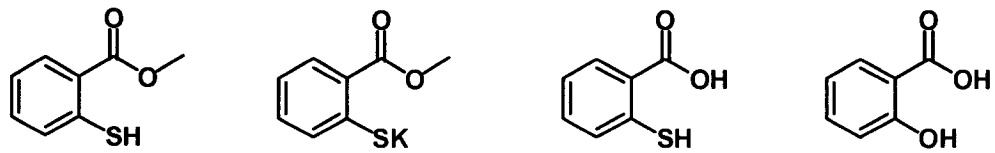

Figure 1.11 Salicylate ligands for bismuth. a) Methylthiosalicylate (MTS), b) potassium methylthiosalicylate (KMTS), c) thiosalicylic acid (TSA), and d) salicylic acid (SA).

Complex ions with stoichiometric ratios of 1:2 Bi:MTS, 1:3:1 Bi:MTS:K, 1:3:1 Bi:MTS:Na, 1:1 Bi:TSA, and 1:2 Bi:TSA were observed. Specifically, from a reaction mixture of $BiCl_3$ and KMTS the base peak observed at *m/z* 543 was assigned to $[Bi(KMTS)_2\text{-}2K]^+$, in which the loss of two potassium ions (-2K) is understood to generate a monocation. Peaks at *m/z* 733 and *m/z* 749 were assigned to cations, $[BiNa(MTS)_3\text{-}3H]^+$ and $[Bi(KMTS)(MTS)_2\text{-}2H]^+$, respectively. Peaks at *m/z* 543 and *m/z* 733 were also observed when $BiCl_3$ was combined with MTS instead of KMTS. $BiCl_3$ in the presence of TSA produced complex ions, $[Bi(TSA)\text{-}2H]^+$ and $[Bi(TSA)_2\text{-}2H]^+$, at *m/z* 361 and *m/z* 515, respectively.[25] All reported bismuth-thiosalicylate assignments were supported by tandem mass spectrometry. For example, the 1:2 Bi:TSA complex ion corresponding to *m/z* 515 underwent collision-induced dissociation (CID) to yield 1:1 Bi:TSA, represented by *m/z* 361 (Figure 1.12).

Two bismuth-thiosalicylate solid state structures have been documented, one of which is a cluster of eight Bi(III) ions, twelve doubly deprotonated thiosalicylate ligands, and twelve neutral molecules of N,N-dimethylformamide (DMF) (Figure 1.13a).[101] The other

structure is a dimer (2:6 Bi:MTS) in which the sulfur atoms in two of six MTS ligands act as μ-thiolate bridges between two bismuth atoms (Figure 1.13b).[25] The latter structure complements the ESI-MS data discussed above, from which the formation of ionic 1:3 Bi:MTS species were also verified.

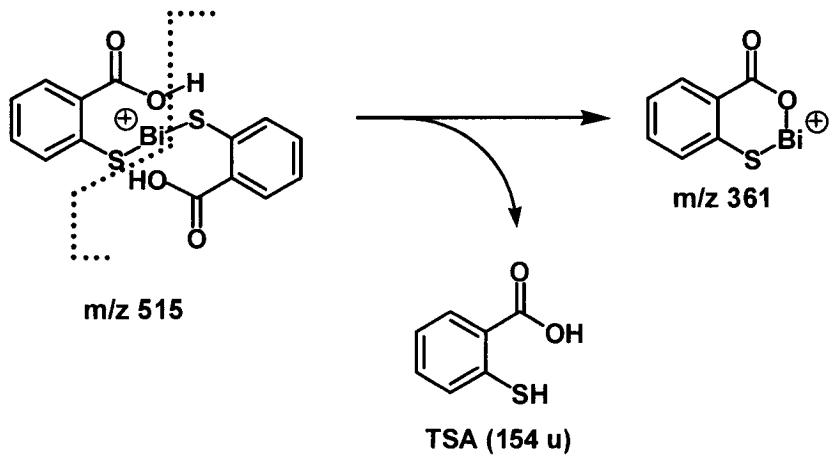

Figure 1.12 Collision-induced dissociation of a 1:2 bismuth:thiosalicylate ion, $[Bi(TSA)_2\text{-}2H]^+$. Concomitant with a neutral loss of TSA, a 1:1 bismuth:thiosalicylate product ion, $[Bi(TSA)\text{-}2H]^+$, is generated.

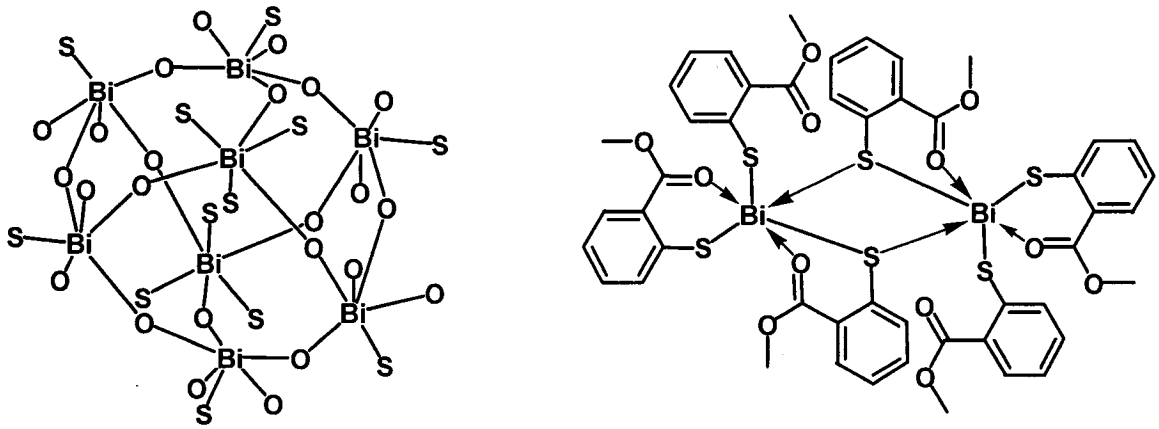

a) b)

Figure 1.13 Bismuth-thiosalicylate compounds characterized in the solid state. a) Shown is the $Bi_8O_{24}S_{12}$ core of dodecathiosalicylate bismuth(III). The oxygen and sulfur atoms are provided by twelve thiosalicylate dianions (twelve DMF solvent molecules are not shown). b) Structural drawing of a solid state dimer of tri(methylthiosalicylate) bismuth(III).

In summary, the use of both ESI-MS and XRD (among other techniques) has allowed for the characterization of interactions between bismuth and a selection of thiosalicylate ligands. In the complexes described above, the comparatively stable links generated between bismuth and sulfur support the formation of weaker bismuth-oxygen ligand interactions. These results highlight not only the significance of the thiophilicity of bismuth, but also draw attention to the propensity of bismuth to form cluster complexes (containing more than one bismuth atom and more than one ligand) involving citrate, salicylate, and other ligands with oxygen[130] and/or sulfur[131] donor atoms. Notably, metal-ligand clusters play an important role in a number of biological systems and medical treatments,[50;132] a fact which may also be relevant for bismuth in a biological milieu. Taken together, all of these factors have prompted further investigations into the role of bismuth-sulfur bonding, especially in the case of medicinally important ligands.

1.3.2 Heteroleptic Bismuth-Thiolate Complexes

Just as it has been possible to prepare a variety of bismuth complexes composed of one or more of the same dithiolate[20] or heterobifunctional thiolate ligands (homoleptic complexes), bismuth-thiolate complexes composed of more than one type of ligand (heteroleptic complexes) can also be generated.[26] In particular, previously reported chlorodithiolate bismuth(III) species[20] were used as reactants in the generation of the first heteroleptic bismuth-thiolate complexes.[26] A metathesis pathway has been proposed to explain the formation of these compounds and an example of this process is shown in Figure 1.14, yielding a heteroleptic dithiolate-hydroxythiolate bismuth(III) compound.

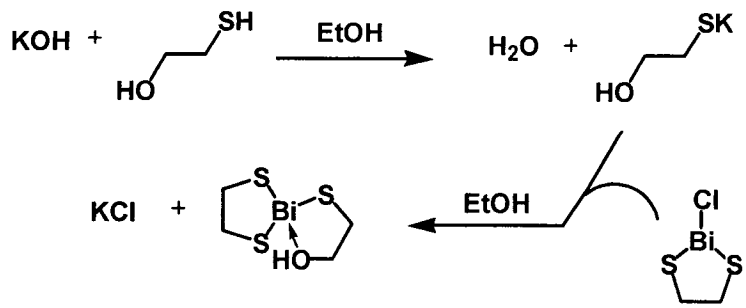

Figure 1.14 Proposed formation of a dithiolate-hydroxythiolate bismuth(III) complex.

As observed previously for homoleptic bismuth-thiolate species, in a series of heteroleptic bismuth-thiolate compounds that have been crystallographically characterized (Figure 1.15), four of the five involve coordination of all ligand donor atoms to bismuth.[26] The exception is the methylthiosalicylate bismocane structure (Figure 1.15d), in which the Bi-$O_{carbonyl}$ distance of 3.55 Å is considerably longer than that typically observed for Bi-$O_{carbonyl}$ interactions in homoleptic compounds. In comparison, the Bi-$O_{carbonyl}$ bond lengths in the aforementioned tri(methylthiosalicylate) bismuth (III) dimer (Figure 1.13b), are 2.72 Å, 2.84 Å and 3.08 Å, all of which are significantly shorter than 3.55 Å.[25] The MTS ligand in the bismocane compound (Figure 1.15d) is therefore considered non-chelating and is drawn such that oxygen is not coordinated to bismuth. In the same structure, the separation between bismuth and the thioether sulfur atom is 3.07 Å. This is longer than typical bismuth-thiol bond lengths, which are often between 2.5 and 2.6 Å; however, because bismuth-thioether interactions are not expected to be as strong as bismuth-thiolate interactions, this difference in bond lengths is reasonable. In addition, the bismocane structure contains four bismuth-sulfur bonds compared to only three bismuth-sulfur bonds per bismuth atom in tri(methylthiosalicylate) bismuth (III). As a result, the Lewis acidity at bismuth is likely too low for significant interaction with oxygen in the MTS ligand of the bismocane compound.

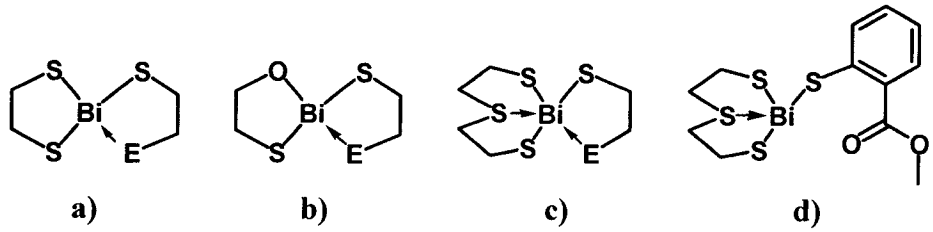

Figure 1.15 Structures of heteroleptic bismuth-thiolate complexes. a) Dithiolate and hydroxythiolate or aminothiolate ligands (E = OH, NR_2), b) hydroxythiolate and aminothiolate ligands (E = NR_2), c) dithiolate and aminothiolate ligands (E = NR_2), or d) dithiolate and thiosalicylate ligands coordinated to bismuth.

Based on the above discussion, it can be noted that bismuth-sulfur bond lengths tend to be similar in heteroleptic and homoleptic bismuth compounds. This indicates that the bismuth-sulfur interaction is not significantly dependent on other factors such as number of ligands, non-thiolate donor atoms, or intermolecular interactions present in the solid state.[26] In general, heteroleptic bismuth thiolate species can be thought of as models for

complex biological proteins which contain a variety of functional groups and are likely targets for bismuth activity. The synthesis of these model systems is a rational and significant step forward in the pursuit of well-defined synthetic strategies for the preparation of medicinally relevant bismuth compounds.

1.3.3 Bismuth-Thiolate Complexes with Amino Acids and Glutathione

To investigate the synthesis and characterization of bismuth compounds containing multifunctional ligands which are present *in vivo*, sulfur-containing molecules endogenous to the human body were considered (Figure 1.16). While examples of sulfur-based carbohydrates, nucleic acids and lipids are limited, L-cysteine (Cys) and L-methionine (Met) are two sulfur-containing amino acids found commonly in human proteins and enzymes. Cysteine is a thiol and can interact with Bi(III) by loss of a proton, thereby forming a stronger interaction than that between bismuth and methionine, a thioether, which is more sterically hindered than cysteine and which can only interact datively with bismuth. Interactions of bismuth with homocysteine (Hcy) have also been examined. This amino acid is involved in the generation of methionine by methylation in all cells.[68] In addition, cysteine forms part of glutathione (GSH), a tripeptide which also contains non-sulfur amino acids, glutamic acid and glycine. GSH exists in significant cellular concentrations (up to 10 mM) and excluding proteins, it is often found to be the most prevalent thiol in human cells.[133] These characteristics have prompted an exploration of the interactions of GSH with various metal ions, including bismuth.

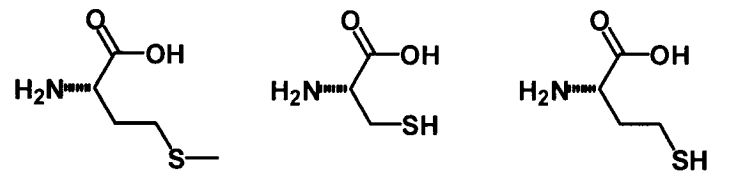

L-methionine (Met) **L-cysteine (Cys)** **L-homocysteine (Hcy)**

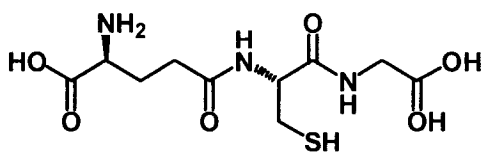

γ-L-glutamyl-L-cysteinyl-glycine

glutathione (GSH)

Figure 1.16 Sulfur-containing amino acids and tripeptide, glutathione.

ESI-MS data has been acquired for several reaction mixtures that pair the biological molecules shown in Figure 1.16 with one of three bismuth starting materials: bismuth(III) chloride, bismuth(III) nitrate, or BSS.[16;17] When any of these bismuth compounds was combined with cysteine (Cys), neither the stoichiometry nor the bismuth salt caused significant changes to the mass spectra obtained. Of particular relevance to the new work described later in this thesis (Chapters 4, 5, 6) is the fact that a number of bismuth-cysteine complexes have been identified through the use of ESI-MS. The base peak (relative intensity 100 %) at *m/z* 328 in bismuth-cysteine spectra was attributed to a 1:1 monocationic Bi:Cys species, $[Bi(Cys)\text{-}2H]^+$, in which the cysteine ligand is dianionic. A possible structure of this cation is shown in Figure 1.17a, reasonable based on the known structures of penicillaminatobismuth(III) chloride (Figure 1.17b),[134] and dinitrato(cysteinato)bismuth(III) phenanthroline (Figure 1.17c).[28]

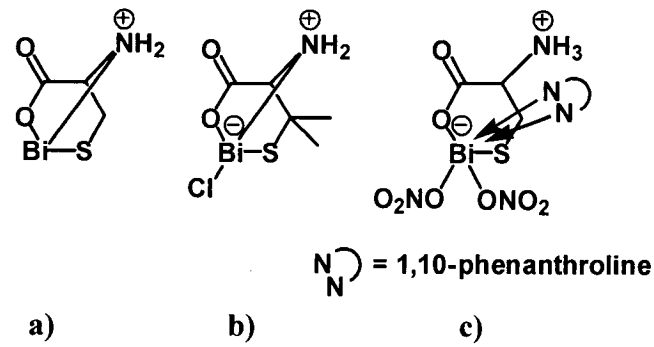

Figure 1.17 Bismuth-cysteine complexes. a) Possible structure of $[Bi(Cys)\text{-}2H]^+$ observed via ESI-MS, b) penicillaminatobismuth(III) chloride, and c) dinitrato(cysteinato)bismuth(III) phenanthroline (one molecule of water has been omitted for clarity).

Despite consensus in the literature that bismuth bioactivity likely involves the coordination of bismuth by cysteine, the structure shown in Figure 1.17c is the first and only crystallographically characterized bismuth-cysteine compound. Cysteine chelates to bismuth in a bidentate fashion through the thiolate and carboxylate functional groups. Two nitrate anions, one molecule of water, and 1,10-phenanthroline are also part of this bismuth:cysteine coordination complex. A 1:3 bismuth-cysteine compound has been characterized by X-ray powder diffraction.[135] Notably, other bismuth-cysteine cations,

$[Bi(Cys)_2\text{-}2H]^+$, $[Bi_2(Cys)_2\text{-}5H]^+$ and $[Bi_2(Cys)_3\text{-}5H]^+$, have been assigned to ESI-MS peaks at *m/z* 449, *m/z* 655, and *m/z* 776, respectively.[17]

In the case of bismuth and methionine, ESI-MS peaks corresponding to ratios of 1:1, 1:2, 2:2 and 2:3 Bi:Met were assigned: $[Bi(Met)\text{-}2H]^+$, $[Bi(Met)_2\text{-}2H]^+$, $[Bi_2(Met)_2\text{-}5H]^+$, and $[Bi_2(Met)_3\text{-}5H]^+$, respectively. In addition, sodiated 1:2 and 2:3 Bi:Met peaks were observed at *m/z* 527 and *m/z* 882.[17] When homocysteine was combined with $BiCl_3$, $Bi(NO_3)_3$, or BSS, ESI-MS peaks corresponding to 1:1, 1:2, 2:2 and 2:3 Bi:Hcy cations were observed. These peaks at *m/z* 342, *m/z* 477, *m/z* 683, and *m/z* 818 are Hcy analogues – $[Bi(Hcy)\text{-}2H]^+$, $[Bi(Hcy)_2\text{-}2H]^+$, $[Bi_2(Hcy)_2\text{-}5H]^+$, and $[Bi_2(Hcy)_3\text{-}5H]^+$ – of the 1:1, 1:2, 2:2 and 2:3 Bi:Cys and Bi:Met complexes mentioned above. All assignments were supported by tandem mass spectra. For instance, fragmentation of the 2:3 Bi:Hcy ion corresponding to *m/z* 818 yielded peaks at *m/z* 342 and *m/z* 477, assigned as the same 1:1 and 1:2 Bi:Hcy cations already discussed.[16;17]

Bismuth was also observed to form 1:1 and 1:2 complexes with GSH via ESI-MS.[16] Peaks at *m/z* 514 and *m/z* 821 were assigned to molecular formulae $[Bi(GS)\text{-}H]^+$ and $[Bi(GS)_2]^+$, respectively, where GS is deprotonated GSH. Glutathione features numerous heteroatoms, meaning that several ligand atoms may coordinate to bismuth. A third interesting signal at *m/z* 385 was observed in which the glutamic acid portion of GSH was lost to yield a bismuth-cysteine-glycine complex cation, $[Bi(C_5H_8N_2O_3S)]^+$. For comparison, MALDI mass spectrometry was also employed in the analysis of bismuth-glutathione species. This alternate technique revealed the same prominent bismuth-glutathione species already identified by way of ESI-MS.[16]

Using ^1H and ^{13}C NMR spectroscopy to examine aqueous reaction mixtures of GSH and RBC has led to the identification of a 1:3 Bi:GSH complex.[13] Proton NMR spectra were obtained for aqueous solutions of free RBC, free GSH, and RBC combined with GSH. Informative differences were observed upon comparison of these three spectra. Chemical shifts of methylene and methine protons attached to carbon atoms (denoted by arrows in Figure 1.18) in α and β positions to -SH in free GSH were found to be 2.9 and 4.6 ppm,

respectively. When GSH was combined with RBC, the aforementioned glutathione proton resonances broadened and were observed at chemical shifts of 4.3 and 4.7 ppm, respectively. Oppositely, citrate proton resonances in the same spectrum were sharper compared to those in a spectrum of free RBC, and were also less deshielded at chemical shifts that are typical of free citrate.[13]

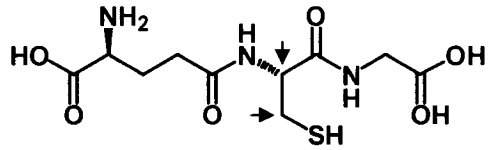

Figure 1.18 Arrows denote glutathione -CH- and -CH_2- units observed to undergo a change in chemical shift upon coordination to bismuth(III).

Information was also obtained by ^{13}C NMR spectroscopy on solutions of RBC and/or GSH at various Bi:GSH stoichiometries. Due to the observation of chemical shifts corresponding to free citrate carbon atoms at a minimum Bi:GSH ratio of 1:3, this stoichiometry was determined to be preferred for bismuth and glutathione in aqueous solution.[13] From the results of ^{1}H and ^{13}C NMR studies, it was unambiguously determined that the thiol moiety in tripeptide glutathione preferentially coordinates to bismuth. Consequently, other NMR studies modeled on those just described will continue to be helpful in examining solutions of bismuth and cysteine or other biologically relevant molecules.

In a broad ESI-MS study of metal-amino acid interactions, bismuth was found to form complexes with seven (cysteine, homocysteine, methionine, histidine, asparagine, glutamine and threonine) of twenty-one amino acids examined, significantly fewer than were observed to form complex ions with other metals.[17] Considering only the sulfur-containing amino acids, Cd(II), Tl(I) and Pb(II) formed one or more complex ions with Cys, Met, and Hcy, while Hg(I) and Hg(II) interacted with Cys and Met, but not with Hcy. In general, metal ions other than bismuth tended to form a greater number of complex ions with methionine than with cysteine or homocysteine. In contrast, bismuth formed similar complex ions with each of these sulfur-containing amino acids.[17] Of most

significance is that bismuth formed a larger number of complex ions with cysteine and homocysteine compared to all other metals investigated (Table 1.1).

The observations summarized in Table 1.1 suggest that while Met, a thioether, is not as selective for a particular metal ion, the thiols, Cys and Hcy, may have a preference for coordination to bismuth over other metals. While homocysteine does not exist in human proteins, on average the mole percent of cysteine in proteins is roughly 1.6 times higher than that of methionine.[64] In general, the likelihood of an *in vivo* bismuth-cysteine interaction is significantly greater than that for bismuth and homocysteine or methionine; therefore, it is of primary importance to pursue a more comprehensive examination of bismuth-cysteine chemistry.

Table 1.1 ESI-MS interactions of metals with cysteine (Cys), homocysteine (Hcy) and methionine (Met). A total of twenty-one amino acids were examined.[17]

	Metal:Amino Acid Complex Ions			Number of Amino Acids Observed to Form Ions with Each Metal
	Cys	Hcy	Met	
Tl(I)	1:1	1:1 2:1	1:1 2:1	21
Hg(I)	1:2	-	1:2 2:2 2:3	16
Hg(II)	1:2 2:3	-	1:1 1:2 2:2 2:3	20
Cd(II)	1:2	2:2 3:2	1:1 1:2 2:2 2:3	21
Pb(II)	1:1 1:2 2:2	1:1 1:2 2:2	1:1 1:2 2:2 3:2	21
Bi(III)	1:1 1:2 2:2 2:3	1:1 1:2 2:2 2:3	1:1 1:2 2:2 2:3	7

1.3.4 Antibacterial Bismuth-Thiolate Complexes

A number of synthetic bismuth thiolate compounds and commercial bismuth complexes (CBS and RBC) have been administered to various species of bacteria including *H.*

pylori.[93;136] Six synthetic compounds (Figure 1.19) were observed to have considerable antimicrobial activity and lower minimum inhibitory concentrations of bacterial growth compared to CBS and RBC. The compounds in Figure 1.19 have similar structural features which may be a basis for the corresponding bioactivities of these complexes.

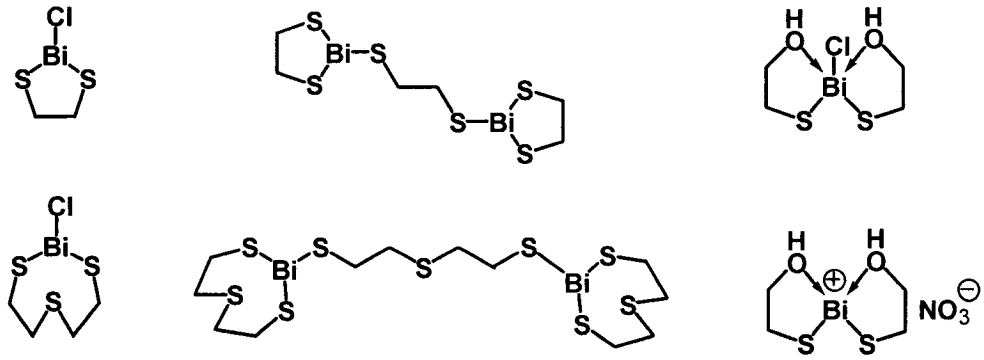

Figure 1.19 Bismuth-thiolate compounds active against bacteria such as *H. pylori*.

It is important to realize that despite the *in vitro* efficacy of bismuth compounds against bacteria, the use of bismuth-thiolate complexes as pharmaceuticals may or may not be beneficial. In fact, the simultaneous administration of bismuth and L-cysteine to mice was found to have a significantly more toxic effect than the independent delivery of either of these components.[137] The water-solubility of bismuth compounds is known to be enhanced in the presence of cysteine, cysteine hydrochloride, homocysteine, glutathione, ascorbic acid, and even grapefruit juice. Solutions of BSS or $Bi(NO_3)_3$ with the aforementioned substances also showed antimicrobial activity toward the virulent bacterium, *Clostridium difficile*.[138]

In summary, the results discussed in Section 1.3 not only support the contention that bismuth-sulfur interactions are biologically important, but the types of complexes that have been reported are enhancing a growing library of known bismuth-biomolecule coordination compounds. ESI-MS has been found to be particularly valuable and complements other techniques in the investigation of the interactions of bismuth compounds with various biologically relevant molecules. Recognizing the pronounced thiophilicity of bismuth – and that thiol-containing peptides and proteins are logical

initial biological binding sites for bismuth – the full therapeutic potential of bismuth chemistry cannot be achieved without a continued, comprehensive investigation of bismuth-thiolate chemistry.

1.4 Characterization of Bismuth Compounds

Notwithstanding examples provided in the previous Sections of Chapter 1, the unambiguous characterization of bismuth complexes has often been elusive due to various challenges associated with the isolation of these species. Bismuth compounds tend to be insoluble in common solvents; therefore, it can be a challenge to obtain crystals of bismuth-biomolecule systems. In addition, bismuth-element bonds are easily broken via hydrolysis, typically generating bismuth oxide precipitates containing the bismuthyl functional group ($^{+}$Bi=O).[27] Upon precipitate formation, the study of the interactions of bismuth with other ligands is compromised. Hydrolysis can be prevented by performing syntheses in a moisture-free environment; however, such syntheses do not represent conditions relevant to biological bismuth chemistry.

Often, single bismuth compounds have been obtained serendipitously, rather than by applying a carefully-designed synthetic strategy meant to yield a series of related bismuth complexes. Unique solid state bismuth structures have been characterized by X-ray crystallography, but many have been isolated based on their ability to crystallize easily under unpredictable conditions. These crystals may or may not be representative of the bismuth compound(s) present in the bulk of a given reaction mixture. In general, there is a need for well-defined strategies for efficient and reproducible preparation techniques for bismuth compounds.

While NMR spectroscopy is useful in yielding structural information, XRD data is also advantageous because it allows for an analysis of bond lengths and angles in the solid state. Relative to the vast number of amino acid complexes that are theoretically possible – even if only a handful of metals (Hg, Tl, Pb, Bi) are considered – very few such complexes have been characterized in the solid state.[28;33;139-142;142-144] Recognizing that bismuth and other metals almost certainly interact with amino acid residues of peptides

and proteins *in vivo*, it is somewhat surprising that a systematic method has not been developed for obtaining solid state information on metal-amino acid and other metal-biomolecule coordination complexes. Indeed, the growth of single crystals of bismuth compounds can be inhibited by a lack of solubility in a variety of solvents, and because bismuth is one of the heaviest elements, absorption of X-rays can be a problem if small crystals cannot be obtained.[1]

To help circumvent the issues described above, it is worth mentioning that a 1,10-phenanthroline ligand was used to stabilize the only known solid state bismuth-cysteine complex (Figure 1.17c, Figure 1.20a).[28] Both 1,10-phenanthroline (phen) and 2,2′-bipyridine (bipy) are known to coordinate relatively strongly to bismuth via nitrogen,[12] and precedence has been set for the use of these compounds as a stabilizing influence.[97] It can be noted that a 1:3 bismuth:salicylate species has been prepared without additional ligand stabilization; however, although the compound was determined by elemental analysis and IR spectroscopy to be $Bi(O_2CC_6H_4\text{-}2\text{-}OH)_3$, it was not crystallographically characterized.[102] Subsequently, the crystallographic characterization of a solid state complex containing bismuth coordinated by two salicylate ligands and 1,10-phenanthroline was achieved (Figure 1.20b). Similarly, a complex containing bismuth coordinated by three salicylate ligands and 2,2′-bipyridine is also known (Figure 1.20c).[97] Both of these solid state structures are dimeric as a result of two carboxylate oxygen atoms – one from a salicylate ligand in each half of the dimer – that bridge two bismuth atoms. For clarity only half of each dimer is shown in Figure 1.20.

Acknowledging the relatively weak interactions between bismuth and oxygen-based ligands like salicylate, the aforementioned examples suggest that it may be possible to exploit the presence of stronger donor ligands, gaining access to the crystallographic characterization of complexes that may not otherwise be easily obtained. More relevant to the discussion at hand, it is possible that cysteine will stabilize interactions of bismuth with other molecules. For instance, Figure 1.20d is an example of a yet unknown bismuth coordination complex that is meant to represent the ADH enzyme active site described in Section 1.2.1. The complex in Figure 1.20d contains two cysteinate ligands, and it is

proposed that the strong bismuth-sulfur bonds between bismuth and cysteine can be considered stabilizing with respect to the weaker bismuth-histidine interactions shown.

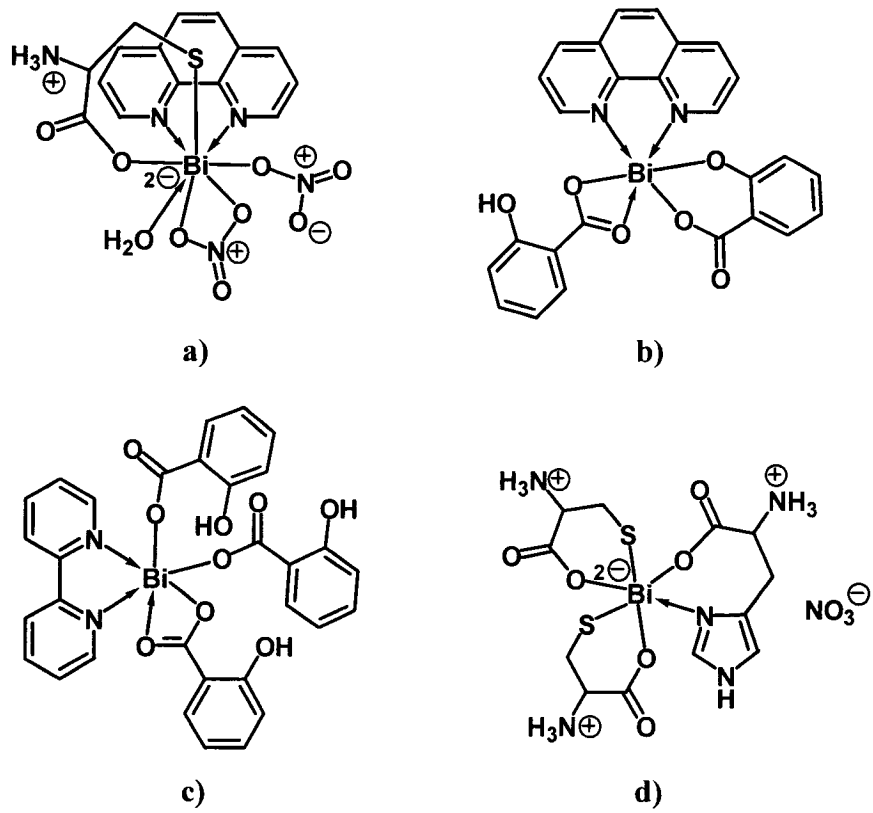

Figure 1.20 Bismuth-biomolecule complexes involving stabilizing ligands. a) 1:1:1 Bismuth:cysteinate:phenanthroline, b) 1:2:1 bismuth:salicylate:phenanthroline, c) 1:3:1 bismuth:salicylate:bipyridine, and d) proposed 1:1:2 bismuth:histidinate:cysteinate structure.

Although ^{209}Bi is 100 % abundant, has a large spin quantum number (I = 9/2), and is relatively sensitive to analysis by nuclear magnetic resonance (NMR) spectroscopy compared to other nuclides (0.137 compared to ^{1}H), it also has a sizeable quadrupole moment, $Q = -0.4 \times 10^{-28}$ m^2.[145] As a result, bismuth nuclei tend to produce broad spectral resonances that can make NMR spectra difficult to interpret, and few instances of the use of ^{209}Bi NMR have been reported. Aqueous $Bi(NO_3)_3$ gives a broad signal for bismuth ($\Delta\upsilon$ = 3200 Hz).[146;147] Solid state spin-spin coupling between ^{209}Bi and ^{19}F in $KBiF_6$ has been observed by to have a magnitude of 2700 ± 300 Hz.[148;149]

A high resolution solution NMR investigation of the hexafluorobismuth(V) anion (countercation = tetramethylammonium) has also been reported.[145] This anion is an appropriate choice for ^{209}Bi NMR because the octahedral symmetry at bismuth reduces resonance broadening. At a frequency of 40.20 MHz, the ^{209}Bi spectrum of $[(CH_3)_4N]^+[BiF_6]^-$ contained a clean septet due to coupling of bismuth to six spin ½ ^{19}F nuclei: J_{Bi-F} = 3823 ± 3 Hz. The chemical shift of ^{209}Bi in $Bi(NO_3)_3$ was found to be 24 ppm upfield of ^{209}Bi in BiF_6^-.[145] Subsequently, the ^{209}Bi NMR spectrum of $[(CH_3)_4N]^+[Bi(OTeF_5)_6]^-$ was examined, and also exhibited octahedral symmetry at bismuth.[150] An YbBiPt compound has been investigated by ^{209}Bi NMR spectroscopy, and in this case it was due to the cubic symmetry at bismuth that sharp resonances were observed.[151] In general, only highly symmetric local geometries reduce bismuth resonance broadening.

A variety of bismuth-biomolecule complexes have been investigated by ^{1}H and ^{13}C NMR spectroscopy.[91;108;110-113;134;152-154] Among other methods for characterization of bismuth compounds are UV-visible spectrophotometry and potentiometry,[155;156] IR radiation spectroscopy[157] and X-ray absorption spectroscopy.[158] Second to atomic absorption spectroscopy, inductively coupled plasma mass spectrometry (ICP-MS) is becoming more common for total bismuth determination analyses.[1] ESI-MS is also being realized as an indispensable means for the definitive identification of bismuth-biomolecule complexes,[16;25;27;28] and this technique is discussed further in Section 1.5. All investigations into the general chemistry of bismuth have improved upon the information that is available regarding the interactions of bismuth with a range of ligands. Still, due to the challenges associated with synthesis, isolation and characterization of bismuth compounds, further investigation is needed to explain the details of the biochemical activity of bismuth.

1.5 Mass Spectrometry

A variety of mass spectrometry (MS) techniques exist, all of which require a method of sample input, generation of ionic species, analysis and detection of these species, and conversion of detected signals into the form of a spectrum for interpretation. In mass spectra, relative ion abundance (%) is plotted as a function of mass-to-charge ratio (*m/z*, i.e., atomic mass units/number of charges). Figure 1.21 is a simple schematic of the sequence of components found in all mass spectrometers.[159]

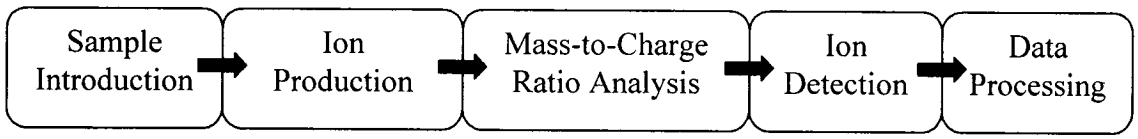

Figure 1.21 The main components of a mass spectrometer.

Ion production is one of the most important processes that occurs in a mass spectrometer because it involves the transformation of sample compounds into charged, gaseous species.[160] The ions are subsequently analyzed, and ultimately identified by the user. Electron ionization (EI) has been in use for several decades and is considered a 'hard' ionization method because the interaction of electrons with sample molecules generally causes significant molecular fragmentation. Typically, electrons used in the EI process possess an energy of 70 eV. Upon collision of these electrons with sample molecules, only a portion of the energy is used in molecular ionization via ejection of one electron. The remaining energy contributes to molecular fragmentations, and consequently, a peak corresponding to the molecular ion is not necessarily observed. Similarly, chemical ionization (CI) involves the interaction of electrons with a reagent gas such as methane or isobutane. Unlike EI, the process of CI involves collision of ionized reagent molecules with sample molecules. The reagent ions have less energy than the initial electrons; therefore, by the CI process, molecular ions are more easily observed and fragmentation is less extensive than when EI is employed.[159]

Gas phase samples are required for analysis by EI- or CI-mass spectrometry; therefore, sample molecules must have relatively low molecular weights and be stable to thermal decomposition. In contrast, biological compounds tend to be significantly polar and

possess high molecular weights, factors which minimize the volatility of these samples.[160] For this reason, newer techniques, specifically electrospray ionization (ESI) and matrix-assisted laser desorption/ionization (MALDI), have entered the scene as formidable options for biological sample analysis. As recently as 2002, one half of the Nobel Prize in Chemistry was awarded for work done on these modern ion production methods.

1.5.1 Electrospray Ionization Mass Spectrometry

In contrast to EI and CI, ESI allows for analysis of samples in aqueous solution, convenient as a simple model of biological conditions.[161] Another benefit of ESI is that it has been designed to yield ions from samples injected into the mass spectrometer at atmospheric pressure. (Atmospheric pressure chemical ionization (APCI) also has this advantage; however, this technique will not be discussed in detail here.) Not only does this mean that the efficiency of ion formation is greatly enhanced, but it is possible to link chemical separation systems, such as high-performance liquid chromatography or capillary electrophoresis, to an electrospray source.[159-161] Electrospray ionization mass spectrometry can be applied not only to biological systems but also to inorganic compounds.[162-165] In particular, ESI-MS has been found to be a versatile and efficient instrumental tool in the definitive identification of a variety of metal-biomolecule interactions.[16;17;25-28;166] Consequently, this report will emphasize ESI-MS as a means of ion production for the mass spectrometric analysis of biologically relevant bismuth samples, and comparisons of bismuth will also be made to analogous samples containing the relatively toxic metals, Hg, Tl, and Pb.

Not unlike the industrial process of spray painting, electrospray ion formation (Figure 1.22) involves exposing a solution sample to an electric field.[161] After the sample is injected into the instrument at a flow rate of 1 to 10 μL/min,[159] it reaches the end of a fine capillary (less than 250 μm, inner diameter).[160] At this position, an electric field is applied to create a potential difference (e.g., 3 to 6 kV) with respect to a counter-electrode located up to two centimeters away from the capillary.[159] A build up of charge (positive or negative, depending on the field direction) results at the solution surface.

Dependent on solvent composition, capillary diameter, and size of the electric potential, an 'electrospray' formally occurs when surface tension in the sample is outweighed by repulsive forces between charges, thus producing a fine suspension of charged, solvated particles.[159;160] In the experiments described in this thesis, a 50:50 ethanol:water solvent ratio was typically employed. Having a lower surface tension than water, ethanol facilitates the production of an electrospray at a suitable capillary voltage.[167]

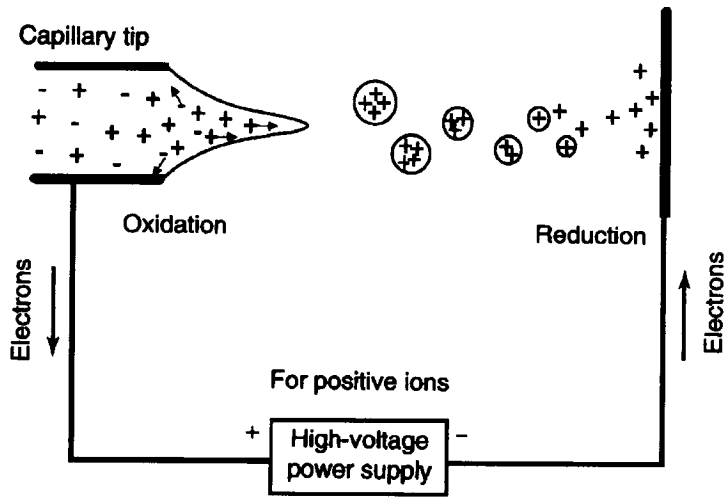

Figure 1.22 Electrospray ionization. (Reproduced with permission from *Mass Spectrometry Principles and Applications*, 2nd ed. de Hoffmann, E.; Stroobant, V. 2002. Copyright John Wiley & Sons, Ltd.)

Introduction of a heated inert gas (e.g., N_2) or passage of the charged particles through a heated capillary assists in desolvation of the sample. As the solvent is removed from each particle, charged species in the particles move closer to one another causing Coulombic forces of repulsion to increase, and eventually causing the particles to divide into smaller droplets.[159] Single ions may be ejected individually from droplets as loss of solvent occurs, or droplets may undergo several cycles of division and further desolvation until single ions remain for analysis and detection.[161]

Ions from the electrospray process are created chiefly as a result of protonation or deprotonation. This is in contrast to electron ionization in which ions are formed by removal of electrons. Acidic and basic moieties in proteins and other biological

molecules often lead to multiply charged species in the electrospray environment. Advantageously, for proteins with large masses and large numbers of charges, mass analyses can be conveniently performed by analyzers which have relatively small mass ranges. The molecular weight of cytochrome c is 12,360 Da and this protein can acquire between ten and twenty protons by ESI. The resulting *m/z* (ca. 1000) is easily analyzed by modern mass spectrometers.[160]

The electrospray ionization method is also useful for small polar molecules,[159] and because reaction mixtures of metal salts and biological ligands contain ionic species, further ionization is not necessarily required upon transfer of these solution species into the gas phase in the mass spectrometer. In addition, given that non-covalent interactions are common in bismuth-biomolecule systems (e.g., solutions of BSS or CBS), the 'softness' of the ESI technique is an advantage. Sample molecules are typically converted into molecular ions, as opposed to undergoing fragmentation, making ESI an ideal choice for mass spectrometric analysis of these systems. As a testament to ESI as a soft ionization approach, an ESI-MS study involving the tobacco mosaic virus can be considered. The virus was observed to preserve its shape, and even its biological activity, after ionization by electrospray, mass analysis, and re-collection.[168]

Once the process of sample ionization is finished, the ions formed by ESI enter a mass analyzer to be separated according to mass-to-charge ratio.[161] For experiments discussed in Chapters 2 to 6, a quadrupole ion trap mass analyzer was used in connection with an ESI source. An advantage of the ion trap is that it allows for tandem mass spectrometry (MS/MS) experiments to be conducted. Sample ions of a particular *m/z* are confined in the mass analyzer and undergo collisions with atoms or molecules of an inert gas (e.g., He), resulting in fragmentation (collision-induced dissociation) of the original ions. Analysis of the resulting tandem mass spectrum contributes to a definitive assignment of the original mass spectral peak by providing information on structural features of the corresponding sample ion.[161] The use of an ion trap is suited to both organic and inorganic samples. The successful study of inorganic and organometallic systems (including air-sensitive compounds), can be accomplished by optimizing the temperature

of the instrument and applying an appropriate sample dilution strategy.[169] More details on the ESI process[170;171] and the operation of quadrupole ion traps[172] have been reviewed by other researchers.

1.5.2 Criteria for Reporting ESI-MS Data

In the following Chapters of this thesis, a number of factors have been taken into account with respect to the interpretation, presentation, and discussion of ESI-MS data obtained from reaction mixtures containing bismuth or other metals with biologically relevant molecules. Given the emphasis on the identification of metal-containing complexes, in most cases spectral peaks are only reported if they are representative of ions composed of one or more metal cations and one or more of the ligands under study. Other peaks are present in all spectra; however, not all of these peaks have been assigned. The base peak is always reported regardless of the corresponding ion composition, and various ligand- or metal-only peaks have also been reported at the author's discretion. Typically, peaks with relative abundances of less than 5 % are not described.

Tabulated mass-to-charge ratios are provided to a precision of one decimal place, and rounded to the nearest whole number when discussed within the text. Relative abundances (%) are given with respect to the 100 % (base) peak, and are consistently rounded to the nearest whole number. Listed mass-to-charge ratios represent chemical species containing only the most abundant isotope of each element, and therefore do not necessarily correspond to the highest intensity signal within a given isotope pattern. As employed in the preceding Sections of Chapter 1, a general ion formula of $[M_a(L)_b\text{-}cH]^{d\pm}$ (M = metal, L = ligand, H = proton; a, b, c, d = integers) can be understood to represent ions of an a:b metal:ligand stoichiometric ratio. Ion formulae include a specified loss of a number, c, of ligand protons, and have an overall positive or negative charge of d.

Tandem mass spectra were obtained for selected ions corresponding to particular *m/z* values, each of which were first rounded to the nearest whole number before applying a helium collision energy of less than 50 (arbitrary units, reported in %). Product ions from collision-induced dissociation were expected within a ± 1 *m/z* range of the chosen integer

values. Numbers listed under a table heading of MS/MS *m/z* correspond to assigned product ions. Tandem mass spectra were often discarded if they did not have a normalized spectral intensity (NL) of at least 2 x 10^4 (arbitrary units). Not all product ions have been listed, and those with relative abundances of less than 5 % are usually not discussed.

Considering that an extensive amount of data is typically acquired from any given mass spectrometry experiment, from a documentation perspective it is important to establish a system of data analysis and archiving that is both efficient and communicable to other researchers. Such an endeavour is dependent on the software used for data analysis. For data presented throughout this thesis, the software program Qual Browser (Version 1.2 from Finnigan Corp. ©1998–2000) has been employed. In order to explicitly distinguish one Qual Browser mass spectrum from another it is recommended that the following specific pieces of information be recorded: the run time (period of data collection, RT, in units of seconds), the time period of subtracted background data (SB, in seconds), and the normalized spectral intensity (NL).

After examining a number of ESI mass spectra from reaction mixtures of bismuth and other metals in the presence of various organic ligands, a number of trends were noted in terms of the types of ions observed. Monocations with whole number metal:ligand ratios and corresponding sodiated analogues were observed most frequently. Therefore, a generic spreadsheet was developed using Microsoft Office software program, Excel, to assist in the interpretation of ESI mass spectra from reaction mixtures of metals and biologically relevant molecules. A sample spreadsheet (Table A.1) is provided in Appendix A for spectra from reaction mixtures containing combinations of Tl(I), cysteine, and cysteinyl-glycine. Comparing experimental spectra with the data in user-defined tables such as Table A.1, has contributed to a more comprehensive procedure for mass spectral analyses.

1.6 Metal Ion Selection and Safety Considerations

Despite the differences in bioactivity between ions of mercury, thallium, and lead, compared to bismuth, these four elements are located as a consecutive series in the sixth row of the periodic table (Figure 1.23). Given that compounds of bismuth are considerably less toxic than those of mercury, thallium, and lead, it is of interest to design experiments that compare the interactions of compounds of these metals[c] with biologically relevant molecules.

Due to relativistic influences, Tl(I), Pb(II), and Bi(III) are more stable oxidation states than Tl(III), Pb(IV), and Bi(V), respectively, chiefly because the loss of the $6s^2$ electrons in the valence shell of each metal is not energetically favourable.[174;175] Consequently, only salts of the lower oxidation state ions of thallium, lead, and bismuth were examined by ESI-MS. Hg(I) and Hg(II) are water-stable ions; therefore, monosaccharide interactions with salts of both mercury ions were investigated.

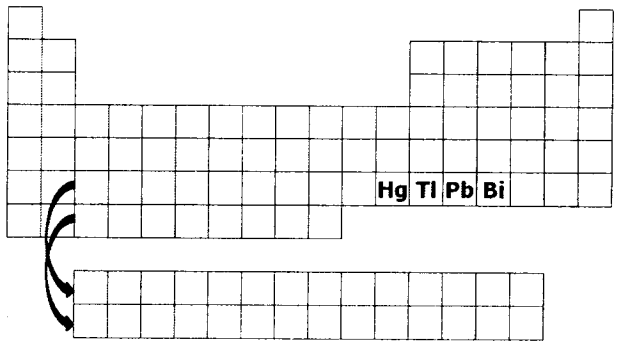

Figure 1.23 Location of mercury, thallium, lead, and bismuth in the periodic table.

In terms of toxicity, minimum lethal doses of elemental mercury, thallium, and lead are approximately 0.5 g, 0.3 g and 10 g, respectively, compared to a minimum lethal dose of 15 g for bismuth,[176] from which a single fatality has been reported.[177] Notably, the consumption of relatively high doses of bismuth compounds has also been associated with encephalopathy.[178-180] Due to the improved water solubility of metal salts compared to neutral metals, Hg(I), Hg(II), Tl(I), and Pb(II) are more noxious than the corresponding elements. Consequently, in conducting the experiments described in this

[c] Due to possible ambiguity with respect to the term 'heavy metal,' this phrase has been excluded from this thesis.[173]

document it was imperative that precautions be taken to preserve the safety of researchers.

Personal protection items, including a laboratory coat, gloves, facial mask, and safety glasses, were worn when handling salts of mercury, thallium, and lead. Solids were weighed in an enclosed space to prevent contamination of surrounding laboratory areas. To avoid unnecessary contamination of communal ESI-MS instrumentation, a separate injection system, including silica capillary, polyetheretherketone (PEEK) tubing, and aluminum plate were used for sample introduction into the mass spectrometer. Glassware in contact with metal-containing samples was bleached between uses, and disposal of metal waste was executed according to local regulations.

Chapter 2 Metal-Monosaccharide Complexes

The primary biological functions of carbohydrates involve production and storage of energy, structural support, and intercellular communication.[71] Many different monosaccharides (sugars) are known with varying carbon backbone lengths, and chains of monosaccharides are connected by glycosidic bonds to form polysaccharides, such as cellulose or glycogen.[71] In contrast to the persistence of L-amino acids in proteins, biological carbohydrates are composed of D-sugars. Interestingly, the predominant production of monosaccharides as D-enantiomers may have been the result of asymmetric catalysis in the presence of amino acids.[181]

D-Glucose (Glc), D-mannose (Man), D-galactose (Gal), and D-fructose (Fru) are the four most common six-carbon sugars.[71] D-Ribose (Rib), a five-carbon sugar, is also important given that derivatives of this monosaccharide exist in all nucleic acids. These five sugars are illustrated in Figure 2.1, recognizing that in aqueous solution these compounds are present primarily as five-membered furanose or six-membered pyranose rings.[71]

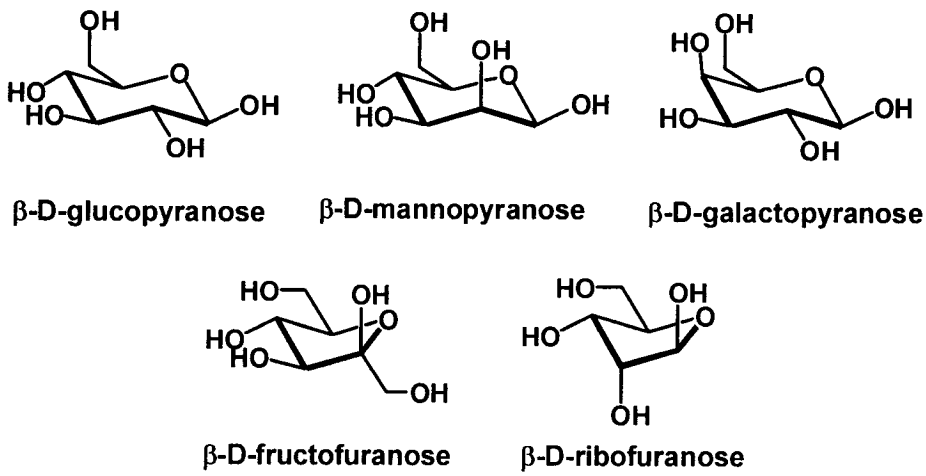

Figure 2.1 Five common monosaccharides, drawn as β-D-stereoisomers.

Although the existence of metalloproteins and metalloenzymes is not paralleled by the biological presence of metallocarbohydrates, research on metal-carbohydrate interactions is of interest from a number of perspectives. Work has been done to investigate the uptake of Tl(I) by starch, in consideration of the usefulness of Tl(I) reagents in organic

synthesis, and previously as rodenticides.[182] Complexes of starch and Bi(III) have been synthesized in view of the medicinal potential of bismuth-based drugs.[183] A solid state network containing methyl-α-D-mannopyranoside coordinated to Bi(III) is also known.[184]

Most biological carbohydrates exist as oligosaccharides linked to proteins or lipids.[185] Such glycoproteins and glycolipids are attached to the outsides of cells and participate in numerous vital biological processes involving intercellular interactions.[186] Given the variety of functional groups featured in glycoproteins, and the range of functions in which these molecules are engaged, it is worthwhile to understand the fundamental chemistry of monosaccharides in the presence of other entities including metal ions.

From a characterization standpoint, carbohydrates are often analyzed by way of mass spectrometry, and the addition of an alkali-, alkaline earth-, or transition metal salt to mixtures of carbohydrates can be a valuable method for the identification of multiple carbohydrate components.[187-191] Recognizing both the toxicity of lead compounds, and the availability of carbohydrates in the natural environment, lead-monosaccharide interactions have been studied using ESI-MS.[192;193]

To supplement the research aforementioned, an ESI-MS survey of common monosaccharides, Glc, Man, Gal, Fru, and Rib, in the presence of bismuth(III) or one of a variety of other relatively toxic metal ions, is described in Section 2.1. Given the presence of aminosugars (e.g., N-acetyl-D-glucosamine) in both bacterial cell walls and in human glycoproteins,[71] endogenous sugars other than those shown in Figure 2.1 have been combined with Bi(III). Results from the latter studies are described in Section 2.2. In consideration of the affinity of sulfur for coordination to bismuth, Section 2.3 details the interactions of Bi(III) with non-endogenous thiosugars.

2.1 Results and Discussion: Metal Complexes with Common Sugars

The main objectives behind the research described in this thesis were to take advantage of the sensitivity and efficiency of data collection offered by ESI-MS in order to characterize complexes of bismuth or other metals with biological molecules. The

ultimate goal of this fundamental work was to elucidate new chemical interactions that are relevant to medicinal inorganic chemistry, and which may help explain how metals affect biological systems. Given that an extensive ESI-MS study of metal-amino acid complexes has been reported,[17] a similar analysis of metal-monosaccharide interactions was the next logical and complementary pursuit. Hg(I), Hg(II), Tl(I), Pb(II) and Bi(III) were examined in the presence of biologically common monosaccharides, Glc, Man, Gal, and Fru. Reaction mixtures of Pb(II) or Bi(III) with Rib were also investigated.

2.1.1 Mercury-Monosaccharide Interactions

Under the reaction conditions described in Section 2.5.1, Hg(I) (from $Hg_2(NO_3)_2$) was not observed to form complexes with Glc or Fru. This was evident given the absence of peaks identified with the natural isotope pattern unique to mercury (^{196}Hg (0.14 %), ^{198}Hg (10.02 %), ^{199}Hg (16.84 %), ^{200}Hg (23.13 %), ^{201}Hg (13.22 %), ^{202}Hg (29.80 %), ^{204}Hg (6.85 %)).[177] Spectra from a reaction mixture of Hg(II) (from $Hg(NO_3)_2$) and Fru may have contained peaks corresponding to mercury-fructose ions; however, due to a relatively noisy baseline, no such ions were definitively assigned.

Mercury-monosaccharide peaks (Table 2.1) have been assigned in spectra from Hg(I) with Man or Gal, and from Hg(II) with Glc, Man, or Gal. In each case, a peak at *m/z* 561 was most relatively abundant, excluding the base peak at *m/z* 383, which corresponds to a complex cation of two monosaccharide (Mon) molecules and sodium(I): $[Na(Mon)_2]^+$.[d] The *m/z* 561 peak was identified as $[Hg(Mon)_2\text{-}H]^+$ (Mon = Man, Gal, or Glc). In the case of Hg(II), one proton is presumably lost from Man, Gal, or Glc to generate a monocation. Comparatively, because *m/z* 561 (and not *m/z* 562: $[Hg(Mon)_2]^+$) is present in spectra from mixtures containing Hg(I), it is believed that oxidation from Hg(I) to Hg(II) occurs within the environment of the mass spectrometer. A match between theoretical[195] and experimental isotope patterns (Figure 2.2) supports the assignment of *m/z* 561 as $[Hg^{II}(Man)_2\text{-}H]^+$, resulting from initial reaction mixtures containing D-mannose and either $Hg_2(NO_3)_2$ or $Hg(NO_3)_2$.

[d] Even when sodium(I) and potassium(I) are not components of reacted compounds, these ions are recognized impurities (e.g., from solvents) that appear in (and sometimes complicate) ESI mass spectra.[194]

Table 2.1 Positive ion mercury-monosaccharide ESI-MS data from reaction mixtures containing $Hg_2(NO_3)_2$ or $Hg(NO_3)_2$ and D-glucose (Glc), D-mannose (Man), or D-galactose (Gal), in 50:50 ethanol:water.

Contents of Reaction Mixture	*m/z*	Relative Abundance (%)	Assignment
$Hg_2(NO_3)_2$/Man	382.7-382.9	100	$[Na(Man)_2]^+$
	542.8-542.9	12-16	$[Hg(Man)_2\text{-}H\text{-}H_2O]^+$
	560.9	51-53	$[Hg(Man)_2\text{-}H]^+$
	582.9	8	$[HgNa(Man)_2\text{-}2H]^+$
	760.5-760.7	7-9	$[Hg_2(Man)_2\text{-}3H]^+$
$Hg_2(NO_3)_2$/Gal	382.8-382.9	100	$[Na(Gal)_2]^+$
	542.9	6-7	$[Hg(Gal)_2\text{-}H\text{-}H_2O]^+$
	560.8-560.9	14-21	$[Hg(Gal)_2\text{-}H]^+$
	583	5	$[HgNa(Gal)_2\text{-}2H]^+$
	760.7	3-4	$[Hg_2(Gal)_2\text{-}3H]^+$
$Hg(NO_3)_2$/Glc	382.9	100	$[Na(Glc)_2]^+$
	542.9	6	$[Hg(Glc)_2\text{-}H\text{-}H_2O]^+$
	560.9	12-15	$[Hg(Glc)_2\text{-}H]^+$
	582.8	8-15	$[HgNa(Glc)_2\text{-}2H]^+$
	760.5-760.8	5-6	$[Hg_2(Glc)_2\text{-}3H]^+$
$Hg(NO_3)_2$/Man	382.9	100	$[Na(Man)_2]^+$
	542.7-542.9	5-15	$[Hg(Man)_2\text{-}H\text{-}H_2O]^+$
	560.9	18-39	$[Hg(Man)_2\text{-}H]^+$
	582.9	8-12	$[HgNa(Man)_2\text{-}2H]^+$
	760.7	7-15	$[Hg_2(Man)_2\text{-}3H]^+$
$Hg(NO_3)_2$/Gal	382.9	100	$[Na(Gal)_2]^+$
	542.9	12-14	$[Hg(Gal)_2\text{-}H\text{-}H_2O]^+$
	560.9	23-26	$[Hg(Gal)_2\text{-}H]^+$
	582.9-583.0	11-13	$[HgNa(Gal)_2\text{-}2H]^+$
	760.7	5-6	$[Hg_2(Gal)_2\text{-}3H]^+$

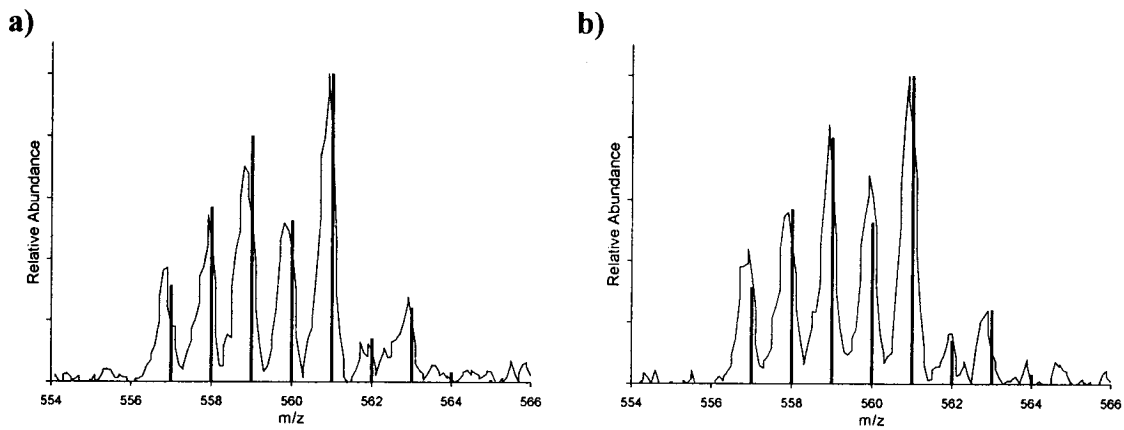

Figure 2.2 Comparison of isotope patterns for $[Hg(Man)_2\text{-}H]^+$ from Hg(I) and Hg(II) starting materials. An experimental ESI-MS isotope expansion (continuous thin line) is shown from a reaction mixture containing a) mercury(I) nitrate or b) mercury(II) nitrate, and D-mannose. Overlaid in each case (dark vertical bars) is the theoretical isotope pattern for the corresponding chemical formula, $HgC_{12}H_{23}O_{12}$.

Sodiated versions of the observed 1:2 mercury:monosaccharide cations identified at *m/z* 561 were also assigned: $[HgNa(Mon)_2\text{-}2H]^+$ at *m/z* 583. Other peaks of interest include *m/z* 543 and *m/z* 761, which presumably represent the loss of water from Mon in $[Hg(Mon)_2\text{-}H]^+$, and a 2:2 Hg:Mon cation, $[Hg_2(Mon)_2\text{-}3H]^+$, respectively. Although relatively intense CID spectra for these peaks have not been obtained, a match between experimental and theoretical isotope patterns typically supports these peak assignments. In some cases the mercury isotope patterns were not clear due to a low spectral signal-to-noise ratio. In the future, increasing the concentrations of examined mercury-monosaccharide reaction mixtures may help to generate improved spectra.

2.1.2 Thallium-Monosaccharide Interactions

When $TlNO_3$ was combined in 1:1 ratios with a variety of monosaccharides, a thallium-monosaccharide cation of the same stoichiometry was observed via ESI-MS: $[Tl(Mon)]^+$ (Mon = Glc, Fru, Man, or Gal) (Table 2.2). The assignment of each 1:1 Tl:Mon complex ion is supported by the observation at *m/z* 385 of an interpretable isotope pattern. In the case of $[Tl(Fru)]^+$, collision-induced dissociation (CID) led to the generation of Tl(I) ions, and also to the loss of water (18 u), yielding a product peak at *m/z* 367.

At first glance, the isotope pattern for *m/z* 385 does not appear to have the expected, normalized 42:100 peak height ratio unique to ^{203}Tl and ^{205}Tl isotopes with 29.5 % and 70.5 % natural abundances,[177] respectively. However, the observed pattern can be attributed to the overlap of *m/z* 385 with a peak at *m/z* 383, assigned to sodiated dimonosaccharide, $[Na(Mon)_2]^+$, as observed in spectra from mercury-monosaccharide reaction mixtures discussed in Section 2.1.1.

If a 1:1 ratio of $[Na(Fru)_2]^+$ and $[Tl(Fru)]^+$ ions is assumed, when the theoretical and experimental isotope patterns for these two ions are overlaid, the patterns do not match exactly (Figure 2.3a). However, the ions represented by peaks at *m/z* 383 and *m/z* 385 are not likely to be present in equal gas phase quantities. Therefore, if the theoretical patterns are mathematically weighted in a ratio of 1:1.86 $[Na(Fru)_2]^+$:$[Tl(Fru)]^+$, a better illustration of how the experimentally-observed isotope pattern is generated can be

achieved (Figure 2.3b). Similarly, a sodiated monosaccharide ion, $[Na(Mon)]^+$ is often observed at *m/z* 203; therefore, this peak was expected to overlap with any $^{203}Tl^+$ that was present.

Table 2.2 Positive ion thallium-monosaccharide ESI-MS data from reaction mixtures containing $TlNO_3$ and D-glucose (Glc), D-mannose (Man), D-galactose (Gal), or D-fructose (Fru), in 50:50 ethanol:water.

Contents of Reaction Mixture	*m/z*	Relative Abundance (%)	Assignment
$TlNO_3$/Glc	203.1	72	$[Na(Glc)]^+$
	205.6	100	Tl^+
	382.9	81	$[Na(Glc)_2]^+$
	384.9	30	$[Tl(Glc)]^+$
$TlNO_3$/Fru	203.1	100	$[Na(Fru)]^+$
	205.6	89	Tl^+
	382.9	51	$[Na(Fru)_2]^+$
	385.0	55	$[Tl(Fru)]^+$
$TlNO_3$/Man	203.1	85	$[Na(Man)]^+$
	205.6	100	Tl^+
	382.9	95	$[Na(Man)_2]^+$
	385.0	47	$[Tl(Man)]^+$
$TlNO_3$/Gal	203.1	69	$[Na(Gal)]^+$
	205.7	70	Tl^+
	382.9	100	$[Na(Gal)_2]^+$
	384.9	26	$[Tl(Gal)]^+$

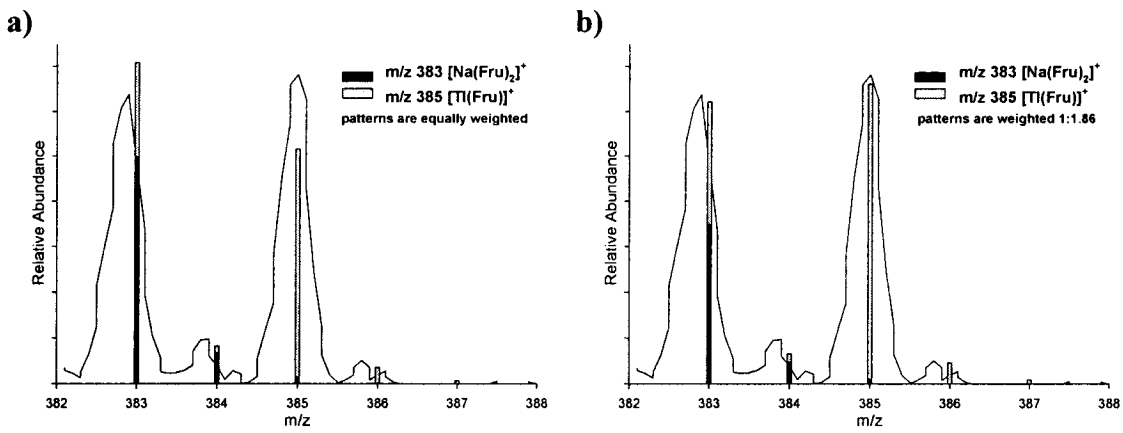

Figure 2.3 Analysis of isotope patterns for $[Na(Fru)_2]^+$ and $[Tl(Fru)]^+$. The sum of the calculated isotope patterns for $[Na(Fru)_2]^+$ at *m/z* 383 (dark vertical bars) and $[Tl(Fru)]^+$ at *m/z* 385 (light vertical bars) is superimposed on the experimental isotope expansion pattern (continuous thin line) from a reaction mixture containing $TlNO_3$ and D-fructose. In a) the calculated patterns are weighted 1:1. A better match is achieved in b) when a weight of 1:1.86 $[Na(Fru)_2]^+$:$[Tl(Fru)]^+$ has been applied.

Also of consequence was a peak at *m/z* 206 in all thallium-monosaccharide spectra, which is one mass unit higher than a peak for $^{205}Tl^{+}$. Although the ESI-MS instrument employed in these experiments does not have the capacity for high resolution ion detection across the full mass range, *m/z* values represent accurate nominal masses within error when rounded from one decimal place to the nearest whole number. Each peak with a rounded value of *m/z* 206 has a unique isotope pattern (Figure 2.4a) indicative of a metal-containing species, but does not correspond explicitly to the presence of Tl^{+}. Thallium(I) is expected to give two peaks at values of *m/z* 203 and *m/z* 205 in a 42:100 ratio of normalized 30:70 relative intensities. Acquiring a ZoomScan™ (high resolution) spectrum of a small range of *m/z* values including *m/z* 206 does reveal a pattern (Figure 2.4c) closer to that which is expected (Figure 2.4b). Ion collection effects at low resolution can result in distorted peak shapes, and this may help to explain the observed pattern at *m/z* 206.[196]

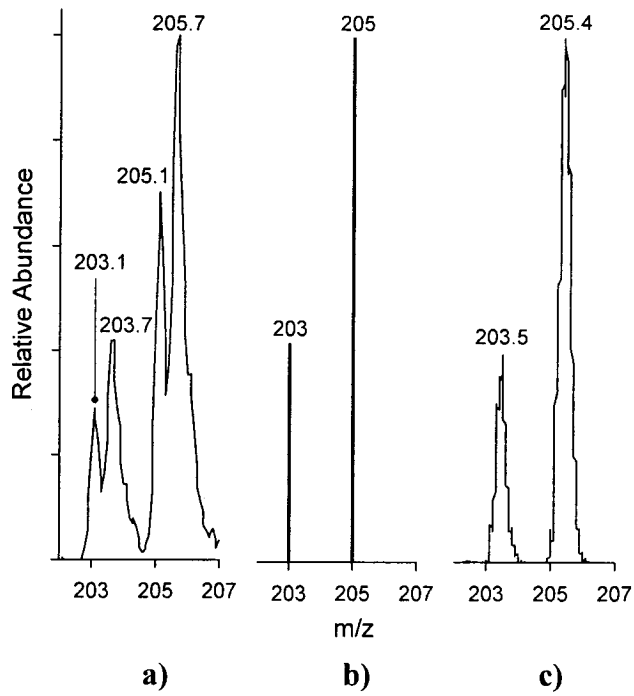

Figure 2.4 Analysis of isotope patterns for Tl^{+} ions represented by *m/z* 206. a) Typical expanded pattern, b) theoretical pattern, and c) ZoomScan™ spectrum. Experimental spectra shown in this figure (a, c) were acquired from solutions containing $TlNO_3$ in 50:50 ethanol:water.

2.1.3 Lead-Monosaccharide Interactions

In contrast to observations of relatively few mercury- and thallium-monosaccharide complex ions, Pb(II) was observed to interact abundantly with Glc, Fru, Man, Gal and Rib. Tandem mass spectrometry and the known isotope pattern unique to lead (^{204}Pb (1.4 %), ^{206}Pb (24.1 %), ^{207}Pb (22.1 %), ^{208}Pb (52.4 %))[177] were exploited where possible to confirm peak assignments. In Figure 2.5, a representative lead-monosaccharide spectrum is shown, obtained from the ESI-MS analysis of a reaction mixture containing lead(II) nitrate and D-glucose. Peak assignments for spectra from all lead-monosaccharide combinations are included in Table 2.3.

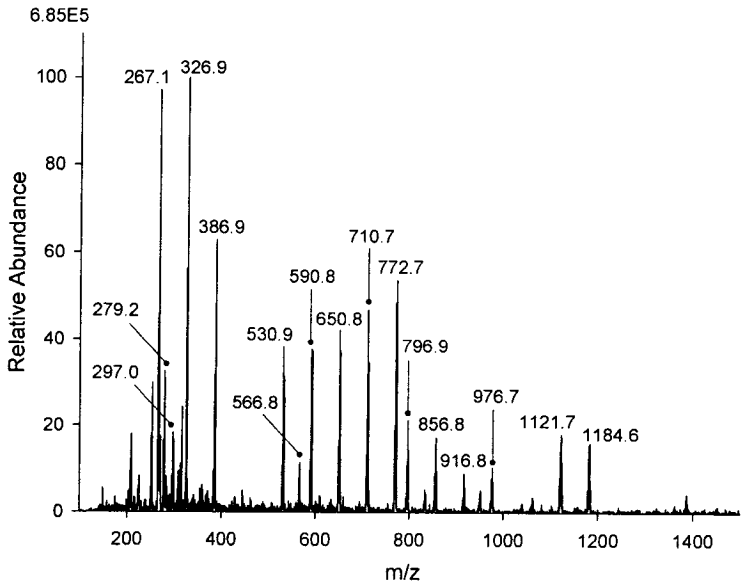

Figure 2.5 Positive ion lead-glucose ESI mass spectrum from a reaction mixture containing $Pb(NO_3)_2$ and D-glucose in 50:50 ethanol:water.[e]

[e] The value at the top left corner of full- and tandem mass spectra in this thesis is the normalized spectral intensity (NL), a value by which the quality of a spectrum can be assessed. Higher NL values indicate that more ions have been detected, increasing the reliability of the spectral results.

Table 2.3 Positive ion lead-monosaccharide ESI-MS data from reaction mixtures containing $Pb(NO_3)_2$ and D-glucose (Glc), D-mannose (Man), D-galactose (Gal), D-fructose (Fru), or D-ribose (Rib), in 50:50 ethanol:water.

Contents of Reaction Mixture	*m/z*	Relative Abundance (%)	Assignment
$Pb(NO_3)_2$/Glc	267.1	97	$[Pb(Glc)-C_4H_9O_4]^+$
	279.2	33	$[Pb(Glc)-C_3H_9O_4]^+$ or $PbOH{\cdot}3H_2O$
	297.0	18	$[Pb(Glc)-C_3H_7O_3]^+$ or $PbOH{\cdot}4H_2O$
	326.9	100	$[Pb(Glc)-C_2H_5O_2]^+$
	386.9	63	$[Pb(Glc)-H]^+$
	532.9	31	$[Pb_2(Glc)-C_2H_7O_2]^+$
	566.8	11	$[Pb(Glc)_2-H]^+$
	592.8	37	$[Pb_2(Glc)-3H]^+$
	652.8	37	$[Pb_2(Glc)_2-C_4H_{11}O_4]^+$
	712.9	35	$[Pb_2(Glc)_2-C_2H_7O_2]^+$
	772.7	54	$[Pb_2(Glc)_2-3H]^+$
	798.9	10	$[Pb_3(Glc)-5H]^+$
	858.8	10	$[Pb_3(Glc)_2-C_4H_{13}O_4]^+$
	918.7	6	$[Pb_3(Glc)_2-C_2H_9O_2]^+$
	978.7	6	$[Pb_3(Glc)_2-5H]^+$
	1124.7	7	$[Pb_4(Glc)_2-C_2H_{11}O_2]^+$
	1184.7	5	$[Pb_4(Glc)_2-7H]^+$
$Pb(NO_3)_2$/Fru	267.0	38	$[Pb(Fru)-C_4H_9O_4]^+$
	279.1	32	$[Pb(Fru)-C_3H_9O_4]^+$ or $PbOH{\cdot}3H_2O$
	297.0	100	$[Pb(Fru)-C_3H_7O_3]^+$
	386.9	57	$[Pb(Fru)-H]^+$
	544.9	23	$[Pb_2(Fru)-CH_7O_2]^+$
	772.6	11	$[Pb_2(Fru)_2-3H]^+$
	888.6	6	$[Pb_3(Fru)_2-C_3H_{11}O_3]^+$
	978.6	16	$[Pb_3(Fru)_2-5H]^+$
	1184.7	3	$[Pb_4(Fru)_2-7H]^+$
$Pb(NO_3)_2$/Man	267.1	35	$[Pb(Man)-C_4H_9O_4]^+$
	279.1	11	$[Pb(Man)-C_3H_9O_4]^+$ or $PbOH{\cdot}3H_2O$
	296.9	29	$[Pb(Man)-C_3H_7O_3]^+$ or $PbOH{\cdot}4H_2O$
	326.8	39	$[Pb(Man)-C_2H_5O_2]^+$
	386.9	100	$[Pb(Man)-H]^+$
	532.9	9	$[Pb_2(Man)-C_2H_7O_2]^+$
	566.8	30	$[Pb(Man)_2-H]^+$
	592.6	8	$[Pb_2(Man)-3H]^+$
	652.8	10	$[Pb_2(Man)_2-C_4H_{11}O_4]^+$
	712.7	4	$[Pb_2(Man)_2-C_2H_7O_2]^+$
	772.7	43	$[Pb_2(Man)_2-3H]^+$
	799.0	3	$[Pb_3(Man)-5H]^+$
	858.7	5	$[Pb_3(Man)_2-C_4H_{13}O_4]^+$
	918.5	1	$[Pb_3(Man)_2-C_2H_9O_2]^+$
	978.7	8	$[Pb_3(Man)_2-5H]^+$
	1124.7	2	$[Pb_4(Man)_2-C_2H_{11}O_2]^+$
	1184.7	2	$[Pb_4(Man)_2-7H]^+$

Contents of Reaction Mixture	*m/z*	Relative Abundance (%)	Assignment
$Pb(NO_3)_2$/Gal	267.1	45	$[Pb(Gal)-C_4H_9O_4]^+$
	279.1	10	$[Pb(Gal)-C_3H_9O_4]^+$ or $PbOH{\cdot}3H_2O$
	296.8	45	$[Pb(Gal)-C_3H_7O_3]^+$ or $PbOH{\cdot}4H_2O$
	326.8	32	$[Pb(Gal)-C_2H_5O_2]^+$
	386.9	100	$[Pb(Gal)-H]^+$
	532.9	11	$[Pb_2(Gal)-C_2H_7O_2]^+$
	566.6	18	$[Pb(Gal)_2-H]^+$
	592.7	10	$[Pb_2(Gal)-3H]^+$
	652.7	12	$[Pb_2(Gal)_2-C_4H_{11}O_4]^+$
	712.7	7	$[Pb_2(Gal)_2-C_2H_7O_2]^+$
	772.8	25	$[Pb_2(Gal)_2-3H]^+$
	798.7	3	$[Pb_3(Gal)-5H]^+$
	858.7	4	$[Pb_3(Gal)_2-C_4H_{13}O_4]^+$
	918.5	1	$[Pb_3(Gal)_2-C_2H_9O_2]^+$
	978.7	12	$[Pb_3(Gal)_2-5H]^+$
	1124.9	3	$[Pb_4(Gal)_2-C_2H_{11}O_2]^+$
	1184.6	6	$[Pb_4(Gal)_2-7H]^+$
$Pb(NO_3)_2$/Rib	267.1	14	$[Pb(Rib)-C_3H_7O_3]^+$
	279.2	8	$[Pb(Rib)-C_2H_7O_3]^+$ or $PbOH{\cdot}3H_2O$
	297.0	17	$[Pb(Rib)-C_2H_5O_2]^+$
	339.0	10	$[Pb(Rib)-H_3O]^+$
	357.0	100	$[Pb(Rib)-H]^+$
	506.8	10	$[Pb(Rib)_2-H]^+$
	563.0	7	$[Pb_2(Rib)-3H]^+$
	580.7	5	$[Pb_2(Rib)_2-C_5H_{11}O_4]^+$
	712.9	10	$[Pb_2(Rib)_2-3H]^+$
	829.0	6	$[Pb_3(Rib)_2-C_3H_{11}O_3]^+$
	919.0	11	$[Pb_3(Rib)_2-5H]^+$
	1124.9	1	$[Pb_4(Rib)_2-7H]^+$

A wide variety of lead-glucose cations were observed, including those with Pb:Glc ratios of 1:1, 1:2, 2:1, 2:2, 3:1, 3:2, and 4:2. Similar spectra were obtained for lead-fructose, -mannose, -galactose, and -ribose reaction mixtures. Peaks in the lead-glucose spectrum shown in Figure 2.5 were comparable to those observed by others.[193] In both published experiments and those reported herein, peaks at *m/z* 387 and *m/z* 567 were assigned to $[Pb(Glc)_b - H]^+$ monocations (b = 1, 2). A 1:3 lead:glucose monocation was also assigned previously; however, the relative abundance of this peak was low (< 5 %).[193] Dicationic peaks were not observed in the lead-glucose spectrum presented in Figure 2.5. In contrast, several $[Pb(Glc)_b]^{2+}$ dications (b = 2 to 12) at *m/z* 284, 374, 464, 554, 644, 734, 824, 914, 1004, 1094, and 1184 have been documented.[193]

Adjusting solution concentration, solvent (from 50:50 ethanol:water to water alone), and reactant stoichiometries to better match those employed in earlier research did not reveal the presence of lead-glucose dications in ESI mass spectra obtained from these subsequent studies. The difference in observations between the literature and the present studies may depend on the application of different instrumental conditions, optimization of which might significantly alter spectral appearance.

The fragmentation of lead-glucose species via tandem mass spectrometry, along with theoretical computations, led to the previous finding that mass units of 60 were often lost from monosaccharides interacting with lead(II).[193] This observation holds true for full lead-monosaccharide spectra, which contain a variety of lead(II) complexes involving only a portion of the monosaccharide under investigation (see Table 2.3). As an example, a diagram of how the fragmentation of $[Pb(Gal)\text{-}H]^+$ may occur is shown in Figure 2.6. Two losses of 60 mass units ($C_2H_4O_2$ x 2) generates $[Pb(Gal)\text{-}C_2H_5O_2]^+$ and $[Pb(Gal)\text{-}C_4H_9O_4]^+$, respectively.

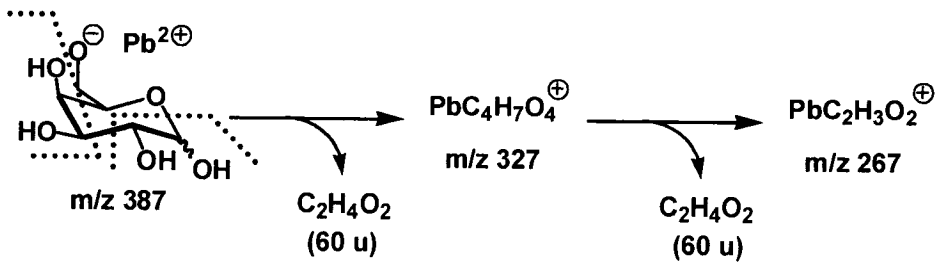

Figure 2.6 Fragmentation of a 1:1 lead:galactose ion ($PbC_6H_{11}O_6^+$) likely involves two neutral losses of 60 u: $C_2H_4O_2$.

2.1.4 Bismuth-Monosaccharide Interactions

Given that naturally occurring ^{209}Bi is 100 % abundant,[177] a characteristic isotope pattern is not observed for this element. For this reason, compared to the other metals investigated, it can often be challenging to identify mass spectral signals which represent ions containing bismuth. Of course, optimized tandem mass spectra can be used to confirm assignments of bismuth-containing peaks. However, some spectra from reaction mixture filtrates containing bismuth(III) nitrate and D-glucose, D-fructose, D-mannose, D-galactose, or D-ribose had relatively noisy baselines from which it was not possible to definitively or consistently assign peaks to ions containing both bismuth and

monosaccharide. In other cases, it may be that metal-containing peaks are present but masked by non-metal peaks at relatively high intensities (e.g., *m/z* 383: $[Na(Mon)_2]^+$).

Despite the previous statements, the results obtained should not be taken to mean that bismuth-monosaccharide complexes cannot form, or that such ions are not observable by way of ESI-MS. A peak that may correspond to a 2:1 bismuth:monosaccharide complex ion (e.g., $[Bi_2(Mon)\text{-}5H]^+$ at *m/z* 593 (Mon = Man, or Gal)) was present at low intensities in some spectra. Likewise, *m/z* 387, proposed to be a 1:1 Bi:Glc cation, has been noted. Due to the insolubility of $Bi(NO_3)_3$, increasing the concentrations of the injected samples may allow for more intense bismuth-monosaccharide peaks to be observed.

2.2 Results and Discussion: Bismuth Complexes with Aminosugars

Given that a number of important biological monosaccharides contain functional groups other than -OH, two biological glucosamines (Figure 2.7) were examined via ESI-MS in the presence of $Bi(NO_3)_3$ or $BiCl_3$. Compared to spectra for each of the free glucosamines, an ESI mass spectrum for each bismuth-glucosamine combination is shown in Figure 2.8.

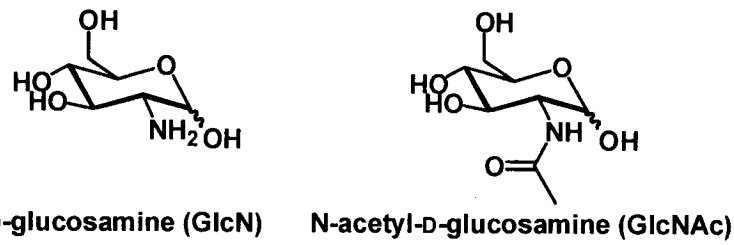

Figure 2.7 Aminosugars examined with $Bi(NO_3)_3$ or $BiCl_3$ via ESI-MS.

In general, no cations were observed to contain both bismuth and one or more intact glucosamine ligand(s). Most of the more intense signals (with relative abundances greater than 15 %) observed in a spectrum corresponding to a reaction mixture of $Bi(NO_3)_3$ and D-glucosamine hydrochloride (GlcN) (Figure 2.8b), are the same as those observed in the spectrum for free GlcN (Figure 2.8a). A few new peaks are observed, including that at *m/z* 460; however, this mass-to-charge ratio does not equate to a bismuth-glucosamine adduct. Due to a ten-fold difference in concentration from the free GlcN reaction mixture

to that containing GlcN and bismuth(III) nitrate, *m/z* 460 and other peaks may correspond to GlcN-only ions that are detected more easily at higher concentrations. Likewise, peaks present in a spectrum from GlcN in combination with bismuth(III) chloride did not appear to contain both bismuth and glucosamine (Figure 2.8c). In the case of $Bi(NO_3)_3$ and N-acetyl-D-glucosamine (GlcNAc) (Figure 2.8e), there are three relatively intense signals, *m/z* 544 (41 %), 629 (9 %), and 765 (10 %), that did not appear in the GlcNAc-only spectrum (Figure 2.8d). Again, the identities of these peaks are not clear, and these peaks are not duplicated in the spectrum from $BiCl_3$ and GlcNAc (Figure 2.8f).

Interestingly, if L-cysteine is included in a reaction mixture with bismuth(III) nitrate and GlcNAc, a new set of peaks is observed (Table 2.4). Underlined peaks in the corresponding full mass spectrum (Figure 2.9a) represent both Bi-Cys-GlcNAc complex ions, as well as 1:1 and sodiated 1:2 Bi:GlcNAc ions, identified at *m/z* 428 and *m/z* 671, respectively. It is important to reiterate that neither of these peaks were observed in the absence of cysteine (Figure 2.8e). Shown in Figure 2.9b is a spectrum from the reaction of $Bi(NO_3)_3$, L-cysteine, and D-glucosamine hydrochloride (GlcN), in which there are still no Bi-GlcN (nor Bi-Cys-GlcN peaks) observed. Table 2.5 contains a list of assignments of other peaks from both spectra in Figure 2.9. In general, it appears that there is some property of cysteine that allows for the generation of previously unobserved complex ions of bismuth(III) and N-acetyl-glucosamine. This phenomenon has been observed using other ligands with bismuth, and is discussed in subsequent Chapters.

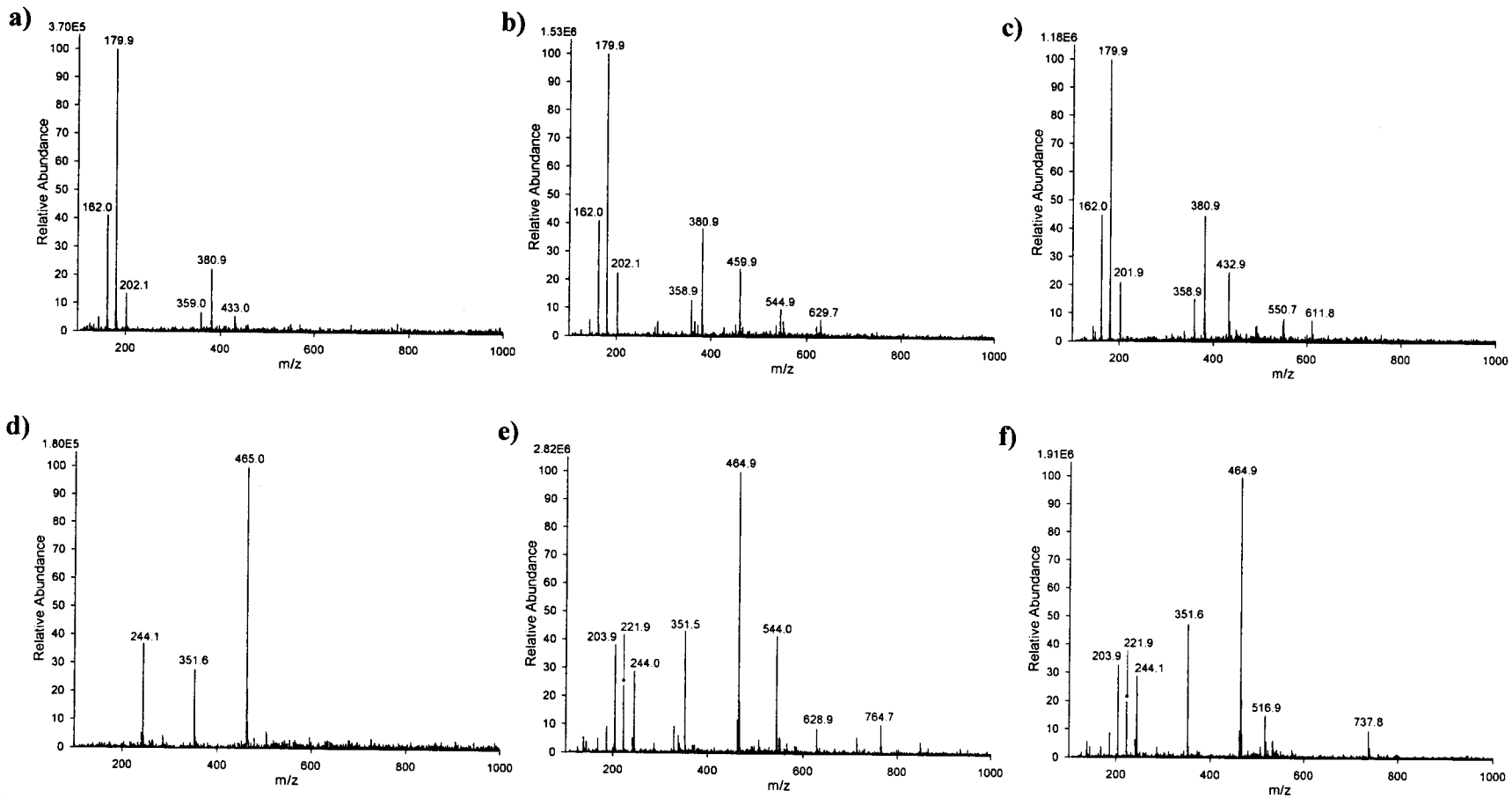

Figure 2.8 Positive ion bismuth-aminosugar ESI mass spectra. Reaction mixtures contained a) D-glucosamine hydrochloride (GlcN), b) $Bi(NO_3)_3$ and GlcN, c) $BiCl_3$ and GlcN, d) N-acetyl-D-glucosamine (GlcNAc), e) $Bi(NO_3)_3$ and GlcNAc, and f) $BiCl_3$ and GlcNAc, in 50:50 ethanol:water.

Table 2.4 Positive ion bismuth-cysteine-aminosugar ESI-MS data from reaction mixtures containing $Bi(NO_3)_3$ with L-cysteine (Cys) and N-acetyl-D-glucosamine (GlcNAc), in 50:50 ethanol:water. Shaded cells highlight peak assignments involving only Bi(III) and GlcNAc. All other listed peaks also contain Cys.

m/z	Relative Abundance (%)	Assignment
447.2	51	$[Bi(GlcNAc)-2H]^+$
548.9	76	$[Bi(Cys)(GlcNAc)-2H]^+$
570.9	17	$[BiNa(Cys)(GlcNAc)-3H]^+$
669.8	7	$[BiNa(GlcNAc)_2-3H]^+$
754.8	72	$[Bi_2(Cys)(GlcNAc)-5H]^+$
875.7	51	$[Bi_2(Cys)_2(GlcNAc)-5H]^+$
897.7	6	$[Bi_2Na(Cys)_2(GlcNAc)-6H]^+$
975.7	7	$[Bi_2(Cys)(GlcNAc)_2-5H]^+$
1081.6	10	$[Bi_3(Cys)_2(GlcNAc)-5H]^+$
1181.7	3	$[Bi_3(Cys)(GlcNAc)_2-5H]^+$
1202.5	14	$[Bi_3(Cys)_3(GlcNAc)-8H]^+$
1203.5	3	$[Bi_3Na(Cys)(GlcNAc)_2-6H]^+$
1224.5	4	$[Bi_3Na(Cys)_3(GlcNAc)-9H]^+$

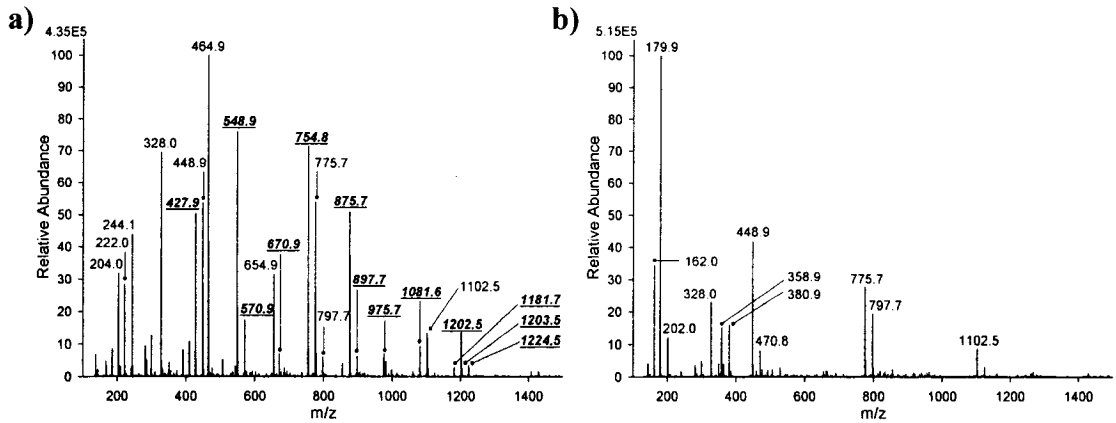

Figure 2.9 Positive ion bismuth-cysteine-aminosugar ESI mass spectra. Reaction mixtures contained $Bi(NO_3)_3$, L-cysteine (Cys), and a) N-acetyl-D-glucosamine or b) D-glucosamine hydrochloride, in 50:50 ethanol:water. Underlined peaks represent ions assigned to Bi-Cys-GlcNAc or Bi-GlcNAc complex ions. No Bi-Cys-GlcN nor Bi-GlcN ions were identified.

Table 2.5 Extended positive ion bismuth-cysteine-aminosugar ESI-MS data from reaction mixtures containing $Bi(NO_3)_3$ with L-cysteine (Cys) and N-acetyl-D-glucosamine (GlcNAc) or D-glucosamine hydrochloride (GlcN), in 50:50 ethanol:water. Peaks associated with ions containing both Bi(III) and aminosugar are listed in Table 2.4.

Contents of Reaction Mixture	*m/z*	Relative Abundance (%)	Assignment
$Bi(NO_3)_3$/Cys/GlcNAc	204.0	32	$[(GlcNAc)-OH]^+$
	222.0	28	$[(GlcNAc)+H]^+$
	244.1	44	$[Na(GlcNAc)]^+$
	328.0	69	$[Bi(Cys)-2H]^+$
	448.9	54	$[Bi(Cys)_2-2H]^+$
	464.9	100	$[Na(GlcNAc)_2]^+$
	654.9	32	$[Bi_2(Cys)_2-5H]^+$
	775.7	54	$[Bi_2(Cys)_3-5H]^+$
	797.7	6	$[Bi_2Na(Cys)_3-6H]^+$
	1102.5	13	$[Bi_3(Cys)_4-8H]^+$
$Bi(NO_3)_3$/Cys/GlcN	162.0	34	$[(GlcN)-OH]^+$
	179.9	100	$[(GlcN)+H]^+$
	202.0	12	$[Na(GlcN)]^+$
	328.0	23	$[Bi(Cys)-2H]^+$
	358.9	15	$[(GlcN)_2+H]^+$
	380.9	16	$[Na(GlcN)_2]^+$
	448.9	42	$[Bi(Cys)_2-2H]^+$
	470.8	8	$[BiNa(Cys)_2-3H]^+$
	775.7	28	$[Bi_2(Cys)_3-5H]^+$
	797.7	19	$[Bi_2Na(Cys)_3-6H]^+$
	1102.5	9	$[Bi_3(Cys)_4-8H]^+$

2.3 Results and Discussion: Bismuth Complexes with Thiosugars

Although little ESI-MS evidence was obtained for complexes between Bi(III) salts and monosaccharides (including glucose, fructose, mannose, galactose, ribose, as well as glucosamine and N-acetyl-glucosamine, excluding cysteine from the reaction mixture), another attempt was made to observe direct bismuth-monosaccharide interactions by exploiting the thiophilicity of bismuth. Thiosugars such as a 1-thio-β-D-glucose sodium salt (TGSS) and 1-thio-β-D-glucose tetraacetate (TGTA) (Figures 1.3, 2.10) are not endogenous biomolecules; however, they are without a doubt biologically significant. As mentioned previously, Auranofin® is a pharmaceutical currently available for the treatment of arthritis, and contains gold(I) coordinated by one TGTA ligand (Figure 1.1h).[61] The compound is a prodrug, and dissociation of the TGTA ligand from the metal allows a second ligand (triethylphosphine) to dissociate, leaving the gold(I) cation free to interact with endogenous ligands that are necessary for transport and bioactivity of

gold(I). Similarly, an examination of the chemistry of bismuth-thioglucose complexes is interesting from both fundamental and medicinal perspectives.

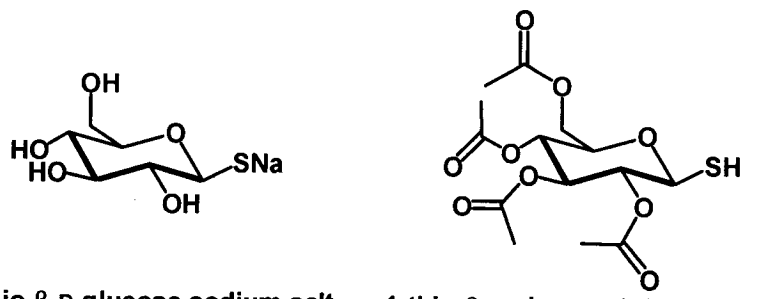

1-thio-β-D-glucose sodium salt (TGSS)

1-thio-β-D-glucose tetraacetate (TGTA)

Figure 2.10 Thiosugars examined in the presence of $Bi(NO_3)_3$ via ESI-MS.

The two thiosugars shown in Figure 2.10 were each combined with bismuth(III) nitrate, and bismuth-thiosugar complex ions were indeed observed using ESI-MS. Relevant *m/z* peaks are reported in Table 2.6. It can be noted that the same samples were injected into the mass spectrometer a second time a few days after the first analysis; however, by that time the spectra were more complex. In general, it has been observed that solutions of these thiosugars decompose readily in air; therefore, experiments must ensure that spectral data is recorded soon after reactants are combined.

An ESI mass spectrum (Figure 2.11a) from a reaction mixture containing $Bi(NO_3)_3$ and TGSS reveals a 1:2 bismuth:thioglucose ion as the base peak: $[Bi(TGSS)_2\text{-}Na\text{-}H]^+$ at *m/z* 621. A sodiated 1:3 bismuth:thioglucose monocation, $[Bi(TGSS)_3\text{-}2Na]^+$, is also prominent (61 %) at *m/z* 817. Likewise, 1:2 and 1:3 bismuth-thioglucose ions were also observed upon combination of $Bi(NO_3)_3$ and TGTA (Figure 2.11b). Peaks at *m/z* 935 (100 %) and *m/z* 1321 (76 %) are the most relatively abundant signals in the spectrum, and correspond to ions, $[Bi(TGTA)_2\text{-}2H]^+$ and $[BiNa(TGTA)_3\text{-}3H]^+$, respectively. The unique isotope pattern of sulfur (^{32}S (95.02 %), ^{33}S (0.75 %), ^{34}S (4.21 %), ^{36}S (0.02 %))[177] makes it possible to validate these peak assignments by way of isotope pattern comparisons (Figure 2.12). Moreover, MS/MS data has been acquired to support some of the peak assignments that have been made (Figure 2.13).

Table 2.6 Positive ion bismuth-thiosugar ESI-MS data from reaction mixtures containing $Bi(NO_3)_3$ and 1-thio-β-D-glucose sodium salt (TGSS) or 1-thio-β-D-glucose tetraacetate (TGTA), in 50:50 ethanol:water.

Contents of Reaction Mixture	*m/z*	Relative Abundance (%)	Assignment
$Bi(NO_3)_3$/TGSS	621.0	100	$[Bi(TGSS)_2\text{-}Na\text{-}H]^+$
	816.9	61	$[Bi(TGSS)_3\text{-}2Na]^+$
$Bi(NO_3)_3$/TGTA	330.9	21	$[TGTA\text{-}SH]^+$
	626.9	7	$[BiNa(TGTA)(S)\text{-}H]^+$
	717.2	3	$[Na(TGTA\text{-}SH)(TGTA\text{-}H)]^+$
	844.6	28	$[BiNa_2(TGTA)(S)(TGTA\text{-}4C_2H_2O)\text{-}2H]^+$
	892.9	29	$[Bi(TGTA)_2\text{-}C_2H_2O\text{-}2H]^+$
	934.9	100	$[Bi(TGTA)_2\text{-}2H]^+$
	1017.1	5	$[BiNa(TGTA)_2(C_2H_4O_2)\text{-}3H]^+$
	1279.0	25	$[BiNa(TGTA)_3\text{-}C_2H_2O\text{-}3H]^+$
	1321.0	76	$[BiNa(TGTA)_3\text{-}3H]^+$
	1496.6	18	$[BiNa_2(TGTA)_3(TGTA\text{-}4C_2H_2O)\text{-}C_2H_2O\text{-}4H]^+$
	1538.5	38	$[BiNa_2(TGTA)_3(TGTA\text{-}4C_2H_2O)\text{-}4H]^+$

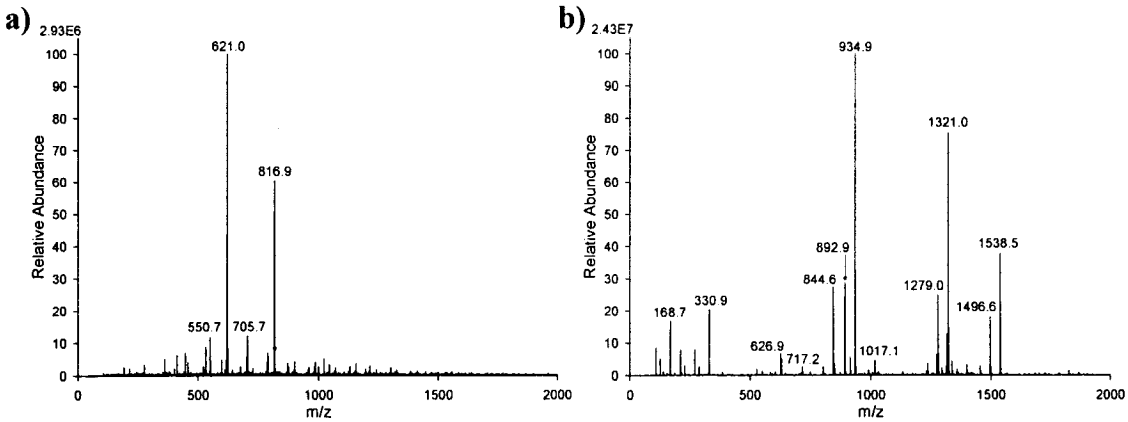

Figure 2.11 Positive ion bismuth-thiosugar ESI mass spectra. Reaction mixtures contained $Bi(NO_3)_3$ and a) 1-thio-β-D-glucose sodium salt (TGSS) or b) 1-thio-β-D-glucose tetraacetate (TGTA), in 50:50 ethanol:water.

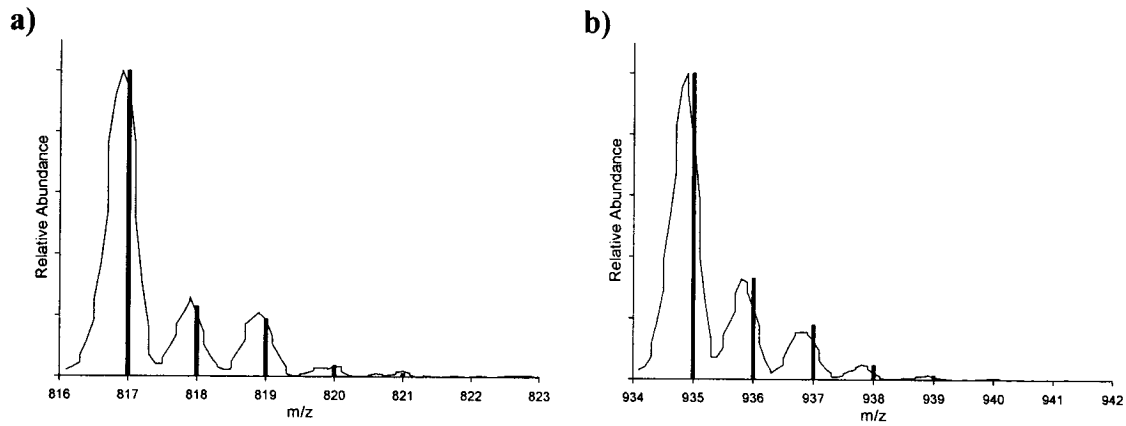

Figure 2.12 Comparison of bismuth-thiosugar isotope patterns. Experimental (continuous thin line) and calculated (dark vertical bars) isotope patterns are shown for a) *m/z* 817, assigned as $[Bi(TGSS)_3\text{-}2Na]^+$ ($BiNaC_{18}H_{33}O_{15}S_3$), and b) *m/z* 935, assigned as $[Bi(TGTA)_2\text{-}2H]^+$ ($BiC_{28}H_{38}O_{18}S_2$).

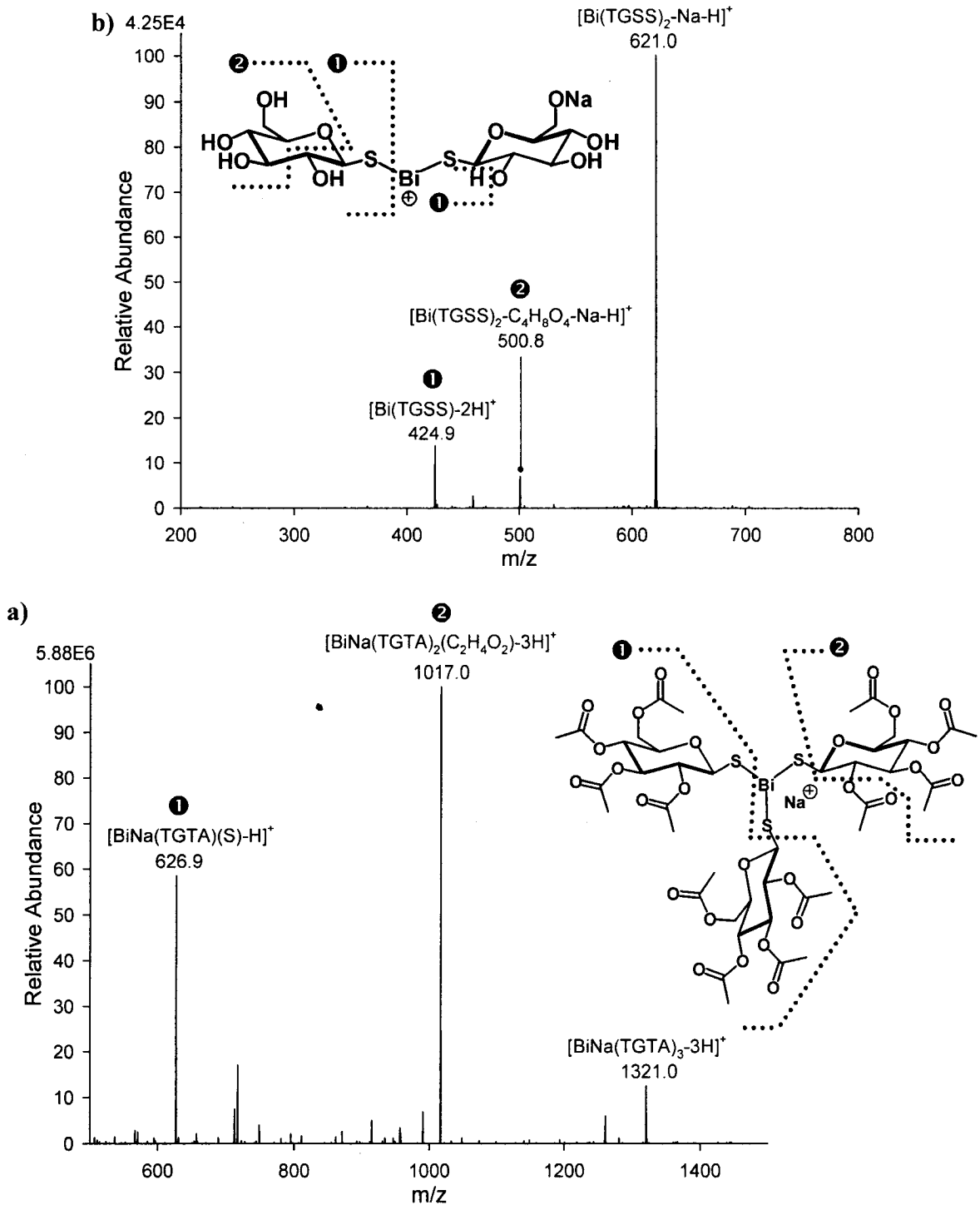

Figure 2.13 Bismuth-thiosugar tandem mass spectra. a) CID of $[Bi(TGSS)_2\text{-}Na\text{-}H]^+$ represented by *m/z* 621 generates product ions at *m/z* 501 and *m/z* 425. b) Ions assigned as $[BiNa(TGTA)_3\text{-}3H]^+$ at *m/z* 1321 undergo CID to yield two main product ions at *m/z* 1017 and *m/z* 627. Potential structures are shown along with dotted lines which suggest axes of ion dissociation.

2.4 Conclusions

Table 2.7 presents a summary of the metal:monosaccharide complex ions observed from ESI-MS studies of Hg(II), Tl(I), Pb(II) and Bi(III) with Glc, Fru, Man and Gal. Notably, Hg(II) complexes of Man and Gal also resulted from Hg(I) reaction mixtures. Hg(I), Hg(II) and Tl(I) are soft acids and are therefore not expected to interact strongly with hard basic donor groups such as ROH or RO^- present in monosaccharides. Pb(II) and Bi(III) are borderline acids, and as such should interact somewhat more strongly with oxygen donors than Hg(I)/(II) and Tl(I). Indeed, as other literature indicates,[193] Pb(II) was observed to interact with common monosaccharides (including Rib) to form numerous lead-sugar species. In contrast, mass spectral peaks corresponding to bismuth-monosaccharide interactions were not readily observed.

Table 2.7 Summary of observed positive ion metal:monosaccharide stoichiometric ratios.

	D-Glucose	D-Fructose	D-Mannose	D-Galactose
Hg(II)	1:2	-	1:2	1:2
	2:2	-	2:2	2:2
Tl(I)	1:1	1:1	1:1	1:1
Pb(II)	1:1	1:1	1:1	1:1
	1:2	-	1:2	1:2
	2:1	-	2:1	2:1
	2:2	2:2	2:2	2:2
	3:1	-	3:1	3:1
	3:2	3:2	3:2	3:2
	4:2	4:2	4:2	4:2
Bi(III)	-	-	-	-

Some of the observations described above can be explained based on the solubility of different metal-monosaccharide combinations in 50:50 ethanol:water. All thallium- and lead-monosaccharide samples were clear, colourless solutions, meaning that full solubility was achieved for each of these metal nitrate salts in the presence of each monosaccharide investigated. For this reason, the dilute concentrations of the lead and thallium reaction mixtures injected into the mass spectrometer can be assumed accurate. In the cases of mercury and bismuth, full solubility was not achieved and solid material was separated from all mercury- and bismuth-monosaccharide reaction mixtures via filtration. Injected sample concentrations were not quantitatively determined; however, it is noted that loss of reactant(s) prior to dilution of filtrates from mercury and bismuth

samples produced concentrations lower than reported in Section 2.5.1 of this account. Although ESI-MS is renowned for analysis of low-concentration samples, at concentrations below ~10^{-4} M the low signal-to-noise ratio of the metal-monosaccharide samples examined was enough to complicate spectral interpretation due to increased relative abundances of baseline peaks.

In general, isolated residues from sample filtrations were also not comprehensively characterized; however, information that was obtained from these residues indicated that the pursuit of their characterization was not necessarily essential. For example, given that bismuth(III) nitrate is insoluble in numerous solvents, it was not surprising that full dissolution of this salt did not occur. Perhaps bismuth-monosaccharide interactions are possible under conditions in which a greater concentration of solubilized bismuth(III) is achieved. Improved solubility of bismuth(III) has been observed previously in the presence of various thiols including cysteine,[138] and it may be the inclusion of cysteine in the aforementioned reaction mixtures that has facilitated the identification of intact complexes of bismuth(III) and N-acetyl-glucosamine.

In an attempt to study the interactions between metals and nucleobases (discussed in Chapter 3) Bi(III) was combined with guanine under reaction conditions similar to those described for lead- and bismuth-monosaccharide reaction mixtures. No bismuth-guanine spectral peaks were observed, and an isolated white residue was examined by Raman spectrometry, only to find that the Raman spectrum matched that of guanine itself. Again, solubility may be the essential reason for which interactions between bismuth (and mercury) salts and biologically relevant molecules such as monosaccharides or nucleobases have not yet been observed by way of ESI-MS. In the future, further information about these metal-biomolecule reaction mixtures could be acquired by comparing the sum of the masses of reactants with the mass of the insoluble components to gauge the extent of solubility achieved.

Although bismuth-containing complex ions were not observed with common monosaccharides, Glc, Fru, Man, Gal, or Rib, nor directly with aminosugars, GlcN or

GlcNAc, it is of interest – and not surprising, given the thiophilicity of bismuth – that 1:2 and 1:3 Bi:TGSS and Bi:TGTA complex ions were observed. Based on these results, the significance of biologically relevant bismuth-sulfur chemistry is emphasized. Bismuth-thioglucose samples have already been observed to undergo a colour change over a period of a few days, making subsequent analyses and growth of crystals by slow evaporation methods difficult. In the future, inert atmosphere techniques may need to be applied to achieve further characterization of these complexes.

2.5 Experimental Methods

Caution: some of the metal salts used in these experiments are toxic to living systems. Safety precautions were taken as outlined in Section 1.6. Mercury(I) nitrate dihydrate and mercury(II) nitrate monohydrate were used as received from Sigma-Aldrich. Lead(II) nitrate was used as received from BDH. Thallium(I) nitrate, bismuth(III) nitrate pentahydrate, bismuth(III) chloride, D-glucose, D-fructose, D-ribose, and 1-thio-β-D-glucose tetraacetate were used as received from Aldrich. D-Mannose, D-galactose, 1-thio-β-D-glucose sodium salt, D-glucosamine hydrochloride, and N-acetyl-D-glucosamine were used as received from Sigma. Ethanol (95 % or HPLC reagent grade) was used as received from Commercial Alcohols, Inc. or Fisher, respectively. All reactions were performed at room temperature using distilled water. Raman spectra were obtained for powdered samples on a Bruker RFS 100 instrument equipped with an Nd:YAG laser (1064 nm).

2.5.1 Reaction Mixtures of $Hg_2(NO_3)_2$ or $Hg(NO_3)_2$ and a Monosaccharide

$Hg_2(NO_3)_2 \cdot 2H_2O$ (0.112 g, 0.200 mmol) was stirred with D-glucose, D-fructose, D-mannose, or D-galactose (0.036 g, 0.20 mmol) in 20 mL 50:50 ethanol:water, yielding concentrations ca. 0.01 M. Each 20 mL reaction mixture initially contained a yellow precipitate. After 26 to 28 h all reaction mixtures were olive green, and upon suction filtration gave an olive green residue and a clear, colourless filtrate. Within 45 to 47 h of preparing the original reaction mixtures, each filtrate was diluted to 0.00025 M and injected directly into the electrospray source of the mass spectrometer.

$Hg(NO_3)_2 \cdot H_2O$ (0.068 g or 0.070 g, 0.20 mmol) was stirred with D-glucose, D-fructose, D-mannose, or D-galactose (0.036 g or 0.037 g, 0.20 mmol or 0.21 mmol, respectively) in 20 mL 50:50 ethanol:water, yielding concentrations ca. 0.01 M. Each 20 mL reaction mixture was initially cloudy. After 22 to 25 h all mixtures were suction filtered, each yielding a pale yellow residue and a clear, colourless filtrate. Within 23 to 26 h of preparing the original reaction mixtures, each filtate was diluted to 0.001 M and injected directly into the electrospray source of the mass spectrometer. Ranges of data in Table 2.1 reflect spectra aquired from two injections of the same Hg(I) or Hg(II) sample.

2.5.2 Reaction Mixtures of $TlNO_3$ and a Monosaccharide

$TlNO_3$ (0.054 g, 0.20 mmol) was stirred with D-glucose, D-fructose, D-mannose, or D-galactose (0.036 g, 0.20 mmol) in 20 mL 50:50 ethanol:water, yielding concentrations ca. 0.01 M. After 22 to 28 h the resulting clear, colourless 20 mL reaction mixtures were suction filtered (no residues were obtained). Within 49 to 51 h of preparing the original reaction mixtures, each filtrate was diluted to 0.0001 M and injected directly into the electrospray source of the mass spectrometer. Data in Table 2.2 reflect spectra acquired from one injection of each Tl(I) sample.

2.5.3 Reaction Mixtures of $Pb(NO_3)_2$ and a Monosaccharide

$Pb(NO_3)_2$ (0.099 g to 0.102 g, 0.299 mmol to 0.308 mmol, respectively) was stirred with D-glucose (0.055 g, 0.30 mmol), D-fructose (0.056 g, 0.31 mmol), or D-ribose (0.045 g, 0.30 mmol) in 30 mL 50:50 ethanol:water, yielding concentrations ca. 0.01 M. Alternatively, $Pb(NO_3)_2$ (0.332 g, 1.00 mmol) was stirred with D-mannose or D-galactose (0.181 g, 1.00 mmol) in 20 mL 50:50 ethanol:water, yielding solution concentrations ca. 0.05 M. After 20 to 24 h, the resulting clear, colourless 20 mL or 30 mL reaction mixtures were suction filtered (no residues were obtained). Within 39 to 45 h of preparing the original reaction mixtures, each 0.01 M sample was injected directly into the electrospray source of the mass spectrometer, and each 0.05 M sample was diluted to 0.0005 M prior to injection. Data in Table 2.3 reflect spectra acquired from one injection of each Pb(II) sample.

2.5.4 Reaction Mixtures of $Bi(NO_3)_3$ and a Monosaccharide

$Bi(NO_3)_3 \cdot 5H_2O$ (0.097 g to 0.099 g, 0.20 mmol) or $BiCl_3$ (0.063 g, 0.20 mmol) was stirred with D-glucose, D-fructose, D-mannose, D-galactose (0.036 g, 0.20 mmol), D-ribose (0.030 g, 0.20 mmol), D-glucosamine hydrochloride (GlcN, 0.043 g, 0.20 mmol), N-acetyl-D-glucosamine (GlcNAc, 0.044 g or 0.045 g, 0.20 mmol), 1-thio-β-D-glucose sodium salt (TGSS, 0.044 g, 0.20 mmol), or 1-thio-β-D-glucose tetraacetate (TGTA, 0.073 g, 0.20 mmol) in 20 mL 50:50 ethanol:water, yielding concentrations ca. 0.01 M. Alternatively, $Bi(NO_3)_3 \cdot 5H_2O$ (0.098 or 0.099 g, 0.20 mmol) was stirred with D-glucosamine hydrochloride (0.043 g, 0.20 mmol) or N-acetyl-D-glucosamine (0.045 g, 0.20 mmol) and L-cysteine (0.024 or 0.025 g, 0.20 or 0.21 mmol, respectively) in 20 mL 50:50 ethanol:water, yielding concentrations ca. 0.01 M. In some cases the $Bi(NO_3)_3 \cdot 5H_2O$ was ground up using a mortar and pestle prior to the addition of this compound to the reaction mixtures. For comparison to bismuth-GlcN and bismuth-GlcNAc reaction mixtures, GlcN (0.043 g, 0.20 mmol) and GlcNAc (0.044 g, 0.20 mmol) were each stirred in 20 mL 50:50 ethanol:water, yielding concentrations of 0.01 M.

Most of the reaction mixtures were initially cloudy grey/white or yellow in appearance (clear and colourless when GlcN or GlcNAc was used in the absence of a bismuth salt). After 15 to 27 h, most of the prepared mixtures were suction filtered to yield a white residue and a clear, colourless or yellow filtrate. One mixture, containing $Bi(NO_3)_3$ and D-fructose, was filtered by gravity through cotton, yielding a nearly clear and colourless filtrate. In some cases, reaction mixtures were passed through a NALGENE® cellulose acetate or polytetrafluoroethylene (PTFE, Teflon®) syringe filter (0.2 μm pore size, 25 mm diameter) to produce clear, colourless or yellow filtrates. Within one to five days of preparing the original reaction mixtures, each sample was either injected directly into the electrospray source of the mass spectrometer or diluted to 0.001 M, 0.0001 M, or 0.0005 M prior to injection. Data in Tables 2.4 to 2.6 reflect spectra acquired from one injection of each sample.

2.5.5 Electrospray Ionization Mass Spectrometry

ESI mass spectra were obtained using a Finnigan^{TM} LCQ^{TM}$_{DUO}$ quadrupole ion trap mass spectrometer. Each dilute filtrate was injected (in 10 or 20 μL aliquots) directly into the electrospray ionization source of the mass spectrometer. The solvent flow rate was set at 1.2 mL/h, the spray voltage at 4.0 kV (4.5 kV for reaction mixtures containing bismuth(III) nitrate and 1-thio-β-D-glucose tetraacetate or 1-thio-β-D-glucose sodium salt), and the capillary temperature at 200 °C (210 °C). Tandem mass spectra were obtained using helium as the collision gas.

Chapter 3 Bismuth-Nucleobase Complexes

It is important to recognize that although the mechanism of bismuth bioactivity probably involves coordination of bismuth by one or more thiolate moieties, not all biomolecules contain sulfur, and other elements (e.g., oxygen, carbon, hydrogen, nitrogen) are also more abundant in the human body. Given the labile nature of bismuth-oxygen interactions in solution, it is likely that BSS, CBS, and RBC act as prodrugs, meaning that once these compounds are inside the human body the original citrate or salicylate ligands coordinated to bismuth are displaced by endogenous donor molecules. Due to the sophistication of human biochemistry, and the capacity of bismuth to form bonds with various heteroatomic donors, bismuth-based compounds may well undergo multiple chemical transformations between intake and elimination of bismuth from the body.

Previously in this document, discussion has been made of bismuth-amino acid and bismuth-monosaccharide complexes in comparison to complexes of other, more noxious metal ions such as mercury(I), mercury(II), lead(II), and thallium(I). Bismuth(III) is known to interact with a selection of amino acids, including those containing sulfur: cysteine, homocysteine, and methionine.[16;17] ESI-MS results described in Chapter 2 indicate that under the experimental conditions applied, bismuth(III) favours coordination to biologically relevant thiosugars compared to monosaccharides which feature only oxygen and/or nitrogen donor atoms. However, it was also noted that adding L-cysteine to a mixture of $Bi(NO_3)_3$ and aminosugar, N-acetyl-D-glucosamine, gave a new set of spectral peaks, some of which were assigned to ions containing both bismuth(III) and the aminosugar. This intriguing result intimates that thiol-containing cysteine somehow facilitates other interactions between bismuth and non-thiol ligands, a concept which is explored further in this Chapter and in Chapter 5. In general, the results summarized in this paragraph are not unexpected given the well-established thiophilicity of bismuth.[12]

The effects of metals on DNA and related biomolecules is of interest;[197-199] therefore, in the current Chapter the ESI-MS examination of interactions of bismuth with nucleobases (NBs), adenine (A), guanine (G), cytosine (C), thymine (T), and uracil (U) will be

described. In particular, the emphasis will be on reaction mixtures containing Bi(III), a nucleobase, and cysteine.

The essential components of ribonucleic acid (RNA) and deoxyribonucleic acid (DNA) are illustrated in Figure 3.1. Nucleic acids are best thought of as the building blocks of life, responsible for storing and reproducing genetic data. These acids are polymers composed of nucleotide links, each of which contains two smaller chemical units: a phosphorylated derivative of ribose and a purine or pyrimidine base. For completeness, it can be noted that a dephosphorylated nucleotide contains only ribose and base, and is referred to as a nucleoside.[72]

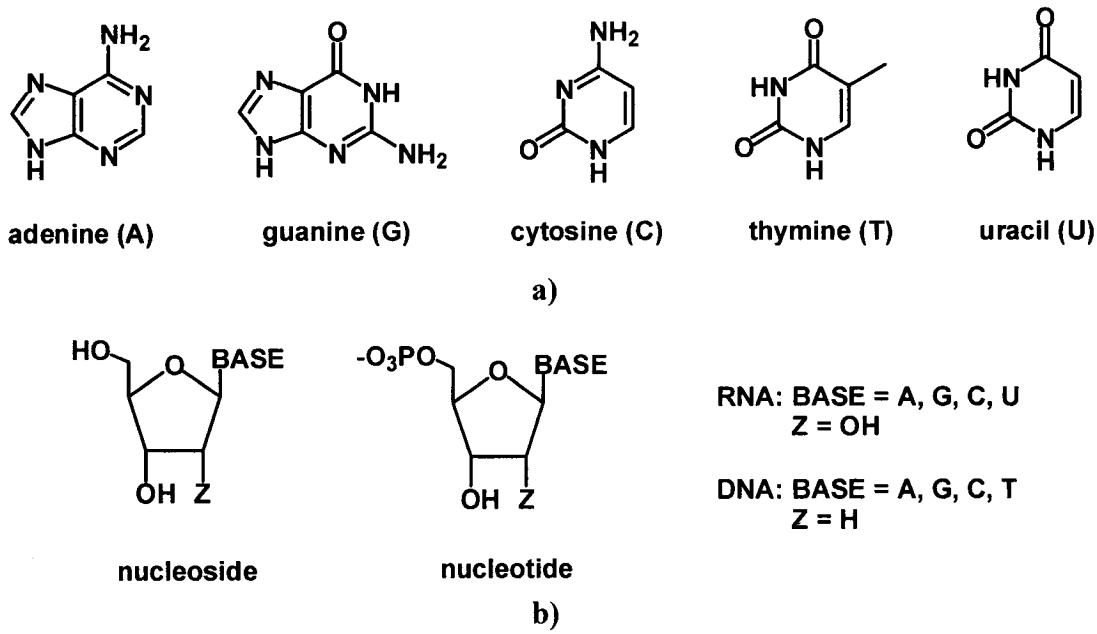

Figure 3.1 Components of nucleic acids. a) Purine (A, G) and pyrimidine (C, T, U) bases. b) General structures of nucleosides and nucleotides.

Relevant previous work in this area includes the mass spectrometric analysis of nucleic acids and constituents,[200;201] as well as complexes formed between these compounds and alkali metal ions.[202-204] A recent report describes the production of two solid state bismuth-nucleoside structures (Figure 3.2).[205] Two oxygen atoms from hydroxyl groups in each of two ribofuranose rings (from two adenosine ligands (Figure 3.2a) or two guanosine ligands (Figure 3.2b)) are coordinated to bismuth. Another solid state structure is known in which bismuth is coordinated by a derivative of

diethylenetriaminepentaacetic acid with two pendant thioaminouracil groups (Figure 3.3).[206] In this structure bismuth(III) is located at the centre of a monocapped square antiprism created by nonacoordination of three amine, five carboxylate, and one aqua donor moieties; therefore, the uracil units do not interact directly with bismuth. From a materials perspective, the adsorption of nucleobase, uracil, onto bismuth electrodes has also been documented.[207;208]

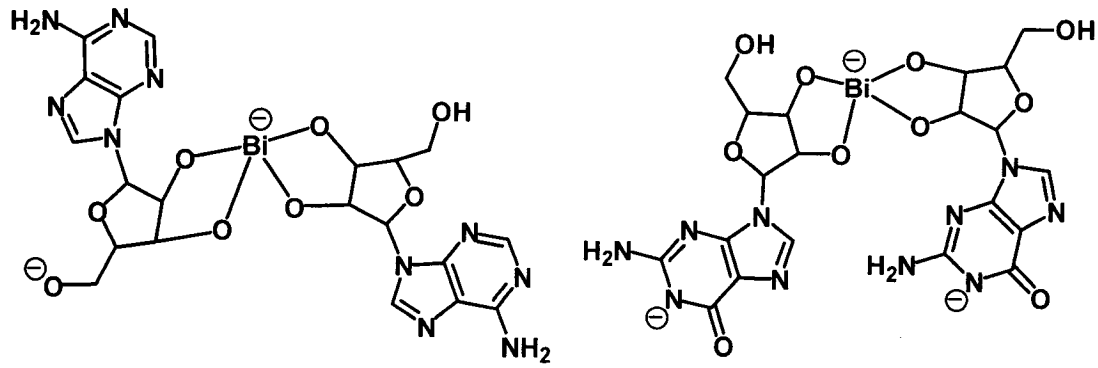

a) b)

Figure 3.2 Solid state bismuth-nucleoside compounds. a) Diadenosinatobismuth(III) counterbalanced by two sodium cations, and b) diguanosinatobismuth(III) counterbalanced by a $[Co(NH_3)_6]^{3+}$ complex cation.

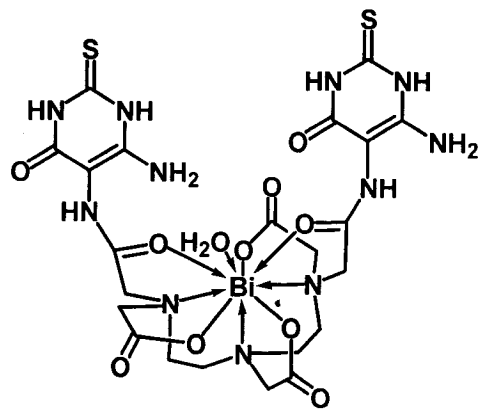

Figure 3.3 Bis(thioaminouracil)-derivatized aquadiethylenetriaminepentaacetato-bismuth(III).

3.1 Results and Discussion: Bismuth Complexes with Nucleobases and Cysteine

In Table 3.1 bismuth-cysteine and bismuth-cysteine-nucleobase complex ions are listed. Both types of ions were assigned in ESI mass spectra generated from three-component reaction mixtures containing bismuth(III) nitrate, L-cysteine, and adenine, guanine, cytosine, thymine, or uracil. A summary of Bi:Cys:NB ratios is provided in Table 3.2.

Similar to the observation described in Chapter 2 of a lack of bismuth-monosaccharide complex ions (monosaccharide ≠ thiosugar), bismuth-nucleobase ions were not identified in ESI mass spectra from reaction mixtures containing only bismuth(III) nitrate and A, C, G, T, or U. However, when Cys was included in these reaction mixtures, several new complex ions were discerned containing all three components (Table 3.1): $[Bi(Cys)(A)-2H]^+$ (*m/z* 463), $[Bi(Cys)(G)-2H]^+$ (*m/z* 479), $[Bi(Cys)(C)-2H]^+$ (*m/z* 439), $[BiK(Cys)_2(C)-3H]^+$ (*m/z* 598), $[Bi(Cys)(T)-2H]^+$ (*m/z* 454), $[BiNa(Cys)(T)-3H]^+$ (*m/z* 476), $[Bi_2(Cys)_2(T)-5H]^+$ (*m/z* 781), $[Bi(Cys)(U)-2H]^+$ (*m/z* 440), and $[Bi_2(Cys)_2(U)-5H]^+$ (*m/z* 767). No complex ions containing bismuth and nucleobase ligands only were observed in the presence of cysteine.

A 1:1:1 Bi:Cys:NB complex ion has been assigned for each combination of bismuth, cysteine and a nucleobase. The 1:1:1 stoichiometry is the only one observed for samples containing a purine, A or G. For pyrimidines T and U, with two carbonyl substituents (Figure 3.1), a 2:2:1 Bi:Cys:NB cation was also observed. In comparison, a potassiated 1:2:1 Bi:Cys:C cation was assigned where pyrimidine cytosine is concerned. Although more information is needed to understand the structures of these bismuth-cysteine-nucleobase complexes, it is reasonable to speculate that the formation of certain types (stoichiometries) of ions containing bismuth and purine or pyrimidine ligands is a function of the structure of the ligand involved.

Table 3.1 Positive ion bismuth-nucleobase ESI-MS data from reaction mixtures containing $Bi(NO_3)_3$ and L-cysteine (Cys) with adenine (A), cytosine (C), guanine (G), thymine (T), or uracil (U), in 50:50 ethanol:water. Shaded blocks indicate ratios corresponding to triple-component bismuth-cysteine-nucleobase complex ions. All other figures correspond to bismuth-cysteine complex ions.

Contents of Reaction Mixture	*m/z*	Relative Abundance (%)	Assignment
$Bi(NO_3)_3$/Cys/A	136.1	100	$[(A)+H]^+$
	328.1	29-52	$[Bi(Cys)-2H]^+$
	449.0-449.1	45-82	$[Bi(Cys)_2-2H]^+$
	[illegible]	[illegible]	[illegible]
	471.0-471.1	8-10	$[BiNa(Cys)_2-3H]^+$
	477.0-477.1	12-17	$[Bi(Cys)_2(CO)-2H]^+$
	504.9-505.0	5-8	$[Bi(Cys)_2(CO)_2-2H]^+$
	654.9-655.0	11-43	$[Bi_2(Cys)_2-5H]^+$
	775.8	51-98	$[Bi_2(Cys)_3-5H]^+$
	797.8	24-34	$[Bi_2Na(Cys)_3-6H]^+$
	803.7	6-15	$[Bi_2(Cys)_3(CO)-5H]^+$
	813.7-813.9	8-11	$[Bi_2K(Cys)_3-6H]^+$
	934.7	8-13	$[Bi_2K(Cys)_4-6H]^+$
	981.6-981.7	2-9	$[Bi_3(Cys)_3-8H]^+$
	1102.5-1102.6	18-48	$[Bi_3(Cys)_4-8H]^+$
	1124.4-1124.5	6-12	$[Bi_3Na(Cys)_4-9H]^+$
	1261.7	9-12	$[Bi_3K(Cys)_5-9H]^+$
$Bi(NO_3)_3$/Cys/G	328.1	61	$[Bi(Cys)-2H]^+$
	356.1	12	$[Bi(Cys)(CO)-2H]^+$
	449.0	94	$[Bi(Cys)_2-2H]^+$
	477.0	32	$[Bi(Cys)_2(CO)-2H]^+$
	[illegible]	[illegible]	[illegible]
	504.9	8	$[Bi(Cys)_2(CO)_2-2H]^+$
	654.9	36	$[Bi_2(Cys)_2-5H]^+$
	775.7	100	$[Bi_2(Cys)_3-5H]^+$
	797.7	14	$[Bi_2Na(Cys)_3-6H]^+$
	803.7	15	$[Bi_2(Cys)_3(CO)-5H]^+$
	981.6	7	$[Bi_3(Cys)_3-8H]^+$
	1102.5	35	$[Bi_3(Cys)_4-8H]^+$

Contents of Reaction Mixture	*m/z*	Relative Abundance (%)	Assignment
$Bi(NO_3)_3$/Cys/C	328.1	43	$[Bi(Cys)-2H]^+$
	[illegible]	[illegible]	[illegible]
	449.0	82	$[Bi(Cys)_2-2H]^+$
	476.9	12	$[Bi(Cys)_2(CO)-2H]^+$
	[illegible]	[illegible]	[illegible]
	654.9	10	$[Bi_2(Cys)_2-5H]^+$
	775.8	100	$[Bi_2(Cys)_3-5H]^+$
	797.7	20	$[Bi_2Na(Cys)_3-6H]^+$
	803.7	8	$[Bi_2(Cys)_3(CO)-5H]^+$
	934.7	5	$[Bi_2K(Cys)_4-6H]^+$
	1102.5	48	$[Bi_3(Cys)_4-8H]^+$
	1124.5	9	$[Bi_3Na(Cys)_4-9H]^+$
	1261.5	10	$[Bi_3K(Cys)_5-9H]^+$
$Bi(NO_3)_3$/Cys/T	328.1	84	$[Bi(Cys)-2H]^+$
	350.1	8	$[BiNa(Cys)-3H]^+$
	356.1	17	$[Bi(Cys)(CO)-2H]^+$
	449.0	100	$[Bi(Cys)_2-2H]^+$
	[illegible]	[illegible]	[illegible]
	470.9	9	$[BiNa(Cys)_2-3H]^+$
	[illegible]	[illegible]	[illegible]
	477.0	34	$[Bi(Cys)_2(CO)-2H]^+$
	505.0	9	$[Bi(Cys)_2(CO)_2-2H]^+$
	654.9	58	$[Bi_2(Cys)_2-5H]^+$
	775.7	92	$[Bi_2(Cys)_3-5H]^+$
	[illegible]	[illegible]	[illegible]
	797.7	26	$[Bi_2Na(Cys)_3-6H]^+$
	803.6	14	$[Bi_2(Cys)_3(CO)-5H]^+$
	981.5	7	$[Bi_3(Cys)_3-8H]^+$
	1102.5	24	$[Bi_3(Cys)_4-8H]^+$
$Bi(NO_3)_3$/Cys/U	328.1	6	$[Bi(Cys)-2H]^+$
	356.1	19	$[Bi(Cys)(CO)-2H]^+$
	[illegible]	[illegible]	[illegible]
	449.1	99	$[Bi(Cys)_2-2H]^+$
	477.0	41	$[Bi(Cys)_2(CO)-2H]^+$
	505.0	8	$[Bi(Cys)_2(CO)_2-2H]^+$
	654.9	62	$[Bi_2(Cys)_2-5H]^+$
	[illegible]	[illegible]	[illegible]
	775.7	100	$[Bi_2(Cys)_3-5H]^+$
	797.7	9	$[Bi_2Na(Cys)_3-6H]^+$
	803.6	18	$[Bi_2(Cys)_3(CO)-5H]^+$
	981.6	9	$[Bi_3(Cys)_3-8H]^+$
	1102.5	29	$[Bi_3(Cys)_4-8H]^+$

Table 3.2 Summary of observed positive ion bismuth:cysteine:nucleobase stoichiometric ratios. Shaded blocks indicate ratios corresponding to triple-component bismuth-cysteine-nucleobase complex ions. All other ratios correspond to bismuth-cysteine complex ions.

Bi:Cys:A	Bi:Cys:C	Bi:Cys:G	Bi:Cys:T	Bi:Cys:U
1:1:0	1:1:0	1:1:0	1:1:0	1:1:0
-	-	-	1:1:0:Na	-
-	-	1:1:0:CO	1:1:0:CO	1:1:0:CO
1:2:0	1:2:0	1:2:0	1:2:0	1:2:0
1:2:0:Na	-	-	1:2:0:Na	-
1:2:0:CO	1:2:0:CO	1:2:0:CO	1:2:0:CO	1:2:0:CO
1:2:0:2CO	-	1:2:0:2CO	1:2:0:2CO	1:2:0:2CO
2:2:0	2:2:0	2:2:0	2:2:0	2:2:0
2:3:0	2:3:0	2:3:0	2:3:0	2:3:0
2:3:0:Na	2:3:0:Na	2:3:0:Na	2:3:0:Na	2:3:0:Na
2:3:0:CO	2:3:0:CO	2:3:0:CO	2:3:0:CO	2:3:0:CO
2:3:0:K	-	-	-	-
2:4:0:K	2:4:0:K	-	-	-
3:3:0	-	3:3:0	3:3:0	3:3:0
3:4:0	3:4:0	3:4:0	3:4:0	3:4:0
3:4:0:Na	3:4:0:Na	-	-	-
3:5:0:K	3:5:0:K	-	-	-

As discussed below (see Figures 3.4 to 3.8), tandem mass spectrometry and isotope pattern analyses[195;209] have been used to validate each of the assigned bismuth-cysteine-nucleobase cations listed in Table 3.1. A full spectrum from the reaction of $Bi(NO_3)_3$, L-cysteine, and adenine is shown in Figure 3.4a, accompanied by a tandem mass spectrum (Figure 3.4b) revealing the collision-induced dissociation of ions represented by *m/z* 463, $[Bi(Cys)(A)-2H]^+$. A reasonable neutral loss of cysteine (121 u) is observed, generating a product peak at *m/z* 342, assigned to what may well be the first known complex containing only bismuth and adenine, $[Bi(A)-2H]^+$. Likewise, a full spectrum from a sample containing $Bi(NO_3)_3$ with L-cysteine and guanine is provided in Figure 3.5a. In Figure 3.5b, fragmentation of *m/z* 479, $[Bi(Cys)(G)-2H]^+$, results in three main product ions, assigned to protonated guanine (*m/z* 152), a CO-adduct (*m/z* 356) of $[Bi(Cys)-2H]^+$, and the first mass spectrometrically observed 1:1 Bi:G cation (*m/z* 358).

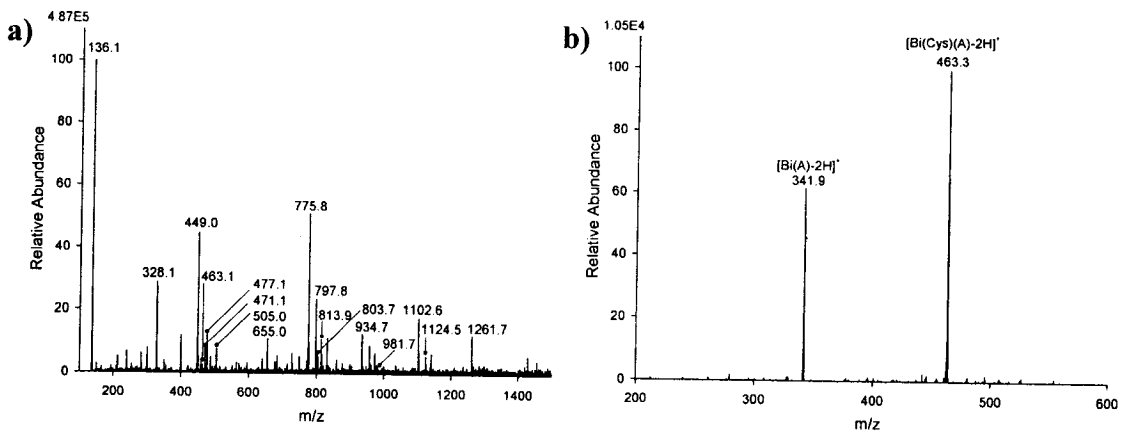

Figure 3.4 Positive ion bismuth-cysteine-adenine ESI mass spectra. Reaction mixtures contained $Bi(NO_3)_3$, L-cysteine, and adenine, in 50:50 ethanol:water. a) Full spectrum. b) CID of *m/z* 463, $[Bi(Cys)(A)-2H]^+$, to yield a product peak at *m/z* 342, assigned as $[Bi(A)-2H]^+$.

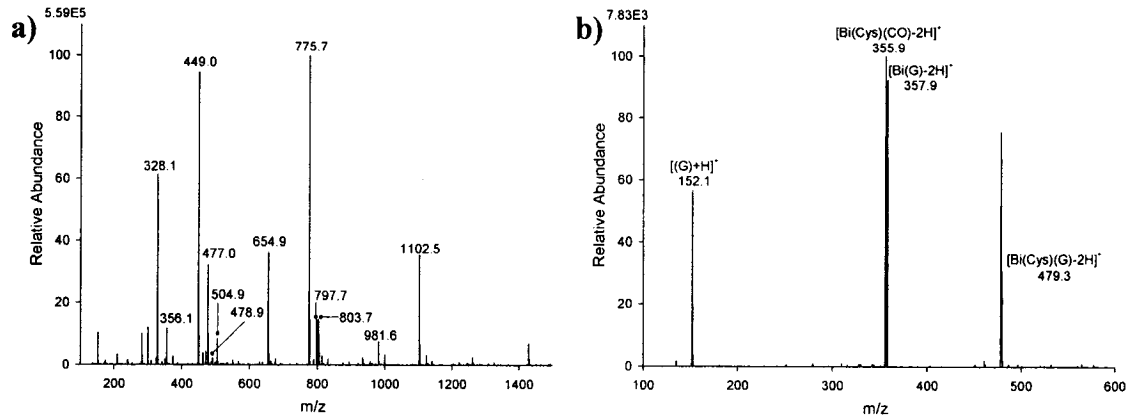

Figure 3.5 Positive ion bismuth-cysteine-guanine ESI mass spectra. Reaction mixtures contained $Bi(NO_3)_3$, L-cysteine, and guanine, in 50:50 ethanol:water. a) Full spectrum. b) CID of *m/z* 479, $[Bi(Cys)(G)-2H]^+$, to yield product peaks at *m/z* 152, *m/z* 356, and *m/z* 358.

In support of bismuth-cysteine-cytosine peaks assigned in the full ESI mass spectrum shown in Figure 3.6a, a tandem mass spectrum showing the results of CID of *m/z* 598, suggested to be $[BiK(Cys)_2(C)-3H]^+$, is given in Figure 3.6b. Neutral losses of cytosine (111 u), and a portion of one doubly deprotonated cysteine ligand ($C_3H_5NO_2$, 87 u) are projected to yield product peaks of $[BiK(Cys)_2-3H]^+$ at *m/z* 487 and $[BiK(Cys)(C)(S)-H]^+$ at *m/z* 511, respectively. The product ion at *m/z* 505 has been assigned to a water-adduct of $[BiK(Cys)_2-3H]^+$. Additionally, Figure 3.6c shows a match between the experimental and theoretical isotope patterns for *m/z* 439, authenticating the assignment of this peak as the 1:1:1 Bi:Cys:C cation aforementioned.

A full spectrum from the reaction of $Bi(NO_3)_3$, L-cysteine, and thymine is provided in Figure 3.7a. In Figure 3.7b, peaks within the observed and calculated isotope patterns corresponding to ions represented by *m/z* 781, assigned as $[Bi_2(Cys)_2(T)-5H]^+$, have similar intensities even though the two patterns are not directly superimposed. This difference between the patterns reflects the fact that the experimentally determined *m/z* values (e.g., *m/z* 780.7) are not necessarily whole numbers like the calculated values that have been used. The two tandem mass spectra given in Figures 3.7c and d clearly reveal neutral losses of thymine (126 u) from both $[Bi(Cys)(T)-2H]^+$ (*m/z* 454), and the sodiated analogue, $[BiNa(Cys)(T)-3H]^+$ (*m/z* 476).

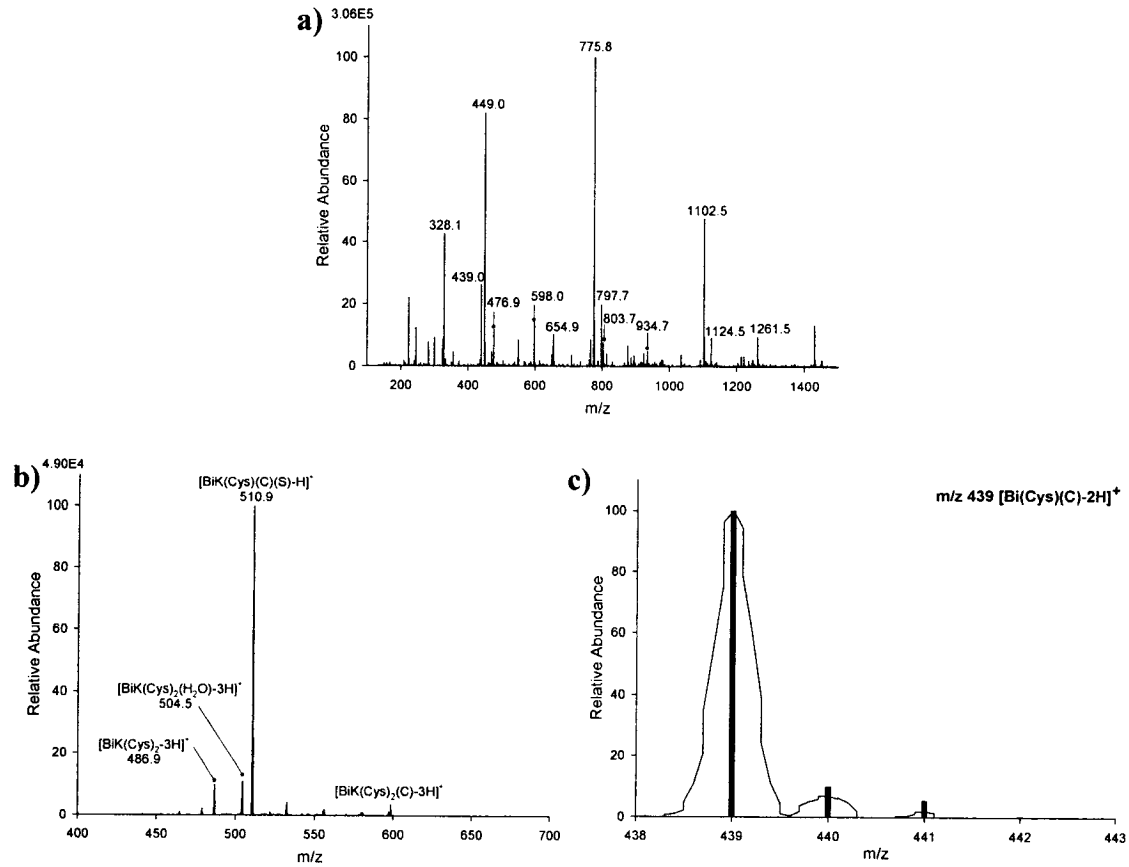

Figure 3.6 Positive ion bismuth-cysteine-cytosine ESI mass spectra. Reaction mixtures contained $Bi(NO_3)_3$, L-cysteine, and cytosine, in 50:50 ethanol:water. a) Full spectrum. b) CID of *m/z* 598, $[BiK(Cys)_2(C)\text{-}3H]^+$, to yield product peaks at *m/z* 487, *m/z* 505, and *m/z* 511. c) Comparison of experimental (continuous thin line) and theoretical (dark vertical bars) isotope patterns for ions represented by *m/z* 439, assigned as $[Bi(Cys)(C)\text{-}2H]^+$.

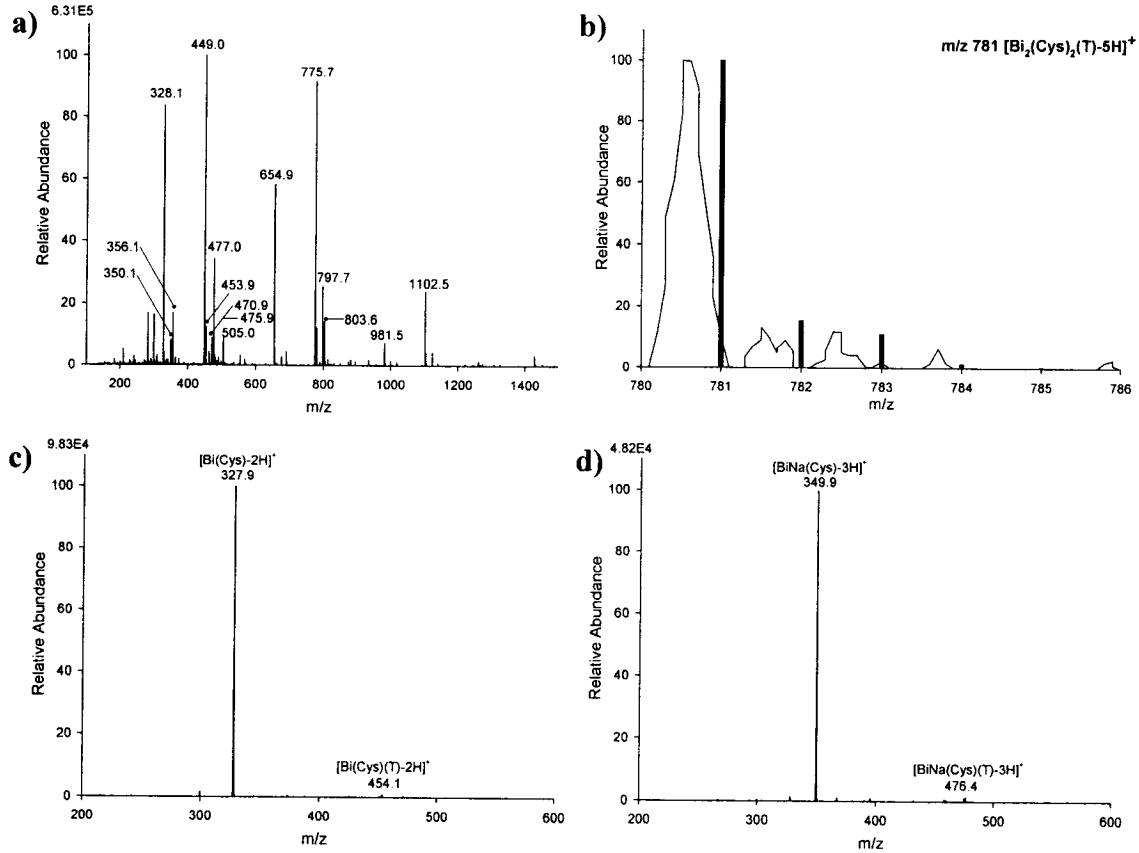

Figure 3.7 Positive ion bismuth-cysteine-thymine ESI mass spectra. Reaction mixtures contained $Bi(NO_3)_3$, L-cysteine, and thymine, in 50:50 ethanol:water. a) Full spectrum. b) Comparison of experimental (continuous thin line) and theoretical (dark vertical bars) isotope patterns for ions represented by *m/z* 781, assigned as $[Bi_2(Cys)_2(T)\text{-}2H]^+$. c) CID of *m/z* 454, $[Bi(Cys)(T)\text{-}2H]^+$, to yield a product peak at *m/z* 328, $[Bi(Cys)\text{-}2H]^+$. d) CID of *m/z* 476, $[BiNa(Cys)(T)\text{-}3H]^+$, to yield a product peak at *m/z* 350, $[BiNa(Cys)\text{-}3H]^+$.

Figure 3.8a contains a full mass spectrum corresponding to a reaction mixture of $Bi(NO_3)_3$, L-cysteine, and final nucleobase, uracil. In Figure 3.8b, the neutral loss of uracil (112 u) from $[Bi(Cys)(U)\text{-}2H]^+$ ions at *m/z* 440 is understood to produce a product peak at *m/z* 328, corresponding to the familiar 1:1 Bi:Cys cation. In support of the assigned uracil-based cations, $[Bi_2(Cys)_2(U)\text{-}5H]^+$ (*m/z* 767), the experimental and theoretical isotope patterns presented in Figure 3.8c are complementary.

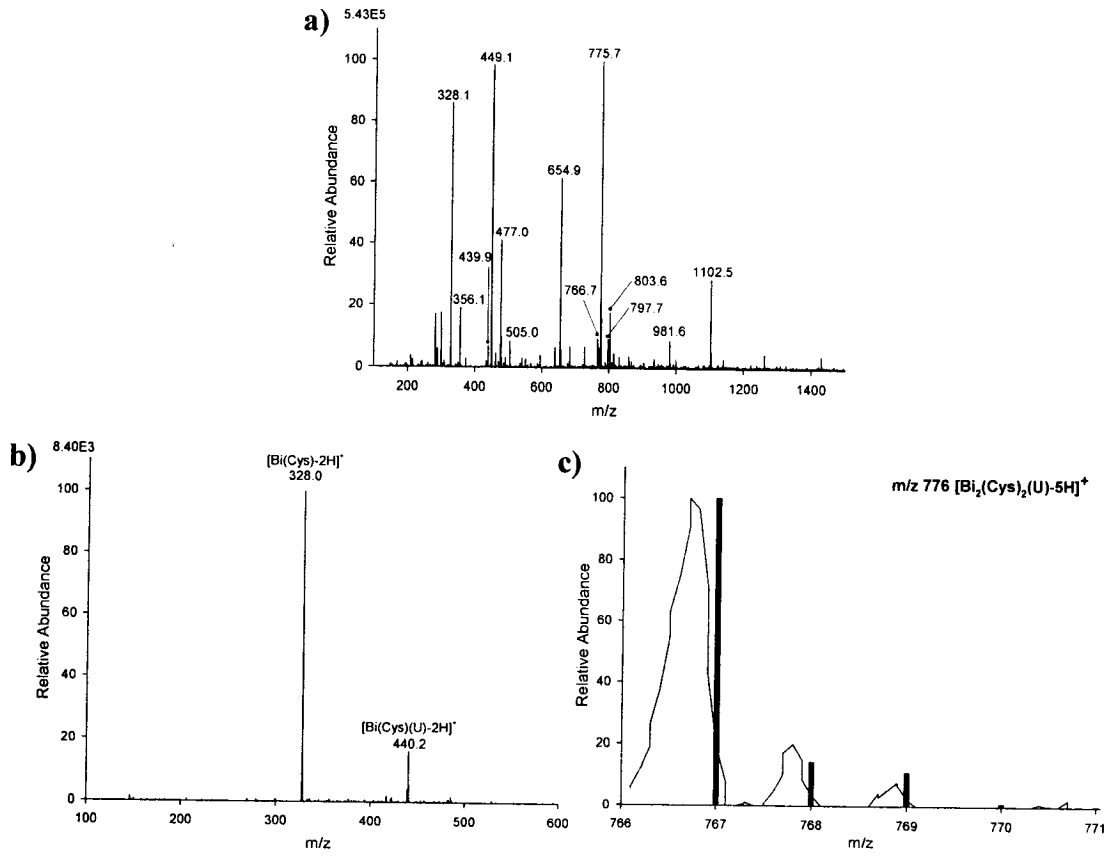

Figure 3.8 Positive ion bismuth-cysteine-uracil ESI mass spectra. Reaction mixtures contained $Bi(NO_3)_3$, L-cysteine, and uracil, in 50:50 ethanol:water. a) Full spectrum. b) CID of *m/z* 440, $[Bi(Cys)(U)-2H]^+$, to yield a product peak at *m/z* 328, $[Bi(Cys)-2H]^+$. c) Comparison of experimental (continuous thin line) and theoretical (dark vertical bars) isotope patterns for ions represented by *m/z* 776, $[Bi_2(Cys)_2(U)-2H]^+$.

Lastly, beyond the assignment of bismuth-cysteine-nucleobase ions (shaded in Table 3.1), numerous bismuth-cysteine complex ions were identified, only some of which (1:1, 1:2, 2:2, and 2:3 Bi:Cys) have been previously reported in the literature.[16;17] New bismuth-cysteine complex ions (2:4, 3:4, 3:5 Bi:Cys) have yet to be confirmed by MS/MS analysis; however, a comparison of experimental and calculated isotope patterns for these peaks is provided in Figure 3.9, revealing a potential match in each case.

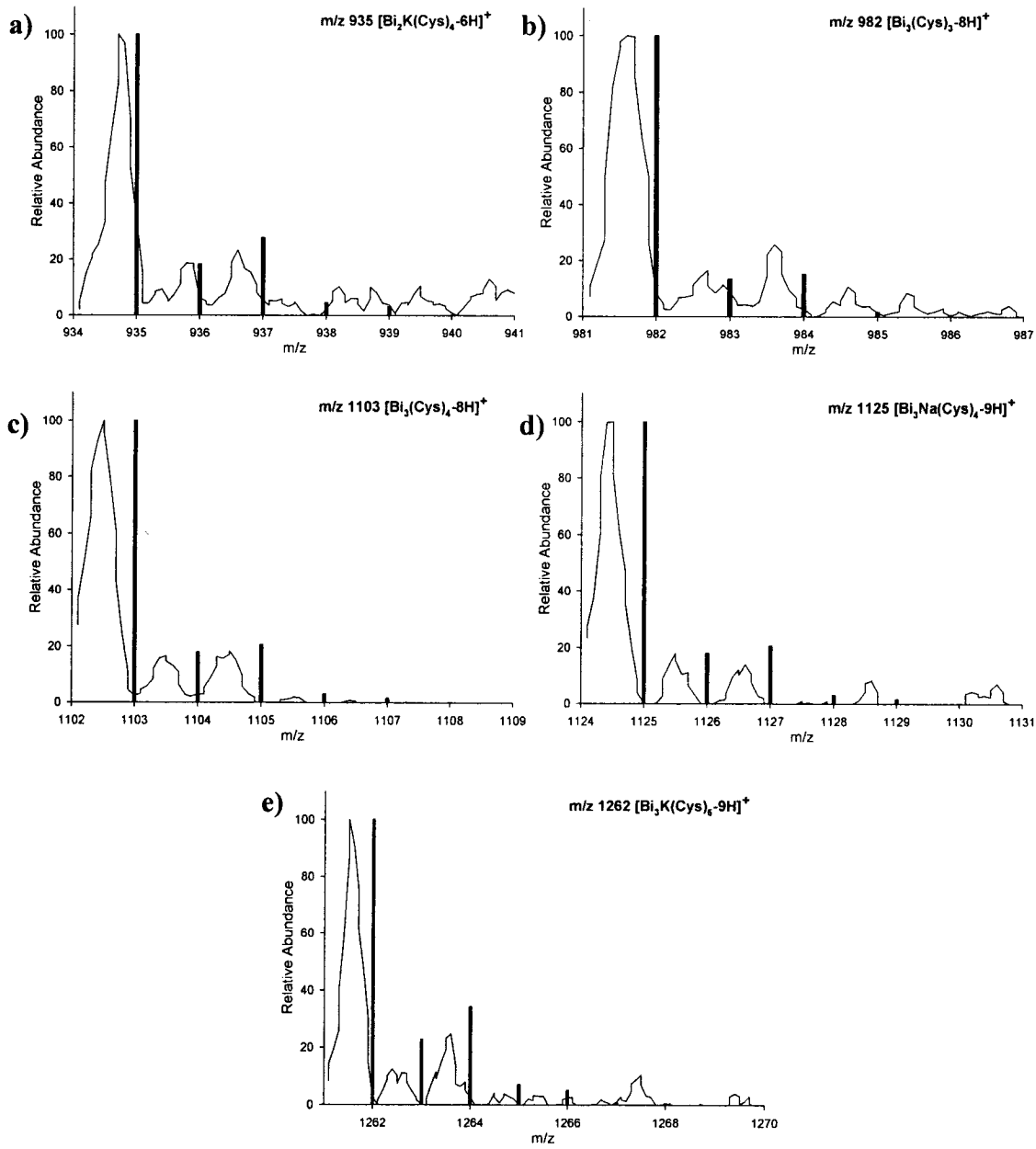

Figure 3.9 Comparison of bismuth-cysteine isotope patterns. Experimental (continuous thin line) and theoretical (dark vertical bars) patterns are shown for new bismuth-cysteine cations represented by a) *m/z* 935: $[Bi_2K(Cys)_4\text{-}6H]^+$, b) *m/z* 982: $[Bi_3(Cys)_3\text{-}8H]^+$, c) *m/z* 1103: $[Bi_3(Cys)_4\text{-}8H]^+$, d) *m/z* 1125: $[Bi_3Na(Cys)_4\text{-}9H]^+$, and e) *m/z* 1262: $[Bi_3K(Cys)_5\text{-}9H]^+$.

3.2 Conclusions

The results herein contribute to the field of metal-nucleobase chemistry by revealing the formation of new bismuth-cysteine-nucleobase complex ions, as well as the first observation of bismuth-adenine and bismuth-guanine complex ions by way of tandem mass spectrometry. The assignment of a total of eight nucleobase-containing ions has been corroborated by a comprehensive analysis of ESI-MS data. These ions – with Bi:Cys:NB ratios of 1:1:1 Bi:Cys:A, 1:1:1 Bi:Cys:G, 1:1:1 Bi:Cys:C, potassiated 1:2:1 Bi:Cys:C, 1:1:1 Bi:Cys:T, sodiated 1:1:1 Bi:Cys:T, 2:2:1 Bi:Cys:T, 1:1:1 Bi:Cys:U, and 2:2:1 Bi:Cys:U – are particularly interesting given the apparently necessary presence of cysteine for ion formation. These results not only affirm the importance of bismuth-sulfur chemistry from a biological viewpoint, but also illustrate that both sulfur, as well as non-sulfur, donor atoms may be present in the biological coordination sphere of bismuth. A subsequent experiment could involve an analysis of bismuth(III) reacted with more than one nucleobase. Perhaps the well-established biological base-pairing of nucleobases A with T or U, and G with C, would play a role in the chemistry observed.

3.3 Experimental Methods

Bismuth(III) nitrate pentahydrate, L-cysteine, adenine, cytosine, guanine, thymine, and uracil were used as received from Aldrich. Ethanol (HPLC reagent grade) was used as received from Fisher. All reactions were performed at room temperature using distilled water.

3.3.1 Reaction Mixtures of $Bi(NO_3)_3$, a Nucleobase, and/or Cysteine

A nucleobase (0.026 g adenine, 0.023 g cytosine, 0.031 g guanine, 0.025 g thymine, or 0.022 g uracil, corresponding to 0.19, 0.20, or 0.21 mmol) was stirred briefly in 10 mL solvent (50:50 ethanol:distilled water), followed by the addition of $Bi(NO_3)_3 \cdot 5H_2O$ (0.097 or 0.098 g, 0.20 mmol) and another 10 mL of solvent. The resulting reaction mixtures were stirred for 21 h. Alternatively, L-cysteine (0.023, 0.024, or 0.025 g, corresponding to 0.19, 0.20, or 0.21 mmol, respectively) was stirred briefly in 10 mL solvent (50:50 ethanol:distilled water), followed by the addition of a nucleobase (0.027 or 0.028 g

adenine, 0.022 g cytosine, 0.030 g guanine, 0.024 g thymine, or 0.021 g uracil, corresponding to 0.19, 0.20, or 0.21 mmol), $Bi(NO_3)_3 \cdot 5H_2O$ (0.096, 0.097, or 0.098 g, 0.20 mmol, ground by mortar and pestle), and another 10 mL of solvent. These reaction mixtures were stirred for 17 to 27 h. All reaction mixtures were then filtered by passage through a NALGENE® PTFE syringe filter (0.2 μm pore size, 25 mm diameter). Each filtrate was diluted ten-fold to a concentration ca. 0.001 M for mass analysis.

3.3.2 Electrospray Ionization Mass Spectrometry

ESI-mass spectra were obtained using a Finnigan™ LCQ™$_{DUO}$ quadrupole ion trap mass spectrometer. Each dilute filtrate was injected (in 5 or 10 μL aliquots) directly into the electrospray ionization source of the mass spectrometer. The solvent flow rate was set at 1.2 mL/h, the heated capillary temperature at 200 °C, the sheath gas ($N_{2(g)}$) flow rate at 20 (arbitrary units), and the spray voltage at a magnitude of 4.00 kV. Tandem mass spectra were obtained using helium as the collision gas, and applying a collision energy of 20 %. In Table 3.1, data is combined from two bismuth-cysteine-adenine samples. Other data in Table 3.1 reflect spectra acquired from one injection of each sample.

Chapter 4 Thallium-Amino Acid and -Peptide Complexes

Thallium and compounds of thallium can be incorporated into mammals via the skin, gastrointestinal tract or respiratory system,[210] and as such, are extremely poisonous to living organisms.[211] Human consumption of 5.7 mg/kg (around 400 mg for a 70 kg person) of thallium metal is known to cause intoxication, and ingesting between 0.2 g and 1 g of thallium(I) sulfate is fatal.[177] Routes by which thallium is damaging likely include the substitution of K(I) by Tl(I), which is essential in biological membrane transport processes.[55] In contrast, a viable treatment for thallium poisoning involves the opposite exchange of Tl(I) and K(I) in order to extract thallium from an organism. This is accomplished using a compound known commonly as Prussian Blue, which contains potassium ions within an inorganic ferric- or potassium ferric hexacyanoferrate crystal lattice.[212] The insoluble form of Prussian Blue, $Fe_4[Fe(CN)_6]_3$, was approved as an antidote for thallium(I) poisoning by the American Food and Drug Administration as recently as 2003.[213] For comparison, organic compound, 2,3-dimercaptosuccinic acid (DMSA), has been studied and used as a chelation therapy for children diagnosed with lead poisoning.[214;215] Notably, a relatively recent study using a rat model determined that Prussian Blue is more effective than DMSA as a remedy for thallium intoxication.[216]

Although thallium is known to accumulate and be distributed easily throughout the human body, the bioactivity of thallium is not understood at a molecular level.[210;217] Despite the fact that thallium compounds once used in rodenticides and insecticides are no longer employed in these industries, thallium is expected to be advantageous in newer applications such as semiconductors and even medical scintillographic imaging.[210;211] For these reasons, an enhanced understanding of the biological chemistry of thallium remains imperative.

Previously, the use of potentiometry has been exploited to ascertain formation constants for the coordination of thallium(I) by cysteine, penicillamine, acetylcysteine and acetylpenicillamine ligands.[218] Using potentiometric and absorbance measurements, the stability constants associated with thallium(I) complexation by L-cysteine were found to be dependent on ionic strength.[219] Cysteine complexes containing a single thallium(I) ion

were the most prominent species observed at a fixed ionic strength.[219] The complexation of methionine to Tl(I) has been likewise investigated, keeping in mind that as a soft acid, Tl(I) should prefer coordination by sulfur over nitrogen, and in turn over oxygen.[220] Complexation of dimethylthallium(III) with cysteine, penicillamine, acetylcysteine, acetylpenicillamine, and glycine was also assessed by potentiometry.[221] Formation constants were found to be highest for binding of cysteine or penicillamine to Me_2Tl^+. For glycine, binding was weakest. Not unlike the situation for bismuth, the conclusion drawn was that coordination of thallium ions by a thiol is favoured over coordination of thallium ions by other donor atoms.

Very few reports have described the use of X-ray diffraction to afford the solid state determination of thallium-amino acid complexes. Of the handful of these compounds that exist, one is a thallium(I) salt of dipenicillaminato iron(III).[144] In two other cases, Tl(III) is coordinated by DL-tryptophan[142] or L-phenylalanine.[222] Therefore, prior to this thesis, to the author's knowledge DL-cysteinatothallium(I)[140] was the only known crystallographically characterized compound containing Tl(I) and one of the twenty amino acids found in human proteins. Structural drawings of the latter three complexes are shown in Figure 4.1. A new, related compound, L-cysteinatothallium(I) has now been generated and is discussed in Section 4.2.

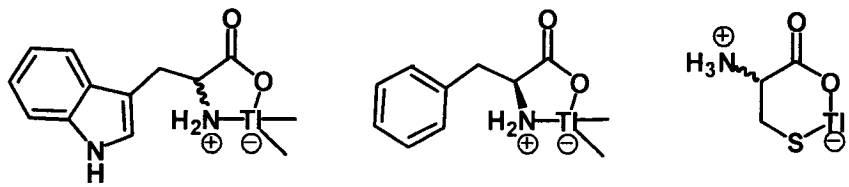

a) **b)** **c)**

Figure 4.1 Solid state structures containing Tl(I) or Tl(III) and an amino acid. a) (DL-Tryptophanato)dimethylthallium(III) monohydrate (one molecule of water has been excluded for clarity), b) (L-phenylalaninato)dimethylthallium(III), and c) DL-cysteinatothallium(I).

It has also been found that solutions of thallium compounds can be effectively examined by way of electrospray ionization mass spectrometry (ESI-MS). To learn more about the

fundamental interactions of thallium(I) with biologically significant molecules, the definitive identification of complex ions containing thallium and each of twenty-one amino acids (including DL-homocysteine) has been accomplished.[17] Complexes have also been identified between thallium and tripeptide, glutathione,[18] as well as other di- and tri-peptides.[223] To continue in pursuit of a systematic and fundamental exploration of biologically relevant thallium(I) chemistry, ESI-MS and other characterization techniques have now been employed to elucidate new interactions of thallium(I) nitrate with two sulfur-containing dipeptides, cysteinyl-glycine and methionyl-glycine (Figure 4.2, Section 4.1), and L-cysteine (Section 4.2).

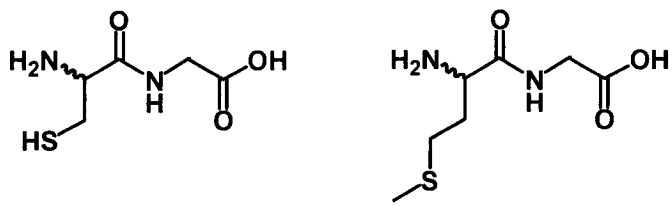

Figure 4.2 Sulfur-containing dipeptides, cysteinyl-glycine and methionyl-glycine.

4.1 Results and Discussion: Thallium Complexes with Dipeptides

Full ESI mass spectra from reaction mixtures containing $TlNO_3$ with either cysteinyl-glycine (Cys-Gly) or methionyl-glycine (Met-Gly) are provided in Figure 4.3. Corresponding mass-to-charge ratios and relative abundances are listed in Table 4.1.

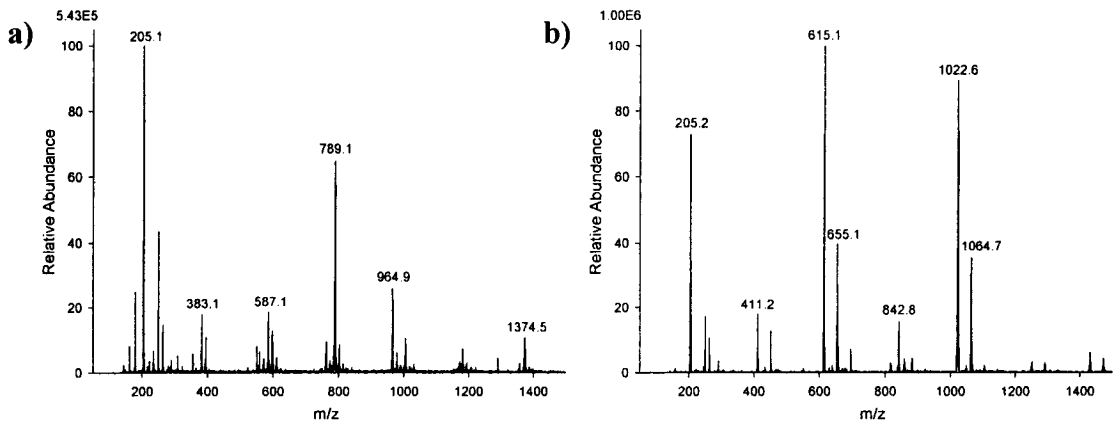

Figure 4.3 Positive ion thallium-dipeptide ESI-MS spectra. Reaction mixtures contained a) $TlNO_3$ and cysteinyl-glycine (Cys-Gly), or b) $TlNO_3$ and methionyl-glycine (Met-Gly), in 50:50 ethanol:water.

Given the growing library of known ESI-MS thallium- and other metal-biomolecule complex ions, it was not unexpected to observe complex ions containing thallium(I) and either Cys-Gly or Met-Gly. In total, five different Tl:Cys-Gly stoichiometric ratios (1:1, 2:1, 2:3:Na, 3:1, 5:2) and six different Tl:Met-Gly stoichiometric ratios (1:1, 1:2:K, 2;1, 2:2:Na, 2:3:K, 3:2) have been verified via CID, or through the analysis of experimental and calculated isotope patterns. For comparison, related thallium:amino acid (Tl:AA) stoichiometric ratios of 1:1 (AA = Cys), 1:1, 2:1 (AA = Met), 2:1, and 3:2 (AA = Gly) have been documented.[17] In addition, (unpublished)[223] data is available on the complex ions formed between thallium(I) and a variety of other dipeptides (DP), included in summary Table 4.2. From this list of Tl:DP ratios, 1:1, 2:1, and 3:2 are noted to be most commonly observed under the applied experimental conditions (described in Section 4.4).

Although it is generally important to construct experiments that are not overly complex, the analysis of progressively more sophisticated biochemical systems is a critical step in understanding the relevant metal-biomolecule nuances in such systems. In particular, the examination of larger and longer peptides as ligands for thallium(I) and other metal ions is important; hence the new thallium-dipeptide complex ions observed using ESI-MS serve to propel forward this field of research and provide new examples of potential biological targets of Tl(I).

Table 4.1 Positive ion thallium-dipeptide ESI-MS data from reaction mixtures containing $TlNO_3$ and cysteinyl-glycine (Cys-Gly) or methionyl-glycine (Met-Gly), in 50:50 ethanol:water.

$TlNO_3$/	*m/z*	Relative Abundance (%)	Assignment	Tl:DP Stoichiometry	MS/MS (*m/z*)	Fragment Assignment
Cys-Gly	205.1	100	Tl^+	-	-	
	383.1	18	$[Tl(Cys\text{-}Gly)]^+$	1:1	205.6	Tl^+
					337.0	$[Tl(Cys\text{-}Gly)\text{-}HCOOH]^+$
					365.0	$[Tl(Cys\text{-}Gly)\text{-}H_2O]^+$
					365.9	$[Tl(Cys\text{-}Gly)\text{-}NH_3]^+$
	587.1	19	$[Tl_2(Cys\text{-}Gly)\text{-}H]^+$	2:1	569.9	$[Tl_2(Cys\text{-}Gly)\text{-}H)\text{-}NH_3]^+$
	791.0	58	$[Tl_3(Cys\text{-}Gly)\text{-}2H]^+$	3:1	568.9	$[Tl_3(Cys\text{-}Gly)\text{-}2H\text{-}TlOH]^+$
					744.9	$[Tl_3(Cys\text{-}Gly)\text{-}2H\text{-}HCOOH]^+$
					773.9	$[Tl_3(Cys\text{-}Gly)\text{-}2H\text{-}NH_3]^+$
	966.9	22	$[Tl_3(disulfide)\text{-}2H]^+$	3:disulfide	790.9	$[Tl_3(Cys\text{-}Gly)\text{-}2H]^+$
	1376.5	7	$[Tl_5(Cys\text{-}Gly)_2\text{-}4H]^+$	5:2	773.8	$[Tl_3(Cys\text{-}Gly)\text{-}2H\text{-}NH_3]^+$
					790.9	$[Tl_3(Cys\text{-}Gly)\text{-}2H]^+$
Met-Gly	205.2	73	Tl^+	-	-	
	411.2	18	$[Tl(Met\text{-}Gly)]^+$	1:1	205.7	Tl^+
					279.8	$[Tl(Met\text{-}Gly)\text{-}C_5H_9NOS]^+$
					307.9	$[Tl(Met\text{-}Gly)\text{-}C_3H_5NO_3]^+$
	615.1	100	$[Tl_2(Met\text{-}Gly)\text{-}H]^+$	2:1	205.6	Tl^+
					483.9	$[Tl_2(Met\text{-}Gly)\text{-}H\text{-}C_5H_9NOS]^+$
					570.9	$[Tl_2(Met\text{-}Gly)\text{-}H\text{-}CO_2]^+$
					596.9	$[Tl_2(Met\text{-}Gly)\text{-}H\text{-}H_2O]^+$
	655.1	40	$[TlK(Met\text{-}Gly)_2\text{-}H]^+$	1:2:K	466.8	$[TlK(Met\text{-}Gly)\text{-}H\text{+}H_2O]^+$
					610.9	$[TlK(Met\text{-}Gly)_2\text{-}H\text{-}CO_2]^+$
	842.8	16	$[Tl_2Na(Met\text{-}Gly)_2\text{-}2H]^+$	2:2:Na	-	
	1024.5	74	$[Tl_3(Met\text{-}Gly)_2\text{-}2H]^+$	3:2	-	
	1064.7	36	$[Tl_2K(Met\text{-}Gly)_3\text{-}2H]^+$	2:3:K	654.9	$[TlK(Met\text{-}Gly)_2\text{-}H]^+$

Table 4.2 Summary of positive ion thallium:dipeptide (DP) stoichiometric ratios. DP = cysteinyl-glycine (Cys-Gly), methionyl-glycine (Met-Gly), glycyl-histidine (Gly-His), glycyl-glutamine (Gly-Gln), glycyl-glutamic acid (Gly-Glu), glycyl-serine (Gly-Ser), glycyl-phenylalanine (Gly-Phe), glycyl-leucine (Gly-Leu), or glycyl-glycine (Gly-Gly).

Tl:Cys-Gly[f]	Tl:Met-Gly[f]	Tl:Gly-His[223]	Tl:Gly-Gln[223]	Tl:Gly-Glu[223]	Tl:Gly-Ser[223]	Tl:Gly-Phe[223]	Tl:Gly-Leu[223]	Tl:Gly-Gly[223]
1:1	1:1	1:1	1:1	1:1	1:1	1:1	1:1	1:1
2:1	2:1	2:1	2:1	2:1	2:1	2:1	2:1	2:1
3:1				3:1				
3:disulfide	3:2	3:2	3:2	3:2	3:2	3:2	3:2	3:2
				4:2				
				4:3				
5:2								

[f] This thesis.

4.2 Results and Discussion: Thallium Complexes with Cysteine

In complement to the mass spectrometry data presented in Section 4.1, the preparation of a new, crystallographically characterized L-cysteinatothallium(I) (TlLCys) compound has been achieved (Figure 4.4). The synthesis of this coordination complex is straightforward, involving the application of heat, followed by slow cooling of the reaction mixture. This procedure is based on a literature precedent for the generation of solid state L-proline complexes of cadmium(II) and mercury(II) from water.[224] Curiously, while the combination of L-cysteine and $TlNO_3$ alone does not generate crystalline material, the inclusion of a stoichiometric amount of L-histidine in the reaction mixture routinely affords single crystals, determined via X-ray diffraction and other characterization techniques to be TlLCys.

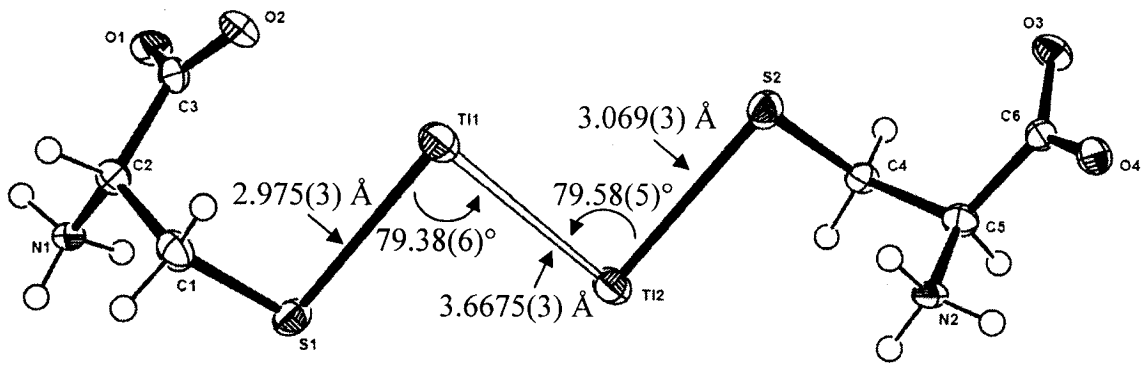

Figure 4.4 An ORTEP view of L-cysteinatothallium(I) (TlLCys). The asymmetric unit contains two uniquely oriented formula units.[g] The open connector drawn between Tl1 and Tl2 represents a thallium-thallium distance that is shorter than the sum (3.92 Å) of two thallium van der Waals radii (1.96 Å).[225] Each L-cysteine ligand is monoanionic, coordinated to one thallium(I) ion through a thiolate functionality. Thermal ellipsoids are shown to 50 % probability, and selected interatomic distances and angles are labeled.

As mentioned earlier, a related DL-cysteinatothallium(I) (TlDLCys) solid state structure is also known[140] (Figure 4.1c, Figure 4.5). The TlDLCys structure is dimeric, involving coordination of both the carboxylate and thiolate moieties in cysteine to each thallium(I)

[g] ORTEP is an abbreviation for Oak Ridge Thermal Ellipsoid Plot. The representation of L-cysteinatothallium(I) in Figure 4.4 was generated using software program, ORTEP-3 (Version 1.08 from L. J. Farrugia, University of Glasgow ©1997-2005).

ion. The structure of TlDLCys is distinct from that of TlLCys because the former[140] was prepared from racemic cysteine, while the more recent preparation employed L-cysteine as a starting material. From a biological perspective, TlLCys is considered to be more relevant than TlDLCys.

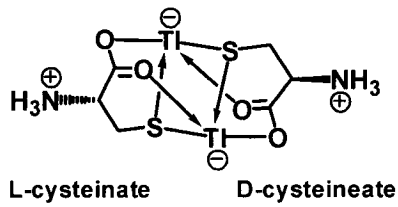

Figure 4.5 DL-cysteinatothallium(I) (TlDLCys). This compound is a dimer involving coordination of oxygen and sulfur donor atoms to thallium(I) from one L- and one D-cysteine molecule.[140]

In TlLCys, thallium-sulfur bond distances of 2.975(3) Å (S1-Tl) and 3.069(3) Å (Tl2-S2) are comparable to 2.890(3) Å and 3.090(4) Å in TlDLCys.[140] All of these thallium-sulfur distances lie within a range of 2.858(2) Å to 3.346(2) Å for various other reported Tl-S bond lengths.[226] The acute TlLCys S1-Tl1-S2 and Tl1-Tl2-S2 angles of 79.38(6)° and 79.58(5)°, respectively, and the resulting bent geometry at each thallium atom, suggest the influence of a stereochemically active lone pair on thallium(I). The contribution of thallium lone pairs was also noted with respect to the square pyramidal geometry about thallium(I) in TlDLCys.[140]

In Figure 4.4, the thallium-thallium contact in TlLCys is shown using an open line, and this distance is one of two such Tl-Tl interactions that occur in the crystalline material. As shown in an extended diagram of the crystal lattice given in Figure 4.6a, the distance between two thallium(I) ions in the asymmetric unit is 3.6675(3) Å, while the distance between two thallium(I) ions in adjacent asymmetric units is 3.6187(3) Å. Both of these distances are longer than a metallic Tl-Tl contact (3.41 Å)[128] and shorter than the sum, 3.92 Å, of two thallium van der Waals radii.[225] The noted thallium-thallium distances also compare well to other known Tl-Tl distances ranging between 3.15 Å and 3.94 Å.[227]

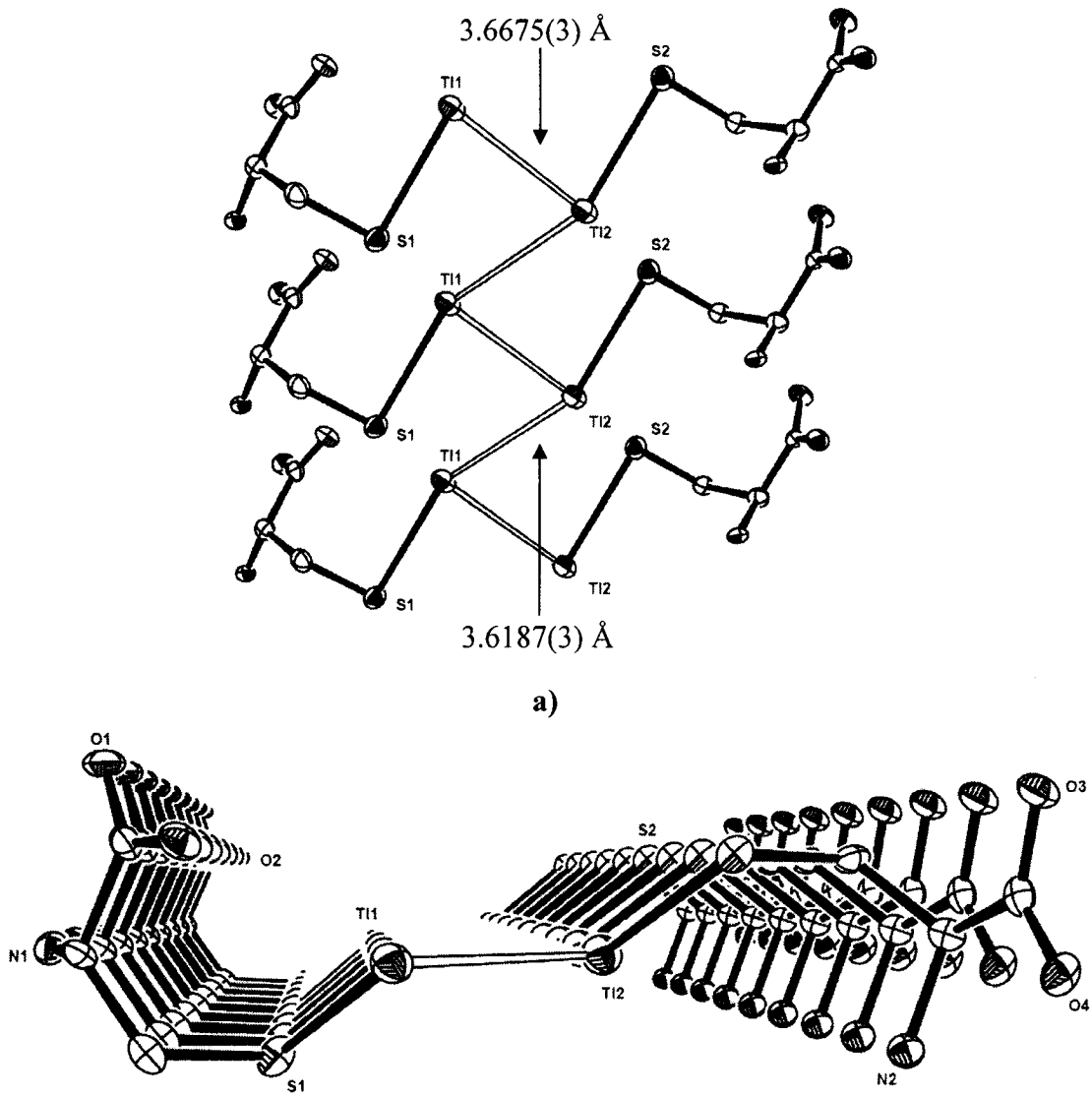

Figure 4.6 Extended diagrams of the L-cysteinatothallium(I) crystal lattice. a) Two distinct Tl-Tl contacts are highlighted, and b) different orientations of two cysteine ligands about the Tl-Tl interaction.

The torsional angle, S1-Tl1-Tl2-S2, in TlLCys is very close to 180° (179.75(10)°), which makes the orientation of these four atoms nearly planar with respect to one another. In Figure 4.6b this near-planarity is more pronounced given the orientation of the structure that is shown. Also more evident in Figure 4.6b is that oxygen atom, O2, is relatively close in proximity to Tl1 compared to the distance between O3 or O4 and Tl2. It may be a result of this relatively close Tl1-O2 contact of 2.913 Å that a shorter S1-Tl1 than S2-

Tl2 distance is observed (Figure 4.4). Table 4.3 contains a comparison of crystallographic data for both known solid state thallium-cysteine compounds.

Table 4.3 Crystallographic experimental details for DL-cysteinatothallium(I) and L-cysteinatothallium(I).

	DL-Cysteinatothallium(I)[140]	**L-Cysteinatothallium(I)**[h]
formula	$TlSO_2NC_3H_6$	$TlSO_2NC_3H_6$
molecular weight (g mol^{-1})	324.5	324.52
colour, habit	colourless, diamond-shaped	orange, plates
crystal system	monoclinic	triclinic
space group	$P2_1/a$	P1
a (Å)	10.841(6)	4.9293(5)
b (Å)	7.672(2)	4.9400(5)
c (Å)	8.391(2)	12.9070(12)
α (deg)	90	96.8762(12)
β (deg)	114.58(3)	97.3518(11)
γ (deg)	90	104.8507(10)
V (Å^3)	634.6	297.46(5)
Z	4	2
$\rho_{calculated}$ (g cm^{-3})	3.40	3.623
λ (Å)	0.71069	0.71073
μ	260 cm^{-1}	27.40 mm^{-1}
goodness-of-fit	-	1.049
R_1† [$F_o^2 \geq 2\sigma(F_o^2)$]	0.063	0.0158
wR_2‡ [$F_o^2 \geq -3\sigma(F_o^2)$]	0.072	0.0376

† $R_1 = \Sigma||F_o|-|F_c||/\Sigma|F_o|$
‡ $wR_2 = [\Sigma w(F_o^2-F_c^2)^2/\Sigma w(F_o^4)]^{1/2}$

Solid state ^{13}C and ^{15}N cross-polarization/magic angle spinning (CP/MAS) NMR spectra support the identification of L-cysteinatothallium(I) and are provided in Figure 4.7. Although L-histidine (spectra of free ligand: Figure 4.7a, b) was included in the reaction mixture from which TlLCys was generated, the ^{13}C and ^{15}N NMR spectra obtained for the product compound (Figure 4.7e, f) resemble only the spectra of free L-cysteine (Figure 4.7c, d). This result was anticipated based on the solid state structure discussed above, in which histidine is not involved. There is a small increase in the chemical shift (27.8 ppm in Figure 4.7c to 28.0 ppm in Figure 4.7e) of the peak associated with the methylene carbon in L-cysteine, suggesting that coordination of sulfur to thallium(I) has occurred (rather than coordination to thallium(I) through the amine or carboxylate functionalities of cysteine).

[h] This thesis.

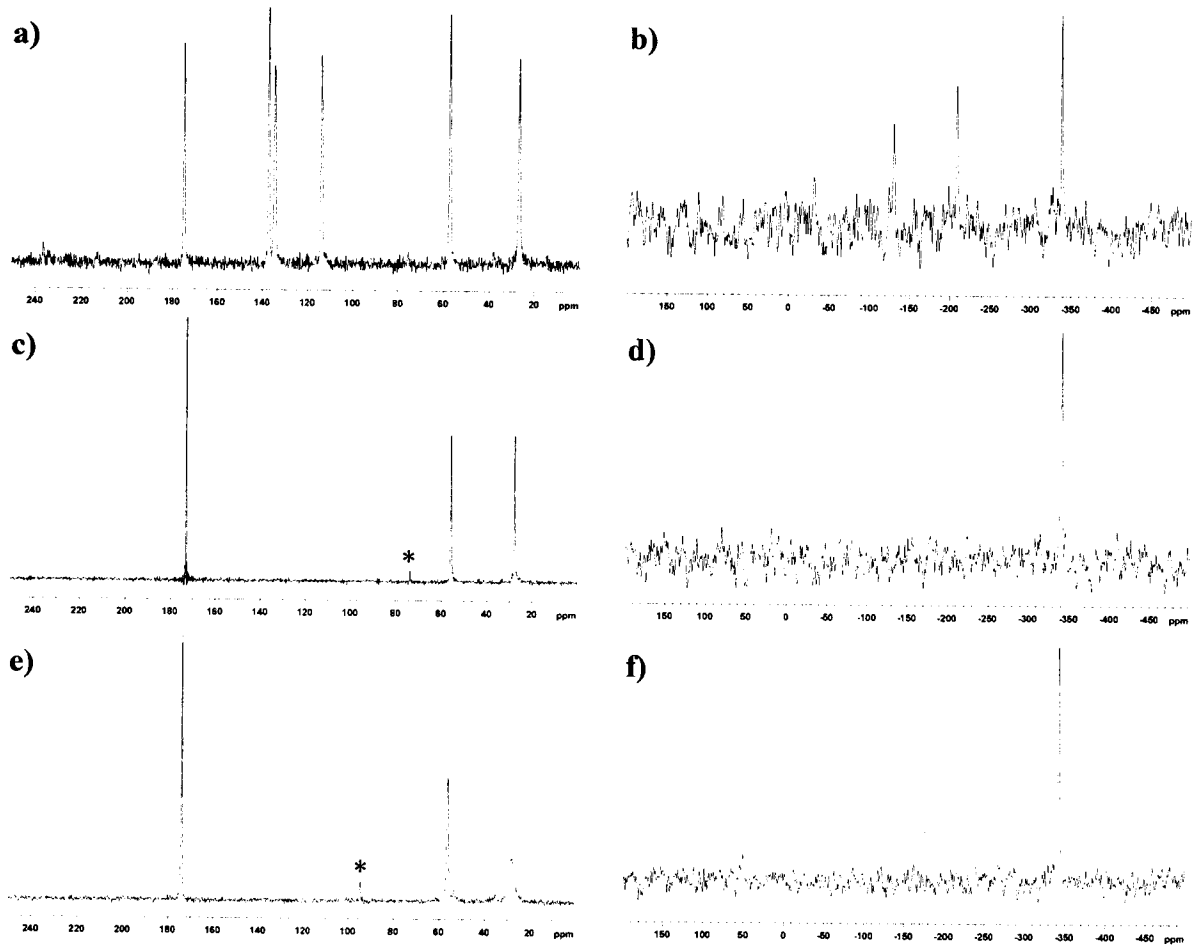

Figure 4.7 Solid state NMR spectra from L-cysteinatothallium(I). a) ^{13}C and b) ^{15}N NMR CP/MAS spectra from L-histidine; c) ^{13}C and d) ^{15}N NMR CP/MAS spectra from L-cysteine; e) ^{13}C and f) ^{15}N NMR CP/MAS spectra from L-cysteinatothallium(I). Asterisks signify spinning side bands.

Even though thallium compounds are significantly water-soluble – a property which contributes to the toxicity of thallium in biological systems[217] – TlLCys was not readily soluble in a variety of common laboratory solvents: chloroform, ethanol, toluene, benzene, water, dimethylsulfoxide, and acetone. However, it was possible to once again take advantage of the sensitivity of electrospray ionization mass spectrometry to examine TlLCys. An ESI-MS spectrum was recorded for both the reaction mixture filtrate (Figure 4.8a) and the supernatant (Figure 4.8b) from TlLCys immersed in distilled water overnight.

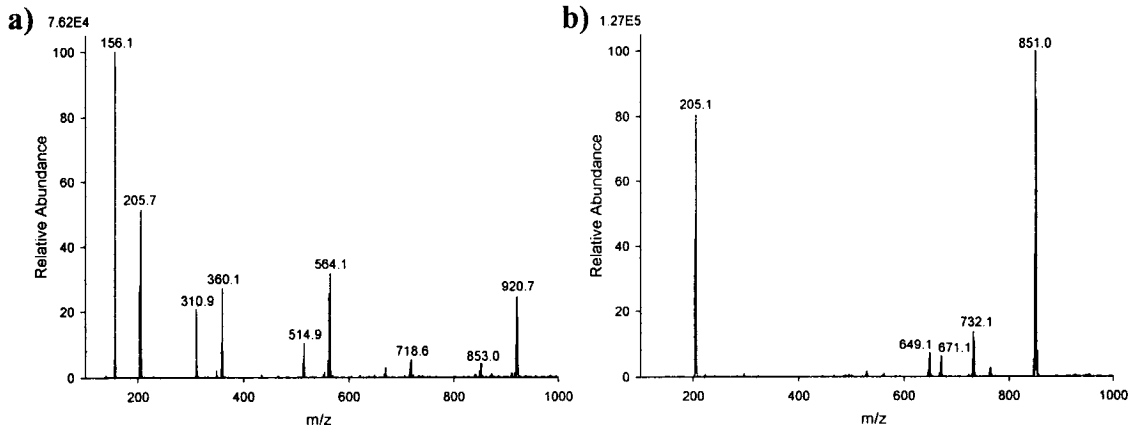

Figure 4.8 Positive ion ESI mass spectra relevant to L-cysteinatothallium(I), generated from a reaction mixture containing $TlNO_3$, L-cysteine, and L-histidine. Spectra shown are from a) the reaction mixture filtrate, and b) the supernatant solution.

As depicted for the TlLCys reaction mixture filtrate in Figure 4.8a (solvent = water), a number of peaks were observed corresponding to the following ions: Tl^+, protonated histidine ($[(His)+H]^+$ at *m/z* 156), protonated dihistidine ($[(His)_2+H]^+$ at *m/z* 311), and various combinations of thallium and histidine that have been previously reported:[17] $[Tl(His)]^+$ at *m/z* 360, $[Tl(His)_2]^+$ at *m/z* 515, and $[Tl_3(His)_2\text{-}2H]^+$ at *m/z* 923. Interestingly, new ions with Tl:His ratios of 2:1 and 2:2 were also observed: $[Tl_2(His)\text{-}H]^+$ at *m/z* 564 and $[Tl_2(His)_2\text{-}H]^+$ at *m/z* 719, respectively. This ESI-MS data validates other data acquired for L-cysteinatothallium(I), indicating that the L-histidine incorporated into the reaction mixture can be primarily located in the filtrate after isolating the solid product.

As mentioned, it was also possible to examine the supernatant from a sample of TlLCys left in water overnight (Figure 4.8b). As might be expected, protonated histidine was not observed in this spectrum, a result which again supports the finding of an absence of histidine in the product compound. The four most abundant peaks in Figure 4.8b were assigned to various thallium-cysteine species; however, neither protonated TlLCys nor protonated biscysteinatodithallium(I) were observed. These peaks might have been expected at *m/z* 326 and *m/z* 651 given the known structure of the starting material. Instead, peaks corresponding to Tl^+, $[Tl_2(Cystine)\text{-}H]^+$ at *m/z* 649, $[Tl_2Na(Cystine)\text{-}2H]^+$ at *m/z* 671, previously observed[17] $[Tl_3(Cys)\text{-}2H]^+$ at *m/z* 734, and $[Tl_3(Cystine)\text{-}2H]^+$ at *m/z* 853 were present (appearing at *m/z* 851, the most intense peak in the isotope pattern for this ion). Cystine (shown in Figure 4.9) is a disulfide, often formed from the oxidation of cysteine, and protonated cystine has been observed at *m/z* 241 in mass spectra from bismuth-cysteine reaction mixtures.[16] Based on the spectrum shown in Figure 4.8b, it appears that the formation of thallium-cystine complexes is favourable from TlLCys in aqueous solution or in the gas phase.

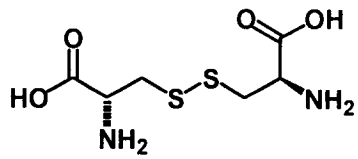

Figure 4.9 Structure of L-cystine.

4.3 Conclusions

Given the toxicity of thallium, and the lack of understanding that surrounds the biochemistry of this metal, it is both critical and potentially hazardous to examine compounds containing this element. However, employing precautionary measures such as those discussed in Section 1.6 have allowed for research to be carried out safely. As a result, the discovery of not only several new gas phase thallium-dipeptide ions, by way of ESI-MS, but also a new, biologically relevant, solid state L-cysteinatothallium(I) coordination complex was made possible. The information and discussion presented in this Chapter again highlight the importance and value of mass spectrometry in

understanding metal-biomolecule species. Equally important is the use of other characterization methods including XRD and NMR to further develop this field of chemistry.

4.4 Experimental Methods

Caution: $TlNO_3$ is toxic to living systems. Safety precautions were taken as outlined in Section 1.6. Thallium(I) nitrate, L-histidine, L-cysteine, cysteinyl-glycine and methionyl-glycine were used as received from Sigma-Aldrich. Ethanol (HPLC reagent grade) was used as received from Fisher. All reactions were performed using distilled water. Melting points were recorded on an Electrothermal melting point apparatus in open capillary tubes and are uncorrected. Raman spectra were obtained for crystalline samples on a Bruker RFS 100 instrument equipped with an Nd:YAG laser (1064 nm). Peaks are reported in wavenumbers (cm^{-1}) with relative intensities in parentheses. Chemical analyses were determined by Canadian Microanalytical Service Ltd., Delta, BC, Canada.

4.4.1 ^{13}C and ^{15}N CP/MAS NMR[i]

Samples were packed into a 4 mm rotor without further preparation. There was enough material to fill the rotor completely. All NMR experiments were carried out on a Bruker Avance NMR spectrometer with a 9.4 T magnet (400 MHz proton Larmor frequency, 100.65 MHz ^{13}C Larmor frequency) or 16.45 T magnet (700 MHz proton Larmor frequency, 176.10 MHz ^{13}C Larmor frequency, 70.96 MHz ^{15}N Larmor frequency) using a double resonance HX or triple resonance HXY probe head for rotors of 4 mm diameter. The samples producing Figure 4.7a-f were spun at two different spinning speeds (between 6.0 and 10.0 kHz) to determine center bands and to identify spinning sidebands. Relaxation times for ^{1}H NMR experiments were determined by inversion recovery sequences. From these experiments a recycle delay of 10.0 seconds (Figure 4.7a, c, e), 5.0 seconds (b, d), or 17.5 seconds (f) for the CP/MAS was determined.

[i] All solid state NMR spectra were acquired in collaboration with Solid-state NMR Coordinator, Dr. U. Werner-Zwanziger, who is affiliated with the Dalhousie University Department of Chemistry, Atlantic Region Magnetic Resonance Centre, and Institute for Research in Materials. Dr. Werner-Zwanziger also provided a template from which Section 4.4.1 was generated.

Other parameters for the ^{13}C and ^{15}N CP/MAS NMR experiments with two-pulse phase-modulation[228] proton decoupling were optimized on glycine or ^{15}N-labeled ammonium nitrate, respectively. The carbonyl resonance of glycine served as an external, secondary chemical shift standard at 176.06 ppm, relative to primary standard, tetramethylsilane. The ammonium resonance of ammonium nitrate served as an external, secondary chemical shift standard at -358 ppm from that of primary standard, nitromethane.[229] For the ^{13}C CP/MAS NMR spectra shown in Figure 4.7, 16 (a, c) or 64 (e) scans were accumulated, using 2600.00 μs CP contact times. For the ^{15}N CP/MAS NMR spectra shown in Figure 4.7, 128 (b, d, f) scans were accumulated, using 5000.00 μs CP contact times.

4.4.2 L-Cysteinatothallium(I)

L-Cysteine (0.195 g, 1.61 mmol) was stirred for several minutes in 10 mL distilled water prior to adding L-histidine (0.252 g, 1.62 mmol), $TlNO_3$ (0.430 g, 1.61 mmol), and a second 10 mL of water (total volume of 20 mL). The reaction mixture was heated, open to the air, in a hot water bath initially at 89 °C. After thirty minutes, heating and stirring of the sample were terminated (the bath temperature was 94 °C). The reaction mixture was allowed to cool to room temperature at the speed of the water bath. Within a few hours, a fiery red solid material precipitated from a clear, colourless solution. The contents of the flask were filtered by suction and the solid was washed with cold distilled water (2 x 10 mL). After drying the solid for thirty minutes under suction, the product was weighed (0.196 g, 0.604 mmol, 38 %). Decomposition point: ca. 140 °C (subsequent preparation of the sample revealed an initial colour change between 115 and 120 °C); Raman (171 mW, room temperature, 4 cm^{-1} resolution, 2000 scans, units of cm^{-1}) 2909 (82), 2887 (29), 2833 (6), 2812 (6), 1580 (6), 1425 (12), 1400 (24), 1355 (12), 1308 (24), 1260 (100), 1206 (6), 1155 (6), 1106 (12), 1058 (6), 973 (6), 888 (12), 844 (6), 791 (6), 675 (35), 588 (6), 535 (6), 492 (12), 164 (6), 133 (41), 115 (18); ^{13}C CP/MAS NMR: δ 174.1 (quaternary), 56.3 (C-H), 28.0 (CH_2). ^{15}N CP/MAS NMR: δ -341.8 (NH_3). Elemental analysis calculated for $C_3H_6NO_2STl$ (324.52): C, 11.10; H, 1.86; N, 4.32. Found: C, 11.24; H, 1.57; N, 4.49.

4.4.3 X-ray Diffraction Analysis[j]

A diffraction-quality crystal of L-cysteinatothallium(I) was coated in Paratone oil then mounted on a thin glass fiber. The crystal was cooled to 193(2) K under a cold N_2 stream and X-ray diffraction data were collected using graphite-monochromated Mo Kα (λ = 0.71073 Å) radiation on a Bruker PLATFORM diffractometer with a sealed tube generator and a SMART 1000 CCD detector. The structure was solved using the direct-methods program *SHELXS-97*,[230] and least-squares refinement (on F^2) was completed using the program *SHELXL-97* (Sheldrick, G. M. *SHELXL-97*. Program for crystal structure determination. University of Göttingen, Germany, 1997). Hydrogen atoms were generated in idealized positions based on the sp^3 hybridizations of their parent nitrogen or carbon atoms, and were given isotropic displacement parameters 120 % of those of their parent atoms. The final model was refined to $R_1(F)$ = 0.0158 (for 2265 reflections with $I > 2s(I)$) and $wR_2(F^2)$ = 0.0376 (for all 2400 unique reflections measured). See Table 4.3 for a summary of crystallographic experimental parameters.

4.4.4 Reaction Mixtures of $TlNO_3$ and a Dipeptide

Thallium(I) nitrate (0.053 g, 0.20 mmol) was combined with cysteinyl-glycine (0.036 g, 0.20 mmol) or methionyl-glycine (0.041 g, 0.20 mmol), each in 50:50 ethanol:water (total: 20 mL). These reaction mixtures were stirred at room temperature overnight (21 to 22 h). Aliquots of the resulting solutions were diluted by a factor of ten to generate samples of a concentration ca. 0.001 M. These dilute samples were analyzed the same day by way of ESI-MS. Data in Table 4.1 reflect spectra acquired from one injection of each Tl(I) sample.

[j] Single crystal X-ray diffraction data was provided by Dr. R. McDonald and Dr. M. J. Ferguson (X-ray Crystallography Laboratory, Department of Chemistry, University of Alberta), who also provided a template from which Section 4.4.3 was generated.

4.4.5 Electrospray Ionization Mass Spectrometry

Mass spectra were obtained using a Finnigan™ LCQ™$_{DUO}$ electrospray ionization quadrupole ion trap mass spectrometer. Each dilute filtrate was injected (in 5 or 10 μL aliquots) directly into the electrospray ionization source of the mass spectrometer. The solvent flow rate was set at 1.2 or 2.0 mL/h, the heated capillary temperature at 200 °C, and the sheath gas ($N_{2(g)}$) flow rate at 20 (arbitrary units). The spray voltage was set at a magnitude of 4.00 kV for the collection of positive ion information. Tandem mass spectra were obtained using helium as the collision gas, and applying a collision energy of 14 to 20 %. Spectra were analyzed and processed using software programs, Qual Browser (Version 1.2 from Finnigan Corp. ©1998–2000) and SigmaPlot (Version 10.0 from Systat Software, Inc. ©2006), respectively.

Chapter 5 Observation of a Cooperative Thiol Effect[k]

Bismuth is anticipated to interact primarily with thiol- or thiolate-containing biological molecules. With this in mind, various bismuth-thiolate compounds have been characterized in solution and in the solid state,[1;2;12;231] and complexes have been identified between bismuth and cysteine-containing biomolecules such as metallothionein[158] and glutathione.[13;16;18;133] In addition, a considerable amount of ESI-MS information has been obtained with respect to complexes formed between bismuth or other metals in the presence of cysteine or other amino acids.[17]

As illustrated in Table 5.1, Hg(I) and Hg(II) have been reported to interact with most amino acids, while Cd(II), Tl(I), and Pb(II) have been observed to form complex ions with all amino acids tested.[17] New (unpublished) data has also revealed that complexes containing Hg(I) and alanine (Ala) are also possible.[232] In contrast, amino acid complex ions of Bi(III) were only documented in seven of twenty-one cases, involving L-histidine, L-threonine, L-asparagine, L-glutamine, L-methionine, L-cysteine, or DL-homocysteine.[17] Not surprisingly, bismuth has been observed to interact with all sulfur-containing amino acids examined. Moreover, the markedly selective nature of non-thiol amino acids for Bi(III) compared to other significantly more toxic metals may help to rationalize the disparate biological activities of these two types of metal elements.

To further probe the amino acid chemistry of bismuth and the importance of biological thiol, L-cysteine, a subsequent preliminary ESI-MS study concerned the reaction mixtures of Bi(III) in the presence of two amino acids: cysteine and a second, non-thiol, amino acid.[233] Interestingly, these experiments led to the observation of new bismuth-amino acid complex ions containing L-tryptophan, L-tyrosine, L-serine, L-lysine, L-arginine, or L-proline, none of which had been previously verified as ligands for bismuth.[233] The same method has since been used to identify complexes of bismuth with two other non-

[k] This thesis Chapter has been published as an article in the Journal of Bioinorganic Chemistry, Vol 101, Phillips, H. A., Eelman, M. D., Burford, N., Cooperative influence of thiolate ligands on the bio-relevant coordination chemistry of bismuth, 736-739, Copyright Elsevier (2007), and has been reproduced here with permission (see Appendix B). Enhancements to the article have been made, including those to ensure that the flow and formatting of the text and diagrams conform to the styles established within the rest of the thesis.

thiol amino acids, as well as citric acid. In addition, this dramatic cooperative effect is not limited to cysteine (Cys), and can be replicated with the structurally related thiols, 3-mercaptopropionic acid (MPA) or 2-mercaptoethylamine (MEA).

5.1 Results and Discussion: Bismuth Complexes with Non-Thiol Amino Acids

For the purposes of reproducibility, previous ESI-MS experiments involving $Bi(NO_3)_3$, Cys and a second amino acid (AA ≠ Cys) with a non-alkyl side chain were repeated, confirming the assignments of many formerly documented ions.[233] In addition, three new bismuth-aspartic acid complex ions, $[Bi(Cys)(Asp)-2H]^+$ (*m/z* 461), $[Bi_2(Cys)_2(Asp)-5H]^+$ (*m/z* 788), and $[Bi_3(Cys)_3(Asp)-8H]^+$ (*m/z* 1115), and corresponding bismuth-glutamic acid species, $[Bi(Cys)(Glu)-2H]^+$ (*m/z* 475), $[Bi_2(Cys)_2(Glu)-5H]^+$ (*m/z* 802), and $[Bi_3(Cys)_3(Glu)-8H]^+$ (*m/z* 1129), have now also been validated by MS/MS data and/or an analysis of experimental and theoretical[195] spectral isotope patterns. The product of a reaction between bismuth(III) iodide and aspartic acid has been examined previously by powder X-ray diffraction.[234] A comprehensive list of mass-to-charge ratios and relative abundances is given in Table 5.2, including data attributed to Bi-AA, Bi-Cys, and Bi-Cys-AA interactions. In addition to previously reported Bi-Cys ions, $[Bi(Cys)-2H]^+$ (*m/z* 328), $[Bi(Cys)_2-2H]^+$ (*m/z* 449), $[Bi_2(Cys)_2-5H]^+$ (*m/z* 655), and $[Bi_2(Cys)_3-5H]^+$ (*m/z* 776),[16;17] a peak at *m/z* 1103 has now also been assigned to the cluster ion formula, $[Bi_3(Cys)_4-8H]^+$.

It is important to recognize that most of the bismuth(III) complex ions that contain a non-thiol amino acid also contain Cys (Table 5.2). Indeed, the interaction of bismuth with non-thiol amino acids may rely on the presence of cysteine within the coordination sphere of the metal. Perhaps even more curious is the fact that some Bi-AA complexes listed in Table 5.2 do not contain cysteine, and yet have not been observed without cysteine in the reaction mixture. Given that bismuth is known to form coordination complexes with a variety of S-, O-, and N-donor ligands,[12] and acknowledging that all tested reaction mixtures were filtered to remove insoluble components prior to analysis, it is unreasonable to propose that complexes of bismuth with non-thiol amino acids are not

formed in solution. Rather, the solubility of any bismuth-non-thiol complexes that are formed may in some cases be too low for detection even via ESI-MS. Alternatively, incorporating Cys into a solution of a non-thiol with Bi(III) exploits the tendency of bismuth to bond with sulfur. This presence of Cys may enhance the solubility of other reaction mixture constituents, perhaps by disrupting extended bismuth-non-thiol structures, thereby allowing for the detection of both Bi-Cys-AA and previously unobserved Bi-AA complex ions: $[Bi(Asn)-2H]^+$, $[Bi(Lys)_2-2H]^+$, $[Bi(His)-2H]^+$, $[BiNa(His)_2-3H]^+$, $[BiNa(His)_3-3H]^+$, and $[Bi(Trp)_2-2H]^+$.

Many of the ions listed in Table 5.2 are best considered as monoanionic or dianionic ligands (conjugate bases of Cys and/or AA) coordinated to a Bi(III) Lewis acid, and are envisaged as chelate complexes (Figure 5.1). In select cases, complex ions are assigned with neutral amino acid ligands (e.g., $[Bi(Cys)(AA)_2-2H]^+$, involving the loss of two protons from two of three amino acids). Complexes containing more than one bismuth center and more than one ligand can be considered as clusters that likely involve ligand bridges between the metal centers, as observed in the solid state for many bismuth complexes.[12;27;31;107-113]

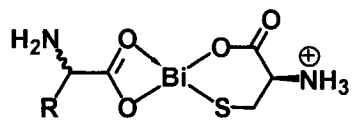

Figure 5.1 Proposed connectivity for a generic bismuth-cysteinate-amino acid complex cation.

Overall, complexes have been identified between bismuth and a total of fifteen different amino acids (Cys, Hcy, Met, His, Thr, Asn, Gln, Ser, Pro, Tyr, Lys, Trp, Arg, Asp, Glu), eight of which have only been shown to form ions containing bismuth when Cys is included in the reaction mixture. A summary of observed Bi-AA and Bi-Cys-AA ion formulae in Table 5.2 is provided in Table 5.3, and a revision of Table 5.1 is given in Table 5.4.

Table 5.1 Summary of reported metal:amino acid interactions. Checkmarks indicate that complex ions have been previously observed between the metal ions and amino acids listed. Blank regions indicate that no interaction was documented.[17]

	Gly	Ala	Val	Leu	Ile	Phe	Trp	Tyr	His	Ser	Thr	Met	Cys	Hcy	Asp	Glu	Asn	Gln	Lys	Arg	Pro
Cd(II)	✓	✓	✓	✓	✓	✓	✓	✓	✓	✓	✓	✓	✓	✓	✓	✓	✓	✓	✓	✓	✓
Hg(I)	✓		✓	✓	✓	✓	✓	✓	✓	✓	✓	✓	✓				✓		✓	✓	✓
Hg(II)	✓	✓	✓	✓	✓	✓	✓	✓	✓	✓	✓	✓	✓		✓	✓	✓	✓	✓	✓	✓
Tl(I)	✓	✓	✓	✓	✓	✓	✓	✓	✓	✓	✓	✓	✓	✓	✓	✓	✓	✓	✓	✓	✓
Pb(II)	✓	✓	✓	✓	✓	✓	✓	✓	✓	✓	✓	✓	✓	✓	✓	✓	✓	✓	✓	✓	✓
Bi(III)									✓		✓	✓	✓	✓			✓	✓			

Table 5.2 Positive ion bismuth-cysteine-amino acid ESI-MS data for reaction mixtures containing $Bi(NO_3)_3$ and L-cysteine (Cys), together with a second amino acid, L-lysine (Lys), L-arginine (Arg), L-tryptophan (Trp), L-serine (Ser), L-threonine (Thr), L-proline (Pro), L-methionine (Met), L-asparagine (Asn), L-glutamine (Gln), DL-homocysteine (Hcy), L-aspartic acid (Asp), L-glutamic acid (Glu), L-tyrosine (Tyr), or L-histidine (His), in 50:50 ethanol:water. Shaded cells highlight examples of Bi-AA or Bi-Cys-AA ions that have not been previously identified.

m/z (Relative Abundance, %)	Assignment Bi/Cys/Lys	*m/z* (Relative Abundance, %)	Assignment Bi/Cys/Arg	*m/z* (Relative Abundance, %)	Assignment Bi/Cys/Trp
147.0 (100)[l,m]	$[Lys+H]^+$	175.1 (100)[l,m]	$[(Arg)+H]^+$	204.9 (100)[l,m]	$[Trp+H]^+$
327.9 (7)[l,n]	$[Bi(Cys)-2H]^+$	327.9 (5)[n]	$[Bi(Cys)-2H]^+$	448.9 (6)[n]	$[Bi(Cys)_2-2H]^+$
448.9 (14)[l,n]	$[Bi(Cys)_2-2H]^+$	448.9 (7)[n]	$[Bi(Cys)_2-2H]^+$	531.9 (17)[l,o]	$[Bi(Cys)(Trp)-2H]^+$
499.0 (1)[l,o]	$[Bi(Lys)_2-2H]^+$	501.9 (14)[l,o]	$[Bi(Cys)(Arg)-2H]^+$	618.0 (7)	$[Bi(Trp)_2-2H]^+$
473.9 (25)[l,o]	$[Bi(Cys)(Lys)-2H]^+$	675.9 (40)	$[Bi(Cys)(Arg)_2-2H]^+$	858.8 (20)[o]	$[Bi_2(Cys)_2(Trp)-5H]^+$
775.8 (12)[n]	$[Bi_2(Cys)_3-5H]^+$			1045.9 (6)	$[Bi(Cys)(Trp)_3-5H]^+$
800.6 (6)[o]	$[Bi_2(Cys)_2(Lys)-5H]^+$				

[l] These peaks have been supported by MS/MS spectra.
[m] Some ligand peaks that do not contain bismuth are included for completeness.
[n] Peaks containing bismuth and Cys (only) are included for completeness, recognizing that some of these peaks have already been reported elsewhere.[16;17]
[o] These peaks (containing bismuth and at least one non-thiol ligand) were also documented previously from preliminary experiments.[233]

m/z (Relative Abundance, %)	Assignment Bi/Cys/Ser	*m/z* (Relative Abundance, %)	Assignment Bi/Cys/Thr	*m/z* (Relative Abundance, %)	Assignment Bi/Cys/Pro
328.0 (46)[n]	$[Bi(Cys)-2H]^+$	119.9 (64)[l,m]	$[(Thr)+H]^+$	116.0 (89)[l,m]	$[(Pro)+H]^+$
350.0 (7)[n]	$[BiNa(Cys)-3H]^+$	328.0 (43)[n]	$[Bi(Cys)-2H]^+$	327.9 (42)[l,n]	$[Bi(Cys)-2H]^+$
432.9 (11)[l,o]	$[Bi(Cys)(Ser)-2H]^+$	350.0 (6)[n]	$[BiNa(Cys)-3H]^+$	442.9 (45)[o]	$[Bi(Cys)(Pro)-2H]^+$
448.9 (100)[n]	$[Bi(Cys)_2-2H]^+$	446.9 (18)[o]	$[Bi(Cys)(Thr)-2H]^+$	448.9 (90)[l,n]	$[Bi(Cys)_2-2H]^+$
[illegible]	[illegible]	448.9 (100)[n]	$[Bi(Cys)_2-2H]^+$	[illegible]	[illegible]
470.9 (20)[n]	$[BiNa(Cys)_2-3H]^+$	[illegible]	[illegible]	470.9 (7)[n]	$[BiNa(Cys)_2-3H]^+$
654.9 (19)[n]	$[Bi_2(Cys)_2-5H]^+$	470.8 (16)[n]	$[BiNa(Cys)_2-3H]^+$	[illegible]	[illegible]
759.8 (13)[o]	$[Bi_2(Cys)_2(Ser)-5H]^+$	654.9 (22)[n]	$[Bi_2(Cys)_2-5H]^+$	654.8 (27)[n]	$[Bi_2(Cys)_2-5H]^+$
775.7 (67)[n]	$[Bi_2(Cys)_3-5H]^+$	773.7 (26)[o]	$[Bi_2(Cys)_2(Thr)-5H]^+$	[illegible]	[illegible]
[illegible]	[illegible]	775.7 (77)[n]	$[Bi_2(Cys)_3-5H]^+$	775.7 (100)[n]	$[Bi_2(Cys)_3-5H]^+$
797.7 (49)[n]	$[Bi_2Na(Cys)_3-6H]^+$	[illegible]	[illegible]	797.8 (12)[n]	$[Bi_2Na(Cys)_3-6H]^+$
1102.5 (21)[n]	$[Bi_3(Cys)_4-8H]^+$	797.7 (43)[n]	$[Bi_2Na(Cys)_3-6H]^+$	[illegible]	[illegible]
1124.6 (8)[n]	$[Bi_3Na(Cys)_4-9H]^+$	[illegible]	[illegible]	1102.6 (18)[n]	$[Bi_3(Cys)_4-8H]^+$
		1102.5 (29)[n]	$[Bi_3(Cys)_4-8H]^+$		

m/z (Relative Abundance, %)	Assignment Bi/Cys/Met	*m/z* (Relative Abundance, %)	Assignment Bi/Cys/Asn	*m/z* (Relative Abundance, %)	Assignment Bi/Cys/Gln
149.9 (100)[l,m]	$[(Met)+H]^+$	132.9 (59)[l,m]	$[(Asn)+H]^+$	146.9 (100)[l,m]	$[(Gln)+H]^+$
328.0 (29)[l,n]	$[Bi(Cys)-2H]^+$	154.9 (8)[m]	$[Na(Asn)]^+$	327.9 (18)[n]	$[Bi(Cys)-2H]^+$
355.9 (4)[l,o,p]	$[Bi(Met)-2H]^+$	328.0 (44)[n]	$[Bi(Cys)-2H]^+$	448.9 (41)[n]	$[Bi(Cys)_2-2H]^+$
448.9 (74)[l,n]	$[Bi(Cys)_2-2H]^+$	338.9 (3)[o]	$[Bi(Asn)-2H]^+$	473.9 (27)[o]	$[Bi(Cys)(Gln)-2H]^+$
470.9 (6)[n]	$[BiNa(Cys)_2-3H]^+$	448.9 (93)[n]	$[Bi(Cys)_2-2H]^+$	[illegible]	[illegible]
476.9 (32)[l,o,p]	$[Bi(Cys)(Met)-2H]^+$	459.9 (37)[o]	$[Bi(Cys)(Asn)-2H]^+$	499.0 (8)[o]	$[Bi(Gln)_2-2H]^+$
[illegible]	[illegible]	471.0 (38)[o]	$[Bi(Asn)_2-2H]^+$	654.9 (8)[n]	$[Bi_2(Cys)_2-5H]^+$
504.9 (3)[l,o]	$[Bi(Met)_2-2H]^+$	[illegible]	[illegible]	775.7 (37)[n]	$[Bi_2(Cys)_3-5H]^+$
654.9 (27)[n]	$[Bi_2(Cys)_2-5H]^+$	654.9 (32)[n]	$[Bi_2(Cys)_2-5H]^+$	800.7 (33)[o]	$[Bi_2(Cys)_2(Gln)-5H]^+$
775.8 (74)[n]	$[Bi_2(Cys)_3-5H]^+$	775.7 (70)[n]	$[Bi_2(Cys)_3-5H]^+$	1102.6 (14)[n]	$[Bi_3(Cys)_4-8H]^+$
797.8 (16)[n]	$[Bi_2Na(Cys)_3-6H]^+$	786.7 (100)[o]	$[Bi_2(Cys)_2(Asn)-5H]^+$	[illegible]	[illegible]
803.7 (35)[o,p]	$[Bi_2(Cys)_2(Met)-5H]^+$	[illegible]	[illegible]		
1102.6 (28)[n]	$[Bi_3(Cys)_4-8H]^+$	[illegible]	[illegible]		
[illegible]	[illegible]	1102.5 (31)[n]	$[Bi_3(Cys)_4-8H]^+$		
		[illegible]	[illegible]		
		1124.5 (7)[n]	$[Bi_3Na(Cys)_4-9H]^+$		
		[illegible]	[illegible]		

[p] These *m/z* values are isobaric with those for CO adducts of Bi-Cys ions: $[Bi(Cys)(CO)-2H]^+$ (*m/z* 356), $[Bi(Cys)_2(CO)-2H]^+$ (*m/z* 477), and $[Bi_2(Cys)_3(CO)-5H]^+$ (*m/z* 804), which have been observed in spectra from reaction mixtures containing $Bi(NO_3)_3$, Cys, and AA ≠ Met.

m/z (Relative Abundance, %)	Assignment Bi/Cys/Hcy	*m/z* (Relative Abundance, %)	Assignment Bi/Cys/Asp	*m/z* (Relative Abundance, %)	Assignment Bi/Cys/Glu
135.9 (27)[l,m]	$[(Hcy)+H]^+$	121.9 (8)[m]	$[(Cys)+H]^+$	148.0 (100)[l,m]	$[(Glu)+H]^+$
328.0 (44)[l,n]	$[Bi(Cys)-2H]^+$	133.9 (70)[l,m]	$[(Asp)+H]^+$	169.9 (6)[m]	$[Na(Glu)]^+$
342.1 (28)[l,o]	$[Bi(Hcy)-2H]^+$	328.0 (51)[n]	$[Bi(Cys)-2H]^+$	328.0 (25)[n]	$[Bi(Cys)-2H]^+$
448.9 (91)[l,n]	$[Bi(Cys)_2-2H]^+$	350.0 (6)[n]	$[BiNa(Cys)-3H]^+$	449.0 (53)[n]	$[Bi(Cys)_2-2H]^+$
462.9 (100)[l,o]	$[Bi(Cys)(Hcy)-2H]^+$	448.9 (100)[n]	$[Bi(Cys)_2-2H]^+$	[illegible]	[illegible]
476.9 (40)[l,o]	$[Bi(Hcy)_2-2H]^+$	[illegible]	[illegible]	476.9 (20)[l]	[illegible]
[illegible]	[illegible]	470.9 (7)[n]	$[BiNa(Cys)_2-3H]^+$	654.9 (10)[n]	$[Bi_2(Cys)_2-5H]^+$
775.7 (31)[n]	$[Bi_2(Cys)_3-5H]^+$	[illegible]	[illegible]	775.7 (24)[n]	$[Bi_2(Cys)_3-5H]^+$
789.7 (55)[o]	$[Bi_2(Cys)_2(Hcy)-5H]^+$	654.9 (15)[n]	$[Bi_2(Cys)_2-5H]^+$	797.8 (11)[n]	$[Bi_2Na(Cys)_3-6H]^+$
803.7 (34)[o]	$[Bi_2(Cys)(Hcy)_2-5H]^+$	775.7 (23)[n]	$[Bi_2(Cys)_3-5H]^+$	801.8 (18)	[illegible]
[illegible]	[illegible]	[illegible]	[illegible]	823.7 (18)	[illegible]
817.7 (8)[o]	$[Bi_2(Hcy)_3-5H]^+$	797.7 (12)[n]	$[Bi_2Na(Cys)_3-6H]^+$	1102.6 (8)[n]	$[Bi_3(Cys)_4-8H]^+$
1102.6 (8)[n]	$[Bi_3(Cys)_4-8H]^+$	[illegible]	[illegible]	1128.7 (11)	[illegible]
[illegible]	[illegible]	1102.6 (7)[n]	$[Bi_3(Cys)_4-8H]^+$		
[illegible]	[illegible]	[illegible]	[illegible]		
[illegible]	[illegible]				

m/z (Relative Abundance, %)	Assignment Bi/Cys/Tyr	*m/z* (Relative Abundance, %)	Assignment Bi/Cys/His
181.9 (100)[l,m]	$[(Tyr)+H]^+$	156.0 (100)[l,m]	$[(His)+H]^+$
327.9 (8)[l,n]	$[Bi(Cys)-2H]^+$	178.0 (3)[m]	$[Na(His)]^+$
448.9 (13)[l,n]	$[Bi(Cys)_2-2H]^+$	328.0 (7)[l,n]	$[Bi(Cys)-2H]^+$
509.0 (11)[l,o]	$[Bi(Cys)(Tyr)-2H]^+$	361.9 (5)[o]	$[Bi(His)-2H]^+$
[illegible]	[illegible]	449.0 (10)[l,n]	$[Bi(Cys)_2-2H]^+$
654.9 (5)[n]	$[Bi_2(Cys)_2-5H]^+$	482.9 (21)[l,o]	$[Bi(Cys)(His)-2H]^+$
775.9 (11)[n]	$[Bi_2(Cys)_3-5H]^+$	[illegible]	[illegible]
[illegible]	[illegible]	517.0 (15)[l,o]	$[Bi(His)_2-2H]^+$
1102.5 (5)[n]	$[Bi_3(Cys)_4-8H]^+$	[illegible]	[illegible]
		775.9 (9)[n]	$[Bi_2(Cys)_3-5H]^+$
		[illegible]	[illegible]
		1102.5 (5)[n]	$[Bi_3(Cys)_4-8H]^+$

Table 5.3 Summary of assigned positive ion bismuth-amino acid and bismuth-cysteine-amino acid chemical formulae. Checkmarks indicate that that an ion of the assigned formula (left column), containing bismuth(III), cysteine (Cys), and/or a non-thiol amino acid (AA), has been observed.[q]

Assigned Formula	Trp	Tyr	His	Ser	Thr	Met	Hcy	Asp	Glu	Asn	Gln	Lys	Arg	Pro
$[(AA)+H]^+$	✓	✓	✓		✓	✓	✓	✓	✓	✓	✓	✓	✓	✓
$[Bi(AA)-2H]^+$							✓							
$[Bi(AA)_2-2H]^+$	✓		✓			✓	✓				✓			
$[Bi_2(AA)_3-5H]^+$							✓							
$[Bi(Cys)(AA)-2H]^+$	✓	✓	✓	✓	✓	✓	✓	✓	✓	✓	✓	✓	✓	✓
$[BiNa(Cys)(AA)-3H]^+$		✓	✓	✓	✓	✓	✓	✓	✓	✓	✓			✓
$[Bi(Cys)(AA)_2-2H]^+$													✓	✓
$[Bi_2(Cys)(AA)_2-5H]^+$			✓				✓							
$[Bi_2(Cys)(AA)_3-5H]^+$	✓													
$[Bi_2(Cys)_2(AA)-5H]^+$	✓	✓	✓	✓	✓	✓	✓	✓	✓	✓	✓	✓		✓
$[Bi_2Na(Cys)_2(AA)-6H]^+$			✓	✓	✓		✓	✓	✓					
$[Bi_2Na(Cys)_3(AA)-6H]^+$										✓				
$[Bi_3(Cys)(AA)_3-8H]^+$							✓							
$[Bi_3(Cys)_2(AA)_2-8H]^+$							✓							
$[Bi_3(Cys)_3(AA)-8H]^+$					✓	✓	✓	✓	✓	✓	✓			✓
$[Bi_3(Cys)_3(AA)_2-8H]^+$										✓				

Table 5.4 Updated summary of reported metal:amino acid interactions. A comparison is shown between bismuth-amino acid interactions observed in the absence (middle row, from Table 5.1) or presence (bottom row) of cysteine (Cys) in the reaction mixture.

	Trp	Tyr	His	Ser	Thr	Met	Cys	Hcy	Asp	Glu	Asn	Gln	Lys	Arg	Pro
Bi(III)[17]			✓		✓	✓	✓	✓			✓	✓			
Bi(III)/ Cys[q]	✓	✓	✓	✓	✓	✓	✓	✓	✓	✓	✓	✓	✓	✓	✓

[q] This thesis.

5.2 Results and Discussion: Bismuth Complexes with Histidine and Citric Acid

To illustrate the potential extent of the cooperative thiolate influence described in Section 5.1, six other three-component (bismuth-thiol-non-thiol) reaction mixtures have been examined by way of ESI-MS. Specifically, $Bi(NO_3)_3$ was combined in 50:50 ethanol:water with a representative amino acid, L-histidine (His), or the pharmaceutically relevant ligand, citric acid (Cit, in CBS), and one of three thiols, Cys, MPA, or MEA (Figure 5.2). In Table 5.5, mass-to-charge ratios and relative abundances are listed as ranges based on spectral data from two or three samples in each case. Formula assignments of *m/z* values have been supported by MS/MS experiments and comparison of experimental and calculated[195] isotope patterns. Data for reaction mixtures containing His and Cys have been expanded from the information presented in Table 5.2. In Table 5.6, a summary is given of all Bi-His and Bi-Cit ion formulae assigned in the presence of Cys, MPA, or MEA. It is noteworthy that substituting the structurally related amino acid, glycine (Gly, Figure 5.2), for Cys, MPA, or MEA, did not produce the same breadth of complex ions, a result which serves to validate the existence of a cooperative thiol effect on bismuth-non-thiol reaction mixtures investigated via ESI-MS.

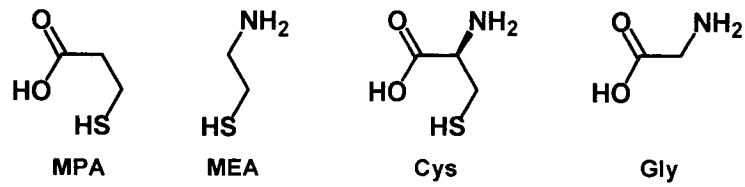

Figure 5.2 Structurally related ligands for bismuth. 3-Mercaptopriopionic acid (MPA), 2-mercaptoethylamine (MEA), L-cysteine (Cys), and glycine (Gly) are shown.

Table 5.5 Positive ion bismuth-thiol-non-thiol ESI-MS data for reaction mixtures containing $Bi(NO_3)_3$ and L-histidine (His) or citric acid (Cit), together with L-cysteine (Cys), 3-mercaptopropionic acid (MPA), or 2-mercaptoethylamine (MEA), in 50:50 ethanol:water.

***m/z* (Relative Abundance, %)**	**Assignment Bi/Cys/His**	***m/z* (Relative Abundance, %)**	**Assignment Bi/MPA/His**	***m/z* (Relative Abundance, %)**	**Assignment Bi/MEA/His**
				152.9 (10)	$[Cystamine+H]^+$
156.0 (100)[r]	$[(His)+H]^+$	156.0 (100)[r]	$[(His)+H]^+$	156.0-156.1 (100)	$[(His)+H]^+$
178.0-178.1 (3-5)	$[Na(His)]^+$	178.0-178.2 (2-6)	$[Na(His)]^+$	177.9-178.1 (3-4)	$[Na(His)]^+$
361.9-362.0 (4-5)	$[Bi(His)-2H]^+$	361.9-362.0 (15-22)[r]	$[Bi(His)-2H]^+$	361.9-362.0 (14-17)	$[Bi(His)-2H]^+$
482.9-483.0 (12-21)[r]	$[Bi(Cys)(His)-2H]^+$	467.9 (8)[r]	$[Bi(MPA)(His)-2H]^+$	439.0-439.1 (21-28)[r]	$[Bi(MEA)(His)-2H]^+$
504.9 (9-13)	$[BiNa(Cys)(His)-3H]^+$	490.0-490.1 (6-10)[r]	$[BiNa(MPA)(His)-3H]^+$	461.0-461.1 (9-11)	$[BiNa(MEA)(His)-3H]^+$
517.0-517.1 (13-16)[r]	$[Bi(His)_2-2H]^+$	516.9-517.0 (28-37)[r]	$[Bi(His)_2-2H]^+$	516.9-517.1 (13-17)[r]	$[Bi(His)_2-2H]^+$
539.0-539.1 (5)[r]	$[BiNa(His)_2-3H]^+$	538.9-539.0 (17-32)[r]	$[BiNa(His)_2-3H]^+$	538.9-539.1 (15-17)	$[BiNa(His)_2-3H]^+$
		671.8-671.9 (9-13)	$[Bi(His)_3-2H]^+$	671.7-671.9 (6-8)	$[Bi(His)_3-2H]^+$
		673.8-673.9 (18-36)	$[Bi_2(MPA)(His)-5H]^+$		
693.8-693.9 (6-13)	$[BiNa(His)_3-3H]^+$	693.9 (20-46)	$[BiNa(His)_3-3H]^+$	693.9-694.0 (18-22)	$[BiNa(His)_3-3H]^+$
		722.9-723.0 (9-16)	$[Bi_2(His)_2-5H]^+$	722.9-723.1 (6-10)	$[Bi_2(His)_2-5H]^+$
809.7 (8-15)	$[Bi_2(Cys)_2(His)-5H]^+$	779.8-779.9 (12-19)	$[Bi_2(MPA)_2(His)-5H]^+$	721.9-722.0 (9-16)	$[Bi_2(MEA)_2(His)-5H]^+$
831.5-831.7 (2-5)	$[Bi_2Na(Cys)_2(His)-6H]^+$	801.9-802.1 (4-6)	$[Bi_2Na(MPA)_2(His)-6H]^+$		
843.7-843.9 (3-8)	$[Bi_2(Cys)(His)_2-5H]^+$	828.7-828.9 (13-22)	$[Bi_2(MPA)(His)_2-5H]^+$	799.9 (15-22)	$[Bi_2(MEA)(His)_2-5H]^+$
		850.8-850.9 (9-16)	$[Bi_2Na(MPA)(His)_2-6H]^+$		
		877.9 (19-31)	$[Bi_2(His)_3-5H]^+$	877.9-878.1 (12-21)	$[Bi_2(His)_3-5H]^+$

[r] These peaks have been supported by MS/MS spectra.

m/z (Relative Abundance, %)	Assignment Bi/Cys/Cit	*m/z* (Relative Abundance, %)	Assignment Bi/MPA/Cit	*m/z* (Relative Abundance, %)	Assignment Bi/MEA/Cit
121.9 (9-16)[r]	$[Cys+H]^+$			152.9 (100)[r]	$[Cystamine+H]^+$
215.0 (11-13)	$[Na(Cit)]^+$	215.0-215.1 (62-100)	$[Na(Cit)]^+$	215.0-215.1 (8-9)	$[Na(Cit)]^+$
448.9 (100)	$[Bi(Cys)_2\text{-}2H]^+$				
519.9 (8-12)[r]	$[Bi(Cys)(Cit)\text{-}2H]^+$	504.9-505.0 (8-9)	$[Bi(MPA)(Cit)\text{-}2H]^+$	475.9-476.1 (4-9)[r]	$[Bi(MEA)(Cit)\text{-}2H]^+$
541.9 (25-35)[r]	$[BiNa(Cys)(Cit)\text{-}3H]^+$	527.0 (25-27)	$[BiNa(MPA)(Cit)\text{-}3H]^+$	497.9-498.0 (2-11)	$[BiNa(MEA)(Cit)\text{-}3H]^+$
		590.9-591.0 (68-72)[r]	$[Bi(Cit)_2\text{-}2H]^+$	590.7-590.9 (8-9)[r]	$[Bi(Cit)_2\text{-}2H]^+$
725.9-726.0 (8)	$[Bi_2(Cys)(Cit)\text{-}5H]^+$	710.9 (16-17)	$[Bi_2(MPA)(Cit)\text{-}5H]^+$		
		796.9-797.0 (100)	$[Bi_2(Cit)_2\text{-}5H]^+$	796.9 (4-16)	$[Bi_2(Cit)_2\text{-}5H]^+$
818.9-819.0 (10-13)	$[Bi_2Na(Cit)_2\text{-}6H]^+$	818.9-819.1 (63-86)	$[Bi_2Na(Cit)_2\text{-}6H]^+$	818.8-819.0 (3-32)	$[Bi_2Na(Cit)_2\text{-}6H]^+$
846.8 (12-15)	$[Bi_2(Cys)_2(Cit)\text{-}5H]^+$				
868.7-868.8 (16-20)	$[Bi_2Na(Cys)_2(Cit)\text{-}6H]^+$	838.7-838.9 (8)	$[Bi_2Na(MPA)_2(Cit)\text{-}6H]^+$		
1123.8 (9)	$[Bi_3(Cys)(Cit)_2\text{-}8H]^+$				
1173.6-1173.7 (7-9)	$[Bi_3(Cys)_3(Cit)\text{-}8H]^+$				
		1194.8-1194.9 (36)	$[Bi_3(Cit)_3\text{-}8H]^+$		
		1216.6-1216.9 (16)	$[Bi_3Na(Cit)_3\text{-}9H]^+$		

Table 5.6 Summary of assigned positive ion bismuth-histidine, bismuth-thiol-histidine, bismuth-citric acid, and bismuth-thiol-citric acid chemical formulae. Checkmarks indicate that that an ion of the corresponding assigned formula, containing bismuth(III), L-histidine (His) or citric acid (Cit), and/or a thiol (X = Cys, MPA, or MEA), has been observed.

Assigned Formula Containing His	X = Cys	X = MPA	X = MEA	Assigned Formula Containing Cit	X = Cys	X = MPA	X = MEA
$[Bi(His)\text{-}2H]^+$		✓	✓	$[Bi(Cit)_2\text{-}2H]^+$		✓	✓
$[Bi(His)_2\text{-}2H]^+$	✓	✓	✓	$[Bi_2(Cit)_2\text{-}5H]^+$		✓	✓
$[BiNa(His)_2\text{-}3H]^+$	✓	✓	✓	$[Bi_2Na(Cit)_2\text{-}6H]^+$	✓	✓	✓
$[Bi(His)_3\text{-}2H]^+$		✓	✓	$[Bi_3(Cit)_3\text{-}8H]^+$		✓	
$[BiNa(His)_3\text{-}3H]^+$	✓	✓	✓	$[Bi_3Na(Cit)_3\text{-}9H]^+$		✓	
$[Bi_2(His)_2\text{-}5H]^+$		✓	✓	$[BiX(Cit)\text{-}2H]^+$	✓	✓	✓
$[Bi_2(His)_3\text{-}5H]^+$		✓	✓	$[BiNaX(Cit)\text{-}3H]^+$	✓	✓	✓
$[BiX(His)\text{-}2H]^+$	✓	✓	✓	$[Bi_2X(Cit)\text{-}5H]^+$	✓	✓	
$[BiNaX(His)\text{-}3H]^+$	✓	✓	✓	$[Bi_2X_2(Cit)\text{-}5H]^+$	✓		
$[Bi_2X(His)\text{-}5H]^+$		✓		$[Bi_2NaX_2(Cit)\text{-}6H]^+$	✓	✓	
$[Bi_2X(His)_2\text{-}5H]^+$	✓	✓	✓	$[Bi_3X(Cit)_2\text{-}8H]^+$	✓		
$[Bi_2NaX(His)_2\text{-}6H]^+$		✓		$[Bi_3X_3(Cit)\text{-}8H]^+$	✓		
$[Bi_2X_2(His)\text{-}5H]^+$	✓	✓	✓				
$[Bi_2NaX_2(His)\text{-}6H]^+$	✓	✓					

The ESI-MS analysis of reactions containing $Bi(NO_3)_3$ and His with (X =) Cys, MPA, or MEA revealed fourteen peaks assigned to Bi-His and Bi-X-His ions (Tables 5.5, 5.6). In comparison, $[Bi(His)_2\text{-}2H]^+$ was the only cation previously assigned in spectra reported from reactions of $Bi(NO_3)_3$ with His.[17] Under the conditions of these experiments, it is clear that the presence of a thiol functionality (cysteine or otherwise) augments the interaction of other functional groups with bismuth.

In view of the positive effects of CBS as a component of some ulcer treatment regimens, the significance of a bismuth-citrate molecular framework cannot be overlooked. Of course, despite the solid state characterization of a number of bismuth-citrate derivatives,[31;107-113] analysis of the solution chemistry of these complexes can be complicated by the formation of extended bismuth-oxygen networks, recognizing also that solid state structures of isolated compounds are influenced by concentration and pH.[1;2] In general, the observation of bismuth-carboxylate complexes by mass spectrometry has not been reported, implicating labile bismuth-ligand interactions.

To the knowledge of the author, this report is the first to document bismuth-citrate complex ions observed by mass spectrometry. Notably, it is possible to observe a peak assigned to $[Bi(Cit)_2\text{-}2H]^+$ in mixtures of $Bi(NO_3)_3$ with Cit alone; however, peaks corresponding to Bi-Cit cations are not consistently observed in the absence of a thiol. In the presence of (X =) Cys, MPA, or MEA, a total of twelve Bi-Cit and Bi-X-Cit ions have been identified. These new Bi-Cit and Bi-X-Cit formulae (Tables 5.5, 5.6) lend insight into the potential compositions of commercially available bismuth preparations in the presence of other biologically relevant ligands.

In particular, ions assigned to $[Bi_2(Cit)_2\text{-}5H]^+$ (*m/z* 797) and $[Bi_2Na(Cit)_2\text{-}6H]^+$ (*m/z* 819) appear in the presence of MPA or MEA and display a striking formula resemblance to the $[Bi_2(Cit)_2\text{-}8H]^{2-}$ dianion observed consistently in the solid state by other researchers.[31;107-109;111;113] Two equally intriguing complex ions are $[Bi(Cys)(Cit)\text{-}2H]^+$ (*m/z* 520) and $[BiNa(Cys)(Cit)\text{-}3H]^+$ (*m/z* 542), which can be regarded as models of possible *in vivo* environments for Bi(III) if the metal cation is transferred directly from CBS to a cysteine-

containing biomolecule. A representative mass spectrum for the reaction of $Bi(NO_3)_3$, Cit and Cys is provided in Figure 5.2a, together with a proposed structural drawing of $[Bi(Cys)(Cit)\text{-}2H]^+$ (*m/z* 520). A tandem mass spectrum is given in Figure 5.2b to illustrate that a reasonable neutral loss of either [Bi(Cys)-3H] (327 u) or Cit (192 u) from *m/z* 542 results in the product ions, $[Na(Cit)]^+$ (*m/z* 215) or $[BiNa(Cys)\text{-}3H]^+$ (*m/z* 350), respectively.

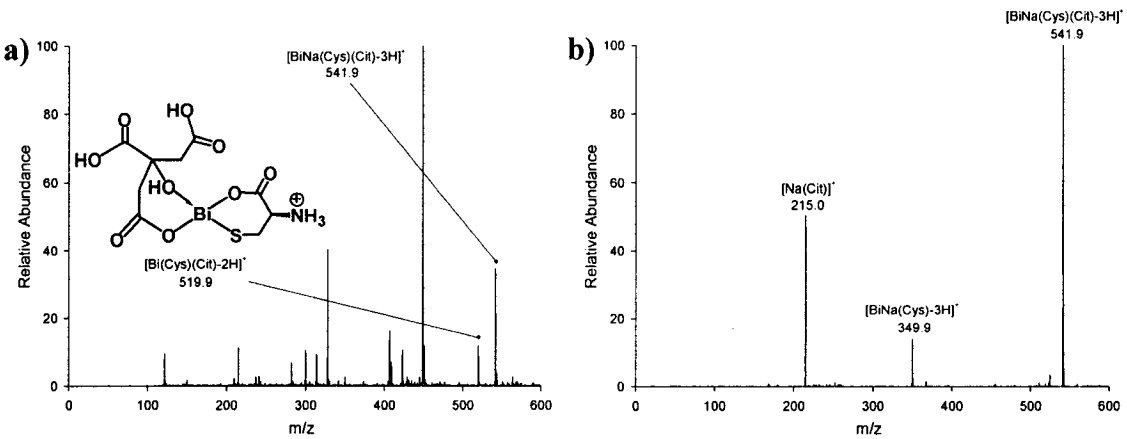

Figure 5.3 Positive ion bismuth-cysteine-citric acid ESI mass spectra. Reaction mixtures contained $Bi(NO_3)_3$, L-cysteine, and citric acid, in 50:50 ethanol:water. a) Full mass spectrum. The proposed connectivity for a bismuth-cysteinate-citrate complex cation assigned to *m/z* 520 is shown. b) Tandem mass spectrum from collision-induced dissociation of $[BiNa(Cys)(Cit)\text{-}3H]^+$ ions represented by *m/z* 542 (15 % collision energy).

5.3 Conclusions

To date, the observation of some complex ions of bismuth with certain non-thiol ligands can only be achieved in the presence of a thiol, a result which may reflect the biological activity of bismuth. As a result of examining various reaction mixtures containing bismuth(III) nitrate with citric acid or a non-thiol amino acid, in the presence of L-cysteine, 3-mercaptopropionic acid, or 2-mercaptoethylamine, it was determined that most bismuth-non-thiol complexes are only observed when a thiol is included in the reaction mixture. Based on previous preliminary work by a colleague,[233] the cooperative influence of a thiol (or thiolate) has been confirmed, and significantly developed, encompassing both bismuth-cysteine-amino acid samples and new bismuth-thiol-non-thiol systems.

The generality of a cooperative thiolate effect is demonstrated by the discovery of an array of new complex cations involving interactions of bismuth with various amino acids and thiols. Altogether, excluding sodiated analogues, more than thirty new bismuth-amino acid complex ions have been reported, including those which also contain Cys, MPA, or MEA. Even though the cooperative effect is not limited to cysteine, the implication is that this feature of bismuth chemistry may play a role in the biological behaviour of this element. In addition to the definitive identification of the first bismuth-citrate interactions by way of ESI-MS, a bismuth-cysteinate-citrate complex ion and corresponding sodiated analogue represent experimental evidence that provides a link between a) related research on administered bismuth drugs and b) potential biological active sites for bismuth. Once again, it has been shown that dilute solutions of bismuth compounds can be effectively analyzed using ESI-MS, thereby enabling the definitive identification of various gas phase species that have not been or cannot be otherwise observed.

5.4 Experimental Methods

Bismuth(III) nitrate pentahydrate, 3-mercaptopropionic acid, 2-mercaptoethylamine, glycine, L-cysteine, L-serine, L-threonine, DL-homocysteine, L-methionine, L-proline, L-tryptophan, L-histidine, L-lysine, L-arginine, L-aspartic acid, L-asparagine and L-glutamine were used as received from Sigma-Aldrich. Ethanol (HPLC reagent grade) and L-tyrosine were used as received from Fisher. L-Glutamic acid was used as received from Fluka. Citric acid monohydrate was used as received from BDH. All reactions were performed at room temperature using distilled water. Due to the hygroscopic nature of 2-mercaptoethylamine, in some instances this compound was weighed under an inert ($N_{2(g)}$) atmosphere prior to continuing the sample preparations in air. It can be noted that massing 2-mercaptoethylamine in air or under $N_{2(g)}$ did not lead to considerably different ESI mass spectra.

5.4.1 Reaction Mixtures of $Bi(NO_3)_3$, a Thiol or Glycine, and a Non-Thiol

Some of the reaction mixtures examined were prepared by combining and stirring a thiol (Cys, MPA, or MEA) or Gly (0.1 or 0.2 mmol), a non-thiol (0.1 or 0.2 mmol) and $Bi(NO_3)_3 \cdot 5H_2O$ (0.1 or 0.2 mmol) in 10 mL or 20 mL of solvent (50:50 ethanol:distilled water), respectively, for a period of 2 to 22 h. For comparison, other reaction mixtures were prepared by combining the thiol (0.2 mmol) or non-thiol (0.2 mmol) with $Bi(NO_3)_3 \cdot 5H_2O$ (0.2 mmol) in 5 mL of solvent (50:50 ethanol:distilled water), followed by a period of stirring from 1 to 3 h. Then, each bismuth-thiol (e.g., Bi-Cys) and bismuth-non-thiol (e.g., Bi-Cit) solution was combined with 5 mL of a non-thiol (e.g., Cit) or thiol (e.g., Cys) solution (0.2 mmol in 50:50 ethanol:distilled water), respectively. Stirring was continued for another 1 to 3 h. It can be noted that the order of addition of reactants did not lead to considerably different ESI mass spectra.

All reaction mixtures were filtered once or twice by suction and/or by passage through a NALGENE® cellulose acetate or PTFE syringe filter (0.2 μm pore size, 25 mm diameter). Filtration by suction or PTFE syringe filter was found to be preferable to filtration by cellulose acetate syringe filter, as contamination from the latter tended to generate spectral interference. Each filtrate was diluted ten-fold to a concentration ca. 0.001 M for mass analysis.

5.4.2 Reaction Mixtures of $Bi(NO_3)_3$, Cysteine, and a Non-Thiol Amino Acid

All reaction mixtures were prepared by combining and stirring an amino acid (L-serine, L-threonine, DL-homocysteine, L-methionine, L-proline, L-tyrosine, L-tryptophan, L-lysine, L-arginine, L-aspartic acid, L-glutamic acid, L-asparagine, or L-glutamine, 0.2 mmol), L-cysteine (0.2 mmol) and $Bi(NO_3)_3 \cdot 5H_2O$ (0.2 mmol) in 20 mL of solvent (50:50 ethanol:distilled water). Reaction mixtures were stirred for 18 to 23 h. A portion of each mixture was filtered by passage through a NALGENE® PTFE syringe filter (0.2 μm pore size, 25 mm diameter). Each filtrate was diluted ten-fold to a concentration ca. 0.001 M for mass analysis.

5.4.3 Electrospray Ionization Mass Spectrometry

Mass spectra were obtained using a Finnigan™ LCQ™$_{DUO}$ electrospray ionization quadrupole ion trap mass spectrometer. Each dilute filtrate was injected (in 3, 5, 10, 15, or 20 μL aliquots) directly into the electrospray ionization source of the mass spectrometer. The solvent flow rate was set at 1.2 mL/h, the heated capillary temperature at 200 °C, the sheath gas ($N_{2(g)}$) flow rate at 20 (arbitrary units), and the spray voltage at a magnitude of 4.00 kV. Tandem mass spectrometry (MS/MS) was achieved using helium as the collision gas, and applying a collision energy of 15 to 20 %. Spectra were analyzed and processed using software programs, Qual Browser (Version 1.2 from Finnigan Corp. ©1998–2000) and SigmaPlot (Version 10.0 from Systat Software, Inc. ©2006), respectively.

Chapter 6 Bismuth-Thiolate-Carboxylate Cluster Complexes

ESI-MS has been employed to identify complexes of Bi with small sulfur-containing biomolecules (amino acids,[16;17;33;70] peptides[16;18]). Such experiments (Chapter 5) have also been discussed in which the presence of a thiol such as cysteine was found to promote the formation of complex ions of bismuth with non-thiol amino acids.[17;70] In support of ESI-MS data, solid state structures of complexes containing bismuth with cysteine or thiolactic acid ligands indicate that both the thiolate and carboxylate functionalities in these molecules engage bismuth.[28]

Recognizing the pronounced thiophilicity of bismuth[2;12] and the prevalence of cysteine in biological systems, a thorough understanding of bismuth-thiolate-carboxylate chemistry is essential. In this context, the following Sections of Chapter 6 describe a comprehensive ESI-MS study of reaction mixtures containing $Bi(NO_3)_3$ with mercaptosuccinic acid (thiomalic acid, TMA), 2-mercaptopropionic acid (thiolactic acid, TLA), 3-mercaptopropionic acid (MPA), or 2-amino-3-mercaptopropionic acid (L-cysteine, Cys). This selected set of four biologically relevant thiol-carboxylic acids (Figure 6.1) provides a palette of complementary ligand frameworks with which to further assess bismuth-thiol coordination chemistry and gain chemical insight into the bioactive behavior of bismuth.

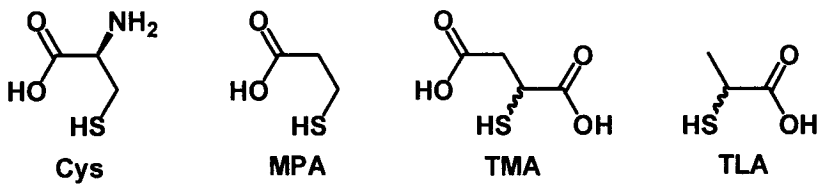

Figure 6.1 Structurally related thiol-carboxylic acid ligands for bismuth. L-Cysteine (Cys), 3-mercaptopriopionic acid (MPA), thiomalic acid (TMA), and thiolactic acid (TLA) are shown.

6.1 Results and Discussion: Homoleptic Bismuth Complexes

ESI-MS data for reaction mixtures containing $Bi(NO_3)_3$ with MPA, TMA, or TLA in 50:50 ethanol:water are presented in Table 6.1. Table 6.2 provides a summary of the stoichiometric ratios observed for Bi:MPA, Bi:TMA, and Bi:TLA complex ions. Mass-to-charge ratios (*m/z*) and relative abundances are listed as ranges over four (TLA, TMA)

or ten sample injections (MPA) from two separate samples for each bismuth-ligand combination. Peaks with relative intensities of less than 5 % are not reported unless the identification of these peaks is useful for comparison between spectra. Tandem mass spectral results are reported from selected MS/MS spectra where the normalized spectral intensity (NL) was $\geq 2 \times 10^4$ (arbitrary units). Not all fragment ions are listed, and in some cases (indicated by a dash in Table 6.1) it was not possible to acquire reliable, intense (NL $\geq 2 \times 10^4$) MS/MS spectra.

Peak assignments in Table 6.1 are presented as generic formulae, $[Bi_v(L)_w\text{-}yH]^z$ (v = 1 to 5; L = MPA, TLA, or TMA; w = 1 to 7; y = 2 to 14; z = ±1), containing one or more bismuth atoms with one or more thiolate-carboxylate ligands. A loss of ligand protons presumably generates the monoionic species that are observed. Multiply charged ions have not been observed. In some cases, sodium, nitrate, or sulfur are involved in the complex ion assignments. Fragment ion formulae (listed in the far right column of Table 6.1) are derived from a neutral mass loss. A comparison of experimental and theoretical[195;209] isotope patterns has been undertaken for all Table 6.1 peak assignments, and corresponding spectra have been compiled in Appendix C.

Bismuth:ligand complex ions with stoichiometric ratios of 1:1 from reaction mixtures containing $Bi(NO_3)_3$ and TMA or TLA were observed in both positive and negative ion modes. Conversely, from reaction mixtures containing $Bi(NO_3)_3$ and MPA, a 1:1:1 Bi:MPA:sulfur peak (*m/z* 345) was observed only in negative ion mode. Given that MPA is the amine-free structural analogue of Cys, and that a 1:1 Bi:Cys cation at *m/z* 328 is consistently observed,[16;17;70] the absence of a 1:1 Bi:MPA complex ion is surprising. It is possible that the amine functionality in Cys plays a role in the coordination of bismuth by cysteine. This supposition is supported by the known solid state structure of the coordination complex shown in Figure 1.17b, involving the interaction of amino, thiolate, and carboxylate functional groups of penicillamine (3,3-dimethylcysteine) with bismuth.[134]

Table 6.1 Positive- and negative ion bismuth-thiolate-carboxylate ESI-MS data from reaction mixtures containing $Bi(NO_3)_3$ with one ligand, L = 3-mercaptopropionic acid (MPA), thiolactic acid (TLA), or thiomalic acid (TMA), in 50:50 ethanol:water.

$Bi(NO_3)_3$/L	*m/z*	Relative Abundance (%)	Assignment	MS/MS (*m/z*)	Fragment Assignment
L = MPA	418.9-419.0	20-32	$[Bi(MPA)_2\text{-}2H]^+$	312.9	$[Bi(MPA)\text{-}2H]^+$
Positive Mode				330.9	$[Bi(SCH_2CH_3)_2]^+$
				358.8	$[Bi(MPA)_2\text{-}2H\text{-}C_2H_4O_2]^+$
				400.8	$[Bi(MPA)_2\text{-}2H\text{-}H_2O]^+$
	440.9-441.1	6-13	$[BiNa(MPA)_2\text{-}3H]^+$	336.9	$[BiNa(MPA)(SCH_2CH_3)\text{-}3H\text{-}C_2H_4O_2]^+$
				368.9	$[BiNa(MPA)(S)\text{-}H]^+$
	730.9	100	$[Bi_2(MPA)_3\text{-}5H]^+$	586.9	$[Bi_2(MPA)(S)_2\text{-}H]^+$
				658.9	$[Bi_2(MPA)_2(S)\text{-}3H]^+$
	752.9-753.0	17-42	$[Bi_2Na(MPA)_3\text{-}6H]^+$	680.9	$[Bi_2Na(MPA)_2(S)\text{-}4H]^+$
	1042.7-1042.8	34-46	$[Bi_3(MPA)_4\text{-}8H]^+$	866.9	$[Bi_3(MPA)_2(O)_2\text{-}4H]^+$
				882.8	$[Bi_3(MPA)_2(S)(O)\text{-}4H]^+$
				898.9	$[Bi_3(MPA)_2(S)_2\text{-}4H]^+$
				954.8	$[Bi_3(MPA)_3(O)\text{-}6H]^+$
				970.8	$[Bi_3(MPA)_3(S)\text{-}6H]^+$
	1460.1-1460.5	1-5	$[Bi_4(MPA)_6\text{-}11H]^+$	-	
	1482.2-1482.5	2-6	$[Bi_4Na(MPA)_6\text{-}12H]^+$	-	
	1772.1-1772.5	2-4	$[Bi_5(MPA)_7\text{-}14H]^+$	-	
L = MPA	344.9	20-26	$[Bi(MPA)(S)\text{-}2H]^-$	241.1	$[Bi(S)]^-$
Negative Mode				273.2	$[Bi(S)_2]^-$
				300.8	$[Bi(MPA)(S)\text{-}2H\text{-}CO_2]^-$
	416.9	100	$[Bi(MPA)_2\text{-}4H]^-$	312.8	$[Bi(MPA)\text{-}2H]^-$
				345.0	$[Bi(MPA)(S)\text{-}2H]^-$
				372.9	$[Bi(MPA)_2\text{-}4H\text{-}CO_2]^-$
	501.8	10-34	$[BiNa(MPA)_2(NO_3)\text{-}4H]^-$	416.9	$[Bi(MPA)_2\text{-}4H]^-$
	791.7	13-27	$[Bi_2(MPA)_3(NO_3)\text{-}6H]^-$	345.0	$[Bi(MPA)(S)\text{-}2H]^-$
				416.9	$[Bi(MPA)_2\text{-}4H]^-$
				719.8	$[Bi_2(MPA)_2(S)(NO_3)\text{-}4H]^-$
	1146.6-1146.7	28-35	$[Bi_3(MPA)_5\text{-}10H]^-$	344.9	$[Bi(MPA)(S)\text{-}2H]^-$
				416.9	$[Bi(MPA)_2\text{-}4H]^-$
				1074.6	$[Bi_3(MPA)_4(S)\text{-}8H]^-$

$Bi(NO_3)_3$/L	*m/z*	Relative Abundance (%)	Assignment	MS/MS (*m/z*)	Fragment Assignment
L = TLA	312.8-312.9	8-10	$[Bi(TLA)-2H]^+$	-	
Positive Mode	418.9-419.0	74-87	$[Bi(TLA)_2-2H]^+$	312.9	$[Bi(TLA)-2H]^+$
				372.8	$[Bi(TLA)_2-2H-CH_2O_2]^+$
				400.7	$[Bi(TLA)_2-2H-H_2O]^+$
	730.7	95-100	$[Bi_2(TLA)_3-5H]^+$	-	
	752.8-752.9	61-86	$[Bi_2Na(TLA)_3-6H]^+$	576.9	$[Bi_2Na(TLA)(O)_2-2H]^+$
				648.8	$[Bi_2Na(TLA)_2-4H]^+$
				664.9	$[Bi_2Na(TLA)_2(O)-4H]^+$
				680.9	$[Bi_2Na(TLA)_2(S)-4H]^+$
	1042.7	76-100	$[Bi_3(TLA)_4-8H]^+$	970.9	$[Bi_3(TLA)_3(S)-6H]^+$
	1460.2-1460.4	12-18	$[Bi_4(TLA)_6-11H]^+$	-	
	1482.3-1482.4	8-14	$[Bi_4Na(TLA)_6-12H]^+$	680.8	$[Bi_2Na(TLA)_2(S)-4H]^+$
				752.9	$[Bi_2Na(TLA)_3-6H]^+$
	1772.3	39-47	$[Bi_5(TLA)_7-14H]^+$	1042.7	$[Bi_3(TLA)_4-8H]^+$
L = TLA	312.9	19-28	$[Bi(TLA)-2H]^-$	209.1	$[Bi]^-$
Negative Mode				268.9	$[Bi(TLA)-2H-CO_2]^-$
	416.9	100	$[Bi(TLA)_2-4H]^-$	312.9	$[Bi(TLA)-2H]^-$
	501.6-501.7	4-10	$[BiNa(TLA)_2(NO_3)-4H]^-$	-	
	791.5-791.7	23-28	$[Bi_2(TLA)_3(NO_3)-6H]^-$	-	
	1146.5	58-69	$[Bi_3(TLA)_5-10H]^-$	-	

$Bi(NO_3)_3$/L	*m/z*	Relative Abundance (%)	Assignment	MS/MS (*m/z*)	Fragment Assignment
L = TMA Positive Mode	357.0-357.1	33-92	$[Bi(TMA)-2H]^+$	241.1	$[Bi(S)]^+$
				312.9	$[Bi(TMA)-2H-CO_2]^+$
				338.7	$[Bi(TMA)-2H-H_2O]^+$
	506.9-507.0	100	$[Bi(TMA)_2-2H]^+$	356.9	$[Bi(TMA)-2H]^+$
				488.9	$[Bi(TMA)_2-2H-H_2O]^+$
	528.9-529.0	37-65	$[BiNa(TMA)_2-3H]^+$	378.9	$[BiNa(TMA)-3H]^+$
	550.9-551.0	9-24	$[BiNa_2(TMA)_2-4H]^+$	-	
	712.9-713.0	12-27	$[Bi_2(TMA)_2-5H]^+$	-	
	734.9-735.0	37-74	$[Bi_2Na(TMA)_2-6H]^+$	379.1	$[BiNa(TMA)-3H]^+$
	862.7-862.9	11-42	$[Bi_2(TMA)_3-5H]^+$	-	
	884.6-884.8	13-21	$[Bi_2Na(TMA)_3-6H]^+$	-	
	906.7-906.9	14-21	$[Bi_2Na_2(TMA)_3-7H]^+$	-	
	1068.7-1068.9	17-20	$[Bi_3(TMA)_3-8H]^+$	-	
	1090.6-1090.7	9-11	$[Bi_3Na(TMA)_3-9H]^+$	-	
	1218.6-1218.9	1-11	$[Bi_3(TMA)_4-8H]^+$	-	
	1240.5-1240.7	3-11	$[Bi_3Na(TMA)_4-9H]^+$	-	
	1262.5-1262.9	8-13	$[Bi_3Na_2(TMA)_4-10H]^+$	-	
	1424.4-1424.9	6-15	$[Bi_4(TMA)_4-11H]^+$	-	
	1446.5-1446.9	12-20	$[Bi_4Na(TMA)_4-12H]^+$	735.0	$[Bi_2Na(TMA)_2-6H]^+$
				1090.6	$[Bi_3(Na(TMA)_3-9H]^+$

$Bi(NO_3)_3$/L	*m/z*	Relative Abundance (%)	Assignment	MS/MS (*m/z*)	Fragment Assignment
L = TMA Negative Mode	356.9-357.1	6-13	$[Bi(TMA)-2H]^-$	114.9	$[(TMA)-3H-S]^-$
				241.1	$[Bi(S)]^-$
				312.9	$[Bi(TLA)-2H]^-$
				338.7	$[Bi(TMA)-2H-H_2O]^-$
	504.9-505.0	100	$[Bi(TMA)_2-4H]^-$	149.0	$[(TMA)-H]^-$
				357.1	$[Bi(TMA)-2H]^-$
				389.0	$[Bi(TMA)(S)-2H]^-$
				486.8	$[Bi(TMA)_2-4H-H_2O]^-$
	526.8-526.9	5-12	$[BiNa(TMA)_2-5H]^-$	-	
	548.9	3-11	$[BiNa_2(TMA)_2-6H]^-$	-	
	860.5-860.6	5-13	$[Bi_2(TMA)_3-7H]^-$	-	
	882.7-882.9	26-34	$[Bi_2Na(TMA)_3-8H]^-$	526.9	$[BiNa(TMA)_2-5H]^-$
				734.9	$[Bi_2Na(TMA)_2-6H]^-$
				766.9	$[Bi_2Na(TMA)_2(S)-6H]^-$
				864.7	$[Bi_2Na(TMA)_3-8H-H_2O]^-$
	904.8-904.9	7-15	$[Bi_2Na_2(TMA)_3-9H]^-$	-	
	1216.6-1216.7	5-12	$[Bi_3(TMA)_4-10H]^-$	-	
	1238.5-1238.6	11-17	$[Bi_3Na(TMA)_4-11H]^-$	-	
	1260.6-1260.7	5-14	$[Bi_3Na_2(TMA)_4-12H]^-$	904.8	$[Bi_2Na_2(TMA)_3-9H]^-$
	1572.5-1572.6	3-8	$[Bi_4(TMA)_5-13H]^-$	-	
	1594.4-1594.5	6-11	$[Bi_4Na(TMA)_5-14H]^-$	882.9	$[Bi_2Na(TMA)_3-8H]^-$
				1238.6	$[Bi_3Na(TMA)_4-11H]^-$
	1616.5-1616.6	3-8	$[Bi_4Na_2(TMA)_5-15H]^-$	-	

Table 6.2 Summary of observed positive- and negative ion Bi:L (L = MPA, TLA, or TMA) stoichiometric ratios.

Positive Mode			Negative Mode		
Bi:MPA	**Bi:TLA**	**Bi:TMA**	**Bi:MPA**	**Bi:TLA**	**Bi:TMA**
-	1:1	1:1	1:1:S	1:1	1:1
1:2	1:2	1:2	1:2	1:2	1:2
1:2:Na	-	1:2:Na	1:2:Na:NO_3	1:2:Na:NO_3	1:2:Na
-	-	1:2:2Na	-	-	1:2:2Na
-	-	2:2	-	-	-
-	-	2:2:Na	-	-	-
2:3	2:3	2:3	-	-	2:3
2:3:Na	2:3:Na	2:3:Na	2:3:NO_3	2:3:NO_3	2:3:Na
-	-	2:3:2Na	-	-	2:3:2Na
-	-	3:3	-	-	-
-	-	3:3:Na	-	-	-
3:4	3:4	3:4	-	-	3:4
-	-	3:4:Na	-	-	3:4:Na
-	-	3:4:2Na	-	-	3:4:2Na
-	-	-	3:5	3:5	-
-	-	4:4	-	-	-
-	-	4:4:Na	-	-	-
-	-	-	-	-	4:5
-	-	-	-	-	4:5:Na
-	-	-	-	-	4:5:2Na
4:6	4:6	-	-	-	-
4:6:Na	4:6:Na	-	-	-	-
5:7	5:7	-	-	-	-

In contrast to the tridentate coordination of a dianionic penicillamine ligand to bismuth as shown in Figure 1.17b,[134] the cysteinatobismuth(III) complex shown in Figure 1.17c contains a bidentate monoanionic cysteinate ligand bound to bismuth via the thiolate and carboxylate functionalities only. While TLA or TMA have the potential to chelate in a bidentate fashion to bismuth to generate a five-membered ring (Figure 6.2a, b, respectively), MPA affords a six-membered chelate ring (Figure 6.2d). Both five-[20;21;23;27;28] and six-membered[20;25;28] chelate heterocycles are known for thiolate or thiolate-carboxylate ligands coordinated to bismuth, but the five-membered chelate ring is most common.[12] It is possible that the absence of a 1:1 Bi:MPA complex ion in ESI mass spectra is due to the inability of MPA to provide a five-membered chelation environment.

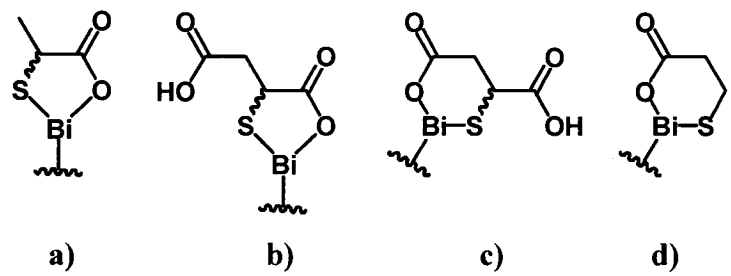

Figure 6.2 Chelation of thiolate-carboxylate ligands to bismuth. This generates five-membered or six-membered rings: a), thiolactic acid, b) and c) thiomalic acid, and d) 3-mercaptopropionic acid.

Complex ions with bismuth:ligand (Bi:L) stoichiometric ratios of 1:2 and 2:3 are observed in both positive and negative ion modes. A greater number of Bi:L ions was identified for bismuth in the presence of TMA compared to MPA or TLA. Considering both ion modes, ions with Bi:TMA ratios of 2:2, 2:3, 3:3, 3:4, 4:4, and 4:5 are observed along with various sodiated analogues. Complex ions that contain an n:n bismuth:ligand ratio (n = 2 to 4) are observed exclusively in positive ion spectra from the combination of $Bi(NO_3)_3$ and TMA. Bi:TMA stoichiometries of 2:2, 3:3, and 4:4 were assigned to peaks with *m/z* values of 713, 1069, and 1425, respectively. For comparison, 2:2 Bi:Cys complex cations have been previously reported.[16;17;70] In addition, the cation, $[Bi_3(L)_4\text{-}8H]^+$, and the anion, $[Bi_3(L)_5\text{-}10H]^-$, are observed for both MPA and TLA. These stoichiometric Bi:L (L = TLA or MPA) ratios of 3:4 (Figure 6.3a) and 3:5 (Figure 6.3b)

are rationalized in terms of L being a dianionic ligand, which limits the stoichiometric options to those observed.

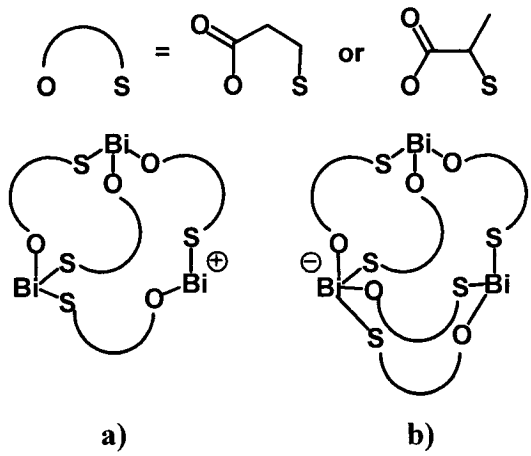

Figure 6.3 Proposed structures of bismuth-thiolate-carboxylate complex ions. a) 3:4 and b) 3:5 Bi:L (L = TLA or MPA).

A larger number of Bi:TMA complex ions are observed than for Bi:MPA or Bi:TLA, perhaps due to the coordinative versatility provided by two carboxylic acid groups in TMA, and the potential for TMA to adopt both five-membered (Figure 6.2b) and six-membered (Figure 6.2c) chelation frameworks. Representative positive and negative ion spectra from reaction mixtures of $Bi(NO_3)_3$ with TMA, TLA, or MPA are shown in Figure 6.4.

Tandem mass spectra have been obtained to support many of the peak assignments listed in Table 6.1. Qualitatively, the signal-to-noise ratio of peaks in MS/MS spectra increases as the normalized spectral intensity (NL) increases. In the experience of the author, when the NL is relatively low (e.g., $< 1 \times 10^4$) there are inconsistencies in the spectral data over time. Therefore, MS/MS peak assignments reported in Table 6.1 are for NL $\geq 2 \times 10^4$. In positive ion mode, neutral losses of intact thiol-carboxylic acid ligands or ligand fragments such as water (18 u), carbon dioxide (44 u), $C_3H_4O_2$ (72 u), or C_3H_4OS (88 u) are typically observed. Figures 6.5 to 6.8 show sample tandem mass spectra and fragmentation pathways for the collision-induced dissociation (CID) of 2:3:1 Bi:TLA:Na and 3:4 Bi:MPA cations.

The fragmentation spectrum of *m/z* 753 shown in Figure 6.5a contains four product ion peaks with relative abundances greater than 5 %. Three of these peaks, *m/z* 577, 665, and 681, have been identified as resulting from neutral losses of two units of C_3H_4OS, one unit of C_3H_4OS, and one unit of $C_3H_4O_2$, respectively. The product ion at *m/z* 649 is thought to be the result of reduction of bismuth, with a concurrent neutral loss of 104 u ($C_3H_4O_2S$, possibly a thiolactate diradical), yielding $[Bi_2Na(TLA)_2\text{-}4H]^+$. Similarly, the loss of a lactate ($C_3H_4O_3^{\bullet}$) radical from a Cu(II) cation, $[Cu^{II}(LA)_2\text{-}H]^+$ (LA = lactic acid), has been observed to produce a Cu(I) species, $[Cu^{I}(LA)]^+$.[235] Moreover, reduction-oxidation reactions are not uncommon for coordination complexes examined by way of ESI-MS.[236] As listed in Table 6.1, the 1:1 Bi:L cations, $[Bi(L)\text{-}2H]^+$ (L = TLA, *m/z* 313 or TMA, *m/z* 357), appear with the same formulae and mass-to-charge ratios in the negative ion mode. Again, this result is presumably due to the reduction of bismuth. The oxidation product in these reactions may be a disulfide of TLA or TMA, although deprotonated disulfide peaks (anticipated at *m/z* 209 and *m/z* 297 for $HOOC\text{-}CH(CH_3)\text{-}S\text{-}S\text{-}CH(CH_3)\text{-}COO^-$ and $HOOC\text{-}CH_2\text{-}CH(COOH)\text{-}S\text{-}S\text{-}CH(COOH)\text{-}CH_2\text{-}COO^-$, respectively) were not present in the recorded mass spectra.

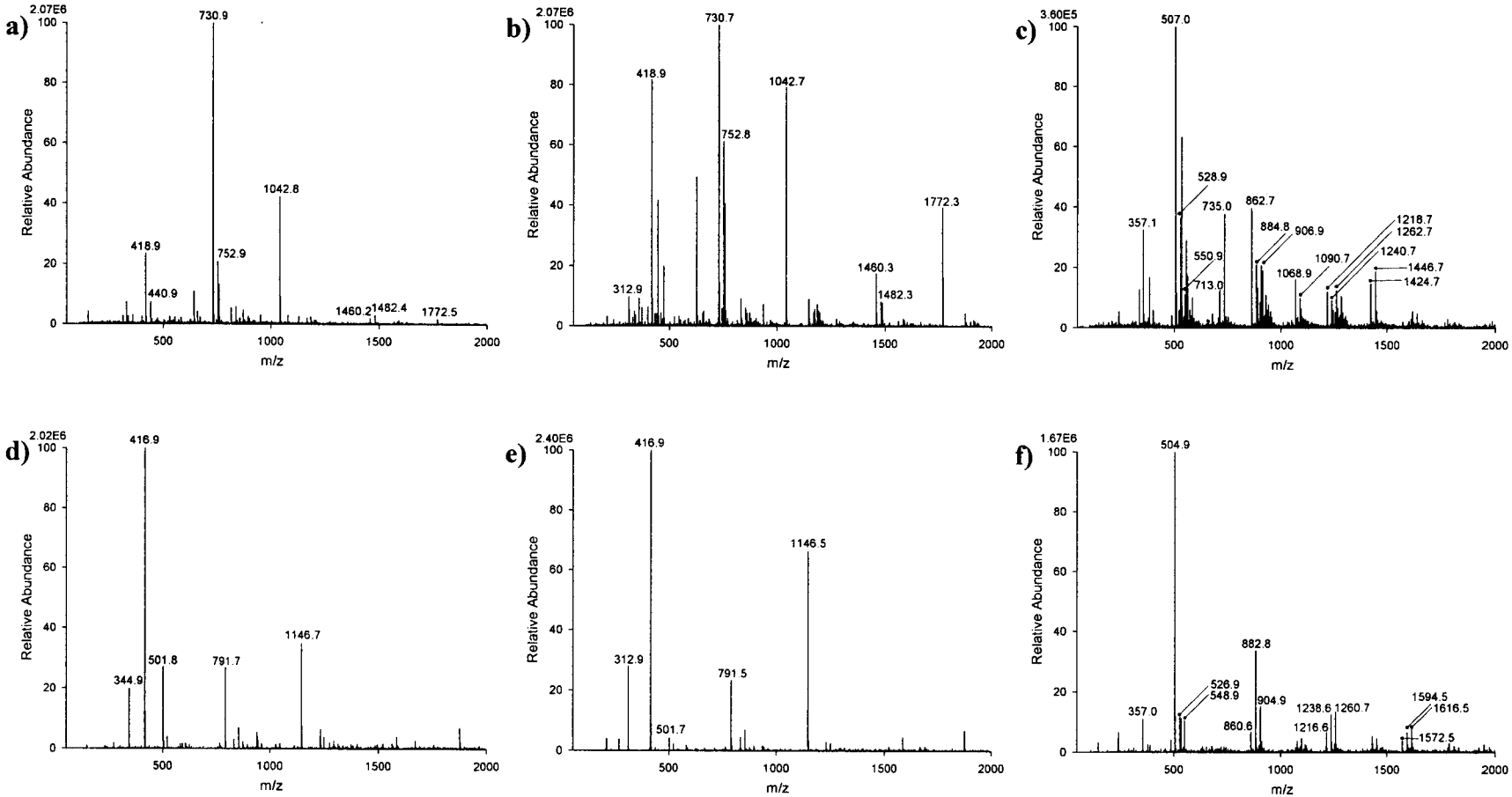

Figure 6.4 Bismuth-thiolate-carboxylate ESI-MS spectra. Reaction mixtures contained a) $Bi(NO_3)_3$ and MPA, b) $Bi(NO_3)_3$ and TLA, and c) $Bi(NO_3)_3$ and TMA (positive ion mode), d) $Bi(NO_3)_3$ and MPA, e) $Bi(NO_3)_3$ and TLA, f) $Bi(NO_3)_3$ and TMA (negative ion mode), in 50:50 ethanol:water. Denoted peaks are also listed in Table 6.1.

In Figure 6.5b, the neutral losses of thiolactate ligand fragments, $C_3H_4O_2$ (72 u), C_3H_4OS (88 u), $2C_3H_4O_2$ (144 u), $C_3H_4O_2$ + C_3H_4OS (160 u), and $2C_3H_4OS$ (176 u), have been assigned to product ion peaks at *m/z* 971, *m/z* 955, *m/z* 899, *m/z* 883, and *m/z* 867, respectively, from CID of 3:4 Bi:MPA ions at *m/z* 1043. Fragmentation pathways consistent with the peak designations in Figures 6.5a and b are provided in Figures 6.6 and 6.7, respectively. A possible mechanism for the fragmentation of $[Bi_2Na(TLA)_3\text{-}6H]^+$ (*m/z* 753) to yield $[Bi_2Na(TLA)_2(S)\text{-}4H]^+$ (*m/z* 681) resembles a gas-phase Meerwein mechanism for the fragmentation of organic 1,3-oxathiolanylium ions using electron ionization mass spectrometry (EI-MS),[237] involving the neutral loss of a functionalized epoxide with a mass of 72 atomic units. A sequential loss of two neutral molecules of $C_3H_4O_2$ (potentially β-propiolactone) from $[Bi_3(MPA)_4\text{-}8H]^+$ (*m/z* 1043) is proposed to yield fragment cations, $[Bi_3(MPA)_3(S)\text{-}6H]^+$ and $[Bi_3(MPA)_2(S)_2\text{-}4H]^+$, at *m/z* 971 and *m/z* 899, respectively.

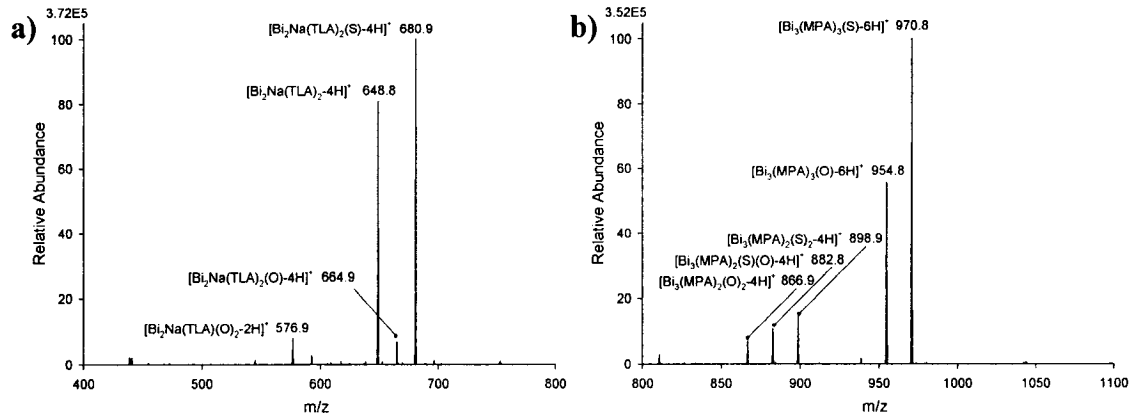

Figure 6.5 Collision-induced dissociation of bismuth-TLA and -MPA ions. a) $[Bi_2Na(TLA)_3\text{-}6H]^+$ ions represented by *m/z* 753 at 30 % collision energy, and b) $[Bi_3(MPA)_4\text{-}8H]^+$ ions represented by *m/z* 1043 at 25 % collision energy.

In general, the experimental isotope patterns for peaks listed in Table 6.1 have assigned chemical formulae that yield matching theoretical isotope patterns. As shown in Figure 6.8, the experimental isotope distributions of peaks at *m/z* 753 and *m/z* 1043 (expanded from Figure 6.4b, a, respectively) are consistent with the theoretical distributions of relative intensities calculated for and $Bi_2NaC_9H_{12}O_6S_3$ (Figure 6.8a) and $Bi_3C_{12}H_{16}O_8S_4$ (Figure 6.8b). Again, given that the abundance of naturally-occurring ^{209}Bi is 100 %,

mass spectral peaks which represent complex ions containing bismuth do not have a unique bismuth isotope pattern by which to efficiently identify bismuth-based peaks. However, all of the peaks of interest correspond to complex ions featuring both bismuth and sulfur. Therefore, the characteristic isotopic distribution of sulfur can been exploited to support peak assignments. Extended data for experimental and calculated isotope patterns are provided in Appendix C.

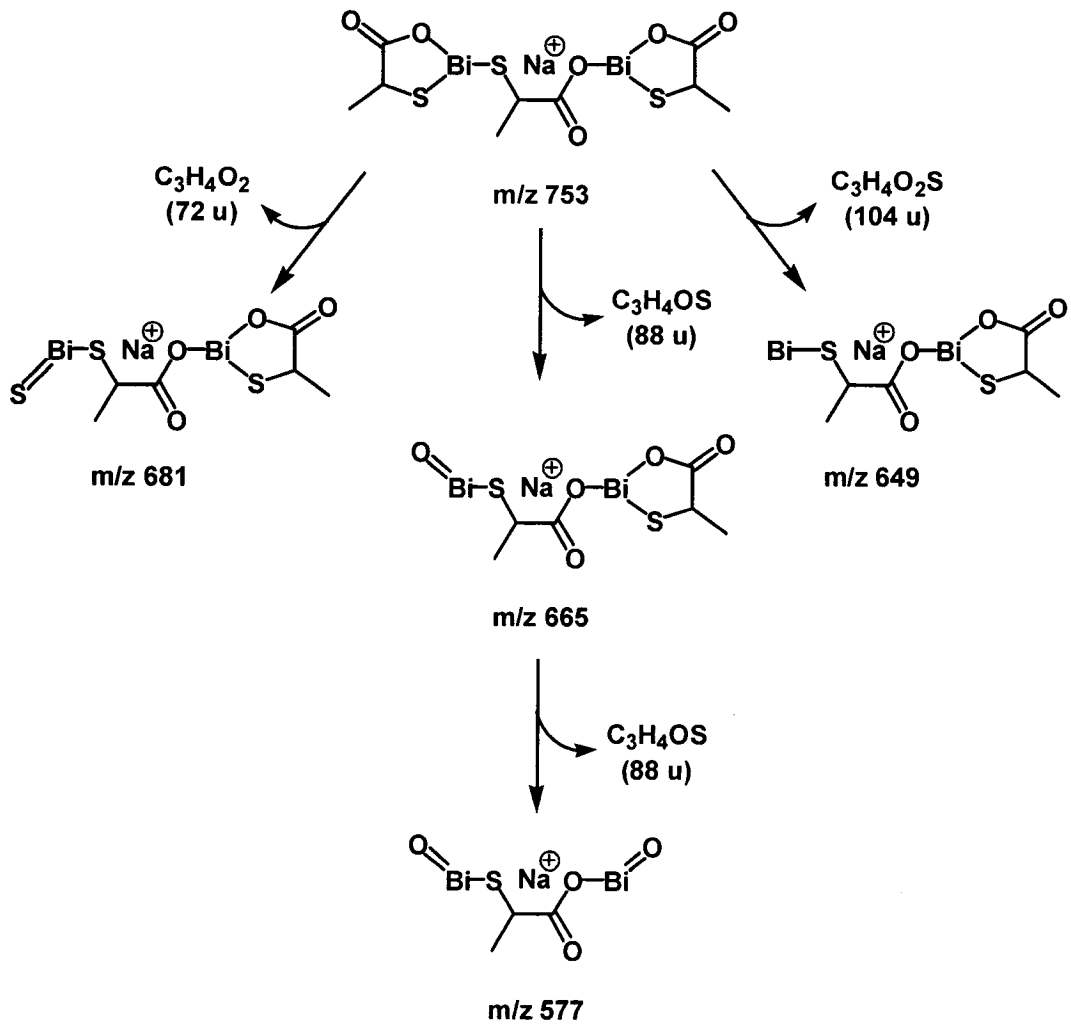

Figure 6.6 Ion fragmentation pathway for $[Bi_2Na(TLA)_3\text{-}6H]^+$ at *m/z* 753.

Multi-bismuth multi-ligand complex ions have been discovered with stoichiometric ratios of up to five bismuth cations coordinated by seven thiol-carboxylic acid ligands: $[Bi_5(TLA)_7\text{-}14H]^+$ (39 to 47 %), $[Bi_5(MPA)_7\text{-}14H]^+$ (2 to 4 %). It is important to recognize that due to the possibility of multi-bismuth multi-ligand clusters forming as a

result of the ESI process itself,[238] it is not possible to directly correlate the solution- and gas-phase chemistries of bismuth-thiol-carboxylic acid reaction mixtures. However, it has been definitively demonstrated that the formation of gas-phase multi-bismuth multi-ligand complexes is possible, and these multi-bismuth multi-ligand complex ions can be justifiably compared to known solid state multi-bismuth multi-ligand cluster compounds that have already had an impact on understanding the biologically relevant chemistry of bismuth.

For example, the 2:2:0 and 2:2:1 Bi:TMA:Na cations assigned to peaks at *m/z* 713 and 735, respectively (Figure 6.4c), along with previously identified 2:2 Bi:Cys and Bi:Cit (Cit = citric acid) cations,[17;70] are comparable to the well-known solid state $[Bi_2(cit)_2]^{2-}$ dimer (cit = tetradeprotonated citric acid, $C_6H_4O_7^{4-}$) counterbalanced by various combinations of sodium, potassium, or ammonium cations.[31;107-113] Other solid state multi-bismuth multi-ligand clusters of bismuth and biologically relevant thiol or carboxylic acid ligands are known, including salicylic acid,[32] 2-ethoxybenzoic acid, and 2-mercaptopropanol.[99]

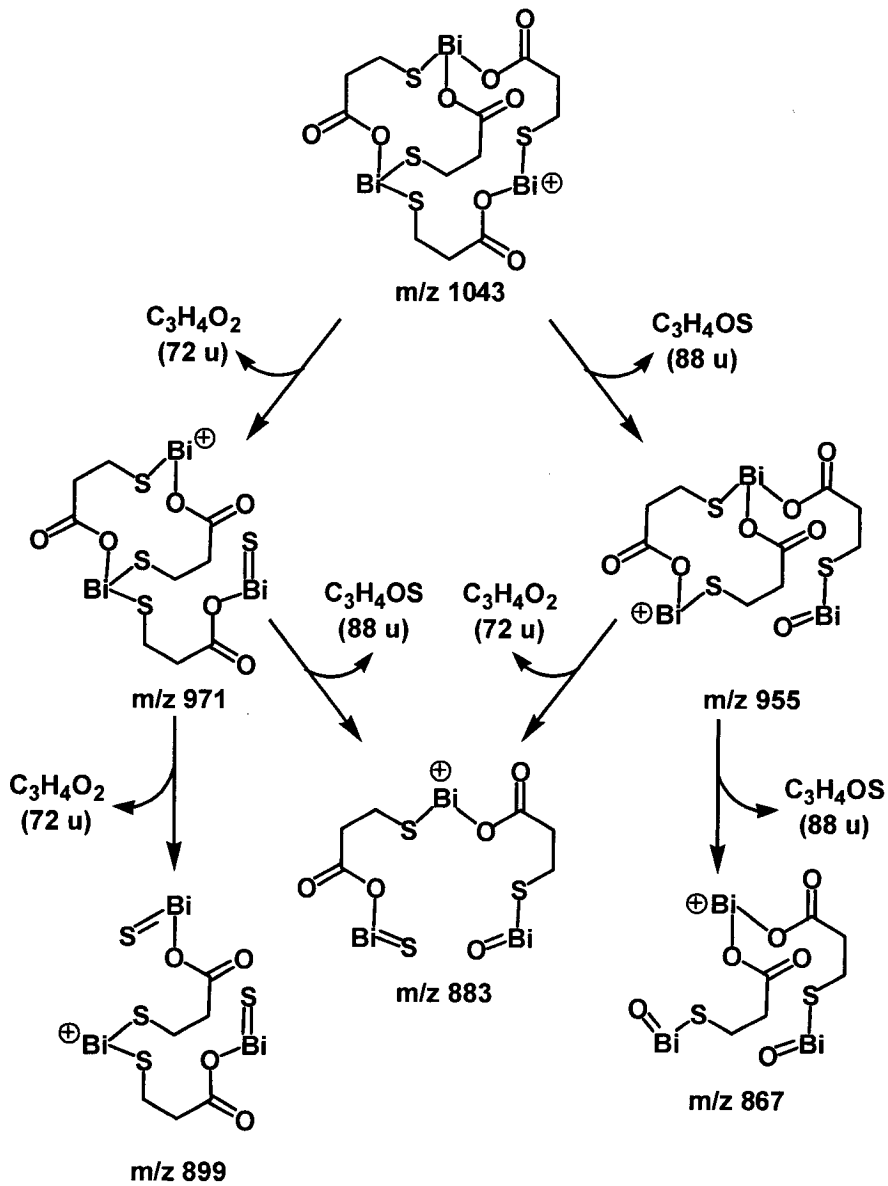

Figure 6.7 Ion fragmentation pathway for $[Bi_3(MPA)_4\text{-}8H]^+$ at *m/z* 1043.

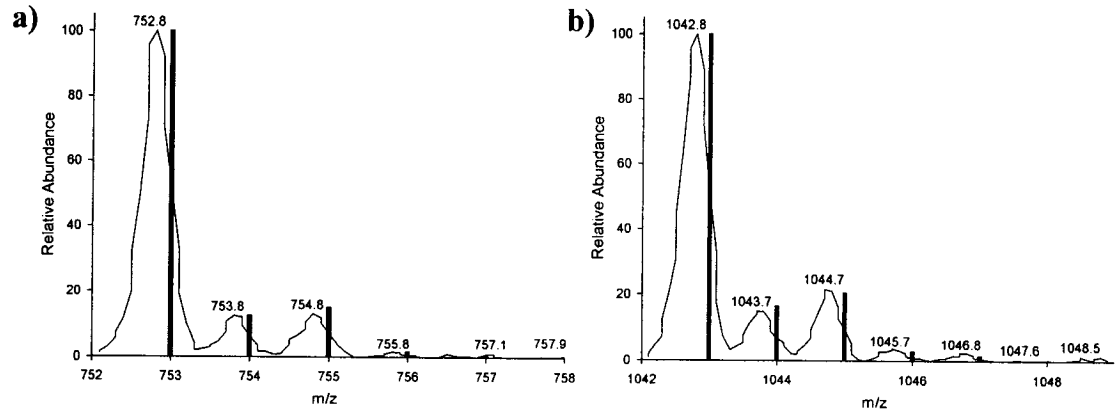

Figure 6.8 Observed and calculated isotope distributions for bismuth-TLA and -MPA ions. a) Experimental (continuous thin line) and theoretical (vertical bars) isotope patterns are shown for *m/z* 753, assigned as $[Bi_2Na(TLA)_3\text{-}6H]^+$, and b) *m/z* 1043, assigned as $[Bi_3(MPA)_4\text{-}8H]^+$.

Ions containing multiple bismuth centers likely involve at least one bridging ligand, as observed in solid state examples including bifunctional ester-thiolates.[27] In this context, a tandem mass spectrum for CID of $[Bi_4Na(TLA)_6\text{-}12H]^+$, represented by *m/z* 1482 (Figure 6.4b), is given in Figure 6.9. The result is a product ion, $[Bi_2Na(TLA)_3\text{-}6H]^+$ at *m/z* 753, is generated via the loss of neutral $[Bi_2(TLA)_3\text{-}6H]$ from the original 4:6:1 Bi:TLA:Na cation. As illustrated in Figure 6.9a, a crown-like complex for $[Bi_4Na(TLA)_6\text{-}12H]^+$ can be envisaged. This ion can also be considered a sodiated dimer, $Na[Bi_2(TLA)_3\text{-}6H]_2^+$ which dissociates into one neutral monomer and one sodiated monomer. Similarly, the spectrum resulting from CID of $[Bi_5(TLA)_7\text{-}14H]^+$, represented by *m/z* 1772 (Figure 6.4b), is shown in Figure 6.10. A neutral loss of $[Bi_2(TLA)_3\text{-}6H]$ is also observed in this case, yielding $[Bi_3(TLA)_4\text{-}8H]^+$ at *m/z* 1043. Again, bismuth-biomolecule complexes containing multiple bismuth ions and multiple ligands are not unreasonable given the known bismuth-citrate dinuclear unit (Figure 6.9c) which is common to solid state structures of CBS.[2]

Despite strong supporting MS/MS evidence for the identities of the ions at *m/z* 1482 and 1772, these rounded whole number *m/z* values are unexpectedly one unit lower than the anticipated nominal masses of 1483 u and 1773 u for 4:6:1 and 5:7:0 Bi:TLA:Na (or Bi:MPA:Na) complex ions. Due to the unit resolution available from the mass

spectrometer in use, spectral peaks have *m/z* values that are typically within ± 0.5 u of the actual monoisotopic masses of ions represented by those peaks. For instance, in Figure 6.4b a peak at *m/z* 1042.7 is different by only 0.2 u compared to the expected monoisotopic ion mass of 1042.9 u for a 3:4 Bi:TLA cation. However, in the same spectrum, peaks at *m/z* 1482.3 and 1772.3 are considerably different (0.6 u) from actual monoisotopic ion masses of 1482.9 and 1772.9 u for 4:6:1 and 5:7:0 Bi:TLA:Na cations, respectively.

Although the Finnigan™ LCQ ™DUO quadrupole ion trap instrument is not a high resolution device, to resolve the mass discrepancies aforementioned a spectrometer function called ZoomScan™ was used. This operation can be applied to a small mass range (10 u), producing a high resolution spectrum within that range.[239] Performing a ZoomScan™ (Figure 6.11) on mass ranges of interest for 4:6:1 and 5:7:0 Bi:TLA:Na cations revealed more accurate *m/z* values of 1482.6 and 1772.6, differing from 1482.9 u and 1772.9 u by only 0.3 u, strongly supporting the assertion that these spectral peaks represent the assigned multi-bismuth multi-ligand bismuth complex ions.

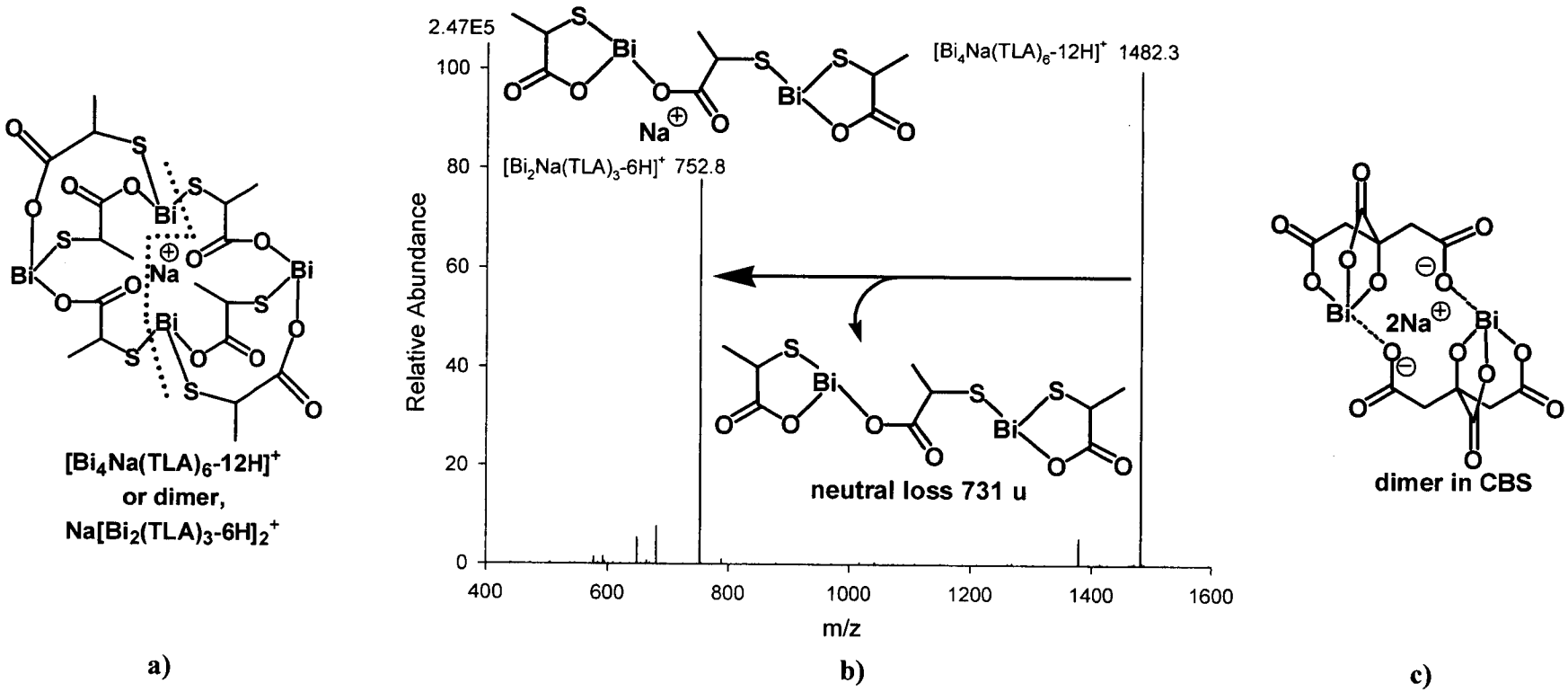

Figure 6.9 Collision-induced dissociation of ions at *m/z* 1483. These ions have been assigned as [Bi4Na(TLA)6-12H]+. a) The fragmentation axis (dotted line) through the proposed structure of a 4:6:1 Bi:TLA:Na ion affords b) a 2:3:1 Bi:TLA:Na product ion and 2:3 Bi:TLA neutral loss (possible structures are shown). The structural drawing in a) can also be considered a sodiated dimer of $[Bi_2(TLA)_3\text{-}6H]$. c) For comparison, the 2:2 multi-bismuth multi-ligand bismuth:citrate dimer found in many solid state structures of CBS is shown.

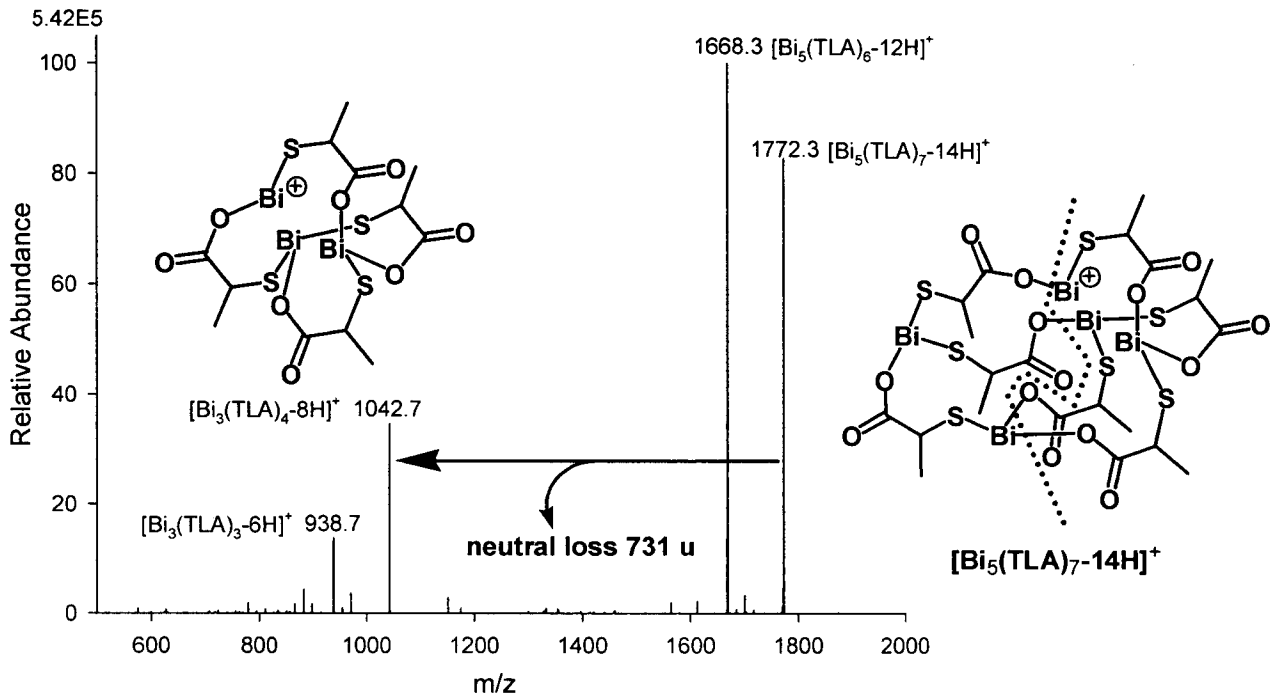

Figure 6.10 Collision-induced dissociation of ions at *m/z* 1772. These ions have been assigned as $[Bi_5(TLA)_7\text{-}14H]^+$ (actual nominal ion mass: 1773 u). From the proposed 5:7 Bi:TLA structure at the right, a neutral loss of 2:3 Bi:TLA yields a 3:4 Bi:TLA product ion.

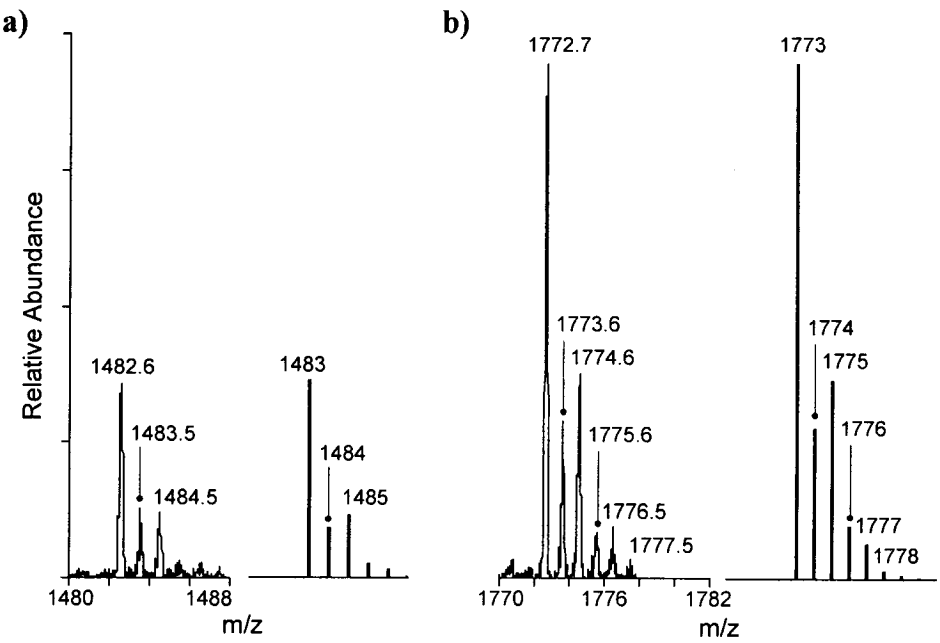

Figure 6.11 Comparison of theoretical and ZoomScan™ spectra for $[Bi_4Na(TLA)_6\text{-}12H]^+$ and $[Bi_5(TLA)_7\text{-}14H]^+$. High resolution (left) and calculated (right) spectra are provided for ions represented by a) *m/z* 1483 and b) *m/z* 1773. Correlation between the two types of spectra is observed in both cases.

6.2 Results and Discussion: Heteroleptic Bismuth Complexes

Given the large number of homoleptic bismuth-thiolate-carboxylate complex ions that have been observed and described in Section 6.1, the next logical step was to consider heteroleptic bismuth-thiolate-carboxylate complexes. This avenue of study was especially attractive, considering that fewer examples of heteroleptic[23;26;28] compared to homoleptic[20-22;24;25;27] bismuth-thiolate complexes have been previously characterized. In light of the complex nature of biological systems, it is possible that bismuth functions in either a homoleptic or heteroleptic environment of amino acids or other biomolecules. More information on bismuth coordination complexes containing multiple different ligands was also expected to enhance and complement the recent observation of several new heteroleptic Bi-Cys-Cit and Bi-Cys-AA complex ions (AA = amino acid) detailed in Chapter 5.

Table 6.3 lists ESI-MS data obtained in both ion modes for reaction mixtures containing equimolar quantities of $Bi(NO_3)_3$ and various combinations of two ligands (L_a, L_b = Cys,

MPA, TLA, or TMA; $L_a \neq L_b$) in 50:50 ethanol:water. Mass-to-charge ratios and relative abundances are listed as ranges observed over two sample injections from two independent samples. Peak assignments are presented as $[Bi_v(L_a)_w(L_b)_x\text{-}yH]^z$ (v = 1 to 3; L_a, L_b = Cys, MPA, TLA, or TMA; $L_a \neq L_b$; w, x = 1 to 3; y = 2 to 10; z = ±1). In general, singly-charged complex ions containing between one and three bismuth(III) cations and various combinations of two different thiol-carboxylic acid ligands have been identified. In some cases, sodium(I) or neutral carbon monoxide are also constituents of ion formulae. Table 6.4 provides a summary of the corresponding $Bi:L_a:L_b$ ratios that have been assigned. Because MPA and TLA are structural isomers (Figure 6.1), it is not possible to distinguish these ligands using mass spectrometry; therefore, this pair of ligands was the only combination not examined. A representative mass spectrum for each three-component reaction mixture is provided in Figure 6.12 (positive ion mode) and 6.13 (negative ion mode).

In Table 6.3 MS/MS results are reported from selected tandem mass spectra where the NL was $\geq 2 \times 10^4$ unless otherwise noted. The applied collision energy was 20 % in each case. Fragment ion formulae represent neutral mass losses, including intact ligands, portions of ligands, water (18 u), and carbon monoxide (28 u). Not all fragment ions are listed, and for reasons not yet elucidated, CID of various ions led to MS/MS spectra with intensities too low to be reliable. Two examples of isotope pattern comparisons are given in Figure 6.14a (3:1:2 Bi:TLA:TMA at *m/z* 1025, see also Figure 6.12e for the corresponding full mass spectrum) and Figure 6.14b (3:1:3 Bi:Cys:TLA at *m/z* 1058, see also Figure 6.12b). In Figure 6.15a a tandem mass spectrum is shown, featuring the unambiguous dissociation of $[BiNa(Cys)(TMA)\text{-}3H]^+$ (*m/z* 500, Figure 6.12c), from which both $[BiNa(Cys)\text{-}3H]^+$ (*m/z* 350) and $[BiNa(TMA)\text{-}3H]^+$ (*m/z* 379) are liberated. Taken in the context of the overall chronicle of bioinorganic data presented herein, Figure 6.15a reflects the highly self-consistent and definitive nature of the abundance of bismuth-thiolate-carboxylate ESI-MS data that has been compiled.

Table 6.3 Positive- and negative ion bismuth-thiolate-carboxylate ESI-MS data from reaction mixtures containing $Bi(NO_3)_3$ with two ligands, L_a, L_b = MPA, TLA, TMA, or Cys, in 50:50 ethanol:water.

$Bi(NO_3)_3/L_a/L_b$	*m/z*	Relative Abundance (%)	Assignment	MS/MS (*m/z*)	Assignment
L_a = MPA	328.0-328.1	81.83-100	$[Bi(Cys)-2H]^+$	-	
L_b = Cys	433.9	40-53	$[Bi(Cys)(MPA)-2H]^+$	327.9	$[Bi(Cys)-2H]^+$
Positive Mode	455.8-455.9	9	$[BiNa(Cys)(MPA)-3H]^+$	-	
	448.9-449.0	95-100	$[Bi(Cys)_2-2H]^+$	-	
	745.7	18-19	$[Bi_2(Cys)(MPA)_2-5H]^+$	-	
	760.7	36-37	$[Bi_2(Cys)_2(MPA)-5H]^+$	-	
	767.7-767.9	7-8	$[Bi_2Na(Cys)(MPA)_2-6H]^+$	-	
	782.7	17-27	$[Bi_2Na(Cys)_2(MPA)-6H]^+$	-	
	1072.5-1072.7	5-6	$[Bi_3(Cys)_2(MPA)_2-8H]^+$	-	
	1087.5-1087.6	13-14	$[Bi_3(Cys)_3(MPA)-8H]^+$	-	
	1109.4-1109.5	3-6	$[Bi_3Na(Cys)_3(MPA)-9H]^+$	-	
L_a = MPA	416.9-417	100	$[Bi(MPA)_2-4H]^-$	-	
L_b = Cys	431.8-432.1	62-63	$[Bi(Cys)(MPA)-4H]^-$	344.9	$[BiS(MPA)-2H]^-$
Negative Mode	743.7-743.8	22-32	$[Bi_2(Cys)(MPA)_2-7H]^-$	-	
	758.7-758.8	33-46	$[Bi_2(Cys)_2(MPA)-7H]^-$	-	
	1070.5-1070.7	8-16	$[Bi_3(Cys)_2(MPA)_2-10H]^-$	-	
	1085.5-1085.7	15-27	$[Bi_3(Cys)_3(MPA)-10H]^-$	-	
L_a = TLA	433.9	77-89	$[Bi(Cys)(TLA)-2H]^+$	327.9	$[Bi(Cys)-2H]^+$
L_b = Cys	448.9	100	$[Bi(Cys)_2-2H]^+$	-	
Positive Mode	455.8-455.9	10-12	$[BiNa(Cys)(TLA)-3H]^+$	349.8	$[BiNa(Cys)-3H]^+$
	461.9	16-18	$[Bi(Cys)(TLA)(CO)-2H]^+$	-	
	639.8-639.9	9-14	$[Bi_2(Cys)(TLA)-2H]^+$	-	
	745.7	67-75	$[Bi_2(Cys)(TLA)_2-5H]^+$	-	
	760.7	60-70	$[Bi_2(Cys)_2(TLA)-5H]^+$	-	
	767.7	22-35	$[Bi_2Na(Cys)(TLA)_2-6H]^+$	-	
	782.7	25-30	$[Bi_2Na(Cys)_2(TLA)-6H]^+$	-	
	1057.6	16-20	$[Bi_3(Cys)(TLA)_3-8H]^+$	-	
	1072.5	21-26	$[Bi_3(Cys)_2(TLA)_2-8H]^+$	-	
	1087.5	13-26	$[Bi_3(Cys)_3(TLA)-8H]^+$	-	
	1109.5	4-5	$[Bi_3Na(Cys)_3(TLA)-9H]^+$	-	

$Bi(NO_3)_3/L_a/L_b$	*m/z*	Relative Abundance (%)	Assignment	MS/MS (*m/z*)	Assignment
L_a = TLA	416.9	100	$[Bi(TLA)_2\text{-}4H]^-$	-	
L_b = Cys	431.8-431.9	15-23	$[Bi(Cys)(TLA)\text{-}4H]^-$	344.8	$[BiS(TLA)\text{-}2H]^-$
Negative Mode	743.6	5-10	$[Bi_2(Cys)(TLA)_2\text{-}7H]^-$	-	
L_a = TLA			$[Bi(TLA)(TMA)\text{-}2H]^+$		$[Bi(TMA)\text{-}2H]^+$
L_b = TMA	462.9	67-93		356.8	$[Bi(TLA)(TMA)\text{-}2H\text{-}H_2O]^+$
Positive Mode				444.7	
	484.8-484.9	9-16	$[BiNa(TLA)(TMA)\text{-}3H]^+$	-	
	490.9	100	$[Bi(TLA)(TMA)(CO)\text{-}2H]^+$	356.9	$[Bi(TMA)\text{-}2H]^+$
				384.9	$[Bi(TMA)(CO)\text{-}2H]^+$
				402.5[s]	$[Bi(TMA)(EtOH)\text{-}2H]^+$
				430.6[s]	$[Bi(TMA)(CO)(EtOH)\text{-}2H]^+$
				472.8	$[Bi(MPA)(TMA)(CO)\text{-}2H\text{-}H_2O]^+$
	512.9	11-20	$[BiNa(TLA)(TMA)(CO)\text{-}3H]^+$	-	
	518.9	24-32	$[Bi(TLA)(TMA)(CO)_2\text{-}2H]^+$	-	
	668.7	7-8	$[Bi_2(TLA)(TMA)\text{-}5H]^+$	-	
	774.5-774.6	12-29	$[Bi_2(TLA)_2(TMA)\text{-}5H]^+$	-	
	796.6-796.7	9-16	$[Bi_2Na(TLA)_2(TMA)\text{-}6H]^+$	-	
	802.7	29-38	$[Bi_2(TLA)_2(TMA)(CO)\text{-}5H]^+$	-	
	818.6	13-37	$[Bi_2(TLA)(TMA)_2\text{-}5H]^+$	463.1[t]	$[Bi(TLA)(TMA)\text{-}2H]^+$
				774.7[t]	$[Bi_2(TLA)_2(TMA)\text{-}5H]^+$
	824.7-824.8	26-27	$[Bi_2Na(TLA)_2(TMA)(CO)\text{-}6H]^+$	-	
	840.6-840.7	7-11	$[Bi_2Na(TLA)(TMA)_2\text{-}6H]^+$	-	
	846.5	11-18	$[Bi_2(TLA)(TMA)_2(CO)\text{-}5H]^+$	-	
	868.5-868.7	4-15	$[Bi_2Na(TLA)(TMA)_2(CO)\text{-}6H]^+$	-	
	1024.6-1024.7	5-9	$[Bi_3(TLA)(TMA)_2\text{-}8H]^+$	-	
	1096.5	9-14	$[Bi_2Na(TLA)_2(TMA)_3\text{-}6H]^+$	-	
	1114.7	6	$[Bi_3(TLA)_3(TMA)(CO)\text{-}8H]^+$	-	

[s] Ethanol (EtOH) is provided by the solvent.
[t] NL > 1 x 10^3

$Bi(NO_3)_3/L_a/L_b$	*m/z*	Relative Abundance (%)	Assignment	MS/MS (*m/z*)	Assignment
L_a = TLA	416.9	100	$[Bi(TLA)_2\text{-}4H]^-$	-	
L_b = TMA	460.9	77-100	$[Bi(TLA)(TMA)\text{-}4H]^-$	311.0	$[Bi(TMA\text{-}H_2O\text{-}CO_2)(O)\text{-}2H]^-$
Negative Mode				312.9	$[Bi(TLA)\text{-}2H]^-$
				344.9	$[BiS(TLA)\text{-}2H]^-$
				356.9	$[Bi(TMA)\text{-}2H]^-$
				442.7	$[Bi(TLA)(TMA)\text{-}4H\text{-}H_2O]^-$
	488.9	8-9	$[Bi(TLA)(TMA)(CO)\text{-}4H]^-$	312.9[t]	$[Bi(TLA)\text{-}2H]^-$
				344.9[t]	$[BiS(TLA)\text{-}2H]^-$
				442.7[t]	$[Bi(TLA)(TMA)\text{-}4H\text{-}H_2O]^-$
	772.6-772.7	24-57	$[Bi_2(TLA)_2(TMA)\text{-}7H]^-$	-	
	816.5-816.6	3-16	$[Bi_2(TLA)(TMA)_2\text{-}7H]^-$	-	
	838.7-838.8	9-16	$[Bi_2Na(TLA)(TMA)_2\text{-}8H]^-$	-	
	844.6-844.8	3-10	$[Bi_2(TLA)(TMA)_2(CO)\text{-}7H]^-$	-	
	1128.5-1128.7	3-14	$[Bi_3(TLA)_2(TMA)_2\text{-}10H]^-$	-	
L_a = MPA	462.9	54-64	$[Bi(MPA)(TMA)\text{-}2H]^+$	356.9	$[Bi(TMA)\text{-}2H]^+$
L_b = TMA				402.6[s]	$[Bi(TMA)(EtOH)\text{-}2H]^+$
Positive Mode				444.9	$[Bi(MPA)(TMA)\text{-}2H\text{-}H_2O]^+$
	484.9	5-13	$[BiNa(MPA)(TMA)\text{-}3H]^+$	378.8[t]	$[BiNa(TMA)\text{-}3H]^+$
	490.9	42-46	$[Bi(MPA)(TMA)(CO)\text{-}2H]^+$	356.9	$[Bi(TMA)\text{-}2H]^+$
				384.9	$[Bi(TMA)(CO)\text{-}2H]^+$
				430.6[s]	$[Bi(TMA)(CO)(EtOH)\text{-}2H]^+$
				472.9	$[Bi(MPA)(TMA)(CO)\text{-}2H\text{-}H_2O]^+$
	513	5-10	$[BiNa(TLA)(TMA)(CO)\text{-}3H]^+$	-	
	518.9-519.0	6-7	$[Bi(TLA)(TMA)(CO)_2\text{-}2H]^+$	-	
	534.9	100	$[Bi(TMA)_2(CO)\text{-}2H]^+$	-	
	668.8-668.9	3-6	$[Bi_2(MPA)(TMA)\text{-}5H]^+$	-	
	774.6-774.7	5-11	$[Bi_2(MPA)_2(TMA)\text{-}5H]^+$	-	
	802.8-802.9	13-15	$[Bi_2(MPA)_2(TMA)(CO)\text{-}5H]^+$	-	
	818.6	15-32	$[Bi_2(MPA)(TMA)_2\text{-}5H]^+$	-	
	846.6	6-11	$[Bi_2(MPA)(TMA)_2(CO)\text{-}5H]^+$	-	
	1096.5-1096.6	10-13	$[Bi_2Na(MPA)_2(TMA)_3\text{-}6H]^+$	-	

[s] Ethanol (EtOH) is provided by the solvent.
[t] NL > 1 x 10^3

$Bi(NO_3)_3/L_a/L_b$	*m/z*	Relative Abundance (%)	Assignment	MS/MS (*m/z*)	Assignment
L_a = MPA	460.9-461.0	28-45	$[Bi(MPA)(TMA)-4H]^-$	310.9[t]	$[Bi(TMA-H_2O-CO_2)(O)-2H]^-$
L_b = TMA				312.9[t]	$[Bi(MPA)-2H]^-$
Negative Mode				344.9[t]	$[BiS(MPA)-2H]^-$
				354.7[t]	$[Bi(TMA-H_2O)(O)-2H]^-$
				442.7[t]	$[Bi(MPA)(TMA)-4H-H_2O]^-$
	482.8-483.0	2-8	$[BiNa(MPA)(TMA)-5H]^-$	-	
	488.9	3-8	$[Bi(TLA)(TMA)(CO)-4H]^-$	-	
	504.9-505	100	$[Bi(TMA)_2-4H]^-$	-	
	772.6-772.9	6-18	$[Bi_2(MPA)_2(TMA)-7H]^-$	-	
	816.5-816.7	13-14	$[Bi_2(MPA)(TMA)_2-7H]^-$	-	
	838.7-838.9	4-20	$[Bi_2Na(MPA)(TMA)_2-8H]^-$	-	
	844.7-844.9	10-14	$[Bi_2(MPA)(TMA)_2(CO)-7H]^-$	-	
	1194.5-1194.7	2-6	$[Bi_3Na(MPA)(TMA)_3-11H]^-$	-	
L_a = TMA	448.9	100	$[Bi(Cys)_2-2H]^+$	-	
L_b = Cys	477.9	48-56	$[Bi(Cys)(TMA)-2H]^+$	327.9	$[Bi(Cys)-2H]^+$
Positive Mode				460.6-460.7	$[Bi(Cys-NH_3)(TMA)-2H]^+$
	499.8-499.9	12-16	$[BiNa(Cys)(TMA)-3H]^+$	349.8	$[BiNa(Cys)-3H]^+$
				378.8	$[BiNa(TMA)-3H]^+$
				482.7	$[BiNa(Cys-NH_3)(TMA)-3H]^+$
	505.9	13-20	$[Bi(Cys)(TMA)(CO)-2H]^+$	-	
	804.5-804.7	6-21	$[Bi_2(Cys)_2(TMA)-5H]^+$	-	
	826.6	5-12	$[Bi_2Na(Cys)_2(TMA)-6H]^+$	-	
	833.5-833.6	6-22	$[Bi_2(Cys)(TMA)_2-5H]^+$	-	
L_a = TMA	475.9	4-5	$[Bi(Cys)(TMA)-4H]^-$	388.9[t]	$[BiS(TMA)-2H]^-$
L_b = Cys	504.9	100	$[Bi(TMA)_2-4H]^-$	-	
Negative Mode					

[t] NL > 1 x 10^3

Table 6.4 Summary of observed positive- and negative ion Bi:L_a:L_b (L_a, L_b = Cys, MPA, TLA, or TMA; L_a, $\neq L_b$;) stoichiometric ratios.

Positive Ion Mode					Negative Ion Mode				
Bi: Cys:MPA	**Bi: Cys:TLA**	**Bi: Cys:TMA**	**Bi: MPA:TMA**	**Bi: TLA:TMA**	**Bi: Cys:MPA**	**Bi: Cys:TLA**	**Bi: Cys:TMA**	**Bi: MPA:TMA**	**Bi: TLA:TMA**
1:1:1	1:1:1	1:1:1	1:1:1	1:1:1	1:1:1	1:1:1	1:1:1	1:1:1	1:1:1
1:1:1:Na	1:1:1:Na	1:1:1:Na	1:1:1:Na	1:1:1:Na	-	-	-	1:1:1:Na	-
-	1:1:1:CO	1:1:1:CO	1:1:1:CO	1:1:1:CO	-	-	-	1:1:1:CO	1:1:1:CO
-	-	-	1:1:1:Na:CO	1:1:1:Na:CO	-	-	-	-	-
-	-	-	1:1:1:2CO	1:1:1:2CO	-	-	-	-	-
-	2:1:1	-	2:1:1	2:1:1	-	-	-	-	-
2:1:2	2:1:2	2:1:2	2:1:2	2:1:2	2:1:2	2:1:2	-	2:1:2	2:1:2
2:1:2: Na	2:1:2:Na	-	-	2:1:2:Na	-	-	-	2:1:2:Na	2:1:2:Na
-	-	-	2:1:2:CO	2:1:2:CO	-	-	-	2:1:2:CO	2:1:2:CO
-	-	-	-	2:1:2:Na:CO	-	-	-	-	-
2:2:1	2:2:1	2:2:1	2:2:1	2:2:1	2:2:1	-	-	2:2:1	2:2:1
2:2:1:Na	2:2:1:Na	2:2:1:Na	-	2:2:1:Na	-	-	-	-	-
-	-	-	2:2:1:CO	2:2:1:CO	-	-	-	-	-
-	-	-	-	2:2:1:Na:CO	-	-	-	-	-
-	-	-	2:2:3:Na	2:2:3:Na	-	-	-	-	-
-	-	-	-	3:1:2	-	-	-	-	-
-	3:1:3	-	-	-	-	-	-	3:1:3:Na	-
3:2:2	3:2:2	-	-	-	3:2:2	-	-	-	3:2:2
3:3:1	3:3:1	-	-	-	3:3:1	-	-	-	-
3:3:1:Na	3:3:1:Na	-	-	-	-	-	-	-	-
-	-	-	-	3:3:1:CO	-	-	-	-	-

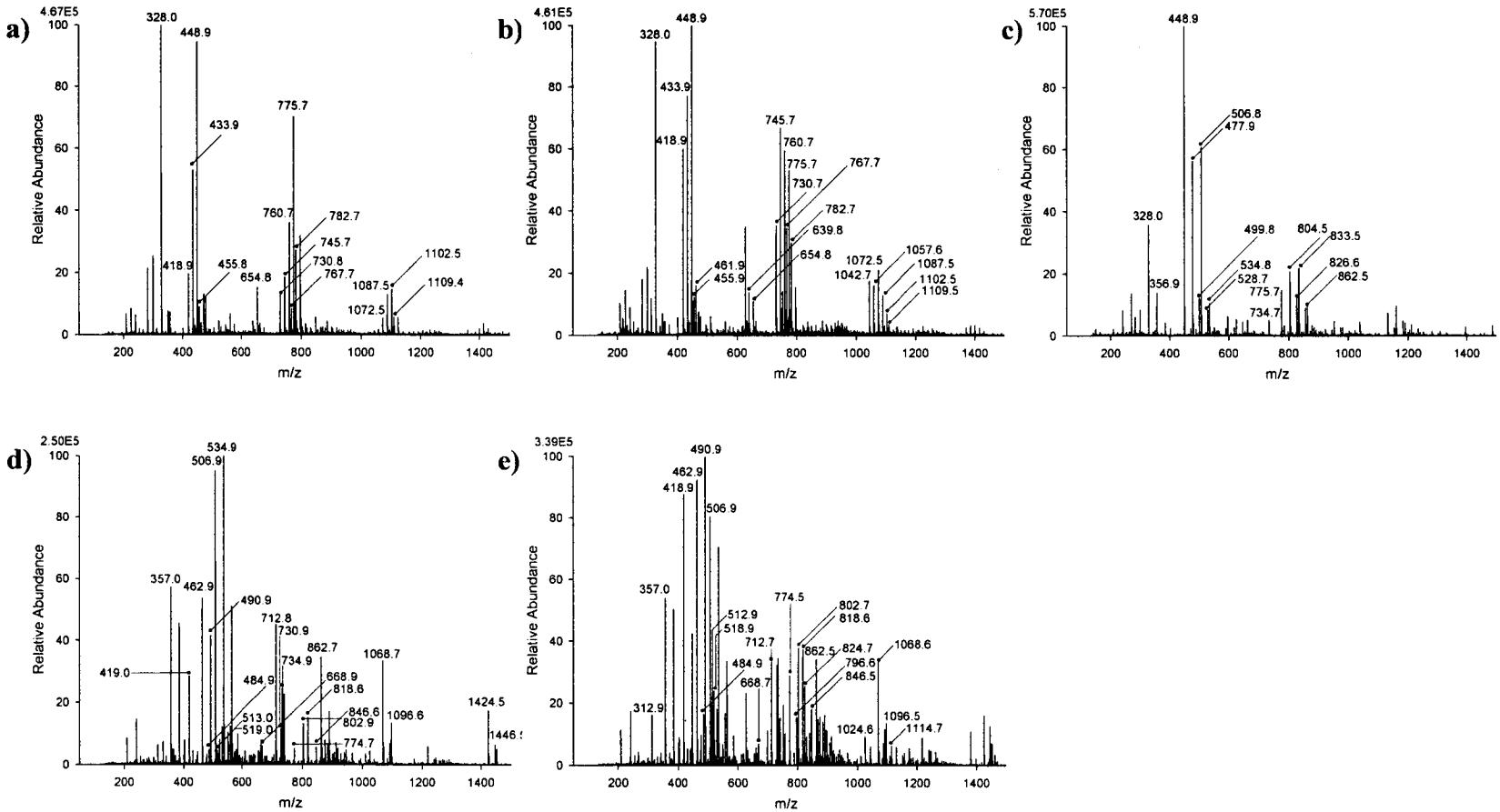

Figure 6.12 Positive ion bismuth-thiolate-carboxylate ESI-MS spectra. Reaction mixtures contained a) $Bi(NO_3)_3$, Cys, and MPA, b) $Bi(NO_3)_3$, Cys, and TLA, c) $Bi(NO_3)_3$, Cys, and TMA, d) $Bi(NO_3)_3$, MPA, and TMA, e) $Bi(NO_3)_3$, TLA, and TMA, in 50:50 ethanol:water. Denoted peaks are also listed in Table 6.3.

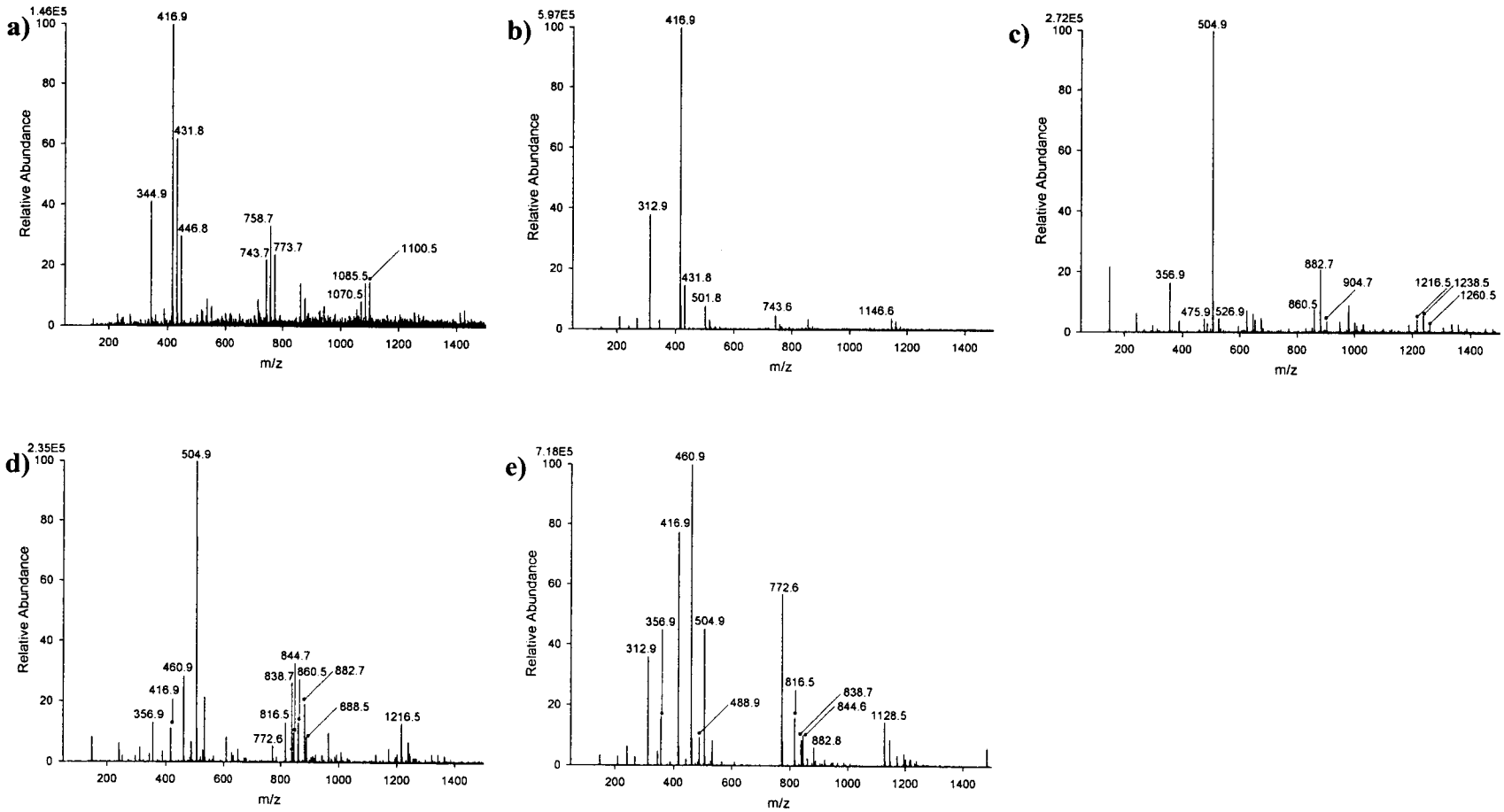

Figure 6.13 Negative ion bismuth-thiolate-carboxylate ESI-MS spectra. Reaction mixtures contained a) $Bi(NO_3)_3$, Cys, and MPA, b) $Bi(NO_3)_3$, Cys, and TLA, c) $Bi(NO_3)_3$, Cys, and TMA, d) $Bi(NO_3)_3$, MPA, and TMA, e) $Bi(NO_3)_3$, TLA, and TMA, in 50:50 ethanol:water. Denoted peaks are also listed in Table 6.3.

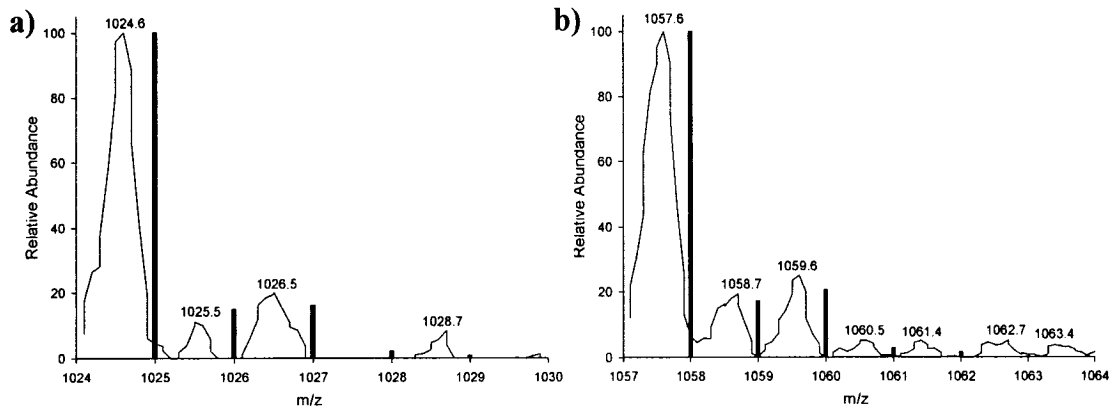

Figure 6.14 Comparison of isotope patterns for bismuth-thiolate-carboxylate cations. Experimental (continuous thin line) and theoretical (vertical bars) isotope patterns are given for a) *m/z* 1025, assigned as $[Bi_3(TLA)(TMA)_2\text{-}8H]^+$, and b) *m/z* 1058, assigned as $[Bi_3(Cys)(TLA)_3\text{-}8H]^+$. In both cases, the vertical bars are positioned at whole number increments, while the line graphs reflect the observed *m/z* values (appearing shifted to the left) within the experimental isotope patterns.

All spectra pertaining to three-component reaction mixtures (Figures 6.12 and 6.13) include at least one peak corresponding to a heteroleptic bismuth(III) complex ion. In the case of $Bi(NO_3)_3$ reacted with Cys and TMA (Figure 6.13h), only one peak was pinpointed as a three-component complex anion: $[Bi(Cys)(TMA)\text{-}4H]^-$ at *m/z* 476. Despite the low relative abundance of this anion (4 to 5 %), employing CID allowed for the identification of a reasonable neutral loss of a cysteine segment ($C_3H_5NO_2$, 87 u), yielding the fragment ion $[BiS(TMA)\text{-}2H]^-$ at *m/z* 389. Although the MS/MS NL was also relatively low (2.21×10^3), in this instance the presence of *m/z* 389 was consistent over a relatively long time frame of 2.45 seconds. This observation reflects the stability of the *m/z* 389 ions, a peak for which was reproduced in a subsequent tandem mass spectrum from the same sample. In comparison, for spectra with NL > 2×10^4, time ranges of less than 0.5 seconds have been confidently accepted for various other tandem spectra reported in this account. Therefore, the MS/MS spectrum containing *m/z* 389 – and other spectra acquired by applying similar parameters – is considered to provide reliable data.

Reviewing Table 6.4 reveals that all combinations of $Bi(NO_3)_3$ with two thiol-carboxylic acids generated spectral peaks assigned to cations or anions with stoichiometries of 1:1:1 $Bi:L_a:L_b$ (L_a, L_b = Cys, MPA, TLA, or TMA; $L_a \neq L_b$). All other three-component

complexes that have been identified are multi-bismuth multi-ligand ions, again reinforcing the idea that bismuth tends to form cluster complexes with thiol-carboxylic acids and other multifunctional donor ligands. Given that the active sites of bacterial and human enzymes – potential biological targets of bismuth[1] – are typically composed of more than one type of amino acid and can in some cases accommodate more than one metal ion, the discovery of new, fundamental heteroleptic multi-bismuth multi-ligand complex ions is particularly important.

Earlier in this report it was noted that 1:1 Bi:MPA ions were not detected (see Table 6.2); however, 1:1:1 Bi:Cys:MPA and Bi:MPA:TMA ions have been confirmed by MS/MS in both ion modes (Table 6.4, and see for example, Figure 6.15b). Both of the anions – $[Bi(Cys)(MPA)-4H]^-$ at *m/z* 432 in Figure 6.13f and $[Bi(MPA)(TMA)-4H]^-$ at *m/z* 461 in Figure 6.13i – were observed to dissociate with the release of a 1:1:1 Bi:MPA:S product anion (*m/z* 345), previously discussed with respect to Figure 6.4d, from a reaction of $Bi(NO_3)_3$ and MPA only. Although the intricacies of such data have not yet been fully rationalized, the idea that an interaction between bismuth and MPA was observed in the presence of Cys or TMA may imply that MPA coordinates to bismuth but does not chelate to the metal. Instead, it is possible that the coordination of MPA to bismuth through one donor atom only (most likely sulfur) occurs with concurrent tridentate chelation by either Cys or TMA.

Along with the three-component $Bi:L_a:L_b$ complexes recognized in spectra provided in Figures 6.12 and 6.13, in most cases there were also two-component $Bi:L_a$ and $Bi:L_b$ ions present, as can be seen from a visual comparison of the corresponding two-component and three-component mass spectra given in Figures 6.4 and 6.12 or 6.13, respectively. It is worth noting that not all two-component ions in Figure 6.4 spectra can be identified in Figure 6.12 or Figure 6.13. For instance, *m/z* 1043, corresponding to $[Bi_3(MPA)_4-8H]^+$ with a significant relative abundance of 34 to 46 % (Figure 6.4a), is absent in spectra containing $Bi(NO_3)_3$, Cys and MPA (Figure 6.12a). Bi:Cys ions were not always observed in negative ion mode. Each spectrum in Figures 6.12 and 6.13 otherwise includes some peaks that can be correlated to Bi:Cys, Bi:MPA, Bi:TLA, or Bi:TMA ions,

thereby making it difficult to generalize about whether or not there is a preference for coordination to Bi(III) of thiol-carboxylic acid L_a compared to L_b. Rather, it appears that regardless of which two thiol-carboxylic acid ligands are reacted with bismuth, one or more two-component complexes are observed.

Although studies have not been done to determine values for the specific binding affinities of various combinations of Cys, MPA, TLA and TMA for bismuth,[u] from solutions containing 1:1:1 molar ratios of $Bi:L_a:L_b$ it can be concluded that there is at least a kinetic preference for the formation of three-component ions containing up to a total of seven metal and ligand units: (i.e., 2:2:3:1 Bi:MPA:TMA:Na and Bi:TLA:TMA:Na; 3:2:2 Bi:Cys:MPA, Bi:Cys:TLA, and Bi:TLA:TMA; 3:3:1 Bi:Cys:MPA, Bi:Cys:TLA, and Bi:TLA:TMA). This data is consistent with other three-component spectra that were recently described (Chapter 5) from reaction mixtures containing equimolar amounts of $Bi(NO_3)_3$, Cys and either citric acid or another amino acid ($\neq$ Cys). Additionally, a 3:3:2 Bi:Cys:Asn cation – containing eight metal and amino acid units – was reported. Overall, more than forty new three-component bismuth-thiolate-carboxylate complex ions have been identified, along with sodiated or CO-complexed analogues, contributing appreciably to a growing catalogue of known bismuth-biomolecule species.

[u] The use of ESI-MS to investigate metal-ligand solution equilibria and stability constants is described in a recent review.[240]

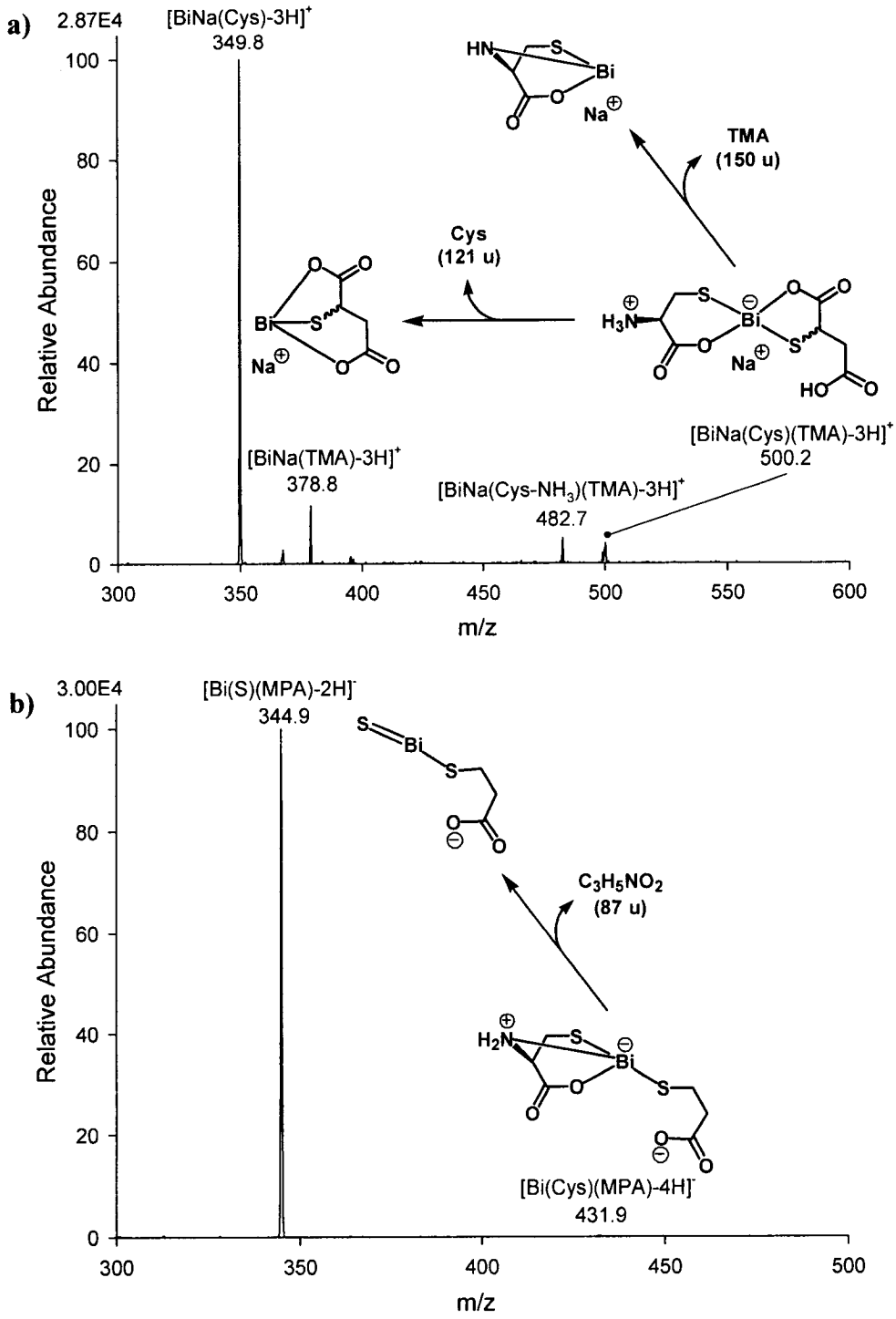

Figure 6.15 Tandem mass spectra for bismuth-cysteine-TMA and -MPA ions. a) $[BiNa(Cys)(TMA)-3H]^+$ at *m/z* 500, and b) $[Bi(Cys)(MPA)-4H]^-$ at *m/z* 432 underwent collision-induced dissociation at collision energy of 20 %. Denoted peaks are also listed in Table 6.3. Fragmentation pathways include proposed structures only.

6.3 Conclusions

As part of a program to develop, expand and understand the chemistry associated with the bioactivity of bismuth, a comprehensive ESI-MS study has been performed on reaction mixtures containing bismuth(III) nitrate and one or two biologically relevant thiol-carboxylic acids, L-cysteine, thiolactic acid, 3-mercaptopropionic acid, and thiomalic acid. A diverse range of more than seventy (two- and three-component) bismuth-thiolate-carboxylate complex ions have been discovered. The identification of such a vast number of bismuth-based species not only enhances the current body of knowledge available on medicinal bismuth chemistry, but also supports the view that bismuth-biomolecule clusters are an important facet of the chemistry of this element. In addition, this work validates the self-consistent and reproducible nature of electrospray ionization mass spectrometry data, tandem mass spectra, and isotope pattern analyses in the exploration and characterization of metal compounds.

6.4 Experimental Methods

Bismuth(III) nitrate pentahydrate, L-cysteine, 3-mercaptopropionic acid, thiolactic acid and thiomalic acid were used as received from Sigma-Aldrich. Ethanol (HPLC reagent grade) was used as received from Fisher. All reactions were performed at room temperature using distilled water.

6.4.1 Reaction Mixtures of $Bi(NO_3)_3$ and One Thiol-Carboxylic Acid

$Bi(NO_3)_3 \cdot 5H_2O$ (0.097 g, 0.20 mmol) was stirred for several minutes in 10 mL solvent (50:50 ethanol:water), followed by the addition of MPA (0.017 mL, 0.20 mmol), TLA (0.018 mL, 0.20 mmol), or TMA (0.030 g, 0.20 mmol), and another 10 mL of solvent. All reaction mixtures were stirred overnight before suction filtering. Each filtrate was diluted ten-fold to a concentration of ca. 0.001 M for analysis by ESI-MS.

6.4.2 Reaction Mixtures of $Bi(NO_3)_3$ and Two Thiol-Carboxylic Acids

MPA (0.017 mL, 0.20 mmol), TLA (0.018 mL, 0.20 mmol), TMA (0.030 g, 0.20 mmol), or Cys (0.025 g, 0.20 mmol) was stirred for several minutes in 10 mL solvent (50:50

ethanol:water), followed by the addition of a different thiol-carboxylic acid: MPA (0.017 mL, 0.20 mmol), TLA (0.018 mL, 0.20 mmol), TMA (0.030 g, 0.20 mmol), or Cys (0.024 g, 0.20 mmol). $Bi(NO_3)_3 \cdot 5H_2O$ (0.097 or 0.098 g, 0.20 mmol) and another 10 mL of solvent were added, followed by stirring overnight. The order of addition of reactants did not lead to considerably different ESI mass spectra. All reaction mixtures were filtered by passage through a NALGENE® PTFE syringe filter (0.2 μm pore size, 25 mm diameter). Each filtrate was diluted ten-fold to a concentration of ca. 0.001 M for analysis by way of ESI-MS.

6.4.3 Electrospray Ionization Mass Spectrometry

Mass spectra were obtained using a Finnigan™ LCQ™$_{DUO}$ electrospray ionization quadrupole ion trap mass spectrometer. The solution was injected (in 5, 10, or 20 μL aliquots) directly into the electrospray ionization source. The solvent flow rate was set at 1.2 mL/h, the heated capillary temperature at 200 °C, the sheath gas ($N_{2(g)}$) flow rate at 20 (arbitrary units), and the spray voltage at a magnitude of 4.00 kV for positive mode spectra and 4.00 kV (two-component reaction mixtures) or 4.50 kV (three-component reaction mixtures) for negative mode spectra. Tandem mass spectra were obtained using helium as the collision gas, and applying a collision energy of 13 to 45 %. In source collision-induced dissociation was deactivated during all experiments. All mass spectra were analyzed and processed using software programs, Qual Browser (Version 1.2 from Finnigan Corp. ©1998-2000) and SigmaPlot (Version 10.0 from Systat Software, Inc. ©2006), respectively.

Chapter 7 Conclusion

An assortment of bismuth compounds have played a role in medicine for over two centuries, and preparations containing bismuth subsalicylate, colloidal bismuth subcitrate, or ranitidine bismuth citrate are currently used widely by patients to overcome pain and discomfort associated with gastrointestinal ailments. Recognizing a relationship between *Helicobacter pylori*, gastrointestinal disorders, and bismuth remedies, it is important to understand the mechanisms by which this element exerts a medicinal influence in the human stomach.

In stark contrast to bismuth, other metals which neighbour bismuth in the periodic table have long been recognized for poisonous effects on living organisms. Despite the widespread application of bismuth compounds as pharmaceuticals, and the well known toxicity of mercury, thallium, and lead compounds, the disparate biological chemistries of these two types of substances are not well understood. Moreover, the specific physical or chemical properties which bring about a therapeutic versus deleterious effect of bismuth compared to mercury, thallium, or lead, respectively, have not been definitively determined.

The overriding goal of the research undertaken and presented in this document was to establish well-defined experimental conditions that facilitate a straightforward and rational characterization or isolation of new coordination complexes featuring bismuth, mercury, thallium, or lead, and one or more biologically significant ligands. Emphasis was placed on uncovering new aspects of bismuth chemistry in order to better understand the unique medicinal potential of this inorganic element. In general, the research was approached from a fundamental (rather than an applied medicinal) perspective. Nevertheless, the wide variety and vast number of new metal-biomolecule complexes that have been investigated certainly afford an improved appreciation of how bismuth and other metals interact with molecules and functional groups that are present in living systems. It is likely that these results will assist other researchers in a variety of scientific disciplines which collectively aim to enhance human health through an understanding of biological chemistry at the molecular level.

7.1 Importance of Electrospray Ionization Mass Spectrometry

In the past, efforts to study medicinal bismuth compounds have been met with synthetic and characterization challenges, primarily resulting from the low solubility of these species, and the tendency of bismuth compounds to hydrolyze in aqueous solution. The most extreme result of these properties is that one of the most commonly consumed over-the-counter gastrointestinal remedies, Pepto-Bismol®, contains an active bismuth ingredient for which only the experimental formula is known. Certainly it is important for patients to have access to effective drugs with limited side effects, regardless of whether or not the detailed chemistry of these drugs has been established. However, if drugs are to be improved, or if the fields of chemistry and medicine are to progress, a more complete understanding of these areas is needed. Considering the biological damage that toxic metals cause, it is also critical that the chemistry of these metals be further explored.

In order to surmount the issue of insolubility, electrospray ionization mass spectrometry has proven to be particularly advantageous. The rapidity with which a reaction mixture spectrum can be obtained (on the order of seconds to minutes) and the low detection limits of the technique have consistently allowed for bismuth- and other metal-biomolecule complex ions to be assigned when other characterization techniques have been unsuccessful. The ESI-MS work in this thesis supports the findings (discussed throughout) of other researchers, verifying that mass spectrometry can be used to examine inorganic compounds. This is an important statement, and underscores the view that mass spectrometry is useful for the development and study not only of organic but inorganic complexes for medicinal or other commercial applications.

The use of ESI-MS and spectral interpretation documented in this thesis was both an exciting and challenging endeavour for the experimentalist given the sheer quantity of data that is generated from a given MS experiment. In order to manage and analyze considerable amounts of ESI-MS data, some recommendations have been made in Section 1.5.2 with respect to metal-biomolecule systems. The use of electronic, user-generated data spreadsheets, including the example provided in Appendix A, were found to be invaluable for the mathematical prediction of spectral peaks and made the analysis

of data more efficient. Given the weight placed in this thesis on a single experimental technique, a variety of approaches were taken to ensure the self-consistency and accuracy of acquired ESI-MS data. The examination of full-, collision-induced dissociation-, and high resolution ZoomScan™ spectra, as well as an extended inspection of spectral isotope patterns, has allowed for confidence in the reported ESI-MS results.

7.2 New Bismuth-Biomolecule Complexes

Recognizing the pronounced thermal and hydrolytic strength of bismuth-sulfur bonds, it is likely that sulfur-containing molecules provide a sink for bismuth in the human body. Given this preference of bismuth for coordination by thiolates, a variety of experiments have been reported which shed light on the structures of bismuth complexes possessing biologically relevant sulfur-containing ligands. New complex ions have been discovered containing bismuth(III) and 1-thio-β-D-glucose sodium salt, 1-thio-β-D-glucose tetraacetate, thiolactic acid, 3-mercaptopropionic acid, thiomalic acid, 2-mercaptoethylamine, or L-cysteine. The identification of such an extended series of bismuth-thiolate ions, involving one or more of the same or different thiolate ligands, undoubtedly illustrates the diversity of bismuth-thiolate chemistry as observed by way of ESI-MS. The majority of ions reported in this thesis contain multiple bismuth cations and multiple ligands, reflecting the inherent propensity of bismuth to form cluster coordination complexes, which may very well model the types of bismuth-biomolecule complexes that are present *in vivo*.

The first bismuth-citrate complexes observed via mass spectrometry have been described, some of which also contain cysteine. The discovery of $[Bi_2(Cit)_2\text{-}5H]^+$ supports previous observations of a solid state bismuth-citrate dimer in examples of CBS. The identification of $[Bi(Cys)(Cit)\text{-}2H]^+$ represents a reasonable biological environment for bismuth, taking into account both the administered and active forms anticipated for this medicinal element. The inclusion of cysteine or other thiols (e.g. MPA, MEA) in a reaction mixture of $Bi(NO_3)_3$ or $BiCl_3$ and a non-thiol ligand is significant. Under such circumstances, it has been possible to observe complexes of bismuth with amino acids, aminosugars, and nucleobases, for which interactions with bismuth were not confirmed in the absence of

cysteine or another thiol. Although a specific chemical rationale for this cooperative thiolate phenomenon has yet to be elucidated, it is proposed that incorporation of a thiol improves the solubility or ability of bismuth to form discrete complexes with other ligands.

7.3 New Metal-Biomolecule Complexes

Due to the proximity of bismuth to mercury, thallium, and lead in the periodic table, it is of interest to probe and compare the chemistry of these elements, seeking reasons for which bismuth is medicinally beneficial while the other metals are poisonous. In comparison to these other metals, bismuth is known from previous ESI-MS studies to show a greater selectivity toward amino acid complexation. Considering monosaccharides as ligands for bismuth (Chapter 2) revealed the consistent formation of gas phase complex ions containing bismuth and thiosugars only. In contrast, a number of mercury-, thallium-, and lead-monosaccharide complex ions were assigned with Glc, Fru, Man, Gal, and/or Rib. It cannot be inferred from these results that complexes between bismuth(III) and common oxygen- or nitrogen-based sugars or amino acids are not possible. Rather, low solubility – potentially involving the formation of extended metal-monosaccharide structures in solution – may have prevented these complexes from being observed. Although ions of mercury, thallium, and lead are also thiophilic, it would not be surprising if the marked affinity of sulfur for bismuth is eventually linked directly to the medical benefits associated with this element.

Extending the published and unpublished data available on thallium ions containing amino acid residues, dipeptide complexes of thallium with cysteinyl- and methionyl-glycine were observed. Additionally, a new L-cysteinatothallium(I) solid state structure was characterized using X-ray diffraction, ^{13}C, and ^{15}N CP/MAS NMR, among other techniques. The existence of this compound supplements a short list of other crystallographically characterized thallium-amino acid compounds, stressing that improved synthetic methods are still required to access other related compounds in the solid state. Curiously, the generation of L-cysteinatothallium(I) has not been achieved without including L-histidine in the reaction mixture. Further experiments will be

required to determine the role of this second amino acid, the requisite presence of which is reminiscent of the cooperative effect of L-cysteine in the generation of various bismuth-non-thiol complex ions.

Due to the poisonous nature of some of the metal ions that have been employed, it is worth reiterating that careful laboratory work has been required in order to safely handle and manage the chemicals and waste produced during these reactions. Research involving metals such as mercury, thallium, or lead is not recommended without first taking necessary safety measures, including those described earlier in Section 1.6.

7.4 Future Endeavours

It is clear that the ESI-MS technique is a fruitful one for the observation or characterization of metal-biomolecule complexes in the gas phase. However, without collecting data via tandem mass spectrometry, ESI-MS does not provide a great deal of structural information about the compounds under investigation. As exemplified in Chapter 4 regarding L-cysteinatothallium(I), the usefulness of NMR spectroscopy, X-ray diffraction, and various other analytical techniques must also be pursued for a more complete understanding these types of compounds.

While a modest number of discrete crystallographically characterized bismuth- and metal-biomolecule complexes are already known, the conditions needed for the growth and isolation of single crystals are still in progress and lack a strategy with reliable and reproducible results. Lead-valine[33] and bismuth-cysteine[28] single crystals have been generated by way of slow solvent evaporation; however, the use of this technique has not been successful for a variety of other metal-biomolecule combinations explored by the author of this thesis.

The main recommendation that can be made is to follow the lead of other researchers with expertise in the area of bismuth chemistry. For example, it is possible to employ triphenylbismuthine as a starting material in the generation of crystallographically characterized compounds of bismuth with 2-ethoxybenzoic acid, *o*-methoxybenzoic acid,

2-picolinic acid, and 1-mercapto-2-propanol,[99;100] all of which can be considered biologically relevant due to the O, S, and/or N functional groups involved. Some of these compounds have been prepared free of solvent, an option which might be advantageous in the preparation of other bismuth- and metal-biomolecule systems that are expected or known to be relatively insoluble or reactive in common solvents. Solid state CP/MAS NMR was also found to be helpful in characterizing not only L-cysteinatothallium(I) (Chapter 4) but other metal-biomolecule compounds that have not been reported herein. However, without other characterization data it is difficult to ascertain the metal:ligand stoichiometries of new solids state complexes; therefore more work in this area is needed.

In many cases, high-performance liquid chromatography is employed in conjunction with mass spectrometry to separate reaction mixture components prior to mass spectral analysis.[241;242] To better assess metal-biomolecule solution chemistry, in the future it would be interesting and advantageous to develop a liquid chromatography/mass spectrometry regime for this purpose. Other types of mass spectrometry can also be used to support and extend the studies that have already been completed. Some preliminary experiments (unpublished, by the author of this thesis) using matrix-assisted laser desorption ionization have been undertaken to assess bismuth-cysteinate and bismuth-citrate chemistry. However, the laser power employed and the matrix:sample ratios used may need to be adjusted to observe more than just bismuth-sulfide peaks. Even in the presence of cysteine, bismuth-salicylate peaks have yet to be observed by way of ESI-MS, making this another viable avenue of pursuit.

To be relatively comprehensive in terms of the types of ligands explored, most other variables were controlled during the ESI-MS investigations that have been described in this thesis. There are numerous other dimensions that can be investigated. Using ESI-MS to examine reaction mixtures containing reactant stoichiometries other than 1:1, higher or lower reaction temperatures, and in particular, different solution pH values, will undoubtedly affect resultant spectra, and provide an even clearer picture of how bismuth and other metals interact with biologically relevant molecules.

7.5 Final Remarks

Bismuth compounds have been useful in many different medicinal applications, and it is through the ongoing exchange of ideas between researchers in various fields – including chemistry, microbiology, and gastroenterology – that the biological chemistry of bismuth is now being better understood from a molecular perspective. The main contribution of the author has been a detailed exploitation of electrospray ionization mass spectrometry as a tool for the rapid and comprehensive analysis of reaction mixtures containing bismuth(III) and one or more biologically relevant molecules. Likewise, to gain a deeper understanding of the fundamental biological chemistry of toxic metal ions of mercury, thallium, and lead, ESI-MS and other characterization techniques have proven to be very effective. Despite the fact that the observed gas-phase ions have not been directly correlated to the solution chemistry of the examined metal-biomolecule systems, the results of this work contribute appreciably to a small but important and growing library of medicinal and toxic inorganic compounds.

Appendix A Sample Spreadsheet for ESI-MS Data Analysis

Table A.1 Sample of an electronic spreadsheet used in the analysis of ESI-MS data from reaction mixtures containing combinations of Tl(I), cysteine (Cys), and cysteinyl-glycine (Cys-Gly). Employing the standard mathematical functions available from Microsoft Office software program, Excel, such a spreadsheet can be created and modified at will by the user to reflect different reaction mixtures. In columns J, L, and N, the term "+22" represents the gain of one sodium ion (nominal mass 23 u) and the corresponding loss of one proton (nominal mass 1 u) compared to the expressions in columns I, K, and M, respectively. Examining the possible *m/z* values in columns I-N gives the experimenter an idea of what to expect in spectra containing specific metal-ligand combinations.

Column A	Column B	Column C	Columns D, E		Columns F, G, H			Column I	Column J	Column K	Column L	Column M	Column N
Nominal Mass of Metal Ion (u)	Nominal Mass of L_a (u)	Nominal Mass of L_b (u)	Stoichiometry of Metal Ion: L_a or L_b		Stoichiometry of Metal Ion: L_a:L_b			Possible Cations (*m/z*) =(D*A) +(E*B) -(D-1)	Possible Sodiated Cations (*m/z*) =(D*A) +(E*B) -(D-1) +22	Possible Cations (*m/z*) =(D*A) +(E*C) -(D-1)	Possible Sodiated Cations (*m/z*) =(D*A) +(E*C) -(D-1) +22	Possible Cations (*m/z*) =(F*A) +(G*B) +(H*C) -(F-1)	Possible Sodiated Cations (*m/z*) =(F*A) +(G*B) +(H*C) -(F-1) +22
Tl	Cys	Cys-Gly	Tl	Cys or Cys-Gly	Tl	Cys	Cys-Gly	Tl: Cys	Tl: Cys: Na	Tl: Cys-Gly	Tl: Cys-Gly: Na	Tl:Cys: Cys-Gly	Tl:Cys: Cys-Gly: Na
205	121	178	1	1	1	1	1	326	348	383	405	504	526
205	121	178	1	2	1	1	2	447	469	561	583	682	704
205	121	178	1	3	1	1	3	568	590	739	761	860	882
205	121	178	1	4	1	1	4	689	711	917	939	1038	1060
205	121	178	1	5	1	1	5	810	832	1095	1117	1216	1238
205	121	178	1	6	1	1	6	931	953	1273	1295	1394	1416
205	121	178	1	7	1	1	7	1052	1074	1451	1473	1572	1594
205	121	178	1	8	1	1	8	1173	1195	1629	1651	1750	1772
205	121	178	1	9	1	1	9	1294	1316	1807	1829	1928	1950
205	121	178	1	10	1	1	10	1415	1437	1985	2007	2106	2128
205	121	178	2	1	1	2	1	530	552	587	609	625	647
205	121	178	2	2	1	2	2	651	673	765	787	803	825
205	121	178	2	3	1	2	3	772	794	943	965	981	1003
Columns continue through higher numbers (user-defined) of metal ions and ligands.													

Appendix B Copyright Release Form for Chapter 5

11 June 2007 Our Ref: CT/HD/Jun07/J030

Heather A. Phillips
Dalhousie University
6247 Coburg Road
B3H 4J3
Halifax
Canada

Dear Heather Phillips,

JOURNAL OF INORGANIC BIOCHEMISTRY, Vol. 101, No. 4, pp 736-739, 2007, Phillips et al, "Cooperative Influence of..." 1 Article Only

Proposed Use: To be published in your Ph.D. thesis for submission to the Faculty of Graduate Studies at Dalhousie University.

As per your letter dated 7 June 2007, we hereby grant you permission to reprint the aforementioned material at no charge **in your thesis** subject to the following conditions:

1. If any part of the material to be used (for example, figures) has appeared in our publication with credit or acknowledgement to another source, permission must also be sought from that source. If such permission is not obtained then that material may not be included in your publication/copies.

2. Suitable acknowledgment to the source must be made, either as a footnote or in a reference list at the end of your publication, as follows:

   "This article was published in Publication title, Vol number, Author(s), Title of article, Page Nos, Copyright Elsevier (or appropriate Society name) (Year)."

3. Your thesis may be submitted to your institution in either print or electronic form.

4. Reproduction of this material is confined to the purpose for which permission is hereby given.

5. This permission is granted for non-exclusive world **English** rights only. For other languages please reapply separately for each one required. Permission excludes use in an electronic form other than submission. Should you have a specific electronic project in mind please reapply for permission.

6. This includes permission for the Library and Archives of Canada to supply single copies, on demand, of the complete thesis. Should your thesis be published commercially, please reapply for permission.

Yours sincerely

C. Truter

Clare Truter
Rights Manager, S&T

Appendix C Extended Data for Chapter 6

Isotope pattern analysis has been used to assess and confirm assigned ESI mass spectral peaks, some of which have also been verified through the collection of MS/MS information. In Figures C.1-C.10, a superposition of experimental (continuous thin line) and calculated (vertical bars)[195;209] isotope patterns are provided for all peaks listed in Table 6.1 (Chapter 6). In most cases there is agreement between the experimental and theoretical patterns. For peaks with low relative abundances the experimental isotope patterns cannot always be distinguished from background spectral noise (e.g., Figure C.2b); therefore, in some cases the existence of corresponding ions can neither be confirmed nor refuted by this method. For higher mass ions (e.g., Figure C.3a, Figure C.4c), the experimental isotope patterns typically appear shifted toward lower *m/z* compared to the low resolution theoretical patterns which are based on whole number isotope masses. It is also possible generate high resolution theoretical isotope patterns, which more accurately represent the expected masses of the ions under study.

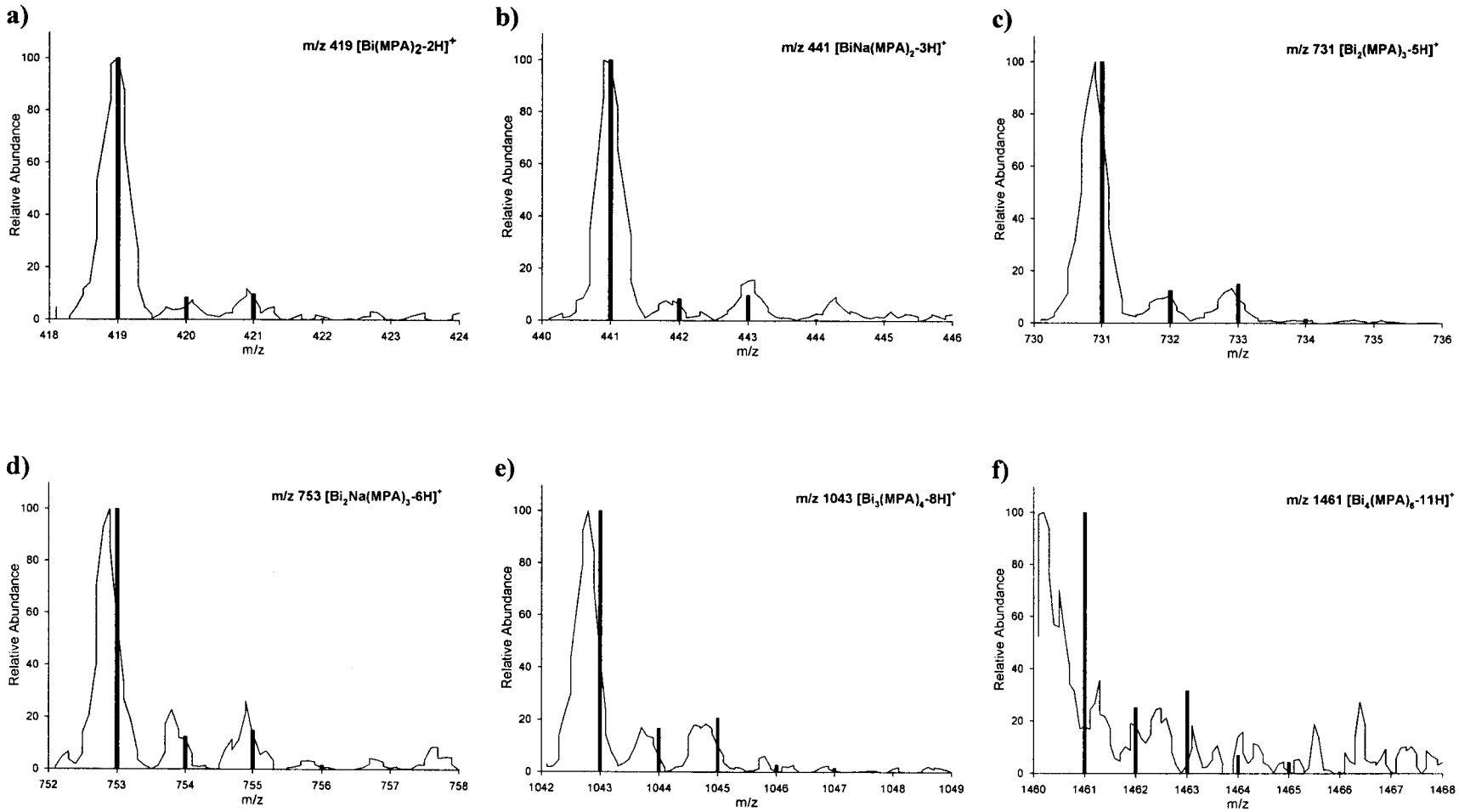

Figure C.1 Observed and calculated isotope peak distributions for Bi/MPA cations. a)-f) Experimental (continuous thin line) and theoretical (vertical bars) isotope patterns are shown for various indicated $[Bi_v(L)_w\text{-}yH]^z$ (L = MPA) complex ions.

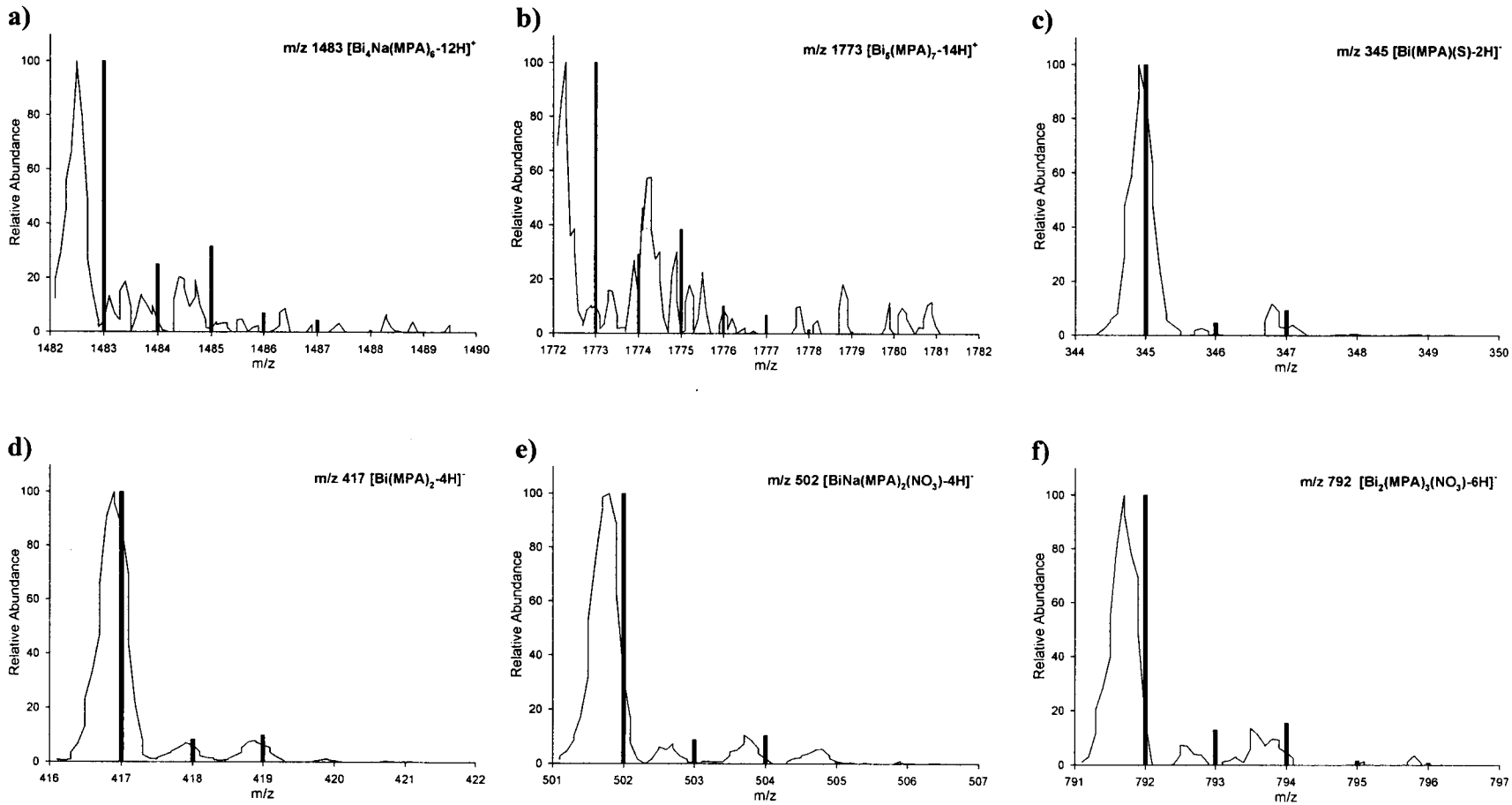

Figure C.2 Observed and calculated isotope peak distributions for Bi/MPA cations and anions. a)-f) Experimental (continuous thin line) and theoretical (vertical bars) isotope patterns are shown for various indicated $[Bi_v(L)_w\text{-}yH]^z$ (L = MPA) complex ions.

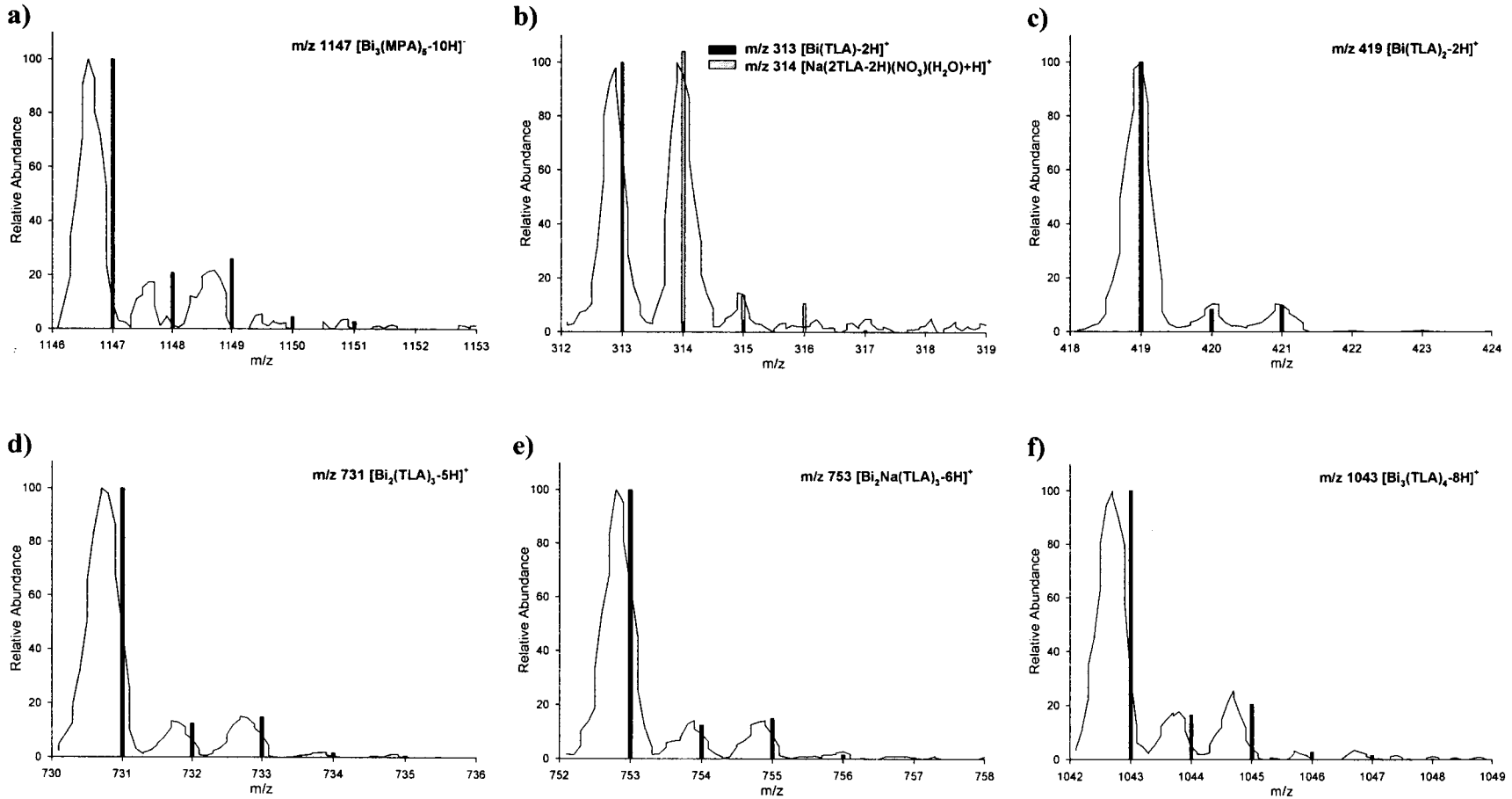

Figure C.3 Observed and calculated isotope peak distributions for Bi/MPA anions and Bi/TLA cations. a)-f) Experimental (continuous thin line) and theoretical (vertical bars) isotope patterns are shown for various indicated $[Bi_v(L)_w\text{-}yH]^z$ (L = MPA, TLA) complex ions.

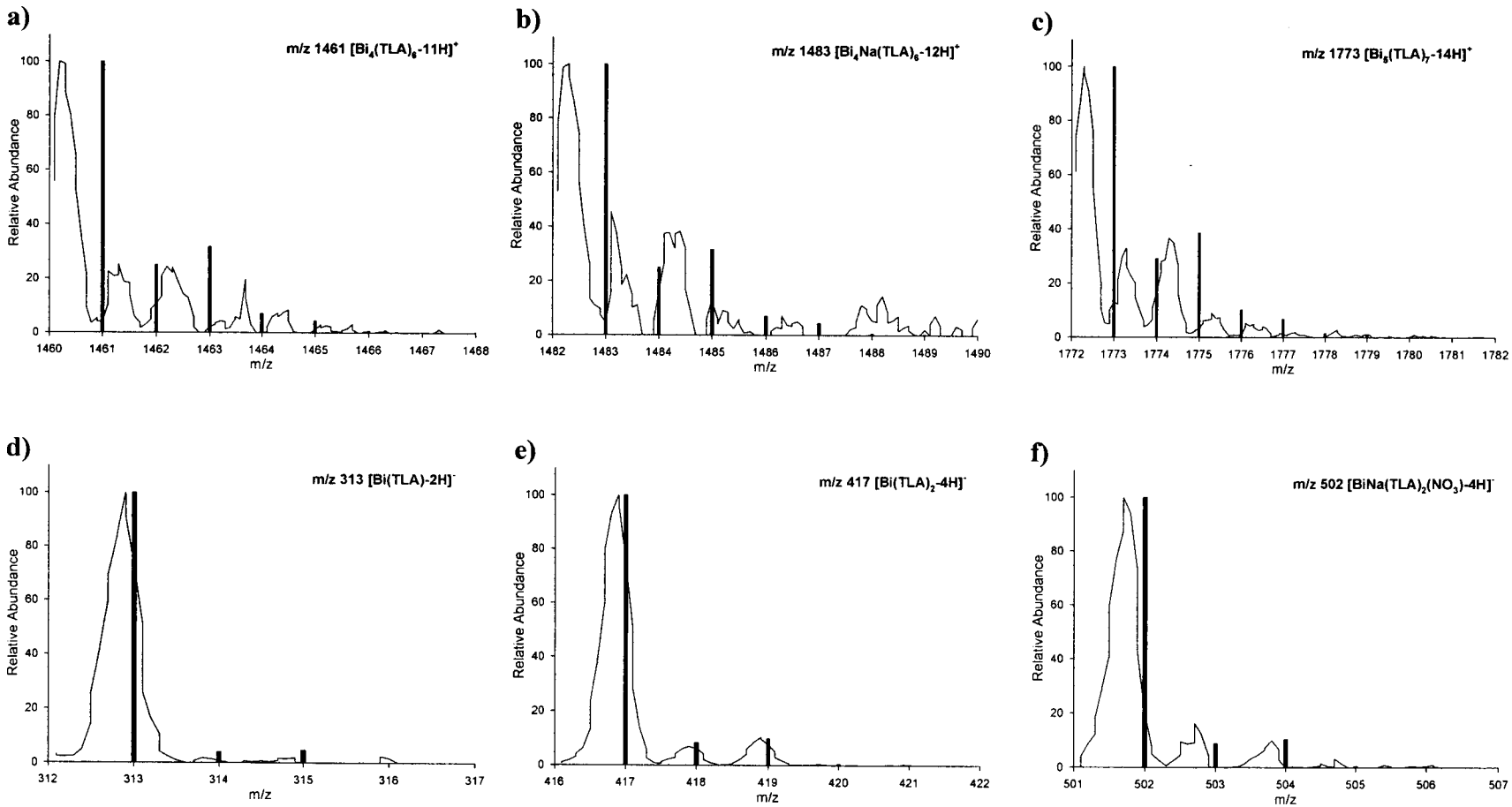

Figure C.4 Observed and calculated isotope peak distributions for Bi/TLA cations and anions. a)-f) Experimental (continuous thin line) and theoretical (vertical bars) isotope patterns are shown for various indicated $[Bi_v(L)_w\text{-}yH]^z$ (L = TLA) complex ions.

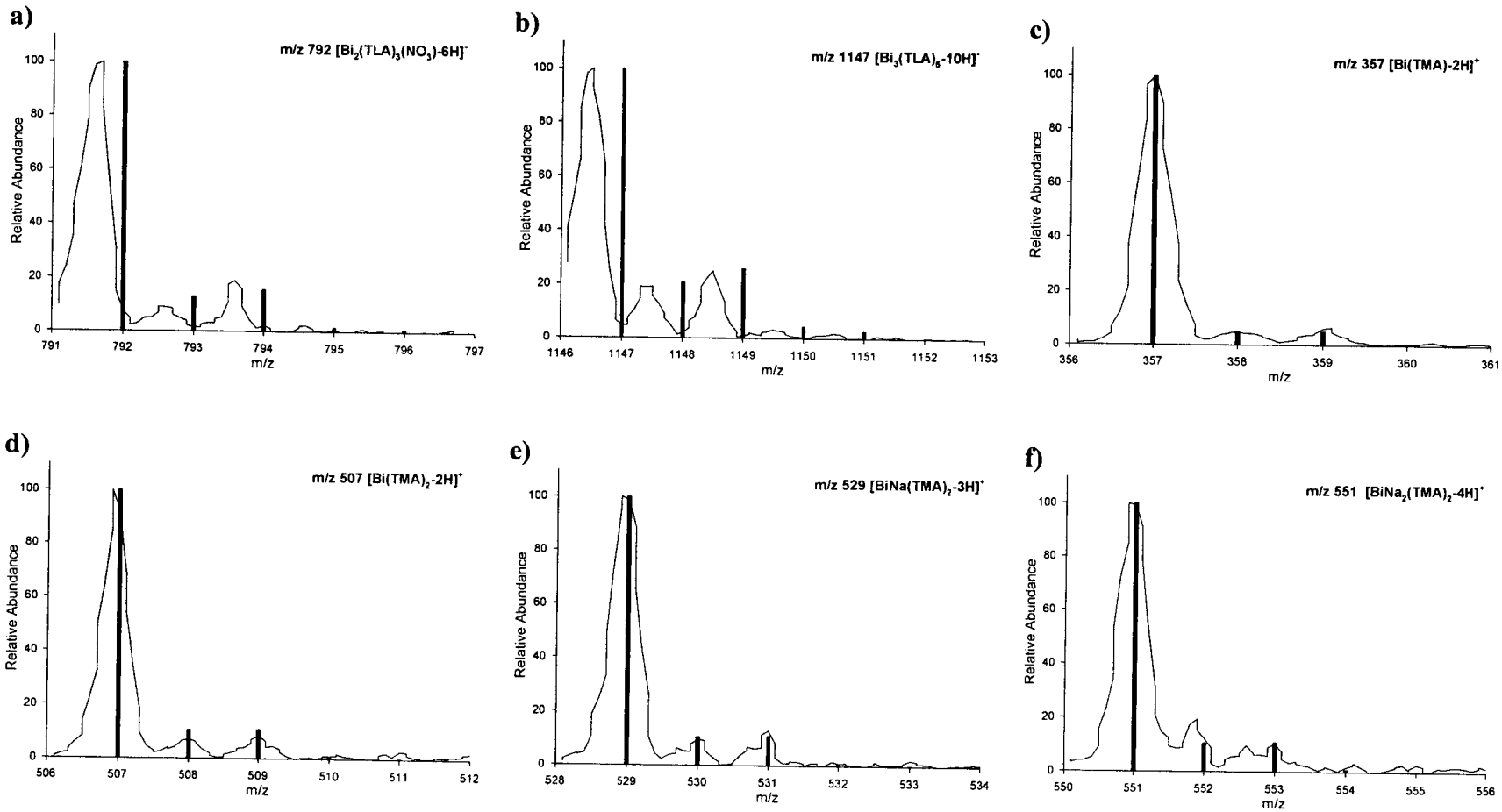

Figure C.5 Observed and calculated isotope peak distributions for Bi/TLA anions and Bi/TMA cations. a)-f) Experimental (continuous thin line) and theoretical (vertical bars) isotope patterns are shown for various indicated $[Bi_v(L)_w\text{-}yH]^z$ (L = TLA, TMA) complex ions.

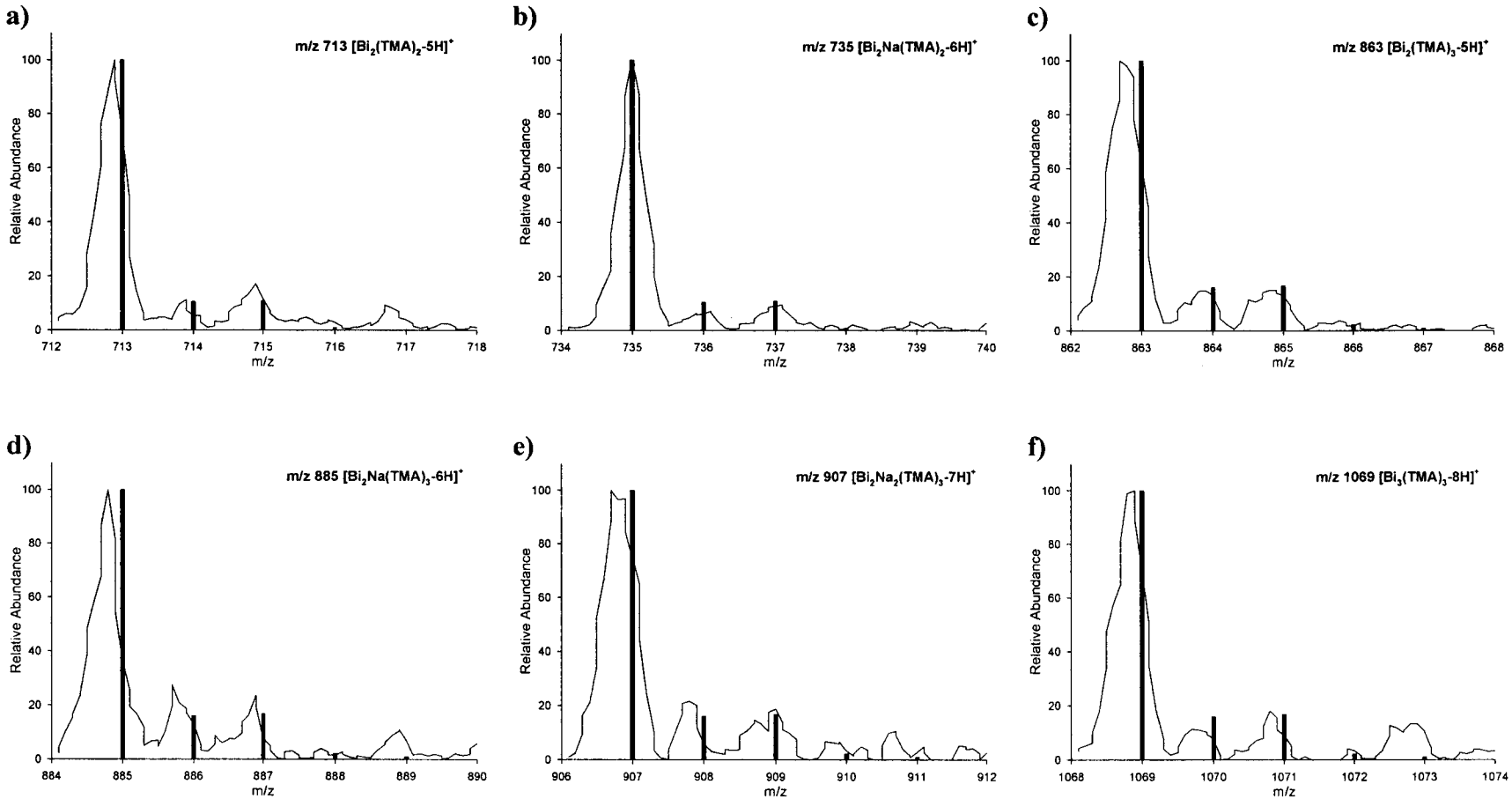

Figure C.6 Observed and calculated isotope peak distributions for Bi/TMA cations. a)-f) Experimental (continuous thin line) and theoretical (vertical bars) isotope patterns are shown for various indicated $[Bi_v(L)_w\text{-}yH]^z$ (L = TMA) complex ions.

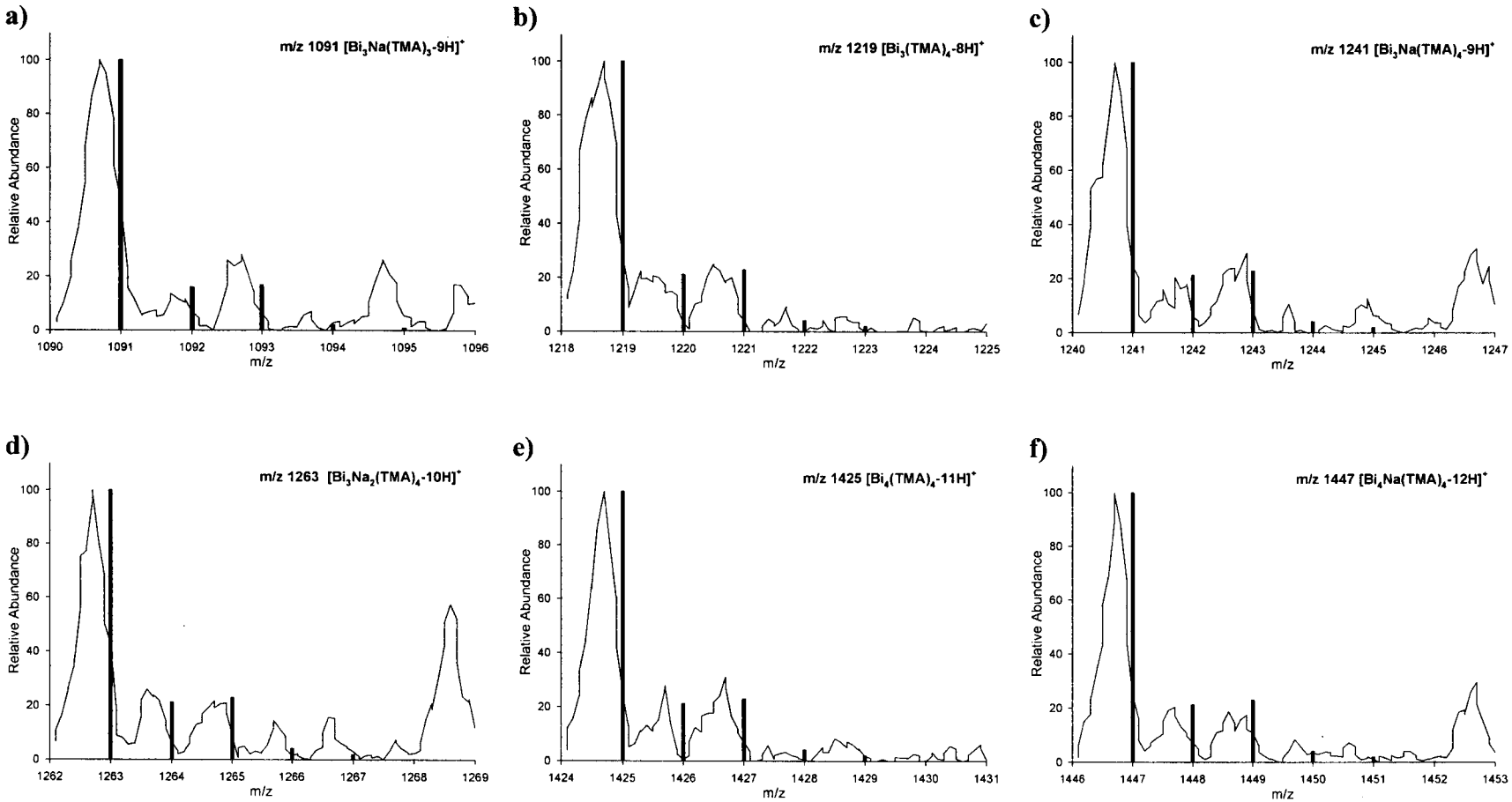

Figure C.7 Continued from Figure C.6. Observed and calculated isotope peak distributions for Bi/TMA cations. a)-f) Experimental (continuous thin line) and theoretical (vertical bars) isotope patterns are shown for various indicated $[Bi_v(L)_w\text{-}yH]^z$ (L = TMA) complex ions.

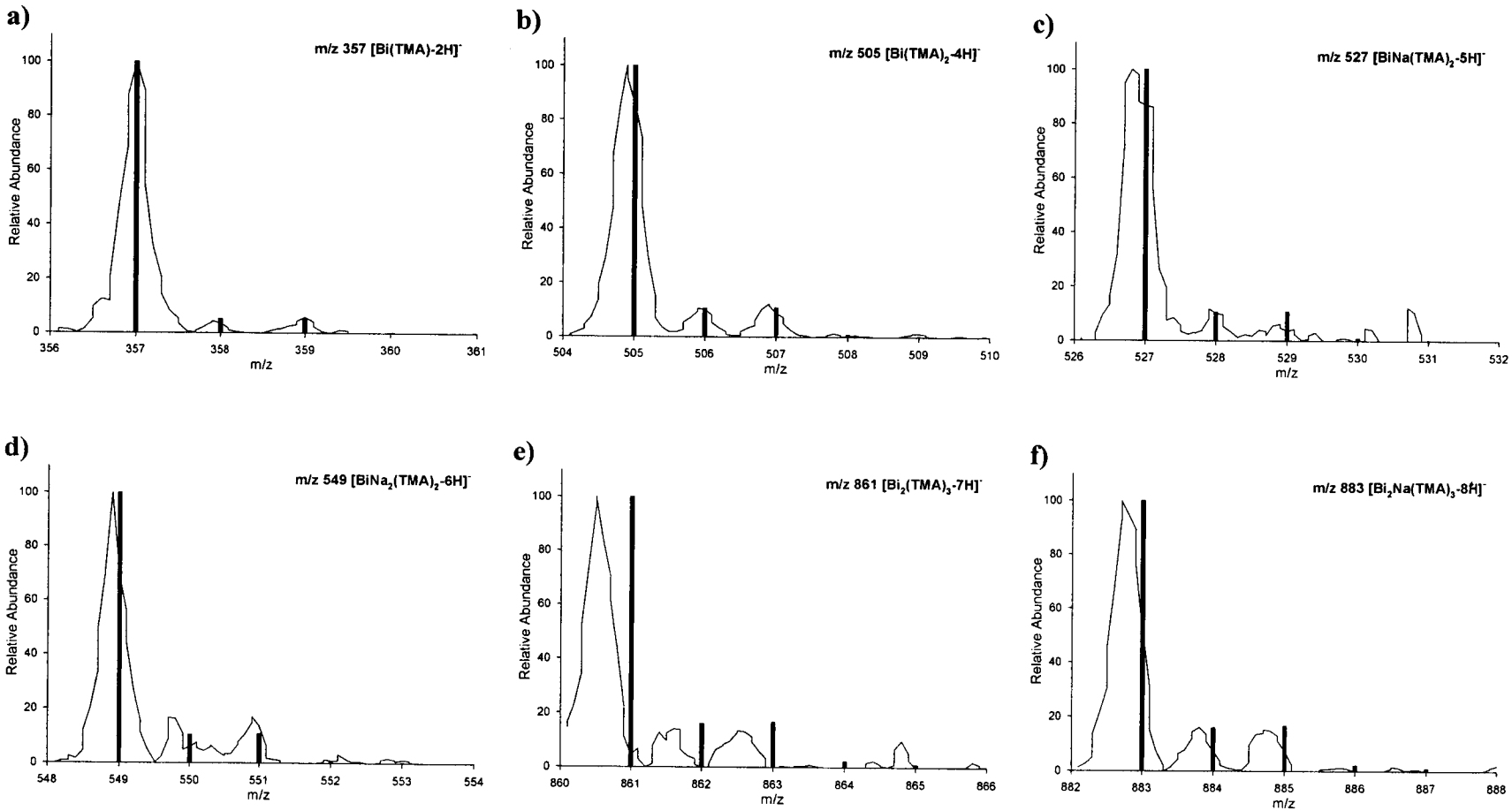

Figure C.8 Observed and calculated isotope peak distributions for Bi/TMA anions. a)-f) Experimental (continuous thin line) and theoretical (vertical bars) isotope patterns are shown for various indicated $[Bi_v(L)_w\text{-}yH]^z$ (L = TMA) complex ions.

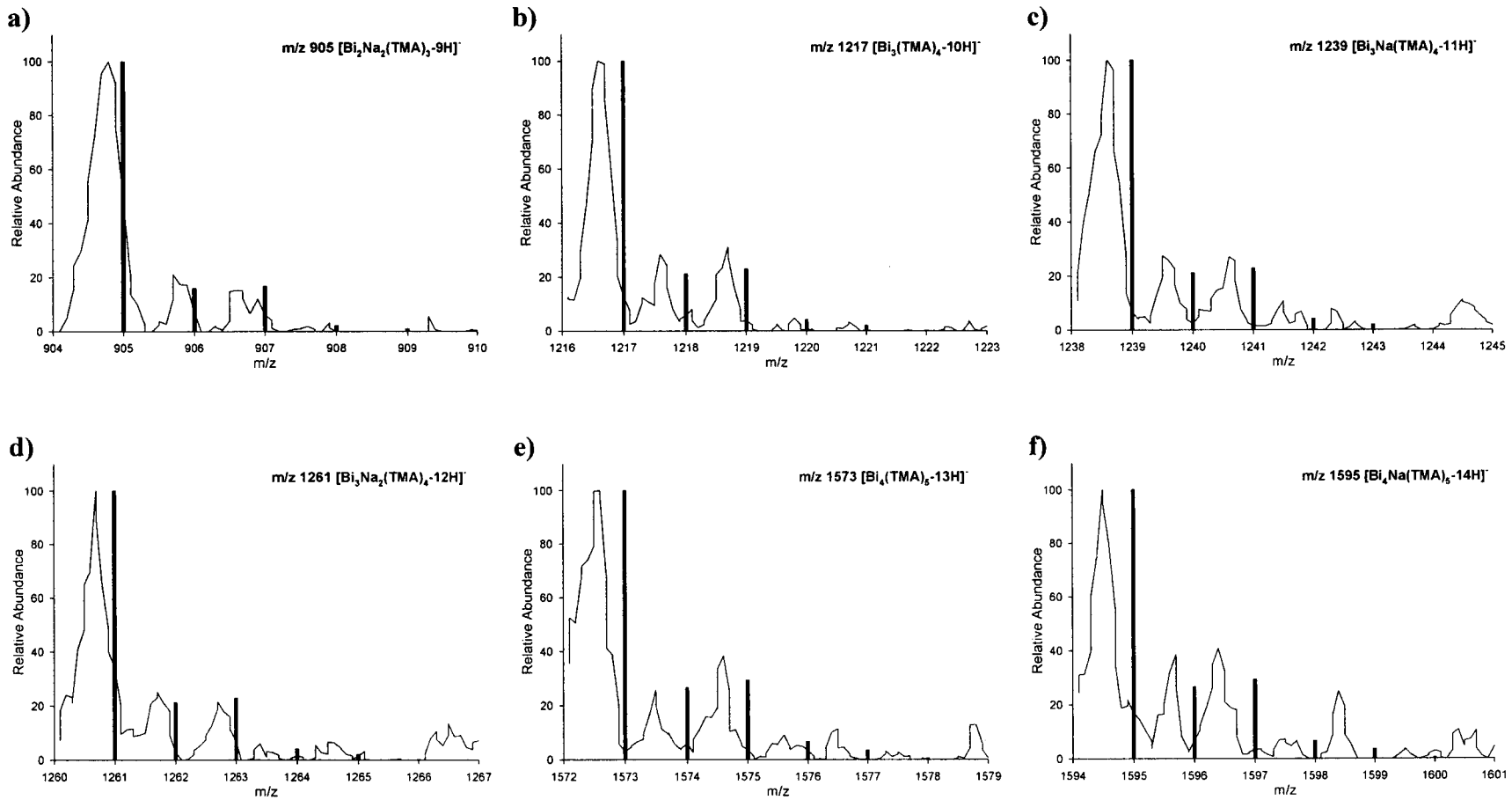

Figure C.9 Continued from Figure C.8. Observed and calculated isotope peak distributions for Bi/TMA anions. a)-f) Experimental (continuous thin line) and theoretical (vertical bars) isotope patterns are shown for various indicated $[Bi_v(L)_w\text{-}yH]^z$ (L = TMA) complex ions.

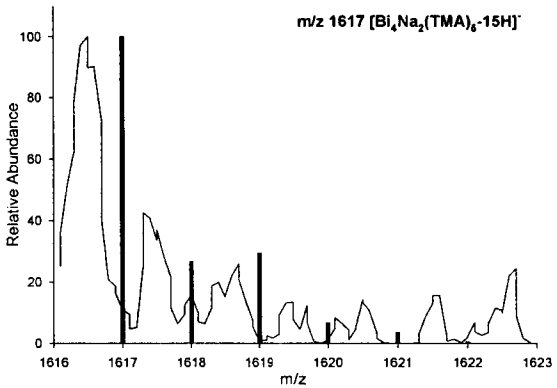

Figure C.10 Continued from Figure C.9. Observed and calculated isotope peak distributions for a Bi/TMA anion. Experimental (continuous thin line) and theoretical (vertical bars) isotope patterns are shown for the indicated $[Bi_v(L)_w\text{-}yH]^z$ (L = TMA) complex ion.

Reference List

(1) Sadler, P. J.; Li, H.; Sun, H. *Coord. Chem. Rev.* **1999**, *185-186*, 689-709.

(2) Briand, G. G.; Burford, N. *Chem. Rev.* **1999**, *99*, 2601-2657.

(3) Abrams, M. J.; Murrer, B. A. *Science* **1993**, *261*, 725-730.

(4) Prewett, E. J.; Nwokolo, C. U.; Hudson, M.; Sawyerr, A. M.; Fraser, A.; Pounder, R. E. *Aliment. Pharmacol. Ther.* **1991**, *5*, 481-490.

(5) Stables, R.; Campbell, C. J.; Clayton, N. M.; Clitherow, J. W.; Grinham, C. J.; McColm, A. A.; McLaren, A.; Trevethick, M. A. *Aliment. Pharmacol. Ther.* **1993**, *7*, 237-246.

(6) Marshall, B. J. *Am. J. Gastroenterol.* **1991**, *86*, 16-25.

(7) McColm, A. A.; McLaren, A.; Klinkert, G.; Francis, M. R.; Connolly, P. C.; Grinham, C. J.; Campbell, C. J.; Selway, S.; Williamson, R. *Aliment. Pharmacol. Ther.* **1996**, *10*, 241-250.

(8) Vondracek, T. G. *Ann. Pharmacother.* **1998**, *32*, 672-679.

(9) Ables, A. Z.; Simon, I.; Melton, E. R. *Am. Fam. Phys.* **2007**, *75*, 351-358.

(10) Marshall, B. J.; Warren, J. R. *Lancet* **1983**, *321*, 1273-1275.

(11) Hellström, P. M. *Scand. J. Gastroenterol.* **2005**, *40*, 1383-1385.

(12) Briand, G. G.; Burford, N. *Adv. Inorg. Chem.* **2000**, *50*, 285-357.

(13) Sadler, P. J.; Sun, H.; Li, H. *Chem. Eur. J.* **1996**, *2*, 701-708.

(14) Sun, H.; Li, H.; Harvey, I.; Sadler, P. J. *J. Biol. Chem.* **1999**, *274*, 29094-29101.

(15) Busenlehner, L. S.; Apuy, J. L.; Giedroc, D. P. *J. Biol. Inorg. Chem.* **2002**, *7*, 551-559.

(16) Burford, N.; Eelman, M. D.; Mahony, D.; Morash, M. *Chem. Commun.* **2003**, 146-147.

(17) Burford, N.; Eelman, M. D.; LeBlanc, W. G. *Can. J. Chem.* **2004**, *82*, 1254-1259.

(18) Burford, N.; Eelman, M. D.; Groom, K. A. *J. Inorg. Biochem.* **2005**, *99*, 1992-1997.

(19) Zhang, L.; Mulrooney, S. B.; Leung, A. F. K.; Zeng, Y.; Ko, B. B. C.; Hausinger, R. P.; Sun, H. *BioMetals* **2006**, *19*, 503-511.

(20) Agocs, L.; Burford, N.; Cameron, T. S.; Curtis, J. M.; Richardson, J. F.; Robertson, K. N.; Yhard, G. B. *J. Am. Chem. Soc.* **1996**, *118*, 3225-3232.

(21) Agocs, L.; Briand, G. G.; Burford, N.; Cameron, T. S.; Kwiatkowski, W.; Robertson, K. N. *Inorg. Chem.* **1997**, *36*, 2855-2860.

(22) Briand, G. G.; Burford, N.; Cameron, T. S. *Chem. Commun.* **1997**, 2365-2366.

(23) Briand, G. G.; Burford, N.; Cameron, T. S.; Kwiatkowski, W. *J. Am. Chem. Soc.* **1998**, *120*, 11374-11379.

(24) Briand, G. G.; Burford, N.; Cameron, T. S. *Chem. Commun.* **2000**, 13-14.

(25) Burford, N.; Eelman, M. D.; Cameron, T. S. *Chem. Commun.* **2002**, 1402-1403.

(26) Agocs, L.; Briand, G. G.; Burford, N.; Eelman, M. D.; Aumeerally, N.; MacKay, D.; Robertson, K. N.; Cameron, T. S. *Can. J. Chem.* **2003**, *81*, 632-637.

(27) Briand, G. G.; Burford, N.; Eelman, M. D.; Cameron, T. S.; Robertson, K. N. *Inorg. Chem.* **2003**, *42*, 3136-3141.

(28) Briand, G. G.; Burford, N.; Eelman, M. D.; Aumeerally, N.; Chen, L.; Cameron, T. S.; Robertson, K. N. *Inorg. Chem.* **2004**, *43*, 6495-6500.

(29) Matzapetakis, M.; Ghosh, D.; Weng, T.-C.; Penner-Hahn, J. E.; Pecoraro, V. L. *J. Biol. Inorg. Chem.* **2006**, *11*, 876-890.

(30) Pannequin, J.; Kovac, S.; Tantiongco, J.-P.; Norton, R. S.; Shulkes, A.; Barnham, K. J.; Baldwin, G. S. *J. Biol. Chem.* **2004**, *279*, 2453-2460.

(31) Li, W.; Jin, L.; Zhu, N.; Hou, X.; Deng, F.; Sun, H. *J. Am. Chem. Soc.* **2003**, *125*, 12408-12409.

(32) Andrews, P. C.; Deacon, G. B.; Forsyth, C. M.; Junk, P. C.; Kumar, I.; Maguire, M. *Angew. Chem. Int. Ed.* **2006**, *45*, 5638-5642.

(33) Burford, N.; Eelman, M. D.; LeBlanc, W. G.; Cameron, T. S.; Robertson, K. N. *Chem. Commun.* **2004**, 332-333.

(34) Crabtree, R. H. Werner Complexes; In *The Organometallic Chemistry of the Transition Metals*; John Wiley & Sons, Inc.: New York, 2001; pp 2-6.

(35) Bowman-James, K. *Acc. Chem. Res.* **2005**, *38*, 671-678.

(36) Rosenfeld, L. *Clin. Chem.* **2002**, *48*, 2270-2288.

(37) Rosenberg, B.; VanCamp, L.; Krigas, T. *Nature* **1965**, *205*, 698-699.

(38) Orvig, C.; Abrams, M. J. *Chem. Rev.* **1999**, *99*, 2201-2203.

(39) Rosenberg, B.; VanCamp, L.; Trosko, J. E.; Mansour, V. H. *Nature* **1969**, *222*, 385-386.

(40) Jamieson, E. R.; Lippard, S. J. *Chem. Rev.* **1999**, *99*, 2467-2498.

(41) Lippard, S. J.; Berg, J. M. *Principles of Bioinorganic Chemistry*; University Science Books: Mill Valley, 1994.

(42) Cowan, J. A. *Inorganic Biochemistry, An Introduction*; Wiley-VCH, Inc.: New York, 1997.

(43) Sadler, P. J.; Guo, Z. *Pure & Appl. Chem.* **1998**, *70*, 863-871.

(44) Roat-Malone, R. M. *Bioinorganic Chemistry, A Short Course*; John Wiley & Sons, Inc.: Hoboken, 2002.

(45) Thompson, K. H.; Orvig, C. *Science* **2003**, *300*, 936-939.

(46) In *Metallotherapeutic Drugs and Metal Based Diagnostic Agents*; Geilen, M., Tiekink, E. R. T., eds. John Wiley & Sons: New York, 2005.

(47) Kraatz, H.-B.; Metzler-Nolte, N. *Concepts and Models in Bioinorganic Chemistry*; WILEY-VCH Verlag GmbH & Co. KGaA: Weinheim, 2006.

(48) Storr, T.; Thompson, K. H.; Orvig, C. *Chem. Soc. Rev.* **2006**, *35*, 534-544.

(49) McMaster, J. *Annu. Rep. Prog. Chem., Sect. A* **2006**, *102*, 564-583.

(50) Bertini, I.; Gray, H. B.; Stiefel, E. I.; Valentine, J. S. *Biological Inorganic Chemistry, Structure and Reactivity*; University Science Books: Sausalito, 2007.

(51) Drennan, C. L.; Tolman, W. B. *Curr. Opin. Chem. Biol.* **2007**, *11*, 113-114.

(52) Garner, C. D. *J. Chem. Soc. Dalton Trans.* **1997**, 3903-3908.

(53) Mann, S. *J. Chem. Soc. Dalton Trans.* **1997**, 3953-3961.

(54) Wittcoff, H. A.; Reuben, B. G. *Industrial Organic Chemicals*; John Wiley & Sons, Inc.: New York, 1996.

(55) Goyer, R. A. Toxic Effects of Metals; In *Casarett & Doull's Toxicology: The Basic Science of Poisons*; Klaassen, C. D., ed. The McGraw-Hill Companies, Inc.: New York, 1996; pp 691-736.

(56) Ferenci, P. *Aliment. Pharmacol. Ther.* **2004**, *19*, 157-165.

(57) Hughes, M. N. *The Inorganic Chemistry of Biological Processes*; John Wiley & Sons, Ltd.: Chichester, 1981.

(58) Woo, L. C. Y.; Yuen, V. G.; Thompson, K. H.; McNeill, J. H.; Orvig, C. *J. Inorg. Biochem.* **1999**, *76*, 251-257.

(59) Sanchez, C. P.; Stein, W.; Lanzer, M. *Biochem.* **2003**, *42*, 9383-9394.

(60) Delhaes, L.; Abessolo, H.; Biot, C.; Berry, L.; Delcourt, P.; Maciejewski, L.; Brocard, J.; Camus, D.; Dive, D. *Parasitol. Res.* **2001**, *87*, 239-244.

(61) Shaw, C. F. I. *Chem. Rev.* **1999**, *99*, 2589-2600.

(62) Guo, Z.; Sadler, P. J. *Angew. Chem. Int. Ed.* **1999**, *38*, 1512-1531.

(63) Koryakin, S. N. *Pharm. Chem. J.* **2006**, *40*, 583-587.

(64) Mathews, C. K.; van Holde, K. E.; Ahern, K. G. Introduction to Proteins: The Primary Level of Protein Structure; In *Biochemistry*; Benjamin Cummings: San Francisco, 2000; pp 126-160.

(65) Ge, R.; Zhang, Y.; Sun, X.; Watt, R. M.; He, Q.-Y.; Huang, J.-D.; Wilcox, D. E.; Sun, H. *J. Am. Chem. Soc.* **2006**, *128*, 11330-11331.

(66) Sun, H.; Li, H.; Mason, A. B.; Woodworth, R. C.; Sadler, P. J. *Biochem. J.* **1999**, *337*, 105-111.

(67) Fitz, D.; Reiner, H.; Plankensteiner, K.; Rode, B. M. *Curr. Chem. Biol.* **2007**, *1*, 41-52.

(68) Townsend, J. H.; Davis, S. R.; Mackey, A. D.; Gregory III, J. F. *Am. J. Physiol. Gastrointest. Liver Physiol.* **2004**, *286*, G588-G595.

(69) Sun, H.; Li, H.; Sadler, P. J. *J. Inorg. Biochem.* **1995**, *59*, 190.

(70) Phillips, H. A.; Eelman, M. D.; Burford, N. *J. Inorg. Biochem.* **2007**, *101*, 736-739.

(71) Mathews, C. K.; van Holde, K. E.; Ahern, K. G. Carbohydrates; In *Biochemistry*; Benjamin Cummings: San Francisco, 2000; pp 278-314.

(72) Mathews, C. K.; van Holde, K. E.; Ahern, K. G. Nucleic Acids; In *Biochemistry*; Benjamin Cummings: San Francisco, 2000; pp 84-125.

(73) Mathews, C. K.; van Holde, K. E.; Ahern, K. G. Lipids, Membranes, and Cellular Transport; In *Biochemistry*; Benjamin Cummings: San Francisco, 2000; pp 315-357.

(74) de Marcillac, P.; Coron, N.; Dambier, G.; Leblanc, J.; Moalic, J.-P. *Nature* **2003**, *422*, 876-878.

(75) Moore, K. L.; Dalley, A. F. *Clinically Oriented Anatomy*; Lippincott Williams & Wilkins: Philadelphia, 1999.

(76) Veldhuyzen van Zanten, S. J. O. *Brit. Med. J.* **2000**, *321*, 648-649.

(77) Gisbert, J. P.; Gisbert, J. L.; Marcos, S.; Moreno-Otero, R.; Pajares, J. M. *Helicobacter* **2007**, *12*, 68-73.

(78) Talley, N. J.; Axon, A.; Bytzer, P.; Holtmann, G.; Lam, S. K.; Veldhuyzen van Zanten, S. J. O. *Aliment. Pharmacol. Ther.* **1999**, *13*, 1135-1148.

(79) Del Giudice, G.; Covacci, A.; Telford, J. L.; Montecucco, C.; Rappuoli, R. *Annu. Rev. Immunol.* **2001**, *19*, 523-563.

(80) Lacy, B. E.; Rosemore, J. *J. Nutr.* **2001**, *131*, 2789S-2793S.

(81) Pounder, R. E.; Ng, D. *Aliment. Pharmacol. Ther.* **1995**, *9 (Suppl. 2)*, 33-39.

(82) Go, M. F. *Aliment. Pharmacol. Ther.* **2002**, *16 (Suppl. 1)*, 3-15.

(83) Marshall, B. J.; Warren, J. R. *Lancet* **1984**, *323*, 1311-1315.

(84) Marshall, B. J. *J. Infect. Dis.* **1986**, *153*, 650-657.

(85) Wright, K. *Discover* **2003**, *24*, 24-25.

(86) de Bortoli, N.; Leonardi, G.; Ciancia, E.; Merlo, A.; Bellini, M.; Costa, F.; Mumolo, M. G.; Ricchiuti, A.; Cristiani, F.; Santi, S.; Rossi, M.; Marchi, S. *Am. J. Gastroenterol.* **2007**, *102*, 951-956.

(87) Vergara, M.; Vallve, M.; Gisbert, J. P.; Calvet, X. *Aliment. Pharmacol. Ther.* **2003**, *18*, 647-654.

(88) Malfertheiner, P.; Mégraud, F.; O'Morain, C.; Hungin, A. P. S.; Jones, R.; Axon, A.; Graham, D. Y.; Tytgat, G.; & The European Helicobacter Pylori Study Group (EHPSG) *Aliment. Pharmacol. Ther.* **2002**, *16*, 167-180.

(89) Ilver, D.; Arnqvist, A.; Ögren, J.; Frick, I.-M.; Kersulyte, D.; Incecik, E. T.; Berg, D. E.; Covacci, A.; Engstrand, L.; Borén, T. *Science* **1998**, *279*, 373-377.

(90) Benini, S.; Rypniewski, W. R.; Wilson, K. S.; Ciurli, S.; Mangani, S. *J. Biol. Inorg. Chem.* **1998**, *3*, 268-273.

(91) Asato, E.; Kamamuta, K.; Akamine, Y.; Fukami, T.; Nukada, R.; Mikuriya, M.; Deguchi, S.; Yokota, Y. *Bull. Chem. Soc. Jpn.* **1997**, *70*, 639-648.

(92) Leung, S. Y.; Chen, X.; Chu, K. M.; Yuen, S. T.; Mathy, J.; Ji, J.; Chan, A. S. Y.; Li, R.; Law, S.; Troyanskaya, O. G.; Tu, I.-P.; Wong, J.; So, S.; Botstein, D.; Brown, P. O. *Proc. Natl. Acad. Sci. USA* **2002**, *99*, 16203-16208.

(93) Mahony, D. E.; Lim-Morrison, S.; Bryden, L.; Faulkner, G.; Hoffman, P. S.; Agocs, L.; Briand, G. G.; Burford, N.; Maguire, H. *Antimicrob. Agents Chemother.* **1999**, *43*, 582-588.

(94) Blaser, M. J. *Scientific American* **2005**, *292*, 38-45.

(95) McCarthy, D. M. *J. Clin. Gastroenterol.* **2007**, *41 (Supp. 2)*, S59-S63.

(96) *The Merck Index*; Merck & Co., Inc.: Rahway, New Jersey, 1983.

(97) Thurston, J. H.; Marlier, E. M.; Whitmire, K. H. *Chem. Commun.* **2002**, 2834-2835.

(98) Stavila, V.; Fettinger, J. C.; Whitmire, K. H. *Organometallics* **2007**, *26*, 3321-3328.

(99) Andrews, P. C.; Deacon, G. B.; Jackson, W. R.; Maguire, M.; Scott, N. M.; Skelton, B. W.; White, A. H. *J. Chem. Soc. Dalton Trans.* **2002**, 4634-4638.

(100) Andrews, P. C.; Deacon, G. B.; Junk, P. C.; Kumar, I.; Silberstein, M. *Dalton Trans.* **2006**, 4852-4858.

(101) Asato, E.; Katsura, K.; Arakaki, M.; Mikuriya, M.; Kotera, T. *Chem. Lett.* **1994**, 2123-2126.

(102) Thurston, J. H.; Whitmire, K. H. *Inorg. Chem.* **2002**, *41*, 4194-4205.

(103) Thurston, J. H.; Ould-Ely, T.; Trahan, D.; Whitmire, K. H. *Chem. Mater.* **2003**, *15*, 4407-4416.

(104) Thurston, J. H.; Whitmire, K. H. *Inorg. Chem.* **2003**, *42*, 2014-2023.

(105) Thurston, J. H.; Trahan, D.; Ould-Ely, T.; Whitmire, K. H. *Inorg. Chem.* **2004**, *43*, 3299-3305.

(106) Thurston, J. H.; Kumar, A.; Hofmann, C.; Whitmire, K. H. *Inorg. Chem.* **2004**, *43*, 8427-8436.

(107) Herrmann, W. A.; Herdtweck, E.; Pajdla, L. *Inorg. Chem.* **1991**, *30*, 2579-2581.

(108) Asato, E.; Driessen, W. L.; de Graaff, R. A. G.; Hulsbergen, F. B.; Reedijk, J. *Inorg. Chem.* **1991**, *30*, 4210-4218.

(109) Herrmann, W. A.; Herdtweck, E.; Pajdla, L. *Z. Krist.* **1992**, *198*, 257-264.

(110) Asato, E.; Katsura, K.; Mikuriya, M.; Fujii, T.; Reedijk, J. *Chem. Lett.* **1992**, 1967-1970.

(111) Asato, E.; Katsura, K.; Mikuriya, M.; Fujii, T.; Reedijk, J. *Inorg. Chem.* **1993**, *32*, 5322-5329.

(112) Asato, E.; Katsura, K.; Mikuriya, M.; Turpeinen, U.; Mutikainen, I.; Reedijk, J. *Inorg. Chem.* **1995**, *34*, 2447-2454.

(113) Barrie, P. J.; Djuran, M. I.; Mazid, M. A.; McPartlin, M.; Sadler, P. J.; Scowen, I. J.; Sun, H. *J. Chem. Soc., Dalton Trans.* **1996**, 2417-2422.

(114) Herrmann, W. A.; Herdtweck, E.; Scherer, W.; Kiprof, P.; Pajdla, L. *Chem. Ber.* **1993**, *126*, 51-56.

(115) Sagatys, D. S.; O'Reilly, E. J.; Patel, S.; Bott, R. C.; Lynch, D. E.; Smith, G. S.; Kennard, H. L. *Aust. J. Chem.* **1992**, *45*, 1027-1034.

(116) Kiprof, P.; Scherer, W.; Pajdla, L.; Herdtweck, E.; Herrmann, W. A. *Chem. Ber.* **1992**, *125*, 43-46.

(117) Udovenko, A. A.; Volkova, L. M.; Sergienko, S. S.; Davidovich, R. L.; Shevenko, V. Ya. *Koord. Khim.* **1983**, *9*, 711-713.

(118) Heinl, U.; Hinse, P.; Mattes, R. *Z. Anorg. Allg. Chem.* **2001**, *627*, 2173-2177.

(119) Kolitsch, U. *Acta Crystallogr., Sect. C: Cryst. Struct. Commun.* **2003**, *C59*, m501-m504.

(120) Vanhoyland, G.; Le Bail, A.; Mullens, J.; Van Poucke, L. C. *Inorg. Chem.* **2004**, *43*, 785-789.

(121) Frutos, A. A.; Sala, L. F.; Escandar, G. M.; Devillers, M.; Salas Peregrín, J. M.; González Sierra, M. *Polyhedron* **1999**, *18*, 989-994.

(122) Sadler, P. J.; Sun, H. *Dalton Trans.* **1995**, 1395-1401.

(123) Yan, N.; Tanner, J. A.; Zheng, B.-J.; Watt, R. M.; He, M.-L.; Lu, L.-Y.; Jiang, J.-Q.; Shum, K.-T.; Lin, Y.-P.; Wong, K.-L.; Lin, M. C. M.; Kung, H.-F.; Sun, H.; Huang, J.-D. *Angew. Chem. Int. Ed.* **2007**, *46*, 6464-6468.

(124) Topol, I. A.; McGrath, C.; Chertova, E.; Dasenbrock, C.; Lacourse, W. R.; Eissenstat, M. A.; Burt, S. K.; Henderson, L. E.; Casas-Finet, J. R. *Protein Sci.* **2001**, *10*, 1434-1445.

(125) Pearson, R. G. *J. Am. Chem. Soc.* **1963**, *85*, 3533-3539.

(126) Huheey, J. E.; Keiter, E. A.; Keiter, R. L. Acid-Base Chemistry: Hard and Soft Acids and Bases; In *Inorganic Chemistry, Principles of Structure and Reactivity*; HarperCollins College Publishers: New York, 1993; pp 350-355.

(127) Miessler, G. L.; Tarr, D. A. *Inorganic Chemistry*; Pearson Education, Inc.: Upper Saddle River, 2004; pp 183-187.

(128) Pauling, L. *The Nature of The Chemical Bond*; Cornell University Press: Ithaca, 1960; pp 93 (electronegativity), 410 (interatomic distances).

(129) Levason, W.; Reid, G. *Dalton Trans.* **2001**, 2953-2960.

(130) Dikarev, E. V.; Zhang, H.; Li, B. *Angew. Chem. Int. Ed.* **2006**, *45*, 5448-5451.

(131) Muller, A.; Zimmermann, M.; Bogge, H. *Angew. Chem., Int. Ed. Engl.* **1986**, *25*, 273.

(132) Castleman, A. W.; Jena, P. *Proc. Natl. Acad. Sci. USA* **2006**, *103*, 10554-10559.

(133) Kosower, E. M. Chemical Properties of Glutathione; In *Glutathione: Metabolism and Function*; Arias, I. M., Jakoby, W. B., eds. Raven Press, Publishers: New York, 1976; pp 1-15.

(134) Herrmann, W. A.; Herdtweck, E.; Pajdla, L. *Chem. Ber.* **1993**, *126*, 895-898.

(135) Golovnev, N. N.; Novikova, G. V.; Vershinin, V. V.; Churilov, T. D.; Golovneva, I. I. *Zh. Neorg. Khim.* **2003**, *48*, 1847-1850.

(136) Sandha, G. S.; LeBlanc, R.; van Santen, S. J. O. V.; Sitland, T. D.; Agocs, L.; Burford, N.; Best, L.; Mahony, D.; Hoffman, P.; Leddin, D. J. *Dig. Dis. Sci.* **1998**, *43*, 2727-2732.

(137) Krari, N.; Mauras, Y.; Allain, P. *Res. Commun. Mol. Pathol. Pharmacol.* **1995**, *89*, 357-364.

(138) Mahony, D. E.; Woods, A.; Eelman, M. D.; Burford, N.; Veldhuyzen van Zanten, S. J. O. *Antimicrob. Agents Chemother.* **2005**, *49*, 431-433.

(139) Taylor, N. J.; Wong, Y. S.; Chieh, P. C.; Carty, A. J. *J. Chem. Soc. Dalton Trans.* **1975**, 438-442.

(140) Freeman, H. C.; Moore, C. J. *Acta. Cryst.* **1977**, *B33*, 2690-2692.

(141) Wong, Y. S.; Carty, A. J.; Chieh, P. C. *J. Chem. Soc. Dalton Trans.* **1977**, 1157.

(142) Henrick, K.; Matthews, R. W.; Tasker, P. A. *Acta Crystallogr., Sect. B: Struct. Crystallogr. Cryst. Chem.* **1978**, *34*, 935-937.

(143) Corbeil, M. C.; Beauchamp, A. L. *Can. J. Chem.* **1988**, *66*, 2458-2464.

(144) Müller, A.; Straube, M.; Krickemeyer, E.; Bögge, H. *Naturwissenschaften* **1992**, *79*, 323-325.

(145) Morgan, K.; Sayer, B. G.; Schrobilgen, G. J. *J. Magn. Reson.* **1983**, *52*, 139-142.

(146) Harris, R. K. Group V - Arsenic, Antimony and Bismuth; In *NMR and the Periodic Table*; Harris, R. K., Mann, B. E., eds. Academic Press Inc. (London) Ltd: London, 1978; pp 379-382.

(147) Brevard, C.; Granger, P. *Handbook of High Resolution Multinuclear NMR*; John Wiley & Sons, Inc.: New York, 1981; pp 210-211.

(148) Fukushima, E.; Mastin, S. H. *J. Magn. Reson.* **1969**, *1*, 648-651.

(149) Fukushima, E. *J. Chem. Phys.* **1971**, *55*, 2463-2466.

(150) Mercier, H. P. A.; Sanders, J. C. P.; Schrobilgen, G. J. *J. Am. Chem. Soc.* **1994**, *116*, 2921-2937.

(151) Reyes, A. P.; Le, L. P.; Heffner, R. H.; Ahrens, E. T.; Fisk, Z.; Canfield, P. C. *Physica B* **1995**, *206 & 207*, 332-335.

(152) Sun, H.; Li, H.; Mason, A. B.; Woodworth, R. C.; Sadler, P. J. *J. Bio. Chem.* **2001**, *276*, 8829-8835.

(153) Zhang, L.; Szeto, K. Y.; Wong, W. B.; Loh, T. T.; Sadler, P. J.; Sun, H. *Biochem.* **2001**, *40*, 13281-13287.

(154) Herrmann, W. A.; Kiprof, P.; Scherer, W.; Pajdla, L. *Chem. Ber.* **1992**, *125*, 2657-2660.

(155) Napoli, A. *Ann. Chim.* **1982**, *72*, 575-583.

(156) Jackson, G. E.; Hancock, R. D. *Polyhedron* **1984**, *3*, 71-73.

(157) Ikram, M.; Powell, D. B. *Spectrochimica Acta* **1972**, *28A*, 59-64.

(158) Sun, H.; Li, H.; Harvey, I.; Sadler, P. J. *J. Biol. Chem.* **1999**, *274*, 29094-29101.

(159) de Hoffmann, E.; Stroobant, V. *Mass Spectrometry Principles and Applications*; John Wiley & Sons, Ltd.: New York, 2002.

(160) Glish, G. L.; Vachet, R. W. *Nature Reviews Drug Discovery* **2003**, *2*, 140-150.

(161) Lambert, J. B.; Shurvell, H. F.; Lightner, D. A.; Cooks, R. G. Mass Spectrometry; In *Organic Structural Spectroscopy*; Prentice-Hall, Inc.: Upper Saddle River, 1998; pp 345-385.

(162) Colton, R.; D'Agostino, A.; Traeger, J. C. *Mass Spectrom. Rev.* **1995**, *14*, 79-106.

(163) Lobinski, R.; Schaumlöffel, D.; Szpunar, J. *Mass Spectrom. Rev.* **2006**, *25*, 255-289.

(164) Traeger, J. C. *Int. J. Mass Spectrom.* **2000**, *200*, 387-401.

(165) Johnson, B. F. G.; McIndoe, J. S. *Coord. Chem. Rev.* **2000**, *200-202*, 901-932.

(166) Burford, N.; Eelman, M. D.; LeBlanc, W. G.; Cameron, T. S.; Robertson, K. N. *Chem. Commun.* **2004**, 332-333.

(167) Ikonomou, M. G.; Blades, A. T.; Kebarle, P. *Am. Soc. Mass Spec.* **1991**, *2*, 497-505.

(168) Siuzdak, G.; Bothner, B.; Yeager, M.; Brugidou, C.; Fauquet, C. M.; Hoey, K.; Chang, C.-M. *Chem. Biol.* **1996**, *3*, 45-48.

(169) Dyson, P. J.; McIndoe, J. S. *Inorg. Chim. Acta* **2003**, *354*, 68-74.

(170) Cole, R. B. *J. Mass Spectrom.* **2000**, *35*, 763-772.

(171) Cech, N. B.; Enke, C. G. *Mass Spectrom. Rev.* **2001**, *20*, 387.

(172) Quarmby, S. T.; Yost, R. A. *Int. J. Mass Spectrom.* **1999**, 81-102.

(173) Duffus, J. H. *Pure Appl. Chem.* **2002**, *74*, 793-807.

(174) Huheey, J. E.; Keiter, E. A.; Keiter, R. L. Periodicity: Periodic Anomalies of the Nonmetals and Posttransition Metals; In *Inorganic Chemistry, Principles of Structure and Reactivity*; HarperCollins College Publishers: New York, 1993; pp 878-885.

(175) Thayer, J. S. *J. Chem. Ed.* **2005**, *82(11)*, 1721-1727.

(176) Arena, J. M.; Drew, R. H. *Poisoning: Toxicology, Symptoms, Treatments*; Charles C Thomas Publishers: Springfield, 1986.

(177) Emsley, J. *The Elements*; Oxford University Press, Inc.: New York, 1998.

(178) Lowe, D. J. *Med. J. Aust.* **1974**, *2*, 664-666.

(179) Martin-Bouyer, G. *Thérapie* **1976**, *31*, 683-702.

(180) Ross, J. F.; Sahenk, Z.; Hyser, C.; Mendell, J. R.; Alden, C. L. *Neurotoxicology* **1988**, *9*, 581-586.

(181) Córdova, A.; Engqvist, M.; Ibrahem, I.; Casas, J.; Sundén, H. *Chem. Commun.* **2005**, 2047-2049.

(182) Baran, W.; Sikora, M.; Tomasik, P.; Anderegg, J. W. *Carbohydr. Polym.* **1997**, *32*, 209-212.

(183) Baczkowicz, M.; Wójtowicz, D.; Anderegg, J. W.; Schilling, C. H.; Tomasik, P. *Carbohydr. Polym.* **2003**, *52*, 263-268.

(184) Klüfers, P.; Mayer, P. *Acta Crystallogr., Sect. C: Cryst. Struct. Commun.* **1998**, *54*, 583-586.

(185) Dwek, R. A. *Chem. Rev.* **1996**, *96*, 683-720.

(186) Sharon, N.; Lis, H. *Scientific American* **1993**, *268*, 82-89.

(187) Fura, A.; Leary, J. A. *Anal. Chem.* **1993**, *65*, 2805-2811.

(188) Kohler, M.; Leary, J. A. *Anal. Chem.* **1995**, *67*, 3501-3508.

(189) Gaucher, S. P.; Leary, J. A. *Anal. Chem.* **1998**, *70*, 3009-3014.

(190) Cancilla, M. T.; Penn, S. G.; Carroll, J. A.; Lebrilla, C. B. *J. Am. Chem. Soc.* **1996**, *118*, 6736-6745.

(191) Xie, Y.; Lebrilla, C. B. *Anal. Chem.* **2003**, *75*, 1590-1598.

(192) Salpin, J.-Y.; Tortajada, J. *J. Mass Spectrom.* **2002**, *37*, 379-388.

(193) Salpin, J.-Y.; Tortajada, J. *J. Phys. Chem. A* **2003**, *107*, 2943-2953.

(194) Emmert, J.; Pfluger, M.; Wahl, F. *Spectroscopy* **2006**, *21*, 62-67.

(195) Manura, J. J.; Manura, D. J. *Isotope Distribution Calculator and Mass Spec Plotter*; Available online at http://www2.sisweb.com/mstools/isotope.htm: accessed July 2007. Scientific Instrument Services, Inc.: Ringoes, New Jersey, 2003.

(196) Du, Z.; Douglas, D. J.; Konenkov, N. *J. Am. Soc. Mass Spectrom.* **1999**, *10*, 1263-1270.

(197) Hartwig, A. *BioMetals* **1995**, *8*, 3-11.

(198) Houlton, A. *Adv. Inorg. Chem.* **2002**, *53*, 87-158.

(199) Freisinger, E.; Sigel, R. K. O. *Coord. Chem. Rev.* **2007**, *251*, 1834-1851.

(200) Nordhoff, E.; Kirpekar, F.; Roepstorff, P. *Mass Spectrom. Rev.* **1996**, *15*, 138.

(201) Banoub, J. H.; Newton, R. P.; Esmans, E.; Ewing, D. F.; Mackenzie, G. *Chem. Rev.* **2005**, *105*, 1869-1915.

(202) Fukushima, K.; Iwahashi, H. *Chem. Commun.* **2000**, 895-896.

(203) Koch, K. J.; Aggerholm, T.; Nanita, S. C.; Cooks, R. G. *J. Mass Spectrom.* **2002**, *37*, 676-686.

(204) Sakamoto, S.; Nakatani, K.; Saito, I.; Yamaguchi, K. *Chem. Commun.* **2003**, 788-789.

(205) Klüfers, P.; Mayer, P. *Z. Anorg. Allg. Chem.* **2007**, *633*, 903-907.

(206) Georgopoulou, A. S.; Ulvenlund, S.; Mingos, D. M. P.; Baxter, I.; Williams, D. J. *J. Chem. Soc. Dalton Trans.* **1999**, 547-551.

(207) Kasuk, H.; Nurk, G.; Lust, K.; Lust, E. *J. Electroanal. Chem.* **2003**, *550-551*, 13-31.

(208) Kasuk, H.; Nurk, G.; Lust, K.; Lust, E. *J. Electroanal. Chem.* **2005**, *580*, 128-134.

(209) Yan, J. *Isotope Pattern Calculator v4.0*; Available online at http://www.geocities.com/junhuayan/pattern.htm: accessed July 2007. Ohio State University: Columbus, Ohio, 2001.

(210) *Thallium and Thallium Compounds Health and Safety Guide (No. 102)*; World Health Organization: Geneva, 1996.

(211) Nriagu, J. O. *C&EN* **2003**, *81*, 153.

(212) Thompson, D. F.; Callen, E. D. *Ann. Pharmacother.* **2004**, *38*, 1509-1514.

(213) U.S.Food and Drug Administration *FDA Approves First New Drug Application for Treatment of Radiation Contamination due to Cesium or Thallium*; Available online at http://www.fda.gov/bbs/topics/NEWS/2003/NEW00950.html: accessed July 2007. FDA: Rockville, Maryland, 2003.

(214) Besunder, J. B.; Super, D. M.; Anderson, R. L. *J. Pediatr.* **1997**, *130*, 966-971.

(215) Chisolm, Jr. J. J. *Clin. Toxicol.* **2000**, *38*, 365-375.

(216) Rusyniak, D. E.; Kao, L. W.; Nanagas, K. A.; Kirk, M. A.; Furbee, R. B.; Brizendine, E. J.; Wilmot, P. E. *Clin. Toxicol.* **2003**, *41*, 137-142.

(217) Peter, A. L. J.; Viraraghavan, T. *Environ. Int.* **2005**, *31*, 493-501.

(218) Bugarin, M. G.; Casas, J. S.; Sordo, J.; Filella, M. *J. Inorg. Biochem.* **1989**, *35*, 95-105.

(219) Gharib, F.; Zare, K.; Taghvamanesh, A.; Shamel, A.; Shafiee, G. *Main Group Met. Chem.* **2002**, *25*, 647-653.

(220) Monajjemi, M.; Gharib, F.; Aghaei, H.; Shafiee, G.; Taghvamanesh, A.; Shamel, A. *Main Group Met. Chem.* **2003**, *26*, 39-47.

(221) Bugarin, M. G.; Garcia, M. E.; Berthon, G.; Casas, J. S.; Sordo, J. *Polyhedron* **1988**, *7*, 2487-2494.

(222) Henrick, K.; Matthews, R. W.; Tasker, P. A. *Acta Crystallogr., Sect. B: Struct. Crystallogr. Cryst. Chem.* **1978**, *34*, 1347-1350.

(223) Groom, K. A. *Identification of Complexes Containing Biologically Relevant Peptides with each of the Heavy Metals As(III), Sb(III), Bi(III), Cd(II), Hg(II), Tl(I) and Pb(II) by Electrospray Ionization Mass Spectrometry*; Department of Chemistry, Dalhousie University: M.Sc. Thesis, 2005.

(224) Ehsan, M. Q.; Malik, K. M. A.; Haider, S. Z. *J. Bangladesh. Acad. Sci.* **1996**, *20*, 175-181.

(225) Bondi, A. *J. Phys. Chem.* **1964**, *68*, 441-451.

(226) Bosch, B. E.; Eisenhawer, M.; Kersting, B.; Kirschbaum, K.; Krebs, B.; Giolando, D. M. *Inorg. Chem.* **1996**, *35*, 6599-6605.

(227) Ghosh, P.; Rheingold, A. L.; Parkin, G. *Inorg. Chem.* **1999**, *38*, 5464-5467.

(228) Edén, M.; Levitt, M. H. *J. Chem. Phys.* **1999**, *111*, 1511-1519.

(229) MacKenzie, K. J. D.; Smith, M. E. NMR of Other Spin-1/2 Nuclei: ^{15}N NMR; In *Multinuclear Solid-State NMR of Inorganic Materials*; Elsevier Science Ltd.: Kidlington, Oxford, 2002; pp 574-575.

(230) Sheldrick, G. M. *Acta Crystallogr.* **1990**, *A46*, 467-473.

(231) Ge, R.; Sun, H. *Acc. Chem. Res.* **2007**, *40*, 267-274.

(232) Saunders, C.; Burford, N.; Werner-Zwanziger, U.; McDonald, R. *Manuscript in preparation:* **2007**, Preparation and Comprehensive Characterization of a Hg(I)-Hg(II)-Alanine Complex.

(233) Eelman, M. D. In *Systematically Developing the Chemistry of Bismuth and Other Heavy Metals with Biorelevant Ligands*; Department of Chemistry, Dalhousie University: Ph.D. Thesis, 2003; pp 72-76.

(234) Jia, R. R.; Wu, C. P.; Wu, S.; Yang, Y. X.; Chen, Y. R.; Jia, Y. Q. *Amino Acids* **2006**, *31*, 85-90.

(235) Kumar, M. R.; Prabhakar, S.; Kumar, M. K.; Reddy, T. J.; Vairamani, M. *Rapid Commun. Mass Spectrom.* **2005**, *19*, 113-120.

(236) Henderson, W.; McIndoe, J. S. The ESI MS Behaviour of Coordination Complexes; In *Mass Spectrometry of Inorganic and Organometallic Compounds*; John Wiley & Sons Ltd: Chichester, 2005; pp 127-173.

(237) Moraes, L. A. B.; Eberlin, M. N. *Chem. Eur. J.* **2000**, *6*, 897-905.

(238) Kebarle, P. *J. Mass Spectrom.* **2000**, *35*, 804-817.

(239) *Finnigan LCQDUO Hardware Manual 97033-97033 Revision B*; Technical Publications, Thermo Electron Corporation: San Jose, 2003.

(240) Di Marco, V. B.; Bombi, G. G. *Mass Spec. Rev.* **2006**, *25*, 347-379.

(241) Petrovic, M.; Barceló, D. *Anal. Bioanal. Chem.* **2006**, *385*, 422-424.

(242) Chen, G.; Pramanik, B. N.; Liu, Y.-H.; Mirza, U. A. *J. Mass Spectrom.* **2007**, *42*, 279-287.